UNDERSTANDING THE REACTIVITY AND SUBSTITUTION EFFECTS OF NITRENES AND AZIDES

by

Harshal Arun Jawale

A Dissertation

Submitted to the Faculty of Purdue University

In Partial Fulfillment of the Requirements for the degree of

Doctor of Philosophy

Department of Chemistry

West Lafayette, Indiana

December 2021

THE PURDUE UNIVERSITY GRADUATE SCHOOL

STATEMENT OF COMMITTEE APPROVAL

Dr. Paul Wenthold

Department of Chemistry

Dr. Chengde Mao

Department of Chemistry

Dr. Corey Thompson

Department of Chemistry

Dr. Jianguo Mei

Department of Chemistry

Approved by:

Dr. Christine Hrycyna

Dedicated to my parents, for their love and encouragement

ACKNOWLEDGMENTS

First and foremost, I'd like to thank my parents for their unconditional love and support throughout my career. They were always supportive of my choices even when they involved leaving and settling down in another country. They have consistently been my pillars of strength and guided me through all the walks of my life. I thank them for shaping me into the individual I am today and for all the sacrifices they have made for me.

I would also like to thank Dr. Paul Wenthold for accepting me as a refugee in his lab and helping me shape my career in mass spectrometry and analytical chemistry. He recognized the difficulties and the several roadblocks I hit during my research but never gave up on me, instead helping me out at every nook and corner of my road to PhD. I thank him immensely for being patient and highly approachable at any point of the day through any medium.

I would also like to thank all my current and ex-lab mates, Dr. Chris Haskins, Dr. Sabyasachy (Babu) Mistry, Dr. Cory Conder, Rachel Knieser and Evan Reeves for helping me out with their guidance and expertise with every problem I encountered in my research. I spent a very memorable time with Dr. Sabyasachy (Babu) Mistry where we both shared our love for soccer and spent countless hours talking about it. I also thank all my lab mates for enduring our talks and sometimes, even making efforts to participate in them.

There are several individuals who I'd like to thank for their mentoring, assistance, friendships and making the grind of graduate school a little easier for me. I would like to thank my roommates and life-long friends in particular, Dr. Swapnil Deshmukh, Dr. Abhijit Talpade, Dr. Piyush Mishra, Abhijit Anil and many others who have helped me get through the most difficult and depressing periods of my PhD life by being there for me and occasionally taking my mind of all the negative thoughts running in my head.

I'd also like to thank Dr. Low for letting me use his laboratory space and services for a project of mine and to his PhD and Post Doc students for helping me and training me on many of their different instruments and teaching me new skills. This experience eventually helped me land a job and pave the way for a career in the pharmaceutical industry. Also, a very special mention to Dr. Lakshmy Ravishankar from Vaze college, University of Mumbai and Dr. Anant Kapdi from Institute of Chemical Technology, Mumbai for encouraging me to pursue my dreams and helping

me to achieve them. I will forever remain grateful to Lakshmy ma'am for recognizing the capabilities in me when I wasn't focused on my career and then talking to my father about the same. That moment gave me immense confidence to completely shift my stance on my career and gave me a ginormous boost to compete for top quality education.

Also, thanks to Manchester United for giving me the 90 mins of respite every week when I cheered and clapped for you and the innumerable times when your failures overshadowed mine to ease off some of my pain. For the same reason, I also thank Roger Federer and the Indian cricket team. Finally, I also thank France A Cordova for the lovely recreational sports center where I spent uncountable number of evenings honing my badminton skills and dropping the shuttle cocks and the crucial few (very few) pounds.

There are a lot of other names I have missed out that would be impossible to list here, but you know who you are! **GGMU!!**

TABLE OF CONTENTS

LIST OF TABLES

LIST OF FIGURES

ABSTRACT

The first chapter reports a study of aryl nitrene intermediates. Although extensively studied over the past 30 years, phenyl nitrenes have a propensity to undergo rearrangement reactions and form polymeric tars. This is in stark contrast to the phenyl carbenes which are known to undergo several important reactions to produce a library of useful organic compounds. One such reaction is the insertion of phenyl carbenes into a double bond to produce a cyclopropane moiety. If aryl nitrenes can be exploited to conjure a similar reactivity, they would be an excellent synthetic route to produce aziridine rings which are a crucial component of many natural products. This review chapter is a collection of all the efforts that have been made in this regard.

In the next chapter, the electronic effect of the azide functional group on an aromatic system has been investigated by using Hammett-Taft parameters obtained from the effect of azide-substitution on the gas-phase acidity of phenol. Gas-phase acidities of 3- and 4-azidophenol have been measured by using mass spectrometry and the kinetic method and found to be 340.8 ± 2.2 and 340.3 ± 2.0 kcal/mol respectively. The relative electronic effects of the azide substituent on an aromatic system have been measured by using Hammett-Taft parameters. The σ_F and σ_R values are determined to be 0.38 and 0.02 respectively, consistent with predictions based on electronic structure calculations. The values of σ_F and σ_R demonstrate that azide acts an inductively withdrawing group but has negligible resonance contribution on the phenol. In contrast, acidity values calculated for substituted benzoic acids gives values of $\sigma_F = 0.69$ and $\sigma_R = -0.39$, indicating that the azide is a strong π donor, comparable to that of a hydroxyl group. The difference is explained as being the result of "chimeric" electronic behavior of the azide, similar to that observed previously for the n-oxide moiety, which can be more or less resonance donating depending on the electronic effects of other groups in the system.

Phenyl nitrenes undergo bimolecular chemistry under very specific circumstances. For example, having an oxide substituent at the para position of the phenyl ring enables the formation of an indophenol product from a photocatalyzed reaction of the nitrene. Although, this reaction has been reported before, the mechanism involved in this reaction has not been fully understood. A two-electron mechanism involving electrophilic aromatic substitution reaction has been proposed in the literature, however we found evidence that did not support this theory. Instead, we

find this reaction analogous to the popular Gibbs' reaction whose single electron transfer mechanism has been extensively studied. The following chapter encompasses a study of the mechanism of the photolysis reaction to look for evidence of a single electron transfer similar to the Gibbs' reaction.

As mentioned earlier, phenyl nitrenes have a proclivity to undergo rearrangement reactions instead of exhibiting bimolecular reactivity that can lead to useful products. One of the strategies to overcome this challenge is to spatially separate the two electrons of an open-shell singlet nitrene so as to minimize electron-electron repulsion. This separation can be achieved by delocalizing the individual electrons over multiple aromatic rings and heteroatoms which can act as radical stabilizers. In this chapter, a short review of literature that sets precedence for developing a unique heteroatom containing aromatic backbone to achieve the necessary stabilization is presented. Our efforts in synthesizing the model azide precursor compound have also been discussed.

CHAPTER 1. INTRODUCTION AND GUIDE TO DISSERTATION

1.1 Introduction and Guide to Dissertation

This dissertation is the collection of several different works, which encompass a variety of chemistry. The title of this dissertation is appropriately broad to ensure all the chemistry is included. In this thesis, I discuss the chemistry of nitrene intermediates and their precursor azides. Nitrenes are known to undergo undesirable reactions in the gas and solution phase. I have tried to address these limitations by studying their reactivity and the mechanisms involved in solutions and discussed strategies to find appropriate solutions. Not just the nitrenes, but their precursor azides are also a bit of an enigma themselves in terms of their electronic properties. These properties along with their implications on an aromatic system have also been studied.

Chapter 2 is a review of several different types of methods employed in the past to harness the reactivity of the phenyl nitrene intermediates. One of the primary focus of my PhD research was to utilize different substituent effects to tune the reactivity of the phenyl nitrenes, which would enable us to do exciting chemistry such as nitrene transfers into alkenes to form an aziridine ring. One such substitution that made possible this transformation was the use of oxide at the ortho position. This chapter is intended to provide an account of various such successful transformations attempted in the past which were the source of inspiration for our work.

Chapter 3 focuses on the chemistry of the most extensively used nitrene precursor in our lab, the azide. The azide is one of the most widely used reagent in click chemistry and a common precursor compound to the nitrene. However, the effects of an azide substituent on the aromatic ring is still a matter of debate due to the conflicting reports about the azide's electronic nature. In this chapter, we have used mass spectrometry as a tool to address this issue by calculating the Hammett-Taft parameters of the azide, which are derived from the gas-phase acidities of the azidophenols calculated by using the kinetic method. These Hammett-Taft parameters have been extensively studied and compared to that of the other common substituents in order to understand the effects of an azide substituent.

During the course of studying the reactivity of the nitrenes in the solution phase, we stumbled upon a unique photolysis reaction of azidophenoxides in water that produced an indophenol product, very similar to the well-known Gibbs reaction. Chapter 4 focuses on

understanding the mechanism of this unique reactivity. The Gibbs reaction is believed to proceed via single electron transfer processes. Herein, we explore all the evidence that suggests that the photolysis of the 4-azidophenoxide also proceeds via single electron transfer mechanisms, drawing parallels to the Gibbs reaction.

Chapter 5 discusses a different approach to tune the reactivity of the phenyl nitrene intermediate. The chapter discusses the background work done in this regard and our attempts to synthesize the appropriate precursor azide with the desired substitution and aromatic back bone rings that could unlock the potential to do exciting chemistry with the nitrene intermediate.

CHAPTER 2. FROM NITRENES TO AZIRIDINES – A REVIEW

2.1 Introduction

Aziridines are 3-membered cyclic amines, comprising of a highly strained ring system. This associated ring strain make these molecules extremely reactive. Despite of such a high reactivity, aziridine ring system is a very common framework in molecules of natural origin. Several aziridine ring containing compounds exhibit potential biological activities.[1]

In the earlier times, synthesis of aziridines was considered to be a challenging venture owing to their high instability and reactivity. However, the synthetic methods for aziridines have made tremendous progress since then where, a number of methods have been developed to synthesize not only racemic but also enantio-enriched aziridines. A deceptively straightforward strategy for the synthesis of aziridines would be direct coupling of a nitrene and an alkene. However, this strategy faces several limitations due to the highly unreactive nature of the nitrenes.

Nitrenes are a fascinating class of intermediates similar to carbenes but exhibit very different reactivity. For example, phenylcarbene in solution readily forms adducts with alkenes and inserts into C-H bonds, whereas phenylnitrene gives mostly polymeric tar. Our lab has previously attempted to understand this reactivity and proposed a solution to activate the bimolecular reactivity of these nitrene intermediates.[2–5] With anionic substitution on the phenyl rings of aromatic nitrenes, we were able to do useful reactions such as proton/hydrogen atom abstraction, Gibbs reaction and nitrene insertion into an alkene with the phenyl nitrene intermediate. This chapter aims at compiling the literature available for such successful conversions of nitrenes into aziridines.

2.1.1 Azides as nitrene precursors

Azides were identified as nitrene precursors much before asymmetric catalysis was discovered.[6–8] Smith and coworkers in 1951 first reported that the thermolysis or photolysis of biphenyl azides produce substituted carbazoles.[7] This result was further expanded to vinyl azides by Hemetsberger and to styryl azides by Sundberg.[9] These thermal and photochemical reactions were identified to proceed through the nitrene intermediates thus, demonstrating the potential of azides to form nitrenes. While these reactions did produce useful N-heterocycles, they were very

limited in scope due to the hyper reactivity of the nitrene intermediate and the harsh conditions required for the conversions. This extreme reactivity of the nitrenes resulted in decomposition of the products and/or poor selectivity. This reactivity could be brought under control by using transition metal catalysts to form the metal nitrenoid intermediates, in turn also normalizing the conditions needed for the reactions.

The use of azides as nitrene precursors in transition metal-catalyzed nitrene transfers have garnered considerably less attention than the other nitrene precursors. The appeal of the azides is mainly because (1) they can be made available easily through sodium azide, (2) their byproduct is only nitrogen gas and (3) they don't require any additives besides the metal catalysts. Thus, development of transition metal-catalyzed. mild and low temperature reactions gained interests in order to utilize the potential of azides to generate important N-heterocycles via nitrenes.

2.1.1.1 Transition metal-catalyzed nitrene aziridinations using azide precursors

Kwart and Khan, in 1967, reported the first metal-catalyzed nitrene transfer from an azide to an olefin (Figure 2.1a).[10] It was reported that benzenesulfonyl azide readily decomposes to its corresponding nitrene in cylcohexene in the presence of copper powder. In addition to the cyclohexene-aziridine product, C-H amination of cyclohexene and benzenesulfonamide products were also observed. This product distribution was consistent with the formation of a nitrene or a nitrenoid intermediate.[11] A radical mechanism was also proposed that accounted for the formation of the observed products.[12] Soon after, exploration of other metals for such type of transfer reactions led Migita and co-workers to develop palladium catalyzed N-atom transfer reactions to olefins (Figure 2.1 b).[13–15]

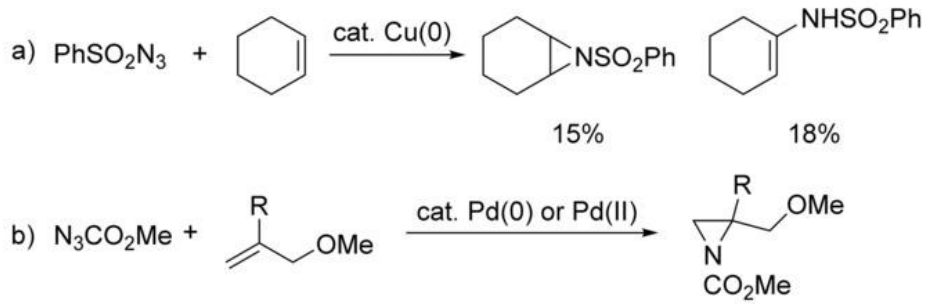

Figure 2.1 Earlier reports of transition-metal-catalyzed nitrogen-transfer reactions of azides to form aziridines

Around the same time, model systems were developed that mimicked catalysis by cytochrome P-450, in which oxygen-atom transfer from idosylbenzene to model organic acceptors was enabled in the presence of metal tetraphenylporphyrins.[16–18] On the basis of these findings Groves and co-workers reported a stoichiometric nitrene-transfer from a nitridomanganese(V) porphyrin to cycloalkenes.[19]

The early work by Migita[13–15] on the stoichiometric transfer of N-atom from azides to olefins by using transition metal and the use of metal porphyrins by Che et al[20] encouraged Cenini and co-workers to further explore metal porphyrins catalysts in the reaction of aryl azides with olefins (Figure 2.2).[21]

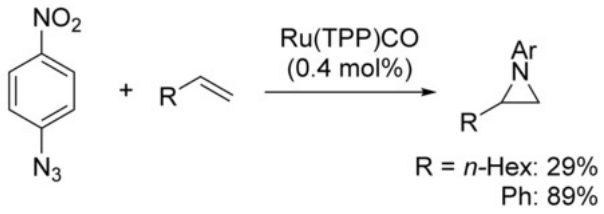

Figure 2.2 Cenini's report of transition-metal-catalyzed nitrogen-transfer reaction of 4-nitrophenyl azide to form aziridine

After examination of a wide range of metal-based porphyrins, Cenini reported that only cobalt and ruthenium-based complexes seemed to catalyze the nitrene transfer from 4-nitrphenylazide to cycloalkenes. Specifically, ruthenium tetraphenylporphyrin (RuTPPCO) and cobalt octaethylporphyrin (CoOEP) provided the best results for the conversion.[22] However, when the nitro substituent was replaced by a methoxy group, only the corresponding aniline was obtained as the by-product, which indicated that the electronic nature of the aryl nitrene seemed to influence the product distribution in the reactions.

The most reactive RuTPPCO complex was then used to carry out nitrene transfers to different types of olefins to yield various aziridine products accompanied by the corresponding side-products (Figure2.3).[21]

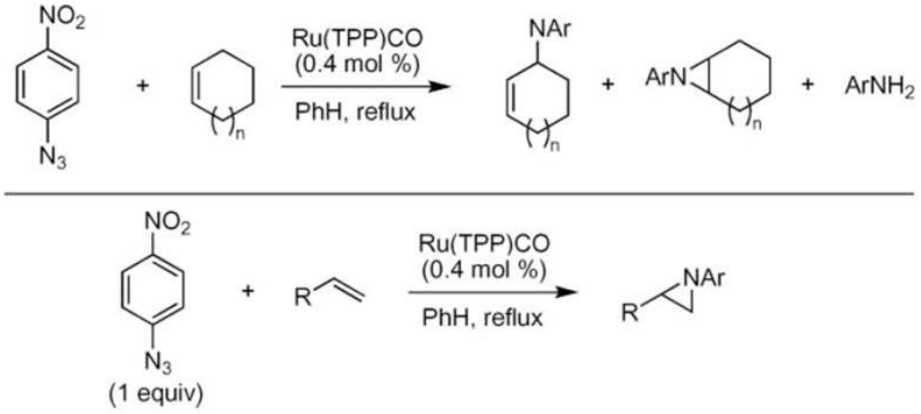

Figure 2.3. Cenini's work on ruthenium porphyrin-catalyzed various aziridine formations from aryl azides

Asymmetric aziridinations using azides

Among the influx of the earlier reports on metal-catalyzed nitrene-transfer reactions, few of the substantial results were reported individually by Jacobson and Muller where they carried out asymmetric aziridinations of styrene, with enantiomeric excess values of 41% and 17% respectively (Figure 2.4 a and b).[23–25]

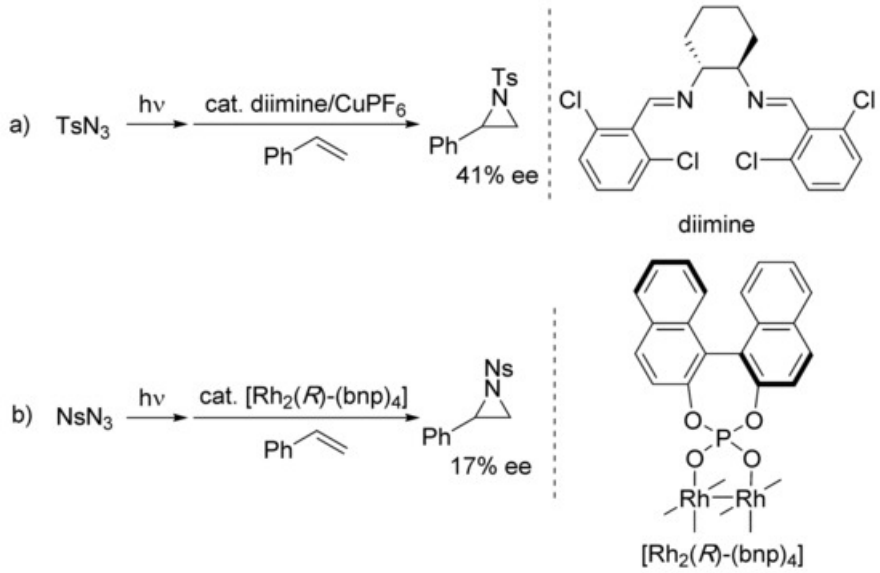

Figure 2.4 a) Jacobson and b) Muller groups' asymmetric aziridination of styrene. Ts=tosyl, Ns=nosyl

Following this seminal work on asymmetric aziridination, further developments in the field were independently achieved by Katsuki and Zhang groups. Katsuki group reported that a chiral ruthenium(II) salen complex can be used to catalyze the formation of aziridines from sulfonyl azides asymmetrically (Figure 2.5).[26]

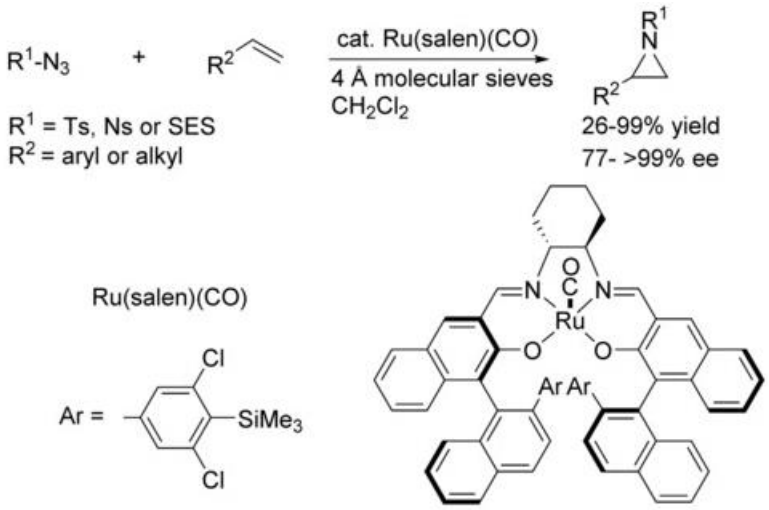

Figure 2.5 Katsuki's work on ruthenium(II) salen catalyzed asymmetric aziridination of olefins.

This complex had been reported previously to catalyze the formation of iminosulfides with large turnover numbers and high enantioselectivities. Katsuki and coworkers realized that, since the mechanism for the formation of iminosulfides involved N-atom transfer the same protocol can also be applied to the formation of aziridines from nucleophilic alkenes. Moreover, they were also able to show that a variety of azides such as NsN_3, SES-N_3, $(PhO)_2P(O)N_3$, and 2,2,2-trichloroethoxysulfonyl azide ($TcesN_3$), besides TsN_3 can also be used in this protocol as nitrene precursors.

One of the main side reactions arising from the above protocol was the allylic C–H bond amination. In order to suppress this side reaction, Katsuki and co-workers designed a new ruthenium(II) salen complex (Figure 2.6).[27]

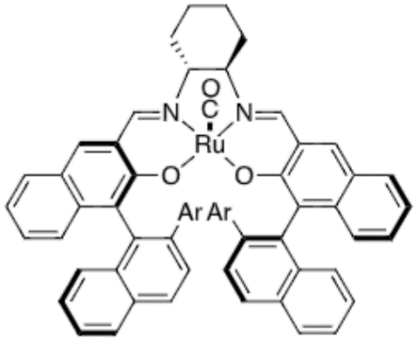

Figure 2.6 Katsuki's new ruthenium(II) salen catalyst for asymmetric aziridination of olefins.

The new catalyst was structurally different than the previous version, where meta-hydrogens on the phenyl groups were replaced by fluorine atoms which would prevent the decomposition of the catalyst due to the nitrenes, making it more robust.

One common drawback of these aziridination protocols was, high reaction rates were only achieved by using *para*-tolylsulfonyl azide and it took relatively harsher conditions like NaNp, DME[27] to remove the group from the aziridine product. However, the newly designed robust catalyst enabled the use of other azides with more easily removable groups.[28,29] 2-(trimethylsilyl)ethanesulfonyl azide ($SESN_3$) and nitrobenzenesulfonyl azide (NsN_3) were examined as nitrene precursors as both the groups could be removed under mild conditions. Both the compounds proved to be efficient sources of nitrenes, although, $SESN_3$ also provided enhanced enantioselectivities. On the other hand, NsN_3 provided improved turn over numbers (TON) (Figure 2.7).

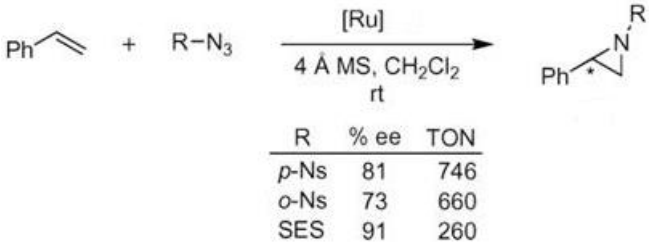

R	% ee	TON
p-Ns	81	746
o-Ns	73	660
SES	91	260

Figure 2.7 Use of new ruthenium(II) salen catalyst for asymmetric aziridination of olefins.

The robust and reactive catalyst also enabled aziridination of non-conjugated olefins as shown in figure 2.8.

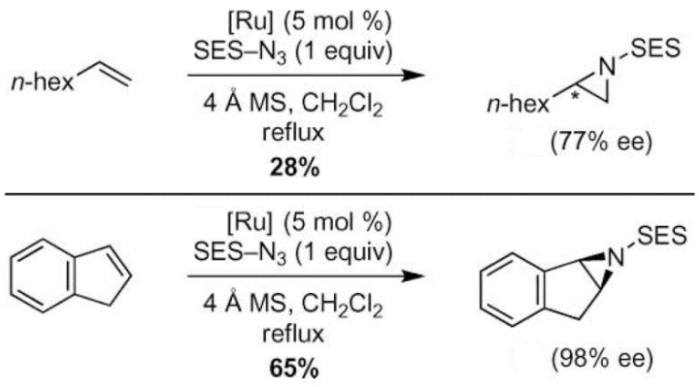

Figure 2.8 Increased substrate scope with ruthenium(II) salen catalyst for asymmetric aziridination of non-conjugated olefins.

Similarly, alkyl substituted alkenes were converted into the corresponding aziridines albeit at higher temperatures (Figure 2.9).

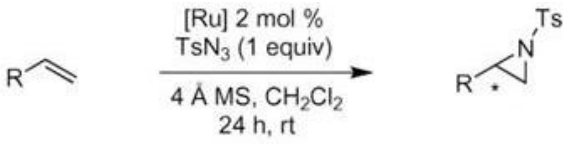

R	%, yield	% ee
C_6H_5	71	87
p-$O_2NC_6H_4$	98	92
$C_6H_5C{\equiv}C$	85	95
2-$C_{10}H_7$	86	87

Figure 2.9 Increased substrate scope with ruthenium(II) salen catalyst for asymmetric aziridination of alkyl substituted alkenes.

Similar to the Katsuki group, the Zhang group also worked on developing protocols to synthesize chiral aziridines containing easily removable groups on the aziridine nitrogen. They developed several aziridination methods that employed the azide based nitrene precursors, diphenylphosphoryl- or nosyl azide.

Diphenylphosphoryl azide was selected as the appropriate nitrene precursor because the phosphorus-nitrogen bond in the aziridine product can be easily hydrolyzed.[30–32] A D2-symmetric chiral porphyrin was developed as the ligand for cobalt catalyst through which high chemical yields with low catalyst loading were obtained (Figure 2.10).[31]

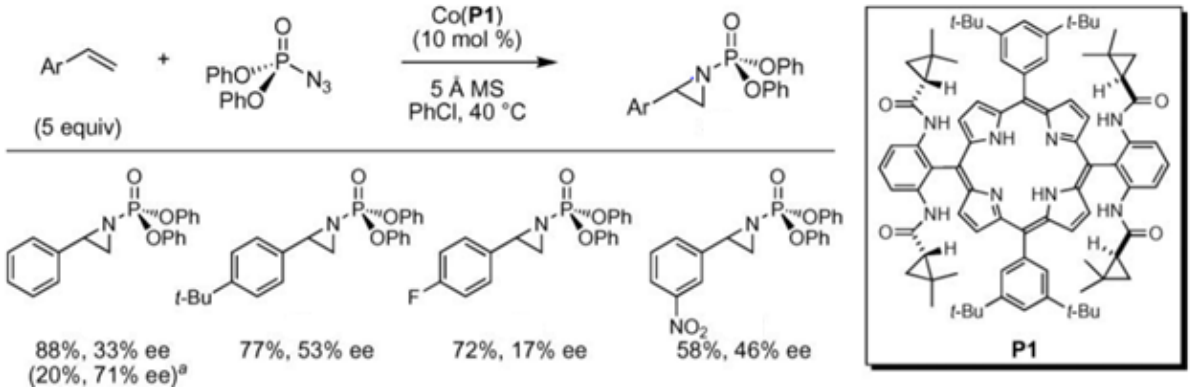

Figure 2.10 Cobalt-catalyzed asymmetric aziridination of styrenes using phosphoryl azide precursor. [a]20 mol% DMAP added

The structural specialty of the ligand lies in its chiral, non-racemic cyclopropyl-substituted amide side chains, which prevent the decomposition of the cobalt amido complex during the reaction. The ligand can be easily synthesized by a palladium-catalyzed quadruple amidation of tetrabromo-substituted porphyrin.[33] Although, the aziridination reaction using diphenylphosphoryl azide as the nitrene source provided only moderate control on the enantioselectivity, it did set precedence for future method development.

When the nitrene source was changed from diphenylphosphoryl to sulfonyl, broader substrate scope and increased product yields were obtained.[34] For this transformation, a non-chiral tetraamide porphyrin P2 was used as the ligand with the cobalt catalyst. The new cobalt P2 porphyrin complex afforded the aziridine products with a high efficiency and a large variety of substituted styrenes (Figure 2.11)

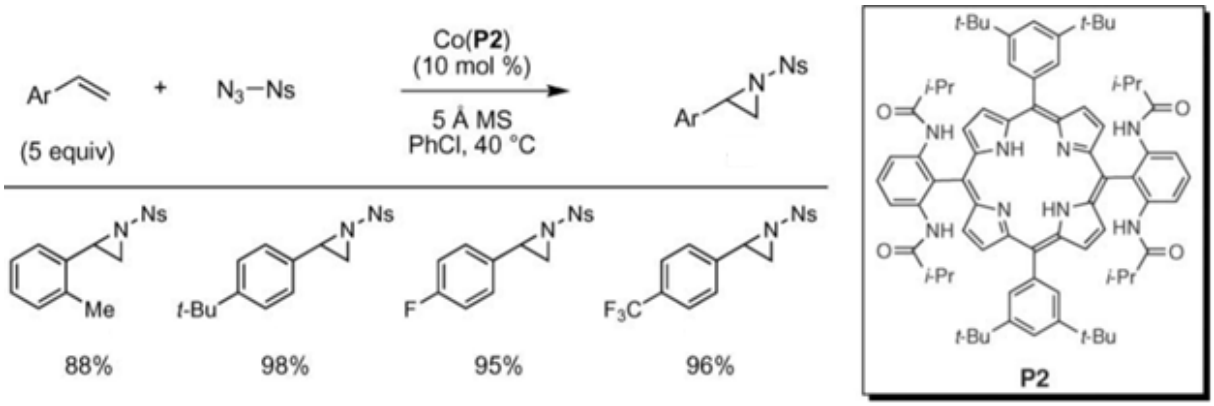

Figure 2.11 Cobalt-catalyzed azirdination of various styrenes using nosyl azide as the nitrene precursor

It was observed that the reaction remained unaffected by the steric or electronic nature of the styrenes and tolerated substrates that contained any kind of ortho-substitution or strong electron-withdrawing groups. Although use of nosyl azide allowed increased substrate scope for the aziridination, the system still remained intolerant to disubstituted or aliphatic styrenes

The cobalt P2 porphyrin complex was designed such that the amide N-H bond was placed closer to the SO_2 group on the nitrene to form a hydrogen bond which would allow for a greater nucleophilicity and impart better stability to the metal nitrenoid intermediate. Computational modelling of the complex calculated the N-H-O bond distance to be only 2.9 Å which would indicate a presence of significant hydrogen bonding between the amide and the nitrenoid. This hydrogen-bonding model thus accounted for the increased reactivity of the aziridination reaction with phosphoryl azide (Figure 2.12).

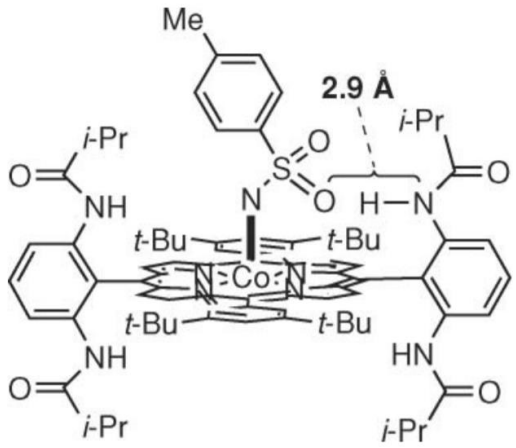

Figure 2.12 Hydrogen-bonding model of the cobalt P2 porphyrin complex

The Zhang group also used the new cobalt P2 porphyrin complex in aziridination reactions using trichloroethoxysulfonyl (TCES) azide as the nitrene precursor (Figure 2.13).[35]

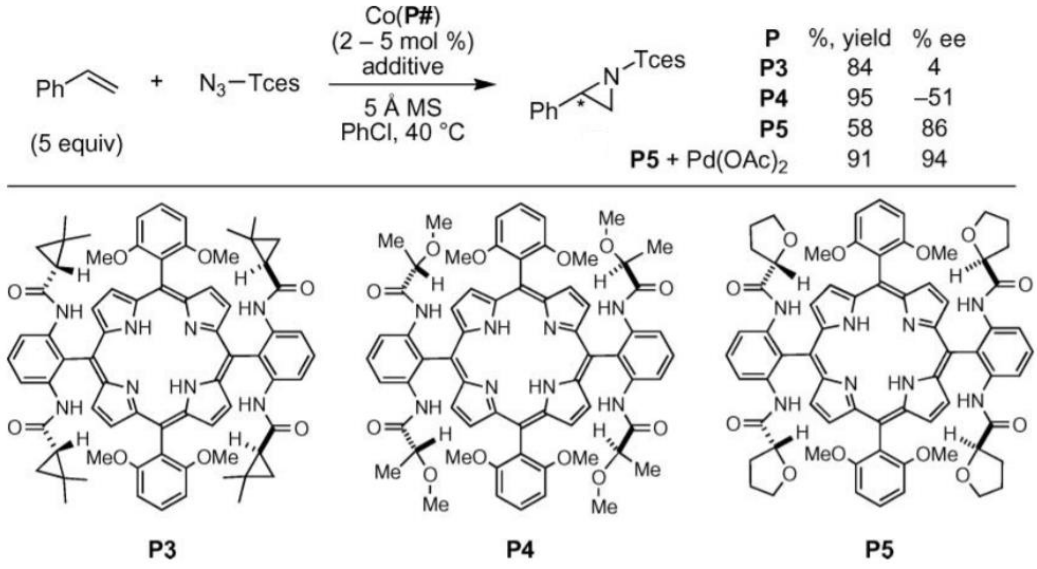

Figure 2.13 Aziridination using trichloroethoxysulfonyl (TCES) azide and various modified porphyrin ligands

The trichloroethoxysulfonyl azide served as a very promising nitrene source for chiral aziridinations owing to the ease of removal of the group from the nitrogen of the aziridine. The porphyrin ligand was further optimized to the porphyrin P5 that resulted in higher enantioselectivities and aziridine yields. Although the other D2-symmetric porphyrins afforded higher yields of the aziridine products porphyrin P5 afforded the highest enantioselectivities. However, this was overcome by the use of palladium acetate additive which was found to improve the yields of the products without affecting their enantioselectivities.

These new model systems enabled aziridination of several different types of alkenes with high enantioselectivities and product yields. Studying the substrate scope of a variety of styrenes revealed that the electronic nature of the styrenes resulted in no difference in the yield and enantioselectivities of the aziridine products. Even dienes and non-conjugated alkenes offered improved yields and enantioselectivities (Figure 2.14).

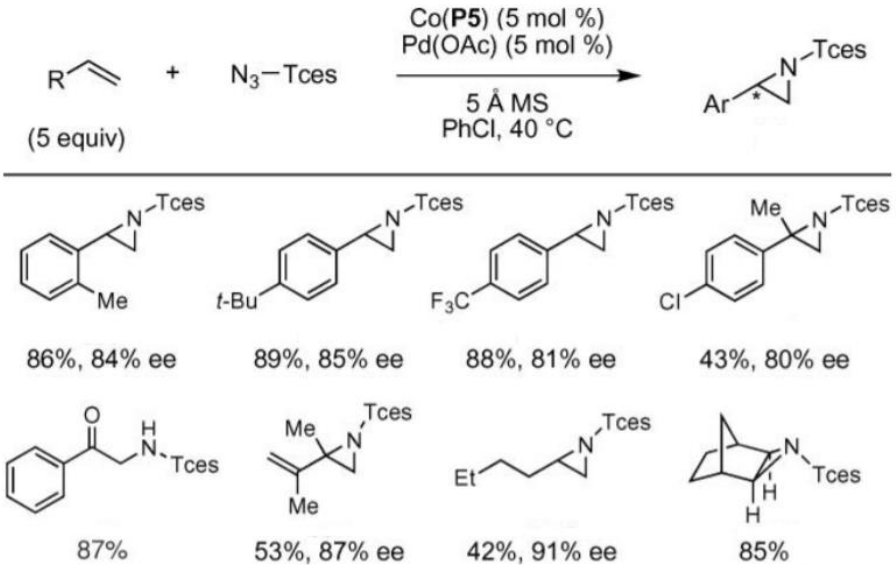

Figure 2.14 Substrate scope of cobalt-catalyzed aziridination of olefins using Tces–Azide and $PdOAc_2$ (5 mol%)

Thus, Zhang group was the first to show that aziridination of olefins can be achieved without any competing side-reactions such as C-H bond amination of the olefins or nitrene dimerization.

2.1.1.2 Transition metal-catalyzed alkene aziridinations using imidoiodinane precursors

Similar to the oxygen transfer reactions reported by Groves et al, the analogous nitrene transfer also became a possibility. Around the same time, sulfonyliminoiodinanes became available as the required nitrene precursors.[36,37] These compounds were found to be excellent sources for nitrenes with some seminal reports also suggesting that iminoiodinanes (PhI=NTs) were more efficient nitrene precursors than the azides in metal-catalyzed N-atom transfer reactions to olefins.[25,38–41] For example, Breslow and Gellman reported highly efficient inter- and intra-molecular nitrene insertions into C-H by using PhI=NTs as the nitrene precursors, catalyzed by $[Rh_2(OAc)_4]$[42] or Mn(III)- or Fe(III)-porphyrins.[43] Similarly, Jacobsen and his coworkers reported similar observations during their work on copper diimine-catalyzed aziridination of olefins.[25] Effective aziridination of olefins using PhI=NTs in the presence of Fe- or Mn-porphyrins was also reported by Gr and co-workers.[41,44,45] In these early reports, the control on the chemoselectivity between the aziridination and allylic amination was quite difficult (Figure 2.15).

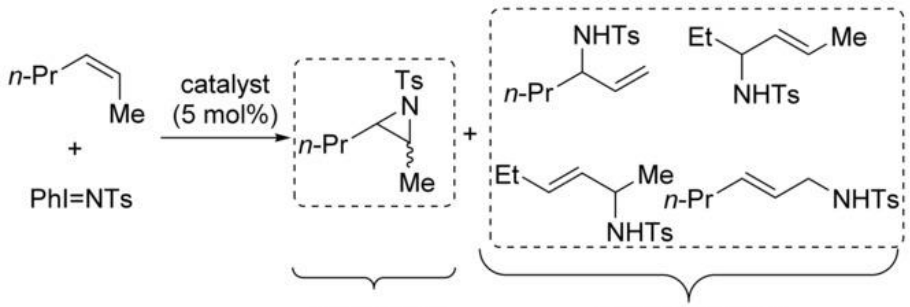

catalyst	yields (%)	
	aziridination	allylic amination
$Fe(TPP)(ClO_4)$	12	20
$Fe(TDCPP)(ClO_4)$	35	13
$Mn(TPP)(ClO_4)$	<2	37
$Mn(TDCPP)(ClO_4)$	11	26

TPP = tetraphenylporphyrine. TDCPP = 5,10,15,20-Tetrakis(2,6-dichlorophenyl)porphyrin

Figure 2.15 Fe– and Mn– based porphyrin-catalyzed reaction of *cis*-hex-2-ene with PhI=NTs

Evans and coworkers, in 1990s, substantially developed the chemistry of aziridination by using iminoiodinanes as the precursors. They reported that Cu^{I} species such as $[Cu(MeCN)_4]ClO_4$, $Cu(acac)_2$ (acac=acetylacetonate), and Cu^{II} species such as copper(II) trifluoromethanesulfonate $[Cu(OTf)_2]$ can be used to catalyze the aziridination of olefins effectively without generating allylic amination side products. Moreover, they also found that phenyl aziridine was produced in 96% yield when using iminoiodinane as the nitrene precursor whereas phenyl aziridine was only produced in 12% yield when using the tosyl azide nitrene precursor (Figure 2.16).[149,40]

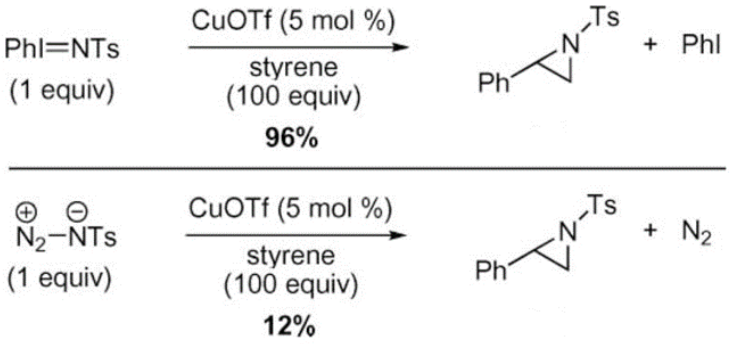

Figure 2.16 Comparison of the efficiency of aziridine formation using iminoiodinane and tosyl azide nitrene precursors

Although these findings lacked much practical applicability, they set precedence for designing efficient systems for catalytic nitrene transfers using iminoiodinanes.

In 1993, Perez and his coworkers reported the synthesis and application of copper-based catalyst [Tp*Cu(C_2H_4)] [Tp*=tris(3,5-dimethyl-1-pyrazolyl)borate] for aziridination of alkene with PhI=NTs. (Figure 2.17)

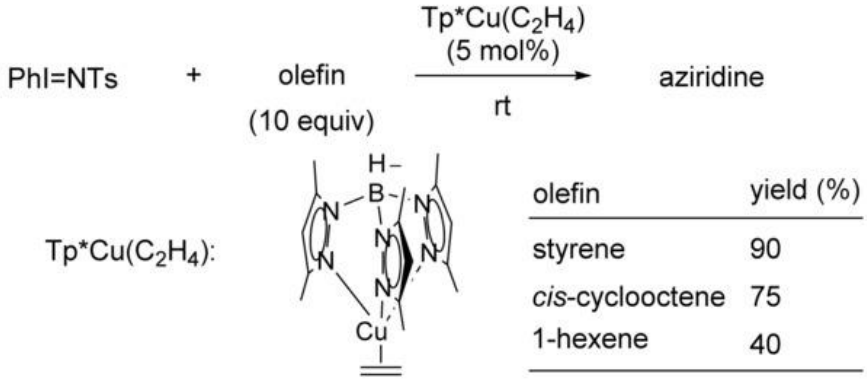

Figure 2.17 Perez's work on Tp*Cu(C_2H_4) catalyzed nitrene-transfer reaction of 4-nitrophenyl azide to form aziridine

Taking inspiration from these works, many different kinds of copper catalysts paired with nitrene-based ligands were reported by Halfen, Caulton and Warren.[47–50] Müller explored other metal complexes such as dirhodium (II,II) $Rh_2(OAc)_4$ as catalyst for aziridination of several aromatic olefins using *p*-nitrobenzenesulfonyl)iminophenyliodinane (PhI=NNs) as the nitrene precursor. This afforded the corresponding aziridines in yields of upto 85% (Figure 2.18).[51–53]

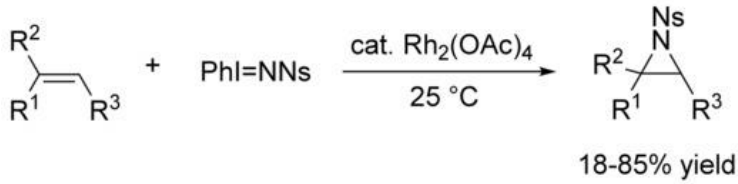

Figure 2.18 Aziridination of olefins using PhI=NNs catalyzed by $Rh_2(OAc)_4$

Similar studies were performed by Che and his co-workers where they used bis(tosyl)imidoruthenium–porphyrin complexes such as $Ru(TPP)(NTs)_2$ to carry out stoichiometric nitrene/imido group transfer reactions.[20] Inspired by the work of Breslow and Gellman,[42,43] Müller also reported selective amination of cyclohexene with PhI=NNs using $Rh_2(OAc)_4$ as catalyst in which the aziridination reactions were completely suppressed. These reactions were also accompanied by C-H insertions into the benzylic and ethereal carbons with good yields (Figure 2.19).

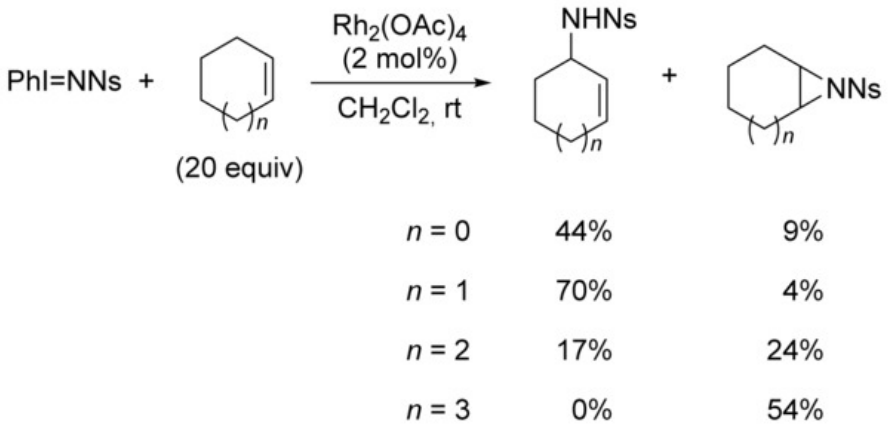

Figure 2.19 Complete suppression of aziridination during selective amination of cyclohexene using PhI=NNs, catalyzed by $Rh_2(OAc)_4$

Although, significant chemistry for aziridination using iminoiodinanes as precursors has been developed, it suffers from setbacks such as short lifetime and explosive potential of the iminoiodinanes which limit their applications in large scale synthesis. To overcome these limitations, various carbamates and sulfonamides were developed as nitrene precursors along with hypervalent iodine(III) oxidants like $PhI(OAc)_2$ or PhI=O. Using there reagents highly efficient nitrene transfer reactions were reported by Che, Du Bois, and Dauban and Dodd such as C-H bond

insertions to yield different products.[54–56] For aziridination, Duban et al reported copper catalyzed intermolecular aziridination of various olefins using different sulfonamides in the presence of PhI=O as oxidants (Figure 2.20).[26]

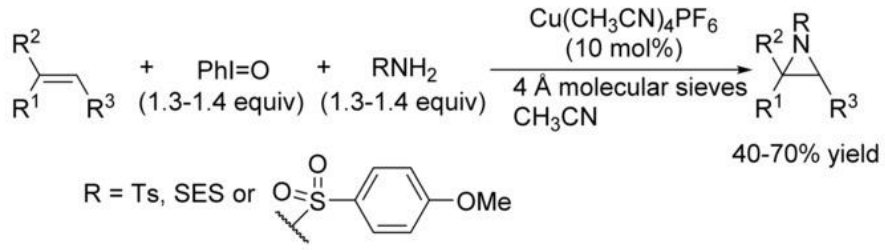

Figure 2.20 Sulfonamides as nitrene precursors in the presence of PhI=O for aziridination of olefins.

Although these Iodine (III) reagents greatly improved the efficiency of N-atom transfer to olefins, they were not as green and atom economical as the azides because they produced a stoichiometric amount of iodobenzene as well.

Asymmetric aziridinations using imidoiodinanes

Copper catalyzed aziridinations

As mentioned earlier, the Evan's group had reported the nitrene transfer reactions to olefins using TsN=IPh and turned them into synthetically useful protocols.[40] The aziridination of various types of olefins was achieved in moderate to excellent yields. Complete stereospecificity was only observed for oct-4-ene, however partial stereospecificity was also observed for β-methyl styrene and *trans*-stilbene. The stereospecificity was found to be dependent on the ligands and the counter-ions associated with the metal. Eventually, Evans also reported enantioselectivity in the aziridinations by using bis(oxazoline)ligands such as the one shown below (Figure 2.21).[46]

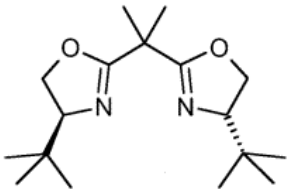

Figure 2.21 Example of a bis(oxazoline)ligand used by Evans to achieve enantioselectivity.

The reactions needed 5% of CuOTf and 6% of ligands and were completed after 24 hrs. Cinnamate esters proved to be the best substrates for the protocols producing aziridines with enantioselectivities of 94-97% and yields of 60-63% in benzene. However, the more simple substrates such as styrenes and methylstyrenes were less suited and provided enantioselectivities of only 63% and 70% respectively (Table 2.1)

Table 2.1. Bis(oxazoline)catalyzed enantioselective aziridinations of olefins

olefin	**solvent, conditions**	**yield, %**	**ee, %**	**conf.**
methyl cinnamate	C_6H_6 (24 h, 21 °C)	63	94	(*S*)
phenyl cinnamate	C_6H_6 (24 h, 21 °C)	64	97	(*S*)
t-butyl cinnamate	C_6H_6 (24 h, 21 °C)	60	96	(*S*)
trans-β-methylstyrene	MeCN (3 d, −20 °C)	62	70	(*S*)
styrene	styrene (2.5 h, 0°C)	89	63	(*R*)

This work encouraged Ghosh to develop several bis(oxazoline) analogues which were used for aziridination of styrenes.[57] One of the seminal works in the aziridination of styrenes was carried out by Masamune who reported enantioselectivities of 88% and yields of 91% using camphor-derived bis(oxazoline) ligand (Figure 2.22).[58]

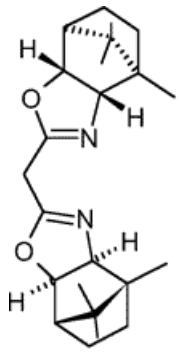

Figure 2.22 Camphor-derived bis(oxazoline) ligands for aziridination of styrenes

Only marginal enantioselectivities for aziridinations of styrene and conjugated dienes were achieved by using tartarate-derived bis(oxazoline)ligands (Figure 2.23).[59]

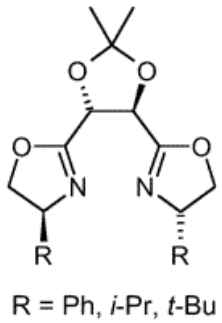

Figure 2.23 tartarate-derived bis(oxazoline) ligands for aziridinations of styrenes and conjugated dienes

Following these reports, several other groups attempted to improve the aziridination systems. Andersson group proposed using NsN=IPh (*p*-nitrophenylsulfonyl iminoiodinane) as the precursor for nitrenes instead of TsN=IPh. The group reported comparable enantioselectivities as that achieved by using the same bis(oxazoline)ligands as used by Evans and coworkers.[60] Moreover, Andersson also reported upto 34% enantioselectivities using anionic di-imine ligands (Figure 2.24 a) and 33% enantioselectivities using the bis(aziridine) ligands (Figure 2.24 b) for the same reaction.

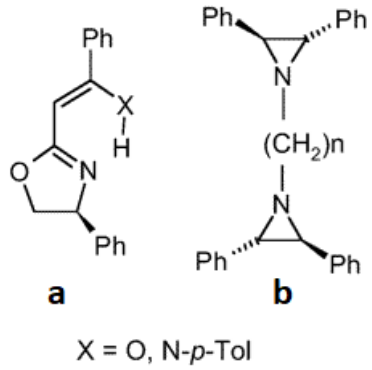

Figure 2.24 a) Anionic di-imine ligands b) chiral bis(aziridine) ligands for aziridination of styrenes

As mentioned earlier, the extent of enantioselectivities in these protocols were observed to vary with the counterions associated with the metal. Thus, Llewellyn et al investigated the effects of counterions used in the aziridination of styrene with bis(oxazoline)- copper catalysts. The idea was to perform asymmetric aziridinations by associating copper ions with a chiral counterion via ion pairing. This was done by using chiral boronate containing binaphthol ligands as counterions to the copper ions. The resulting aziridination reactions however, only showed about 7% enantioselectivity (Figure 2.25)

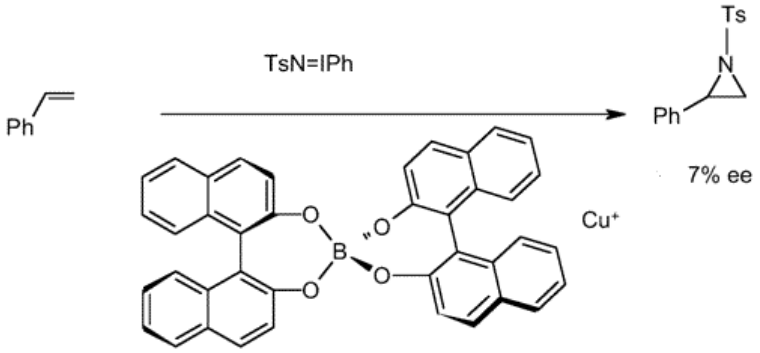

Figure 2.25 Chiral boronate containing binaphthol ligands as counterions to copper ions for asymmetric aziridination

Around the same time, Hutchings and his coworkers developed a copper exchange zeolite (CuHY) which they reported to be a highly efficient heterogenous catalyst for the aziridination of olefins.[61–64] This zeolite was modified with the bis(oxazoline)ligands such as in Figure 2.22. and used in the aziridination of styrenes which led to enhanced enantioselectivities. The highest yields

of the aziridine products were obtained when the nitrene source was switched from TsN=IPh to NsN=IPh, which was used in a slight excess over the styrene. The enantioselectivity was observed to be as high as 95% with 77% yield using TsN=IPh and 80% with 99% yield using NsN=IPh. These were the first few reports which showed that heterogenous catalysts were capable of inducing higher enantioselectivities than the homogenous catalysts.[65] Although the details of the system are not yet been fully understood, EPR studies showed direct evidences for a copper(II)−bis(oxazoline) complex inside the Y zeolite pores.[65] Although, leaching of Cu from the pores of the zeolite does happen, it is very limited. Moreover, it has also been shown that the leached Cu does not interfere with the aziridination process.[65] Thus, this system offers an advantage where the catalyst can be recovered at the end of the reaction.

Similar to the bis(oxazoline) ligands, aziridination using chiral diimine based-catalysts was also studied thoroughly. The Jacobsen group developed many chiral 1,2-diimine derivatives[25] in the presence of different Cu(II) salts and carried out many asymmetric aziridinations of olefins carrying atleast one aromatic substituent, with high enantioselectivities.[66] It was noticed that the number of co-ordination sites on the copper played a very crucial part in the catalyst design. Best results were obtained with two co-ordination sites on the copper instead of four. The best ligand of choice was the bis(imine) derived from 2,6-dichlorobenzaldehyde and 1,2-diaminocyclohexane (Figure 2.26).

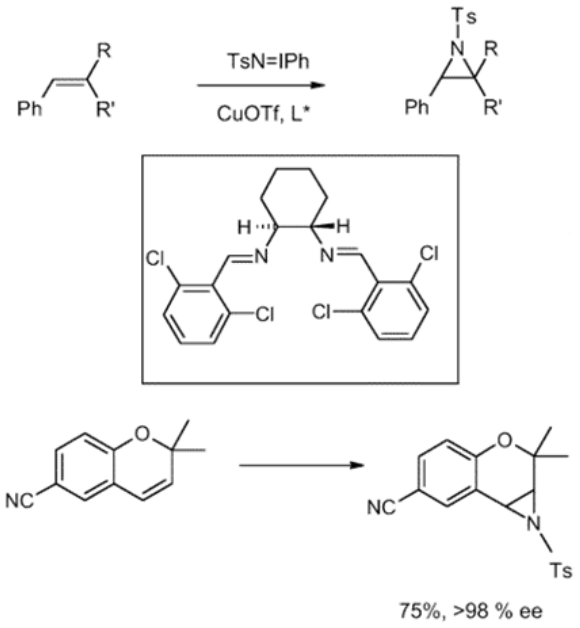

Figure 2.26 Aziridination of olefins with atleast one aromatic group catalyzed by bis(imine) complex (in the box)

The Jacobsen protocol afforded high enantioselectivities with the *cis*-olefins whereas the Evans protocol was more suited for the trans-isomers. The best result using the Jacobsen protocol was seen with 6-cyano-2,2-dimethylchromene which afforded the corresponding aziridine with enantioselectivity of more than 98% (Table 2.2). However, the simpler olefins resulted in only low to moderate enantioselectivities. For example, styrene reacted with only 66% enantioselectivity. Furthermore, the Jacobsen protocol required a high amount of catalyst loading of 5-10 mol% resulting in poor turnovers.

Table 2.2. Cu catalyzed aziridination of olefins using Jacobsen's ligand (Figure 2.26)

olefin	**aziridine, yield, %**	**ee, %**	**abs. conf.**
styrene	79	66	(*R*)
cis-β-methylstyrene	79 (*c*/*t* = 3:1)	67 (cis)	(1*R*,2*S*)
		81 (trans)	(1*S*,2*S*)
1,2-dihydronaphthalene	70	87	(1*R*,2*S*)

Table 2.2. continued

Indene	50	58	(1*R*,2*S*)
6-cyano-2,2-dimethylchromene	75	>98	(3*R*,4*R*)

Further developments in the Jacobsen's approach where brought about by Kim and his co-workers where, they used C2-symmetric bis(ferrocenyldiamines) (Figure 2.27) as ligands and observed moderate yields and enantioselectivities even with simple olefins like hexenes and styrenes.[67–69]

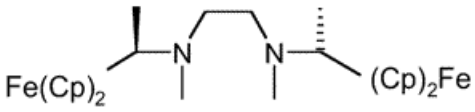

Figure 2.27 C2-symmetric bis(ferrocenyldiamines) as ligands for aziridinations of olefins

However, these reactions still required 10 mol% of catalyst loading along with a ten-fold excess of olefin. On a similar note, a chiral salen-type ligand derived from binaphthyldiimine (Figure 2.28) was also tested with styrene and showed unsatisfactory results, although indene and cinnamate esters seemed to react more effectively with the same ligand.[70]

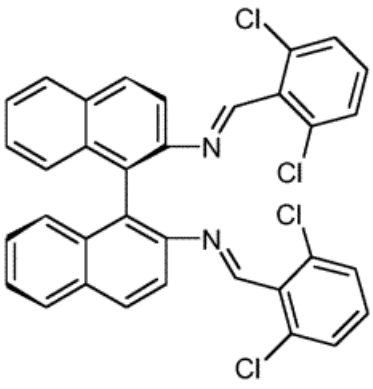

Figure 2.28 Chiral salen-type binaphthyldiimine ligands for aziridination of olefins

Meanwhile, Cu-catalyzed asymmetric aziridinations using TsN=IPh in the presence of chiral (bis)imine and bis(oxazoline)ligands were being explored further and enantioselectivities of

upto 52% were achieved with cyclic and acyclic enol derivatives.[71] Around the same time, the Scott group developed monomeric copper complexes with biaryl Schiff bases as ligands (Figure 2.29) which catalyzed aziridinations with TsN=IPh.[72]

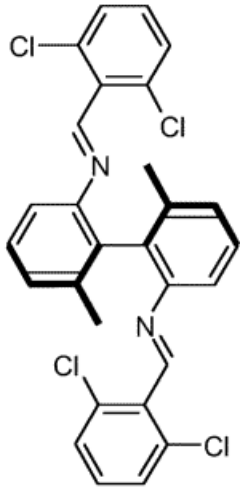

Figure 2.29 Biaryl Schiff bases as ligands for aziridination of olefins

This system worked the best for cinammate esters affording 88-98% enantioselectivities. The catalysts also gave upto 99% enantioselectivity in the aziridination reaction of 6-acyl-2,2-dimethylchromene. The enantiomeric excess of the product was found to have linear relationship with the enantiomericexcess of the ligand and the %conversion seemed to have no significant effects on the enantiomeric excess of the products as well. These results were consistent with a catalyst whose nature does not change during the course of the reaction and consists of only one ligand attached to it. However, styrenes and other simpler alkenes did not offer good selectivities as the absence of polar substitutents resulted in no secondary binding interactions. (Table 2.3) The reactions were completed in minutes in DCM and acetonitrile solvents at room temperature.

Table 2.3. Cu catalyzed aziridination of olefins using the biaryl Schiff's bases as ligand (Fig 2.29)

olefin (1)	***T***	**aziridine (2) yield, %**	**ee, %**	**abs. conf.**
t-butyl cinnamate	−40 °C	77	89	(2*S*,3*R*) (−)
t-butyl *p*-bromocinnamate	r.t.	45	96	(−)
t-butyl *p*-bromocinnamate	−40 °C	59	98	(−)
trans-β-methylstyrene	−40 °C	88 (*t*/*c* = 97:3)	28 (trans)	(2*R*,3*R*)
styrene	r.t.	91	27	n.i.
trans-stilbene	−40 °C	66	5.1	n.i.
1,2-dihydronaphthalene	r.t.	60	54	(2*S*,3*R*)
6-acylchromene	−40 °C	87	99	n.i.

Thus, Scott's system turned out to be highly superior to the other Cu-catalyzed aziridinations reported before due to the enhanced reactivities and selectivities.

Due to the extensive studies conducted on the Cu-catalyzed aziridinations, it becomes imperative to explore the mechanistic aspects of the reaction. The main factors that need to be considered for the aziridinations are formation of the Cu-nitrene intermediate, nature of the nitrene transfer, and the oxidation states of the metal. The experimental evidences for the formation of metal-nitrene intermediate has been provided by the Jacobsen group.[23] They found that the enantioselectivities of the aziridination reactions of several olefins using the copper (bis)imine catalysts were independent of the substitutions on iodobenzene which implies that iodobenzene plays no part in nitrene transfers. This indicates that PhI does not play a part via Lewis acid mechanism in the selectivity determination step. Moreover, the tosyl nitrenes generated from the TsN_3 produced similar enantioselectivities as the nitrenes generated from TsN=IPh. The DFT calculations for the Jacobsen system model carried out by Andersson and Norrby groups, revealed

the presence of a Cu-bound sulfonyl nitrene (Figure 2.3) intermediate along with a co-ordination of the oxygens on the sulfonyl group with the metal.[73]

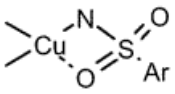

Figure 2.30 Structure of the nitrene intermediate in the Jacobsen system as predicted by DFT calculations

On the other hand, DFT calculations of the Scott system revealed the structure of the metal nitrene intermediate in which there was no such metal-oxygen interaction but instead, an interaction between the sulfonyl oxygens with the nitrene (Figure 2.31)

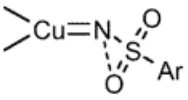

Figure 2.31 Structure of the nitrene intermediate in the Scott system as predicted by DFT calculations

It has now been well accepted that the aziridination reactions proceed via metal-nitrene intermediate. Kinetic investigations of the Jacobsen model revealed that the reaction was first order with respect to the olefin and catalyst concentration and thus second order overall. This was consistent with the rate-determining attack of metallonitrene on the olefins.[23] However, further studies conducted by Andersson and Norrby revealed that the reaction was zero-order for olefins despite the fact that single-experiments appeared to obey first-order kinetics.[73] Thus, the DFT calculations were found to be in agreement with the rate-determining step of formation of metallonitrene.

Since the bis(oxazoline) catalyst used by Evans and derived from Cu(I) and Cu(II) also produced the same extent of enantioselectivity, it was suggested that TsN=IPh oxidizes Cu(I) to Cu(II) and it is this Cu(II) species that exists in the catalyst. However, the Jacobsen group later suggested the existence of a Cu(III) species as the reactive intermediate in the Cu oxidation-reduction cycle. This explanation was also backed by the calculations of Andersson and Norrby where they confirmed that the Cu(I) species is the active catalyst and that Cu(II) may react with

TsN=IPh and play a part in the Cu(I)/Cu(III) catalytic cycle. However, Scott suggested that Cu(II) could also be an active catalyst or it could also be reduced to Cu(I) in situ, implying that conversion of Cu(I) to Cu(II) may not necessarily be required to show any activity.

The mechanistic aspects of the stereochemistry of the aziridine formation is not fully understood. Evans found that aziridination of *cis*-oct-4-ene with Cu catalysts proceeded with high stereospecificity, but aziridinations of *cis*-stilbene and *cis*-β-methyl styrene showed produced both isomers in varied amounts, depending on the counter ions used. Counter ions that were involved in strong co-ordinations (acetylacetonate, chloride etc) were found to favor the *trans*-aziridines. In contrast, the aziridination of *cis*-stilbene using Scott's Cu-diimine ligands afforded a 5:95 trans/cis stereospecificity and no *cis*-isomers were detected in the aziridinations of *trans*-cinnamate esters.[72] These reports suggest the existence of two competing pathways for aziridination –

1. A concerted and stereospecific nitrene transfer from the metallocarbenes to olefins.[74]
2. A two-step radical pathway which is favored by substrates that remarkably stabilize the intermediate radicals.[75]

The DFT calculations by Andersson and Norrby also show that metallonitrene has a ground state triplet state which is very close to the singlet state energetically. The stereospecificity in the aziridination may occur due to the singlet nitrene species whereas the lack of stereospecificity maybe attributed to the triplet state or the intermediate singlet biradical formed by the addition of metallonitrene to olefin (Figure 2.32).

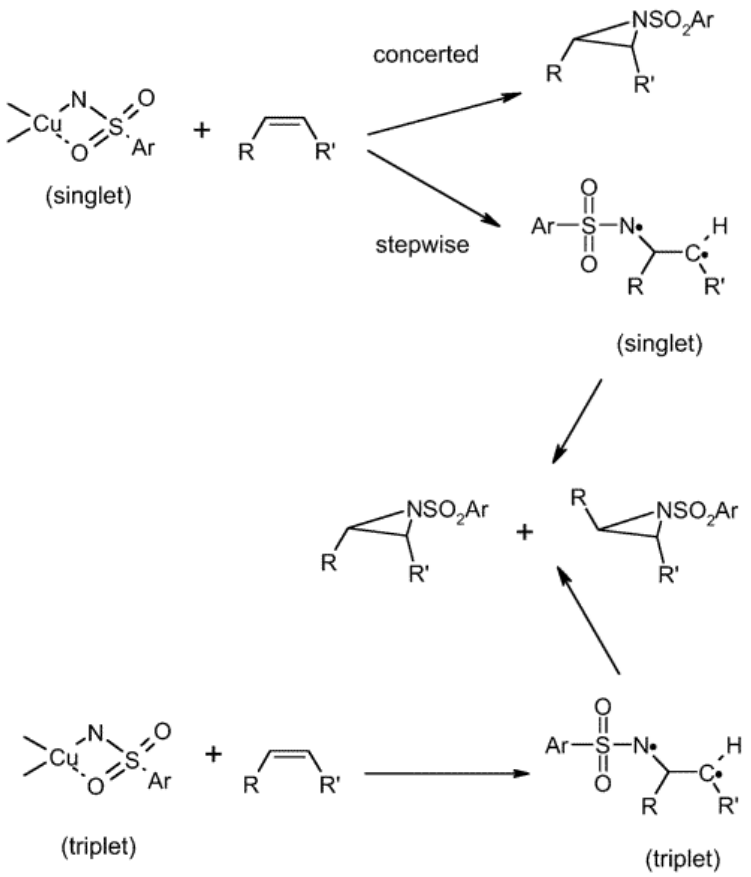

Figure 2.32 Proposed mechanisms for the stereospecific and non-stereospecific aziridination of olefins via triplet and singlet nitrenes.

The electronic substituent effect for the aziridination has also been studied by means of competing experiments. Müller group calculated a ρ-value of -0.49 vs σ^+ for reaction of substituted styrenes with NsN=IPh in the presence of [Cu(acac)$_2$] as the catalyst,[53] whereas Scott group calculated a ρ-value of -0.65 vs σ for the reactions of cinnamate esters in the presence of copper complexes with biaryl Schiff bases. This range of values is also observed for the concerted carbene transfer to olefins indicating an early transition change with a small positive charge buildup.[76]

Alongside the aforementioned works, several other achiral ligands have been introduced for aziridinations with TsN=IPh in the presence of Cu-metal which have show potential for asymmetric aziridinations. The Halfen group introduced a new Cu-1-(2-pyridylmethyl)-5-methyl-1,5-diazacyclooctane trifluoroacetate complex which afforded aziridinations of styrenes with remarkable efficiency (Figure 2.33).[77]

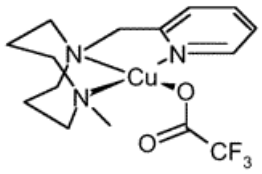

Figure 2.33 Cu-1-(2-pyridylmethyl)-5-methyl-1,5-diazacyclooctane trifluoroacetate complex for aziridination of olefins

Similar results were obtained by using Cu-1,4,7-tri*iso*propyl-1,4,7-triazacyclononane-bis(trifluoroacetate) complex (Figure 2.34).[47]

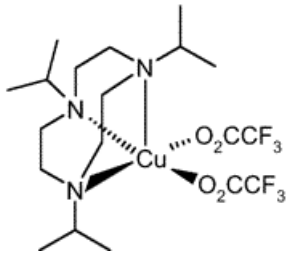

Figure 2.34 Cu-1,4,7-tri*iso*propyl-1,4,7-triazacyclononane-bis(trifluoroacetate) complex for aziridination of olefins

At the same time, Brookhart's Cu-tris(3,5-trimethylpyrazolyl)borate catalyst were synthesized and used for aziridinations. These catalysts offered moderate reactivities for aryl olefins but below par reactivities for aliphatic olefins. (Figure 2.35).[78]

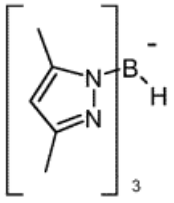

Figure 2.35 Brookhart's Cu-tris(3,5-trimethylpyrazolyl)borate ligands for aziridination of olefins

Other ligands that offered excellent efficiencies were the tris(pyrazolyl)borate ligands stabilized with trifluoromethyl substituents which formed Cu(I) ethylene adducts. (Figure2.36).[79]

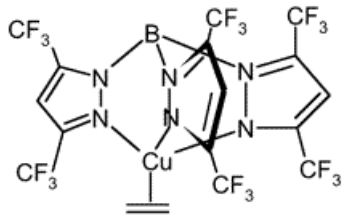

Figure 2.36 Tris(pyrazolyl)borate ligands stabilized with trifluoromethyl substituents forming Cu(I) ethylene adducts for aziridination of olefins

Remarkable improvement in the sythetic potential of the aziridination was brought about by Dauban and Dodd when they isolated phenyl imino iodinanes from aliphatic sulfonimides. They developed trimethylsilylethanesulfonyl (Ses) based reagent (SesN=IPh) for the aziridination reactions and obtained decent yields for the aziridine products of simple olefins using CuOTf as catalyst.[79] The successful development of SesN=IPh reagent from aliphatic sulfonimides introduced the possibility of intramolecular aziridinations which proceeded with acceptable yields using CuOTf as catalyst (Figure 2.37).[80]

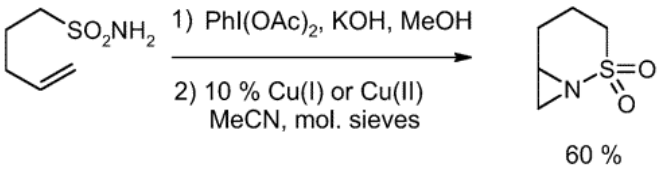

Figure 2.37 Intramolecular aziridination with SesN=IPh reagent and using CuOTf as catalyst

A Rh(II) catalyzed asymmetric intramolecular aziridination was also reported thereafter.

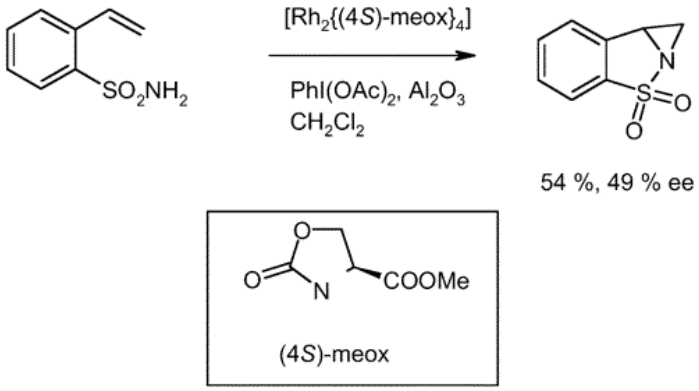

Figure 2.38 Rhodium metal catalyzed intramolecular aziridination

Even more promising development in this regard was the generation of phenyl iodinanes from sulfonamides[81] and sulfamates[82] in situ with idosylbenzene. The asymmetric bis(oxazoline) ligands were found to be compatible with these reactions (Figure 2.39).

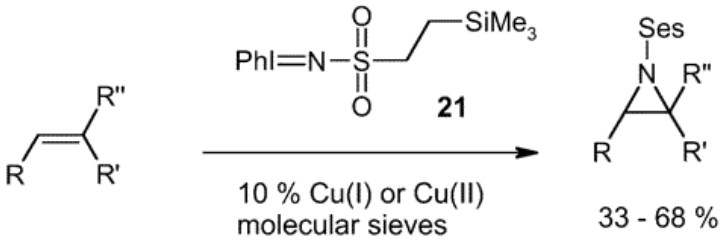

Figure 2.39 Aziridination with phenyl iodinanes generated from sulfonamides in situ

Rhodium catalyzed aziridinations

After the initial reports on the success of Rhodium catalysts, some groups focused on developing the aziridination protocols centered around Rh(II) catalysts. Rh(II) catalysts have been known to be complementary to Cu(I) catalysts in carbene transfer reactions.[83–89] Their use as nitrene transfer catalysts have been contemplated very early, but since Cu catalysts were found to be far superior in aziridinations using TsN=IPh, works on the development of Rh(II) catalysts were abandoned. However, it was later found that $[Rh_2(OAc)_4]$ in combination with NsN=IPh was also efficient in the aziridinations.[51] Aziridinations of β-methylstyrene and hex-2-ene were completely stereospecific although, *cis*-stilbene afforded very low yield and a mixture of cis and trans aziridines. With some electron-rich olefin substrates, the aziridines underwent ring-opening followed by cycloaddition to the excess olefins to form pyrrolidines.

Aziridinations of *cis*-β-methylstyrene and styrene with Pirrung's $[Rh_2\{(R)\text{-bnp}\}_4]$ catalyst were found to provide the highest enantioselectivities of 35% and 27% respectively (Figure 2.40).[90]

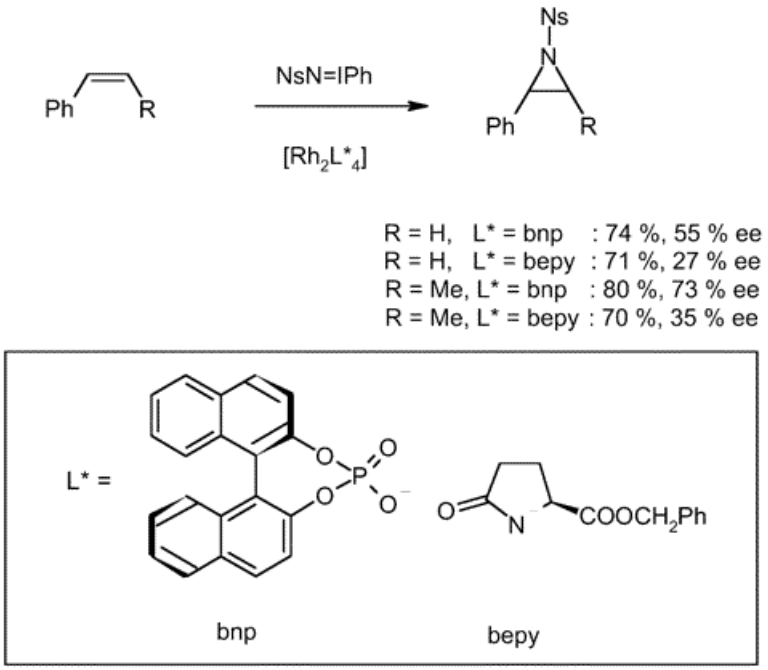

Figure 2.40 Enanatioselective aziridination of stryene and *cis*-β-methylstyrene with NsN=IPh and Pirrung's [Rh_2{(*R*)-bnp}$_4$] catalyst

On the other hand, the analogue of Doyle's Rh(II)-carboxamidate catalyst, [Rh_2{2*S*)-bepy}$_4$] provided less satisfactory results with enantiomeric excess of 35% and 27% respectively (Figure 2.40). The other Rh(II) catalysts provided little to no enantioselectivities and thus were less effective.

On a similar note, Du Bois reported Rh(II)-catalyzed olefin aziridinations using phenyliodinanes generated in situ from trichloroethylsulfamate ester (Figure 2.41).[91]

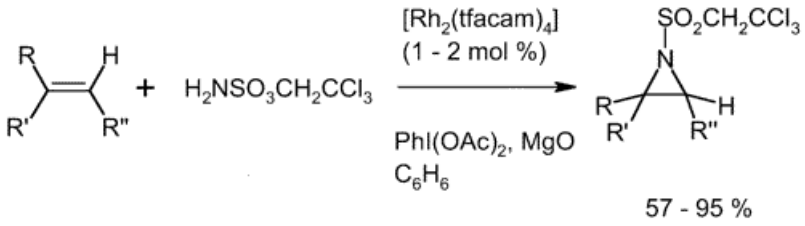

Figure 2.41 Rh(II)-catalyzed olefin aziridination using in situ generated phenyliodinanes derived from trichloroethylsulfamate ester

The most suitable catalyst for the transformation was found to be [Rh_2(tfacam)$_4$] (tfacam = CF_3CONH_2). The iodinane was generated from $PhI(OAc)_2$ in the presence of MgO. Using this

protocol, stereospecific aziridination of β-methylstyrene was achieved. Typical yields of aziridine ranged from 57-95% with different olefins. The system tolerated both alkyl and aryl substituents. This protocol was also successfully applied to phosphoramidates, sulfamate esters and intramolecular aziridinations.

Similar intramolecular aziridinations using Rh(II) catalysts, $PhI(OAc)_2$ in the presence of Al_2O_3 and in situ generated phenyliodinanes from unsaturated sulfonamides were reported by Che and coworkers.[91] Out of all the catalysts studied, Doyle's [Rh_2{(4*S*)-meox}$_4$] catalyst gave the best possible results with an enantiomeric excess of 49% and yield of 54%.

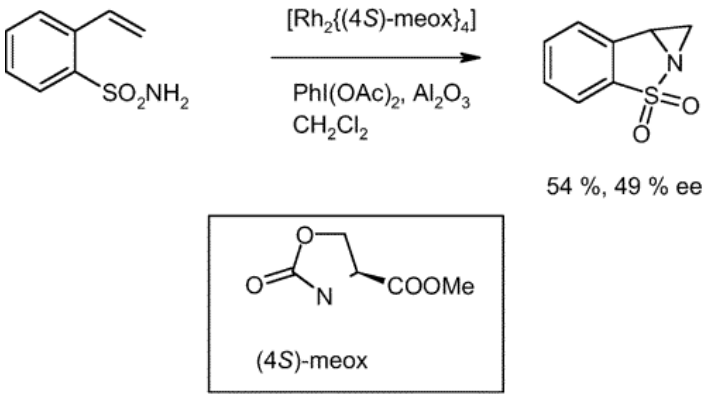

Figure 2.42 Doyle's [Rh_2{(4*S*)-meox}$_4$] -catalyzed intramolecular aziridination using in situ generated phenyliodinane derived from unsaturated sulfonamide

In one of the synthetic methodologies developed by the Rojas group, amidoglycosylation of allal carbamate was carried out by decomposition of in situ generated phenyliodinanes from carbamates and PhI=O and catalyzed by Rh(II). The reaction was proposed to proceed via an aziridine intermediate which is eventually attacked by acetate to afford the corresponding acetate product. The reaction also proceeded in the presence of Cu-catalysts albeit with lower yields (Figure 2.43).[92]

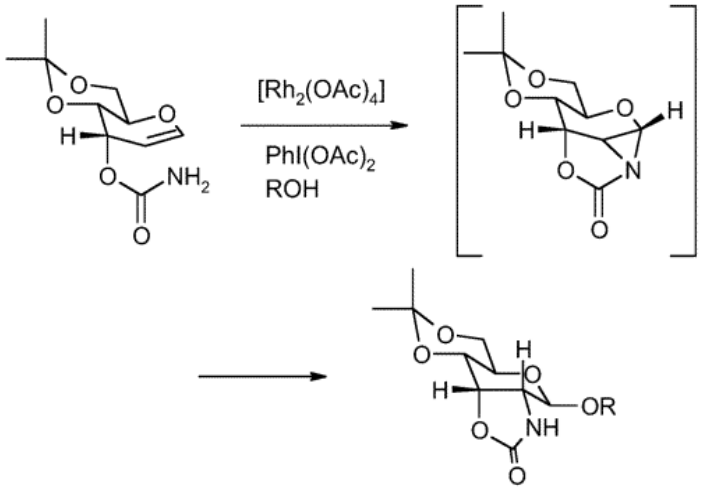

Figure 2.43 Amidoglycosylation of allal carbamate using phenyliodinanes and catalyzed by Rh(II)

In another synthetic route, aziridination of an indolyl substituted carbamate **1** was carried out using $PhI(OAc)_2$ in the presence of $[Rh_2(OAc)_4]$. The reaction proceeded via formation of a zwitterion, **2** which was attacked by AcOH to afford spiro-oxazolidinone, **3.** The reaction was proposed to go through a metallonitrene intermediate. However, similar reaction of cycloalkenyl carbamate **4**, with $PhI(OAc)_2$ took place even without the presence of a catalyst to yield the aziridine **5** (Figure 2.44).[93]

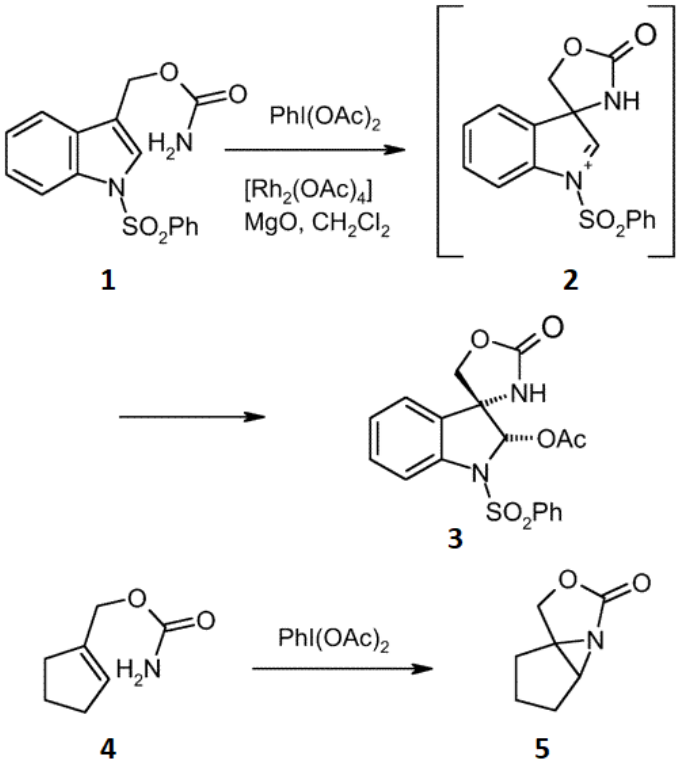

Figure 2.44 $Rh_2(OAc)_4$-catalyzed aziridination of an different substituted carbamates using $PhI(OAc)_2$

These reactions thus mark the first instance of an uncatalyzed aziridination using phenyliodinane where, the phenyliodinane intermediate directly reacts with the electron-rich double bond of the substrate. A similar reaction with the carbon analogue viz, uncatalyzed intramolecular cyclopropanation using phenyliodonium methanides has been repeatedly observed before.[94–97]

Manganese-catalyzed aziridinations

Some other metals that have been studied for aziridination of olefins are Mn and Fe. As described previously, the Mansuy group described the first racemic olefin aziridination catalyzed by Mn- and Fe- porphyrins and using TsN=IPh.[18,41,44,45] Seminal studies on extending this protocol to chiral Mn(III) salen complexes provided no selectivities in the aziridinations of *cis*-β-methylstyrene and styrene.[98] Later, Groves introduced a procedure for aziridination by using nitridomanganese complexes[99] which was further developed by Du Bois and Carreira to form

aziridine intermediates ultimately leading to amidation of enol ethers.[100–103] Even more developments to the reaction were brought about by the Komatsu group who used a chiral 1,2-diaminocyclohexane based nitridomanganese complex (Figure 2.45).[104–106]

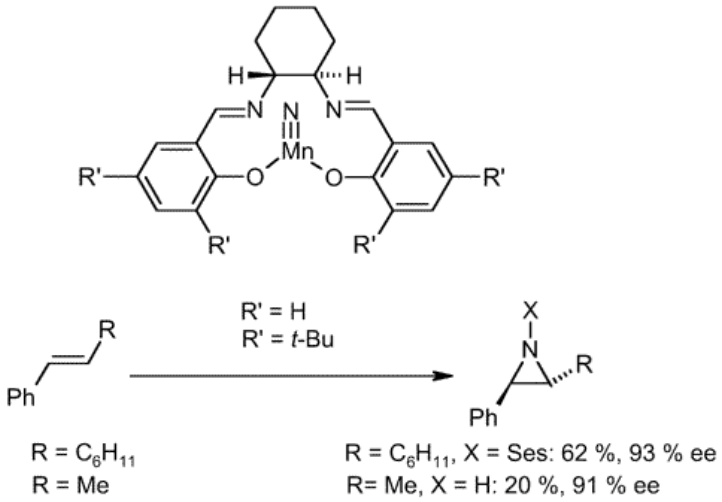

Figure 2.45 Chiral 1,2-diaminocyclohexane based nitridomanganese reagent for asymmetric olefin aziridination

The complex reacted with alkenes in the presence of Ts_2O or sulfonyl chlorides to produce aziridines with yields in the range of 50-87% and enantiomeric excess of upto 93%. The reaction was also found to be stereospecific with β-methylstyrene. When sulfonyl chlorides were replaced by acid chlorides as initiators, oxazolines were produced via aziridine intermediates in 53-85% yields. Poor enantioselectivities were observed in the oxazoline formation with styrene, α-methylstyrene and cis-disubstituted styrenes, but they were excellent with trans-disubstituted styrenes. When the Mn(V)nitrido complexes were activated using Bronsted or Lewis acids such as BF_3 and trifluoroacetic acid (TFA) instead of acid chlorides or sulfonyl chlorides, olefin aziridination proceeded towards unprotected aziridines. For example, *trans*-β-methylstyrene afforded the corresponding aziridine with enanatioselectivity of 91%, albeit with only a 20% yield.[107]

In parallel to these works, Nishikori and Katsuki optimized a chiral salen complex to carry out Mn-catalyzed asymmetric aziridination reactions (Figure 2.46).[38,108,109]. Using this complex, they achieved upto 94% enantiomeric excess for aziridination reactions of styrene with TsN=IPh

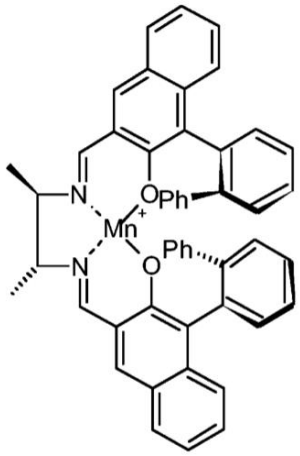

Figure 2.46 Nishikori and Katsuki's optimized chiral Mn-salen complex

Higher enantioselectivities were obtained in the presence of catalytic amounts of 4-phenyl-pyridine-*N*-oxide.

In a different study, another chiral Mn(III) porphyrin complex (Figure 2.47) with TsN=IPh, afforded the aziridination products with decent yields and enantioselectivities.[110,111]

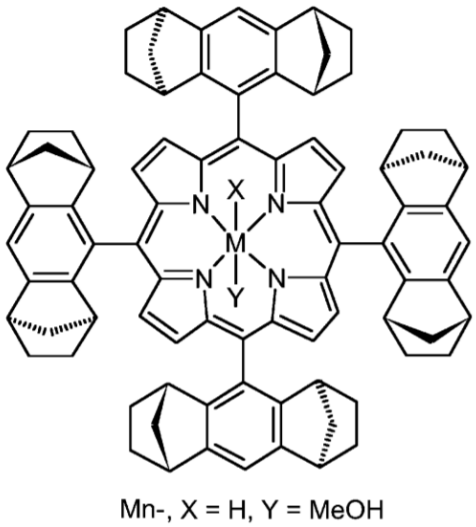

Figure 2.47 Che's Mn(III) porphyrin complex for aziridination

Similarly, Marchon and coworkers developed another chiral Mn(III)-porphyrin catalyst (Figure 2.48) and reported an enantiomeric excess of 57% for the aziridiantion of styrene using

TsN=IPh.[112] When the same ligand was used with Fe(II), aziridines with oppposite absolute configurations were produced than those in Mn(III)-complex.

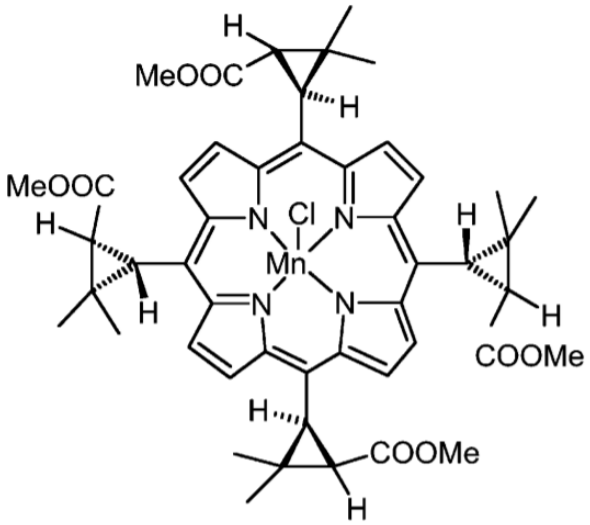

Figure 2.48 Marchon's modified Mn(III) porphyrin complex for aziridination

Besides manganese, efforts were also made to develop and characterize ruthenium catalysts for aziridination. In a report by Che, bis(tosyl)imidoruthenium(VI)−porphyrin complexes (Figure 2.49) afforded stoichiometric aziridinations of various olefins. The complexes were prepared by ligand displacement from [Ru(II)(por)(CO)(MeOH)] with TsN═IPh and characterized by X-ray crystallography.[20]

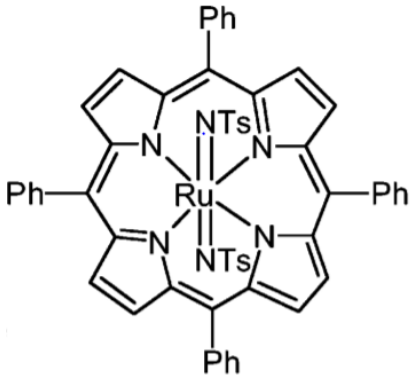

Figure 2.49 Che's modified bis(tosyl)imidoruthenium(VI)−porphyrin complex for aziridination

The mechanism for the aziridination has also been extensively studied which is proposed to go through stepwise aziridination involving radical intermediate.[113]

Ruthenium-catalyzed aziridinations

Similar to their studies on Mn(III) porphyrin complexes, Che et al replaced the Mn metal with Ru in the complex (Figure 2.50) but observed the enantioselectivities to be half of that obtained with the Mn(III) porphyrin complexes.[110]

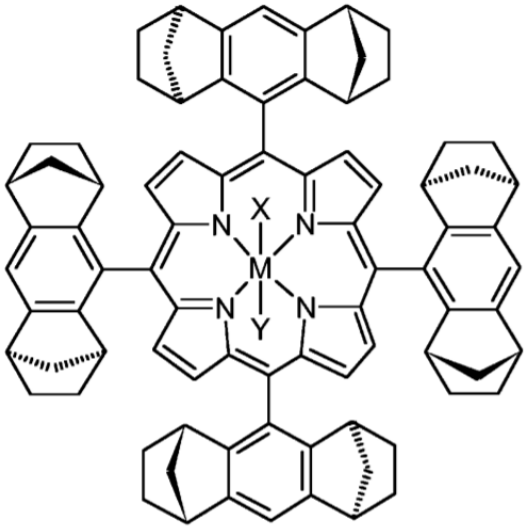

Ru- X = CO, Y = EtOH

Figure 2.50 Che's Ru(III) porphyrin complex for aziridination

Che et al also developed another chiral Ru-based Schiff base catalysts which were found to be highly efficient in amidations of silyl enol ethers with enantioselectivities of upto 97% which proceeded via isolable aziridine intermediates (Figure 2.51).[114]

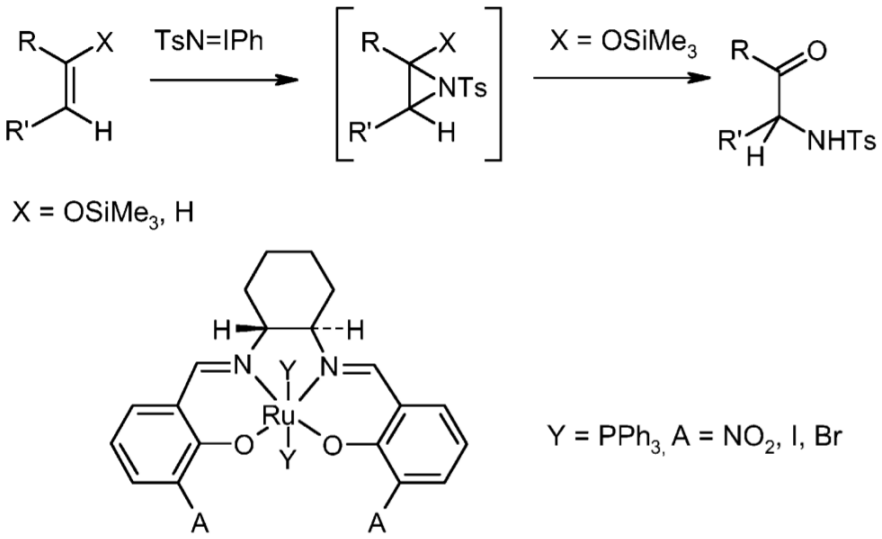

Figure 2.51 Aziridination of sily enol ethers catalyzed by Che's Ru-based Schiff base catalysts

In another work, an achiral Ru-porphyrin catalyst was combined with polyethylene glycol to afford a polymer supported soluble catalyst which was used for aziridinations.[115] With respect to rhenium metal, methyltrioxorhenium (MTO) was also found to execute nitrene transfer reactions using TsN=IPh albeit with low yields with styrenes (28-32%). However, α-methylstyrene reacted exceptionally well with 70% yield.[116]

2.1.2 Nitrene transfers without transition metals

The laboratory of Platz attempted nitrene insertions into olefins without the use of metal-catalysts. Platz utilized pentafluoro-substitutions in phenyl nitrene to control the reactivity of the nitrene instead of using the traditional metal catalysts.[117–125]

As mentioned earlier, phenyl nitrenes have a proclivity of forming polymeric tars from its rearranged products. These intramolecular rearrangements stem from the ability of the phenyl nitrenes to access their high energy π^2 electronic state, which frees an in-plane p-orbital to accept electrons from the aryl ring.[126] This process goes through the formation of a ketenimine via a benzazirine transition state eventually leading to polymerization. Platz tried to hinder this formation of ketenimine by introducing electron-withdrawing fluorines that would raise the energy barrier associated with the insertion of the nitrene into the ring. This extends the lifetime of the singlet phenylnitrene into tens of nanoseconds rather than hundreds of picosecond, giving them enough time to undergo insertions into olefins. It is also predicted that, the σ electron-withdrawing

and the π-donating ability of the fluorines would also stabilize the σ^2 and the σπ electronic states relative to the π^2 configuration thus making it difficult to access the reactive π^2 state. This synergistic combination of effects enabled different insertion reactions of phenyl nitrenes including nitrene transfers (Figure 2.52).

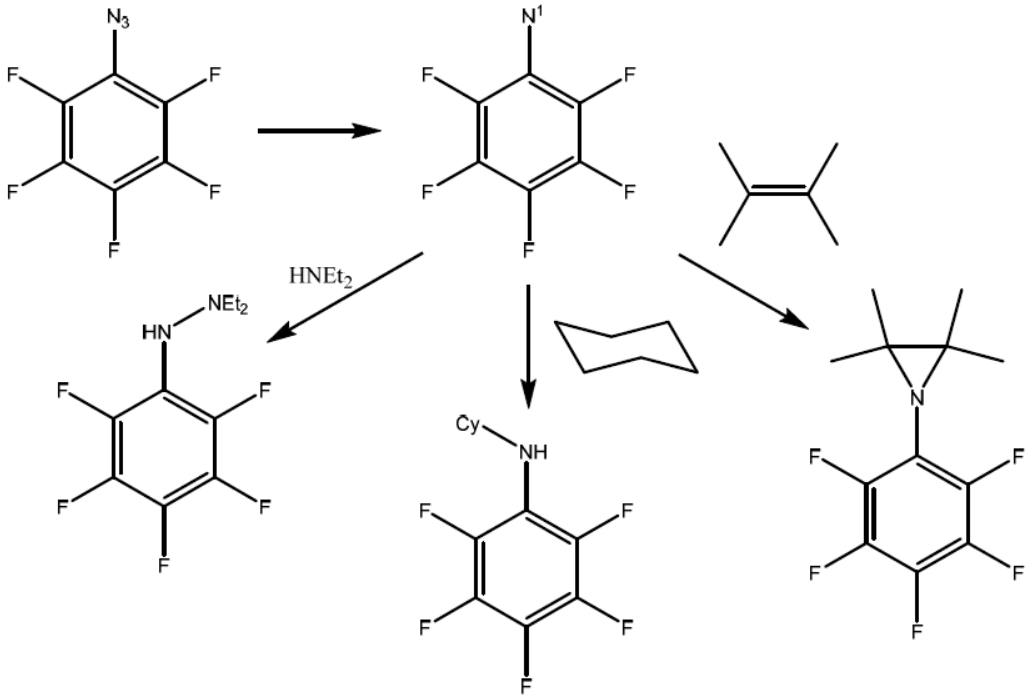

Figure 2.52 Reactivity of pentafluorophenyl nitrenes

Hilinski and Johnson are also one of the very few authors to report aziridination reactions using metal-free conditions.[127] They employed an iminium salt as the organic catalyst to promote the aziridination of styrenes using TsN=IPh (Figure 2.53)

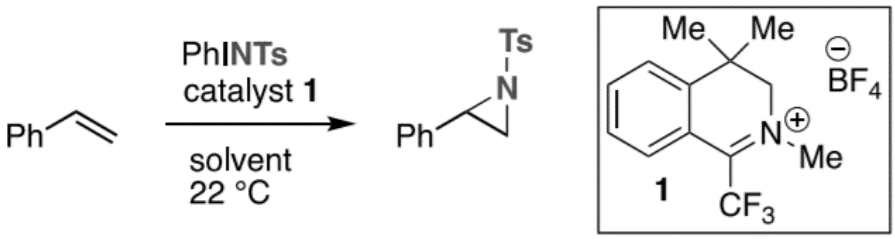

Figure 2.53 Reactivity of pentafluorophenyl nitrenes

In terms of the substrate scope, a variety of mono-substituted styrenes underwent aziridinations in acceptable yields. The yields were found to increase with stronger π-electron donating substituents whereas, presence of strong deactivating groups drastically affected the reaction performance resulting in lowest yields of the aziridine products. The negative influence of the deactivating groups was also seen on the rate of reaction where significant amount of starting materials remained unconsumed. The reaction also tolerated the presence of acid-sensitive group such as tert-Butyldimethylsilyl ether (TBS) and boronic ester pinacol borane (B(pin)).

Mechanistically, it was proposed that the nucleophilic attack of TsN=IPh takes place on the iminium catalyst forming a diaziridinium. The highly electrophilic nitrogen of the diaziridinium then adds to the alkene in a polar, step-wise fashion to produce a cationic intermediate which undergoes ring closure to produce aziridines. (Figure 2.54)

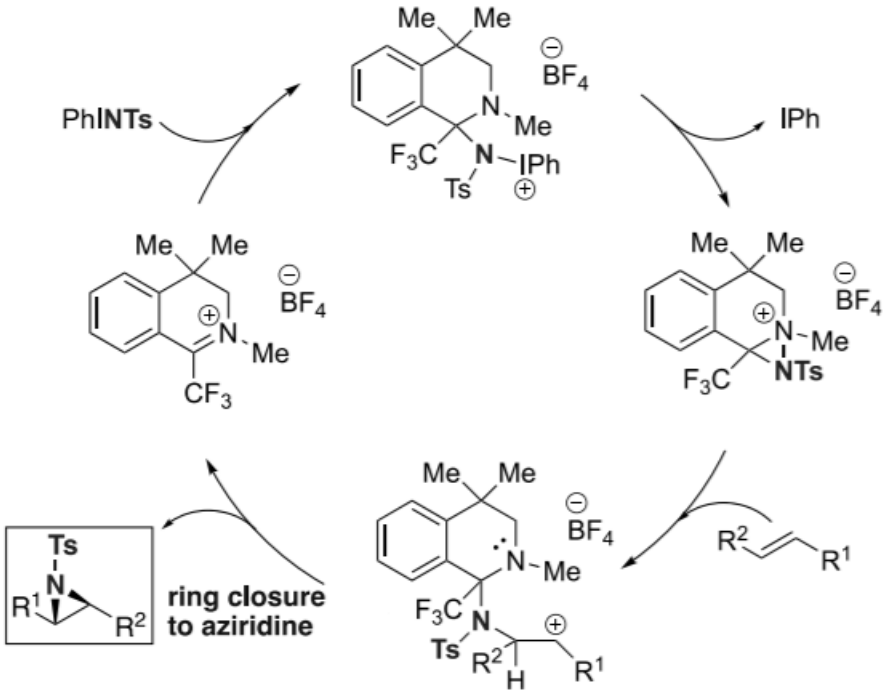

Figure 2.54 Aziridination mechanism proposed by Hilinksi

A unique approach for oxidative nitrene transfer to olefins using an electrochemical approach was reported by Yudin et al. They group developed a simple combination of platinum electrodes, acetic acid and triethyl amine to carry out highly efficient nitrene transfer from N-aminophthalamide to cyclohexene at room temperature (Figure 2.55)

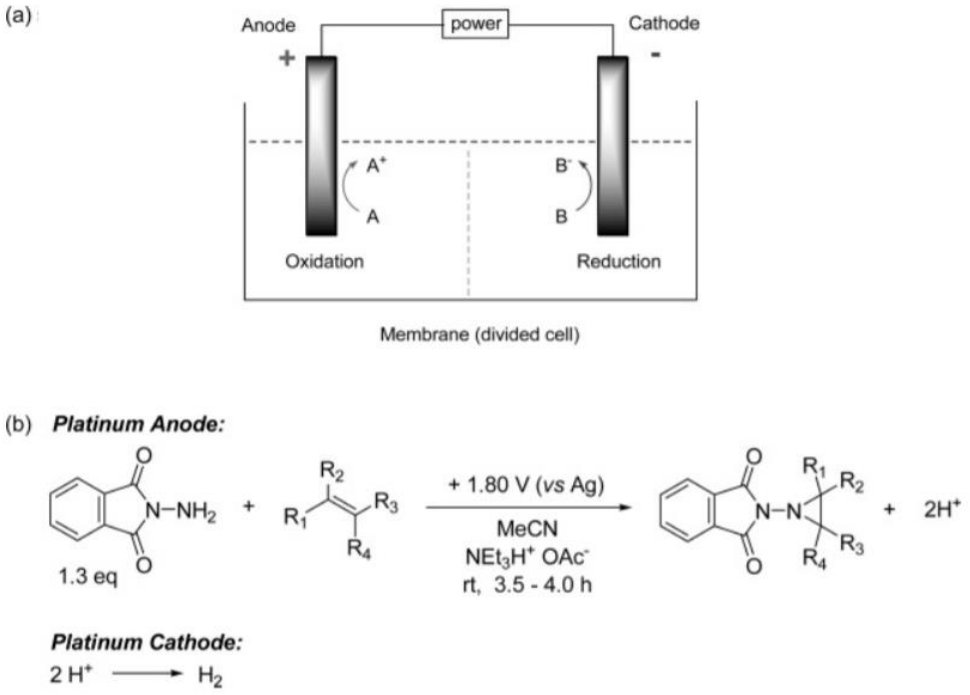

Figure 2.55 a) Schematic representation of the electrochemical cell b) electrochemical olefin aziridination

The reaction cell consisted of a silver wire as pseudo-reference electrode and used a small excess of the N-aminophthalamide relative to the olefin. The formation of the aziridine was relative to the cell current and stopped when the current dropped below 5% of its original value. The driving force behind the reaction was attributed to *overpotential,* which is essentially the additional potential beyond the thermodynamic requirement, required to drive forward a reaction at a certain rate. This overpotential can be used to selectively oxidize the N-aminophthalamide in the presence of a thermodynamically similar acceptor such as an olefin without any competing reactions and side-products. Thus, the *overpotential* can be considered to be the driving force or the catalyst for the reaction which replaces the transition metals in the traditional aziridination approaches.

This approach successfully provided aziridines in moderate to excellent yields from both electron-rich and electron-deficient olefins under anodic oxidation conditions. However, aziridination of certain olefins such as methyl acrylate, allyl bromide, hex-1-ene, succinic anhydride and dimethyl maleate proved to be unsuccessful using this protocol. The use of acetic acid is very crucial in this protocol as the acetate anion is prevents the formation of the unwanted nitrene dimer.

2.2 Conclusion

This review chapter lists the developments in the field of aziridinations of olefins particularly using metal catalysts. This area has witnessed tremendous development with the discovery of new efficient routes for the chiral aziridine synthesis which for a long time has remained undeveloped especially compared to the other three membered cyclopropanes and epoxides. Today, a large number of various functionalized aziridines have been efficiently synthesized in excellent yields and enantioselectivities. This review clearly demonstrates that the asymmetric aziridination reaction plays a vital role in organic synthesis, still attracting a considerable amount of interest due to the potential use of enantiopure aziridines as crucial intermediates in the complex molecule synthesis, and to the intriguing biological activities of numerous aziridine-containing products including important natural compounds. The development of new catalytic systems for the synthesis of certain highly useful synthetic intermediates is, however, to be expected in the next few years.

CHAPTER 3. INVESTIGATION OF THE SUBSTITUENT EFFECTS OF THE AZIDE FUNCTIONAL GROUP USING THE GAS-PHASE ACIDITIES OF 3- AND 4-AZIDOPHENOLS

3.1 Introduction

Phenyl azides have garnered significant interest since their discovery in 1864 due to their applicability in various fields.[128–133] Currently, it is one of the most commonly used functional group in click chemistry[134–141] which involves combining a biomolecule and a substrate of choice to generate a large library of compounds that find employment in various disciplines. A typical click reaction is the combination of an azide with an alkyne to yield a very useful, 5-membered triazole ring: an azide-alkyne cycloaddition (Figure 3.1).[141]

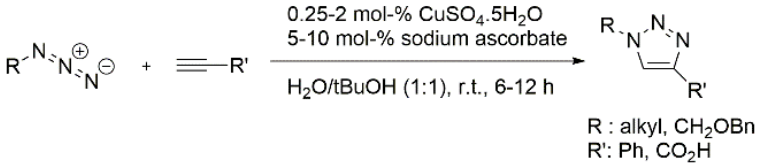

Figure 3.1 Example of an azide-alkyne click cycloaddition

Synthesis of drug analogs is very pertinent to the field of medicinal chemistry and drug discovery, and triazoles constitute a vital part of multiple bioactive molecules,[142] being one of the most widely used bio-isosteres.[143–145] They have good stability along with various structural characteristics such as rigidity and polarity along with the ability to act as both a hydrogen bond donor and acceptor, which helps them to mimic the traits of various functional groups which establishes their potential applicability in medicinal chemistry,[137,146–149] agriculture,[150,151] bioconjugation,[152] chemical synthesis[153] and supramolecular chemistry.[154]

Azides are also popular precursors of nitrenes in nitrene chemistry. Azides readily decompose in the presence of light, heat and catalysts under reagent free conditions to yield nitrenes which have attracted tremendous interests recently.[155–163] The presence of an exceedingly good leaving group dinitrogen imparts a high chemical reactivity to the azide functionality, enabling it to act as electrophile, nucleophile and radical acceptor, which makes it highly useful in synthetic chemistry.[164] However, even though the azide is a versatile and energy-rich functional

group widely studied for its applications, not much is known about its electronic nature. Considering that the azide is a cumulated system of π-electrons, it would be expected to interact with π system, such as in aromatic molecules, though conjugation. On examining the possible resonance structures, the azide can be rationalized to be either a π-electron donor or an acceptor as shown in figure 3.2.

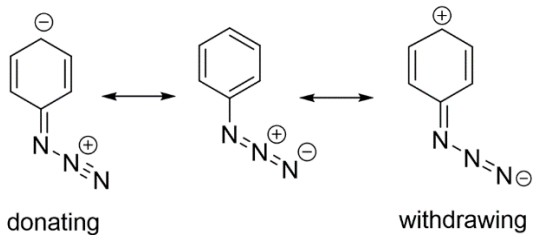

Figure 3.2 Azide as a π-acceptor and a π-donor

For example, an azide could exhibit π-electron donating capabilities, as shown in the left side of Scheme 1. The advantage in this case is that all the atoms maintain filled octets, at the cost of transferring negative charge from nitrogen to carbon. In contrast, as a withdrawing group, negative charge stays on the nitrogen and positive charge is transferred to the carbon. Literature reports have supported characteristics of azide that sometimes contradict each other. Azides are found to not participate as π-electron donors in charge transfer, resulting in blue-shifted absorptions.[165] On the contrary, Streitwieser and Pulver have shown that azides can act as powerful electron donors in situations of strong electron demands in non-aromatic systems.[166] It is also known that an azide permits direct nitration of benzene and naphthalene rings with the nitro groups directed to the ortho and para positions of the phenyl azide[167] or α- and β- positions in napthyl azide.[168] Bromination of phenyl azide is known to produce para-bromophenyl azide whereas that of 2-napthyl azide produces 1-bromo-2-napthyl azides.[169] These instances of electrophilic aromatic substitutions demonstrate a π-donating character of azides. Another study by Stankovský and Kovăc found that the integrated absorption intensity in the ν_{as}(NNN) band increases in the presence of electron-donating substituents or electron-withdrawing substituent, hinting at a possibly dual electronic nature of the azide group.[170] With all the uncertainty surrounding the true electronic nature of an azide group, it warrants a systematic investigation to elucidate the electronic effects of an azide group.

The electronic properties of the azide group can be interpreted by evaluating their Hammett parameters. The original Hammett equation related substituent constant, σ with the reaction constant, ρ by the following equation:

$$\rho\sigma_x = log\,(k_x/k_H)$$

where k_H is the ionization constant of unsubstituted compound and k_x is the corresponding constant for meta- and para-substituted compound. The parameter σ is dependent on the position of the substituent whereas, ρ was position independent.[171] Although this idea of quantifying substituent effects in terms of the substituent constants was a milestone, it combined all the different types of substituent effects into just one variable resulting in lack of a detailed study of the substituents. Taft[172] has provided an alternate approach where the substituent effects are separated into different components, including inductive/field effects, σ_F, mesomeric/resonance effect, σ_R, polarizability, σ_α, and electronegativity, σ_χ, and related to the difference in the free energies, $\partial\Delta G°$ of the substituted and unsubstituted compounds. For most substituents and reactions, the most important parameters are the inductive/field and resonance effects, σ_F and σ_R, respectively. In the Hammett-Taft model, the effect on the energetics for a defined chemical process follows the relationship below, where A° is a small constant.

$$\delta\Delta G_{acid} = \rho_F\sigma_F + \rho_R\sigma_R + A^o \qquad (1)$$

Because different reactions respond differently to the inductive and mesomeric effects, the reaction constants ρ are considered to be position dependent, whereas the substituent constants, σ, are position independent. The Hammett-Taft parameters obtained by using this approach provide a fundamental understanding of the substituent behavior[172] and can be very effective in gaining insights into the electronic nature of a wide variety of substituents.

In this work, we report an experimental investigation of the Hammett-Taft parameters of the azide substituent within the 3- and 4-azidophenol systems. According to the Taft and Topsom approach,[172] the σ_F and σ_R values for the azide substituent in the azidophenols are related to the difference in gas-phase acidities of the azidophenols and unsubstituted phenol. The gas-phase acidities of 3- and 4-azidophenols have not been reported in the literature, and thus have now been determined using the kinetic method with mass spectrometry.[173] The electronic effects of the azide substituent have also been investigated in the azidobenzoic acid system using computational

methods, and show the azide to have a dual electronic nature in terms of π-electron delocalization, which is influenced by the nature of other substituents in the aromatic system.

3.2 Experimental section

All the reagents, solvents and reference phenols were obtained from commercial sources and used as supplied. The azidophenols were synthesized by using procedures similar to those reported previously.[174,175]

3.2.1 Procedure for synthesis of 3-azidophenol

To a solution of 2-hydroxyaniline (9.16 mmol) in DCM (15 mL) at 0°C was added 8 ml of concentrated HCl with constant stirring. A solution of sodium nitrite (11.0 mmol) in 10 mL water was then added dropwise over a period of 10 min with stirring. After 1h, a solution of sodium azide (11.91 mmol) in water (5 mL) was added to the reaction mixture with constant stirring. The reaction mixture was warmed to room temperature and stirred for further 4 h. The solution was then poured into water, extracted with DCM (3 × 20 mL), dried over magnesium sulfate, filtered and concentrated in vacuo to give 3-azidophenol as a viscous yellow oil, which was used for the studies without any further purification.

3.2.2 Procedure for synthesis of 4-azidophenol

To a round bottom flask, 9.16 mmols of 3-hydroxyaniline was dissolved in 25 ml of deionized water and 8 ml of concentrated HCl with stirring. The solution was then cooled to 0^{o}C in an ice bath. Once cooled, 9.16 mmols of sodium nitrite was added to the solution in small portions and the mixture was allowed to stir for 10 minutes. 10.89 mmols of sodium azide was then added to the solution in small portions with constant stirring. Once the addition was complete, the solution was allowed to warm to room temperature and stirred for an additional hour. The solution was then extracted with ethyl acetate (3 x 25 ml). The combined organic layers were washed with sodium bicarbonate and brine, dried over magnesium sulfate and the solvent was evaporated under reduced pressure to yield 4-azidophenol as a dark brown oil which was used without further purification.

For prolonged use, the azidophenols were stored under cold and dark conditions.

3.2.3 General procedure for sample preparations

The substituted reference phenols selected for the experiments along with their gas-phase acidities are listed in Table 3.1.

Table 3.1. Reference phenols and their gas-phase acidities

Reference	Gas-phase acidities[b]
3-fluorophenol	343.7 ± 2.8[b]
ethyl-3-hydroxybenzoate	343.9 ± 2.1
4-fluorophenol	346.7 ± 2.1
3-trifluoromethyl phenol	339.2 ± 2.1
3-hydroxybenzaldehyde	340.5 ± 2.1
methyl-3-hydroxybenzoate	343.8 ± 2.1

[a] *Values in kcal/mol. All the gas-phase acidity values from ref* [176] *unless otherwise noted.*

[b] *Ref* [177]

One molar stock solutions of each of the reference phenols and the azido phenols were prepared by dissolving the necessary amounts in methanol. The stock solutions of the azido phenols were kept in the dark and stored in a freezer. Samples were prepared by mixing 7 µl of a reference stock solution with 7 µl of the azido phenol stock solution and 7 µl of 0.5 M potassium hydroxide (in water). The solutions were diluted to 1ml in water-methanol solvent system (1:1) for ESI-MS analysis. All of the samples were stored and analyzed in the dark.

3.2.4 Spectra collection

Electrospray ionization mass spectra were obtained on a Waters Micromass (Milford, Massachusetts) Quattro Ultima Pt triple quadrupole mass spectrometer, equipped with ESI source, operating in negative ion mode. Sample solutions were introduced into the source directly at a flow rate of 10 µL/min. Electrospray and ion focusing conditions were varied to maximize the signal of the proton bound dimer of the phenoxide ions.

3.2.5 Collision-induced dissociation (CID) studies

The phenoxide cluster ions were isolated on the basis of their mass-to-charge ratio and subjected to collision with argon target at energies of 4, 6, 8, 10, 13, 17 and 20 volts (center-of-lab frame). Primary product ions observed were *m/z* 134 (azido phenoxide) and the phenoxide of the corresponding reference phenol. CID of ions containing *p*-azidophenoxide also resulted in formation *m/z* 106, presumably the quinonimide ion (*p*-$NC_6H_4O^-$) formed by secondary fragmentation. Intensities of the product ions were recorded for each collision energy. The experiments were repeated at least four times on separate days.

3.2.6 Kinetic method for determination of gas-phase acidities

As mentioned in the introduction, gas-phase acidities of azido phenols required to determine their Hammett-Taft parameters have not been reported. In this work, we have measured them by using the kinetic method.[173]

Deprotonated phenols form proton-bound dimers with neutral phenols in the gas phase. When such dimers are subjected to collision with neutral molecules, they undergo fragmentation and the yields of the products depend on the relative gas-phase acidities of the respective phenols. Knowing this, it is possible to determine the gas-phase acidities of the azido phenols by using the set of substituted reference phenols with known gas-phase acidities. In the kinetic method, we consider the dissociation of a proton bound dimer [$AP^- H^+ P_i^-$], where AP^- is the azido phenoxide and P_i^- is the reference whose corresponding phenol has known gas-phase acidity. Fragmentation of this complex leads to either APH + P_i^-species or AP^- + P_iH species.

In the mass spectroscopic measurement for the kinetic method, the difference in the acidities of the reference phenols (P_iH) and the azido phenol (APH) is related to the branching ratios $R_{E,i}$ of the AP^- and P_i^- species, by eq 2, where T_{eff} is the effective temperature of the dissociation,[178,179] $\delta\Delta S$ is the difference in activation entropies for the formation of P_i^- and AP^- from the proton-bound dimer,[180–183] and the E and i subscripts indicate the terms that are dependent on the collision energy of the dissociation and the reference phenol respectively. The branching ratio $R_{E,i}$ is the ratio of *m/z* 134 + *m/z* 106 (corresponding to AP^-) to the *m/z* of the reference phenoxide (P_i^-).

$$lnR_{E,i} = \frac{\Delta H_{acid}(P_iH) - \Delta H_{acid}(APH) - T_{eff,E}\,\delta\Delta S}{-RT_{eff,E}} \quad (2)$$

The kinetic method, in its simplest form,[184] relies on the entropy term in the equation to be negligible, thus enabling acidity calculations through a plot of $\ln R_i$ Calculated at a single collision energy vs ΔH_{acid}, for a series of reference acid P_iH. However, the extended kinetic method,[183,185] includes the entropy component to the branching ratio. Thus, from eq 2, a plot of $\ln R_{E,i}$ vs $\Delta H_{acid}(P_iH)$ at a given energy has a slope m_E = -1/$RT_{eff,E}$ and an intercept y_E = [ΔH_{acid}(APH) + $T\delta\Delta S$]/$RT_{eff,E}$. In accordance with the extended kinetic method, when the dissociation is carried out at a series of collision energies, a second regression plot of y_E vs -m_E can be constructed, where the slope would be the acidity, ΔH_{acid}(APH) and the intercept would be $\delta\Delta S/R$.

It has been noted[173] that the slopes and intercepts obtained from the best fit of the data in the first linear regression are interdependent. This means that, the second regression plot will result in an excessive correlation between the derived slopes and intercepts. This correlation can be removed[173] by simply plotting $\ln R_{E,i}$ versus $\Delta H_{acid}(P_iH) - \Delta H_{acid}(P_iH_{,avg})$, as the first regression plot where $\Delta H_{acid}(P_iH_{,avg})$ is the average of the gas-phase acidities of the reference phenols. In this approach, the second regression plot has an intercept of $\delta\Delta S/R$ and a slope of $\Delta H_{acid}(APH) - \Delta H_{acid}(P_iH_{,avg})$, from which the acidity of azidophenol can be obtained.

3.3 Results

The collision-induced dissociation of phenoxide proton-bound dimers was carried out at seven different energies, from 4-20 V in the lab frame. The first regression plots of $\ln R_{E,i}$ versus $\Delta H_{acid}(P_iH) - \Delta H_{acid}(P_iH_{,avg})$ for 3- and 4-azidophenols at all the collision energies are provided in Figure 3.3, where $\Delta H_{acid}(P_iH_{,avg})$ = 343.0 kcal/mol

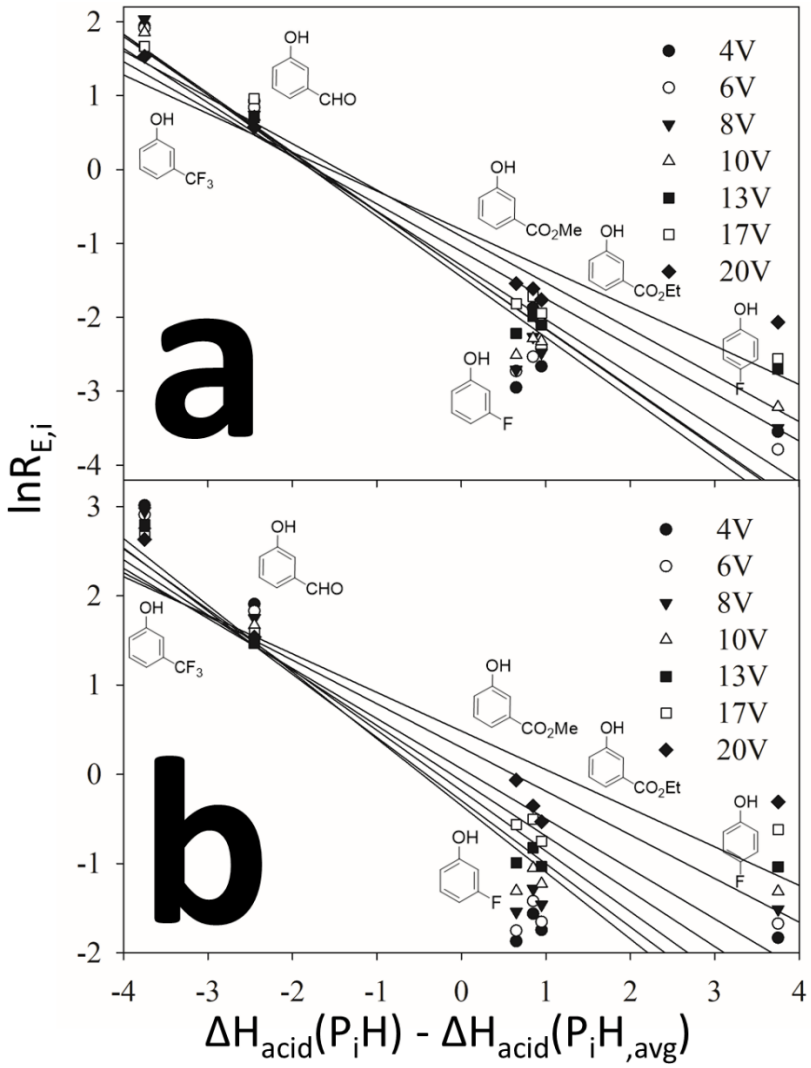

Figure 3.3 First regression plots of $\ln R_{eff,E}$ vs $\Delta H_{acid}(P_iH) - \Delta H_{acid}(P_iH_{,avg})$ at a series of energies for a) 3-azidophenol and b) 4-azidophenol

The subsequent second regression plots have slopes equal to 2.2 and 2.7 kcal/mol and intercepts equal to 0.3 and 1.6 e.u. for 3- and 4- azidophenols respectively (Figure 3.4).

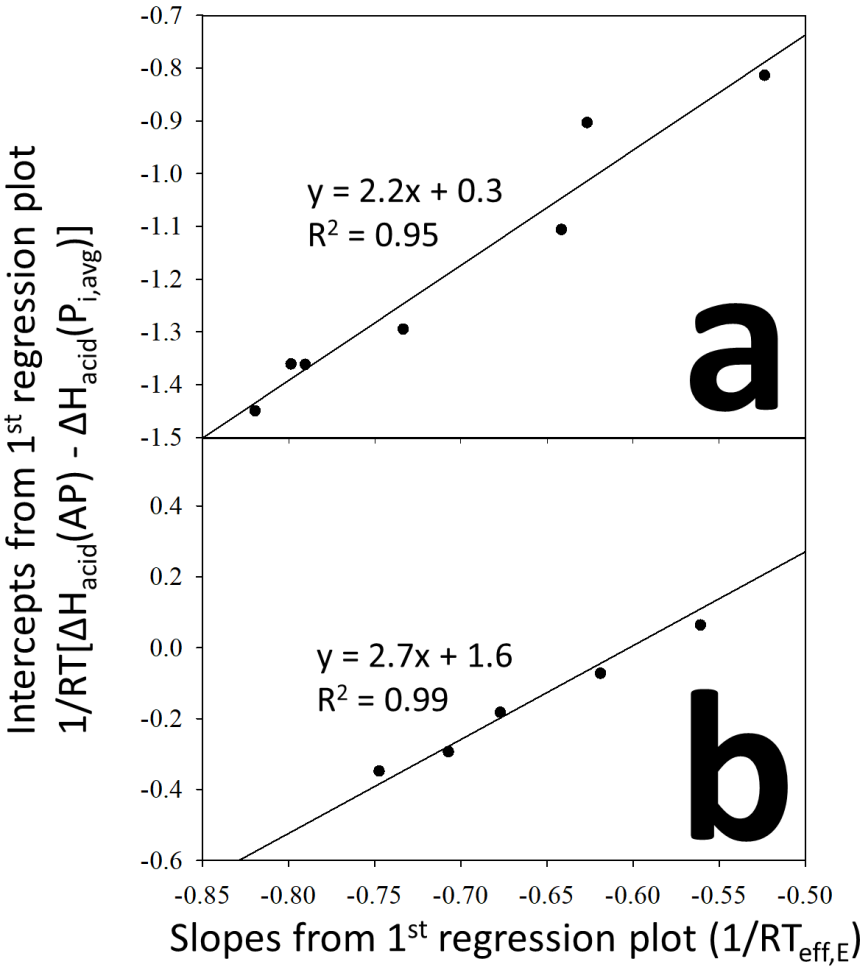

Figure 3.4 Second regression plot for a) 3-azidophenol and b) 4-azidophenol

In the analysis, the gas-phase acidities of the azidophenols are calculated from the slopes of the 2nd regression plot by the equation $\Delta H_{acid}(APH) = \Delta H_{acid}(P_iH_{,avg}) - \text{slope}$. From this work, the gas-phase acidities of 3-azidophenol and 4-azidophenol are found to be 340.8 kcal/mol and 340.3 kcal/mol, respectively. From the intercept values, $\delta\Delta S$ is calculated to be 0.6 and 3.2 eu for 3- and 4-azidophenols respectively. The small values of $\delta\Delta S/R$ indicate minimal differences in the activation entropies for the two dissociation pathways.

The slopes obtained from fitting the data shown in Figure 3.4, have uncertainties (δ_{slope}) of ±0.6 and ±0.3 kcal/mol for 3- and 4-azidophenols respectively, referring to statistical 95% confidence levels.[173] This, however, does not include the possible errors due to uncertainties in the reference gas-phase acidities, and those intrinsic to the kinetic method itself. The uncertainty in the measured gas-phase acidities is determined by combining the uncertainties in the slope with

the uncertainty in $\Delta H_{acid}(P_iH_{,avg})$. If the uncertainties of the reference acidity values are the same, then the uncertainty in $\Delta H_{acid}(P_iH_{,avg})$ would nominally be $\frac{\partial \Delta H_{acid}}{\sqrt{n}}$, where n is the number of references. However, the gas-phase acidities for the references are likely not independent and random, many having come from the same source using the same methodology, utilizing relative measurements that are anchored to the same reference. Therefore, the systematic uncertainty is not improved with more references. As described previously,[186] we approximate that half of the uncertainty in the reference values is independent and random whereas half are due to systematic errors, as shown in eq 3. Using the reported $\delta\Delta H_{acid} = 2.1$ for the references, that gives independent and random and systematic uncertainties of ±1.5 kcal/mol.

$$\delta^2\Delta H_{acid} = \delta^2\Delta H_{acid,i\&r} + \delta^2\Delta H_{acid,systematic} \qquad (3)$$

Finally, in calculating the uncertainty we conservatively include a ±1 kcal/mol contribution due to potential error in the kinetic method model. Combining the systematic error, random statistical uncertainty, uncertainty in the kinetic method model and the δ_{slope}, the overall uncertainties in the ΔH_{acid}(APH) for 3- and 4-azidophenols are calculated to be ± 2.0 and ± 1.9 kcal/mol, respectively.

The measured acidities and the corresponding ΔG values for both the azidophenols are listed in Table 3.2, where $\Delta G = \Delta H - T\Delta S$. The entropy term, ΔS_{acid}(APH), required for the calculation is obtained by using frequencies calculated at the B3LYP/6-31+G* level of theory.

Table 3.2. Gas-phase acidities of azidophenols determined in this work.

Phenol	ΔH_{acid}[a]	ΔS_{acid}[b]	ΔG_{acid}[c]
3-azidophenol	340.8 ± 2.0	25.5	333.1 ± 2.0
4-azidophenol	340.3 ± 1.9	25.4	332.7 ± 1.9
phenol	349.0[d]		340.8[d]

[a] Values in kcal/mol [b] Values in eu, obtained by using unscaled calculated frequencies of neutral azidophenol and conjugate base anion azidophenoxide obtained at B3LYP/6-31+G level of theory. [c] Values in kcal/mol at 300 K, obtained by using the equation $\Delta G_{acid} = \Delta H_{acid} - T\Delta S_{acid}$ [d] Reference* [187]

3.3.1 Hammett parameters for the azide group

The determination of the Hammett parameters σ_F and σ_R, for the azide group from the gas-phase acidities are described in this section. As discussed earlier, Taft[172] related the Hammett parameters of the azide to the difference in the gas-phase acidities of 3- and 4- azidophenols with the unsubstituted phenol as shown in eq 4a and 4b.

$$7.7 = 12.2\sigma_R + 19\ \sigma_F + 0.2 \qquad (4a)$$

$$8.1 = 49\sigma_R + 18.6\ \sigma_F + 0.1 \qquad (4b)$$

Solving this pair of equations gives values of σ_F and σ_R to be 0.38 and 0.02, respectively.

3.4 Discussion

To help understand the electronic behavior of the azide, the calculated Hammett-Taft parameters of the azide can be compared with those of some of the common substituents in Table 3.3

Table 3.3. Substituent parameters for some common substituents[a]

Substituent	σ_F	σ_R
COCN	0.66	0.28
CHO	0.31	0.19
NO_2	0.65	0.18
CN	0.60	0.10
CF_3	0.44	0.07
N_3	**0.38**	**0.02**
CH_3	0.00	-0.08
Cl	0.45	-0.17
F	0.44	-0.25
HO	0.30	-0.38
C_2H_5O	0.25	-0.45
σ radical[b]	0.57	-0.47
NH_2	0.14	-0.52

[a] *All values are from ref* [172] *and* [188] *unless noted*
[b] *Reference* [4]

The large, positive σ_F value for N_3 is interpreted to mean that the azide group on an aromatic ring is an inductively electron withdrawing group, comparable to that of CF_3 (0.44), Cl (0.45) and F (0.44) (Table 3.3).[188] For σ_R, a positive value indicates π-electron withdrawing properties of a functional group, whereas a negative value is characteristic of it having π-electron donating abilities. As shown in the Table 3.3, the azido group in a phenol has a value nearly 0 for σ_R, which indicates it has little resonance contribution, and, if there is any, it is withdrawing. This value of σ_R is somewhat surprising in that the azide, a system consisting of multiple π-electrons in conjugation with the aromatic ring and cumulative double bonds, has effectively no contribution to the resonance in the aromatic ring whereas even functional groups like CF_3 and CH_3 have σ_R values of 0.07 and -0.08 respectively.

To explore whether the σ_R value could be a result of an error in our acidity measurements, we have corroborated the results by using electronic structure calculations. The energies of the proton transfer reactions (Figure 3.5) have been computed at the B3LYP/6-31+G* level of theory.

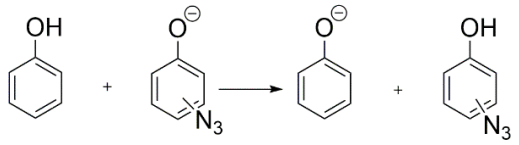

Figure 3.5. Proton-transfer reaction of azidophenols and substituted phenol

As shown in Table 3.4, the calculated relative acidities for the azidophenols are in good agreement with the experimental values.

Table 3.4. Experimental and calculated $\partial\Delta G_{acid}$ and $\partial\Delta H_{acid}$ of the azidophenol isomers[a]

	3-azidophenol		**4-azidophenol**	
	Exp[b]	**Calc[c]**	**Exp[b]**	**Calc[c]**
$\partial\Delta G_{acid}$	7.7	7.5	8.1	8.4
$\partial\Delta H_{acid}$	8.2	8.1	8.7	9.0

[a] Values in kcal/mol.
[b] Values obtained at B3LYP/6-31+G level of theory.*
[c] Values obtained by using literature values of ΔG_{acid} and ΔH_{acid} of unsubstituted phenol (ref [187])

More importantly, the calculated free energy changes, used with the Hammett-Taft equations, lead to predicted σ_F and σ_R values of 0.36 and 0.03 respectively, very similar to the experimentally determined values. In particular, the very small, predicted value of 0.03 for the σ_R is indicative of a negligible π-withdrawing ability of the azide group, similar to what was deduced from the experimental acidities.

Although the lack of π-donating ability seems surprising, it likely can be attributed to the presence of the oxide (O^-) in the phenoxide ring. Considering that the azide is capable of π-donation, there is a competition between its electron donating abilities with that of the other substituents in the system, including the hydroxyl group in the phenol and the oxide in the anion. In other words, the azide is not able to act effectively as a donor because it has to compete with the strong donor ability of the oxide group. This observation has prompted further investigation of azide under a different electronic environment.

To determine the effect of an azide by itself, it can be studied without a competing group. For example, the π-electrons on a carboxylate oxygen are delocalized within the carboxylate group,

thus effectively isolating the system from taking part in any type of resonance contribution with the benzene ring ($\sigma_R = 0$).[172] Therefore, a carboxylate does not create a competing resonance effect, and presents a very different electronic environment to study the azide. Therefore, carboxylic acids could also be used to determine Hammett-Taft parameters. Unfortunately, proton-bound dimer clusters of the benzoates are not formed easily in our mass spectrometer. However, as shown with the phenols, the electronic effect can be accurately predicted by using electronic structure calculations.

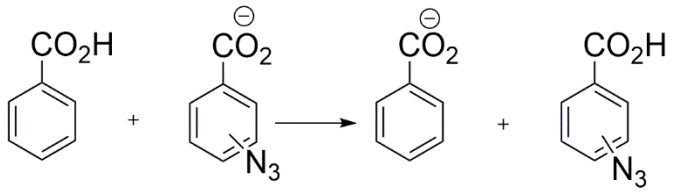

Figure 3.6 Proton-exchange reactions of azidocarboxylic acids and unsubstituted carboxylic acid

Calculations at the B3LYP/6-31+G* level of theory for the proton exchange reaction in eq 6 find $\partial\Delta G_{acid}$ values of 5.6 and 4.5 kcal/mol for 3-azido- and 4-azidobenzoic acid, respectively. The corresponding σ_F and σ_R values for azide in benzoic acid are determined using the relative acidities and the ρ values for deprotonation to be 0.69 and -0.39 respectively.[172] While still having strong electron-withdrawing inductive effects, the large negative value of σ_R indicates a very strong π-donating effect, similar to that of the hydroxy group ($\sigma_R = -0.38$). This result is in stark contrast to the negligible π-effect of the azide as in the azidophenols.

This difference in behavior can be explained by a simple resonance model. In an azidophenol system, there is a competition between the π-donating abilities of the oxide and the azide, as mentioned above. However, resonance theory favors the structures with complete octets and minimal charge separation (Figure 3.7, Scheme 2) which are only possible when the oxide acts as a π-donor and the azide as a π-acceptor. The azide as a π donor (Figure 3.7, Scheme 3) creates unfavorable interaction of negative charges in the ring.

Differences in the calculated geometries of phenoxide ions is consistent with the resonance interpretation shown in Figure 3.7, Scheme 2. The optimized C-O bond lengths in phenoxide and 4-azidophenoxide are found to be 1.275 Å and 1.270 Å, respectively. The shorter C-O bond length in 4-azidophenoxide can be attributed to the increased contribution of the carbonyl-containing

resonance structure in the overall resonance hybrid, which can happen when the azide is a π-accepting group. If the azide were acting as a π donating group, the C-O bond length would be expected to increase due to the increased electron density in the aromatic ring. Therefore, the effect on the geometry is consistent with what would be expected for a π withdrawing group.

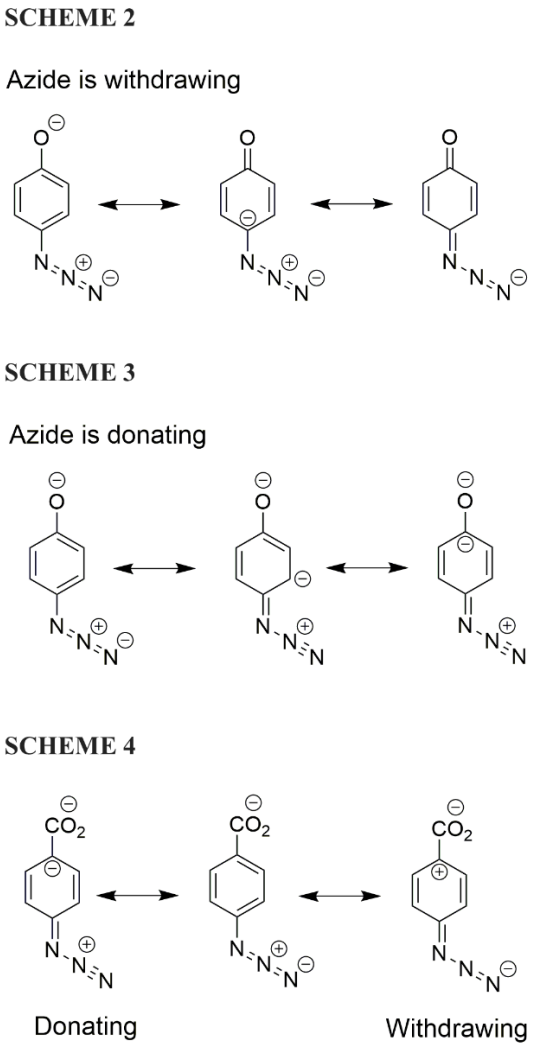

Figure 3.7 Resonance structures of azides in the presence of electron donating (oxide) and neutral (carboxylate) functional groups

With the carboxylate (Figure 3.7, Scheme 4), a π-accepting azide does not have as much stabilizing effect by resonance when compared to the azidophenoxide system. Conversely, a π-donating azide does not have any unfavorable resonance effects on the molecule unlike in the case of the azidophenoxide system. Hence, in situations where the electron demands of the system do

not require it to be a π-acceptor, azide acts nominally as a π-donor, reflected in its σ_R value of -0.39.

This interpretation is also supported by comparing the computed bond lengths for the azidocarboxylate and phenoxide. Calculations at the B3LYP/6-31+G* level of theory predict the terminal N-N bond lengths of the azide to be 1.157 Å in 4-azidophenoxide and 1.148 Å in 4-azidobenzoate. The shorter terminal N-N bond length in 4-azidobenzoate is indicative of more triple bond character, which results from azide acting as a π-donor (Scheme 4). Similarly, the longer terminal N-N bond in 4-azidophenoxide hints at a double bond character where the azide is π-withdrawing (Figure 3.7, Scheme 2). Furthermore, the higher calculated absorption frequency of the NNN stretch at 2229 cm^{-1} for 4-azidobenzoate versus the 2201 cm^{-1} for 4-azidophenoxide is also consistent with increased bond order between the terminal nitrogen atoms. Finally, calculated Mulliken charges at the terminal nitrogen atoms are -1.083 and -1.211 for 4-azidobenzoate and 4-azidophenooxide, respectively, indicating that azide in azidophenoxide is more π accepting.

The different results depending on the competing substituents are indicative of a rare (but not novel) dual electronic nature. The ability to change the electronic effect in response to the environment has been described by Poole as a "*chimeric*" behavior.[189] This dual electronic nature demonstrated by the azide is very similar to that displayed by the N-oxide moiety, which can similarly be explained by its resonance structures (Figure 3.8). Pyridine N-oxides are known to be more reactive than pyridines, displaying penchants for both nucleophiles[190–193] and electrophiles[194–196] depending on the electronic environments.[189] In this respect, we might also consider the azide group to be chimeric, or, perhaps, chameleonic may be more appropriate, in that it can change its properties in response to the environment.

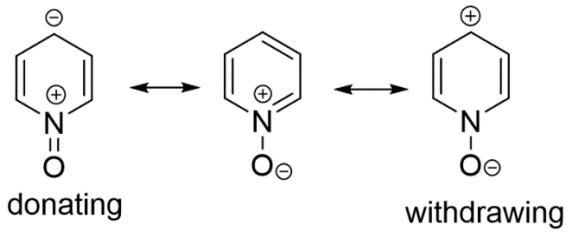

Figure 3.8 Resonance structures of N-oxide as π-donor and acceptor

Poole's assessment in also in agreement with our theoretical predictions of the electronic effect of the N-oxide. Using the same procedures as above, with gas-phase acidities calculated at the B3LYP/6-31+G* level of theory, the effective substituent parameter, σ_R, for the N-oxide moiety, is found to be -0.43 (donating) when using carboxylic acids and 0.07 (withdrawing) with phenols, reflecting chimeric behavior.[189]

The dual nature of the electronic effects of azide have been described previously in the literature. For example, the electron withdrawing and donating abilities of the azide affect the integrated absorption intensities of the NNN bands in infrared spectroscopic studies of substituted phenyl azides.[170,177] Our observations are consistent with the conclusions described in these reports.

3.5 Conclusion

Analysis of the dissociation of proton bound dimers of azidophenols over a series of collision energies provide the gas-phase acidities of 340.8 ± 2.2 and 340.3 ± 2.0 kcal/mol for 3- and 4-azidophenol isomers respectively, resulting in resonance (σ_R) and inductive (σ_F) values of 0.02 and 0.38, respectively. The absence of a significant resonance effect for substitution at the para-position of the azidophenoxide is surprising considering that the azide functional group is a system with delocalizable π-electrons in conjugation with an aromatic system. To test the influence of the strongly donating oxide group in the phenoxide on the substituent parameters, they have been re-examined computationally using the carboxylic acids, and, in that system, the azide is found to be a strong π-donating group, similar to a fluorine, hydroxyl or alkoxy group. However, unlike the other strong π-donors, the azide can modulate the amount of π donation depending on the electronic needs of the system. In this way, the azide group is chameleonic in its resonance effect, always adapting to provide the maximum benefit.

CHAPTER 4. INVESTIGATION OF THE MECHANISM FOR THE CONVERSION OF 4-AZIDOPHENOXIDE TO INDOPHENOL

4.1 Introduction

Nitrenes are one of the most widely studied reaction intermediates with unfilled electronic valences that lead to their high reactivity.[126,197–210] Although structurally similar to carbenes, they exhibit very different reactivity. This difference is attributed to the structure of the lowest energy singlet and the energy difference between the singlet and the ground state triplet of the nitrenes.[211,212] These electronic states and their effects on the gas-phase reactivity of nitrenes have been extensively studied in our lab.[2,3,5] This chapter describes our attempts to carry out bimolecular chemistry of phenyl nitrenes in the condensed phase and explore the mechanism of the observed reactivity.

4.1.1 Bimolecular reactivity of phenyl nitrenes

Phenyl nitrenes have been known to not exhibit carbene like chemistry owing to their inability to access the closed-shell singlet electronic state.[126,197,213] Our lab has previously reported the formation of a closed-shell singlet phenyl nitrene in the gas phase by introducing anionic π-donors such as oxo and methanide. Such substitution unlocked the potential to do bimolecular chemistry with phenyl nitrenes. Photolysis of ortho-azidophenoxide in water revealed the formation of a new product which is proposed to be the ortho-quinonimide formed through H-abstraction of water by the corresponding nitrene (m/z 106). This was further verified by HD exchange experiment that shifted the product mass by one unit (m/z 108). Photolysis of para-azidophenoxide is known to exhibit very different reactivity than that of the ortho isomer.[214] While monitoring the reaction using mass spectrometer, we observed the formation of m/z 198 which was attributed to the indophenol product, similar to the product observed by Grinstein and his coworkers after photolysis of 4-oxidophenylpentazole (OPP).[214] This formation of m/z 198 was accompanied by considerable decrease in the intensity of m/z 269 which corresponds to the proton-bound dimer of the deprotonated azidophenols, whereas m/z 134 (4-azidophenoxide) and m/z 106 (4-oxidophenyl nitrene) didn't change significantly. We decided to investigate this unique reactivity and study the mechanism for the formation of indophenol using mass spectrometry.

4.1.2 Previous studies of the photolysis of para-azidophenol

Grinstein and his coworkers carried out photolysis experiments of OPP in water and acetonitrile and observed the formation of 4-azidophenoxide which further undergoes photochemical reactions to produce subsequent products such as 4-benzoquinoneimine and indophenol.[214] The mechanism for the photolysis of 4-azidophenoxide is proposed to go via a singlet 4-oxidophenylnitrene intermediate resulting in the formation of indophenol as listed in figure 4.1.

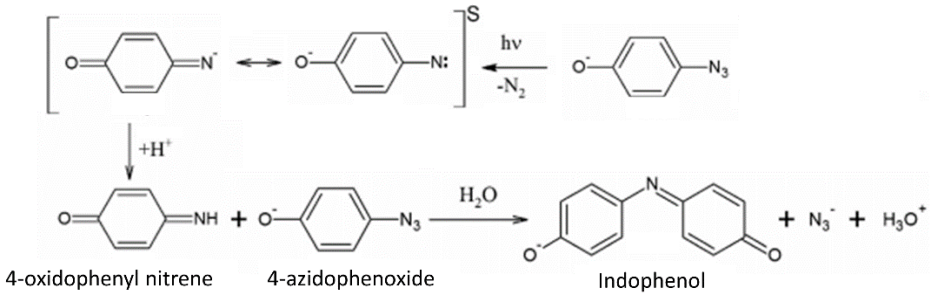

Figure 4.1 Grinstein and coworkers' proposed mechanism for the photolysis of 4-azidophenoxide

According to the proposed mechanism, the azidophenoxide produces the nitrene intermediate upon photolysis by exclusion of a nitrogen molecule and is formed in its singlet state. The singlet nitrene abstracts a proton from the protic solvent to form benzoquinone imine, which then undergoes electrophilic aromatic substitution at the para position of 4-azidophenoxide thus forming indophenol along with the release of an azide anion. However, the mass spectrometric studies of the reaction dispute some of the assumptions made in the above mechanism.

Grinstein considered the loss of nitrogen molecule from the azide as a photochemical step. Our initial photolysis studies conducted on mass spectrometers in the dark reveal the presence of the phenyl nitrene (m/z 106) alongside the azidophenoxide (m/z 134). This indicates that phenyl nitrene is not really a short-lived intermediate in the photolysis reaction as assumed by Grinstein but more so, a species that co-exists with the azidophenols. Its formation could be catalyzed by light, but the requirement to consider nitrene as an intermediate in the formation of indophenol is not necessarily true.

The true nature of the phenyl azide with respect to its electrophilicity and nucleophilicity has always been a matter of debate.[165–170] Our recent studies on the electronic nature of the azide

group (Chapter 3) have shown that azide can act as both π-acceptor or π-donor depending on the nature of its surroundings. In the presence of a strongly π-donating group such as an oxide, azide acts a π-electron withdrawing group imparting a double bond character to the C-N bond in its most stable resonance form (Figure 4.2).

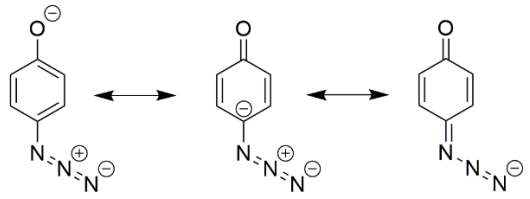

Figure 4.2. Resonance structures of azide as a π-electron donor.

Thus, the assumption of an electrophilic attack by benzoquinone imine at the para-position of the 4-azidophenoxide displacing the azide anion does not hold true. Besides, if the reaction is considered to be an electrophilic aromatic substitution, the leaving group should be electrophilic in nature which N_3^- is clearly not. Furthermore, there is no evidence to suggest that N_3^- could be a reasonable nucleophilic leaving group either, to account for a different kind of aromatic substitution pathway.

In our quest to determine the mechanism for the formation of the indophenol, we stumbled upon the popular Gibbs reaction which is widely used in the determination of phenolic compounds.[215] The highly similar nature of the reaction of phenols with the Gibbs reagent encouraged us to investigate deeper into the mechanistic aspects of the Gibbs reaction.

4.1.3 The Gibbs reaction

The Gibbs reagent (2,6-dichlorobenzoquinone-4-chloroimine) is a very popular analytical reagent used in the detection of phenolic compounds.[216–224] The Gibbs' reaction generally occurs para to the hydroxyl group of the phenoxide and the efficacy of the reaction is determined by the leaving ability of the substituent at the para-position of the phenol. This can include a wide variety of substituents such as carboxylic acids, halogens and alkoxy groups producing the corresponding intensely colored indophenols.[215,225,226]

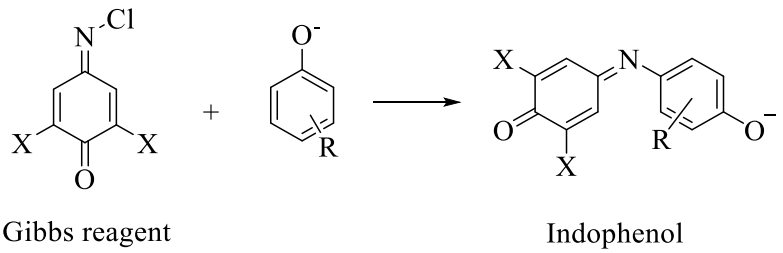

Figure 4.3. The Gibbs' reaction

The mechanism for the reaction has been extensively studied by Pallagi and his co-workers.[225–229] It is reported to proceed via a single electron transfer (SET) to the N-chloroimine, possibly through an external electron source or from the phenoxide to produce 2,6-dichlorobenzoquinone-4-chloroimine radical anion. The chlorimine radical anion can then form indophenols by three different pathways: it combines directly with the free phenoxy radical or it initiates a chain reaction where it reacts with another chlorimine radical anion ($S_{RN}2$ mechanism) or it is transformed into a benzoquinone imine (Figure 4.4). The Pallagi lab's work thus strongly suggests the possibility of a SET mechanism for the Gibbs reaction instead of a two-electron electrophilic aromatic substitution.

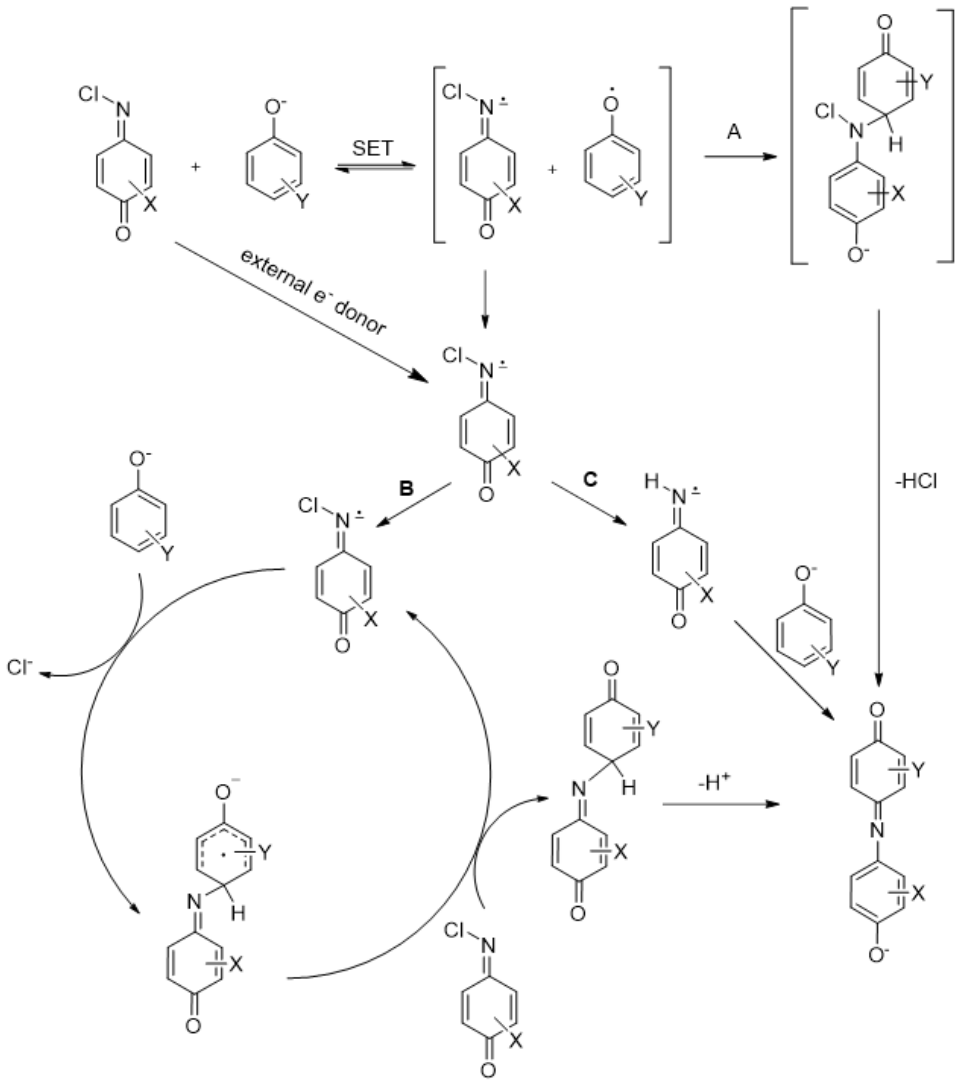

Figure 4.4. Pallagi lab's proposed mechanism of the Gibbs' reaction

We draw parallels between the Gibbs reaction and our photolysis experiments of para-azidophenoxide, where we can compare the role of the Gibbs reagent in the Gibbs reaction to that of the para-oxido phenylnitrene in order to study its reactivity. The para-oxido phenyl nitrenes can be considered to be structurally similar to the Gibbs reagent where the two chlorines on the ring are replaced by hydrogens and the C=N-Cl by C=N-H after a proton abstraction by the nitrene from the solvent. The chlorine attached to the imine in the Gibbs reagent has been proven to play no role in the reactivity. In fact, in aqueous alcoholic solutions, the chlorine gets replaced by a hydrogen thus reducing the chlorimine to an imine.[228] In the Gibbs reagent, the highly electron withdrawing chlorines at the 2- and 6- positions make the benzoquinone imine highly electron

deficient and thus very susceptible to SETs, which is the driving force behind the Gibbs reaction. In the photolysis experiments with para-azidophenoxide, using an external source of energy such as an incandescent light bulb could provide enough energy to compensate for the loss of electron deficiency due to absence of chlorines, to promote SET to the quinone imine. Thus, in theory, the photolysis of para-azidophenol to produce indophenols can be considered to be analogous to the Gibbs reaction and thus warrants further investigations into a possible SET mechanism.

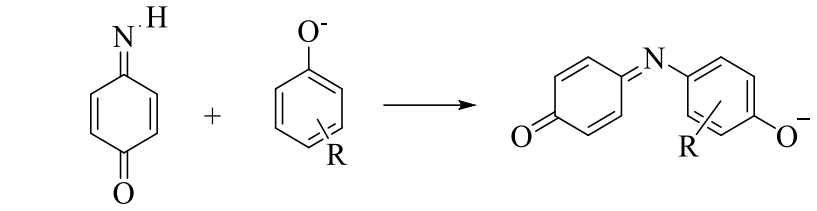

benzoquinone-4-imine indophenol

Figure 4.5. Formation of indophenol from benzoquinone-4-imine

In this project, we have carried out multiple photolysis reactions of para-azidophenoxides in presence of different single-electron donating and accepting agents to explore the possibility of SET mechanism. These SET reagents should only affect the formation of indophenols if the involved mechanism is a single-electron mechanism.

4.2 Experimental

All the reagents, solvents and additives were obtained from commercial sources and used as supplied. The 4-azidophenol was synthesized by using procedure similar to those reported previously.[175]

4.2.1 Procedure for synthesis of 4-azidophenol

To a round bottom flask, 9.16 mmols of 3-hydroxyaniline was dissolved in 25 ml of deionized water and 8 ml of concentrated HCl with stirring. The solution was then cooled to 0^{o}C in an ice bath. Once cooled, 9.16 mmols of sodium nitrite was added to the solution in small portions and the mixture was allowed to stir for 10 minutes. 10.89 mmols of sodium azide was then added to the solution in small portions with constant stirring. Once the addition was complete,

the solution was allowed to warm to room temperature and stirred for an additional hour. The solution was then extracted with ethyl acetate (3 x 25 ml). The combined organic layers were washed with sodium bicarbonate and brine, dried over magnesium sulfate and the solvent was evaporated under reduced pressure to yield 4-azidophenol as a dark brown oil which was used without further purification.

For prolonged use, the azidophenols were stored under cold and dark conditions.

4.2.2 General procedure for sample preparation

The SET influencing agents selected for the photolysis experiments are 1,4-Benzoquinone, Benzophenone, 4'-Fluoroacetophenone, 7,7,8,8-Tetracyanoquinodimethane (TCNQ), Indophenol, Methylene blue and 2′,3′,4′,5′,6′-Pentafluoroacetophenone.

Stock solutions of the azidophenol and each of the additives were prepared in Methanol with concentration of 10mg/ml. A 0.5 M stock solution of KOH was prepared in water to be used as a base for deprotonation of the azidophenol. Samples for ESI were prepared by mixing 200 µl of stock 4-azidophenol solution, 50 µl of the additive stock solution (7 µl in case of TCNQ as its highly intense peaks dominated the mass spectrum), and 14 µl of the KOH solution. The solutions were diluted to 1ml in water-methanol solvent system (1:1) for ESI-MS analysis.

4.2.3 Spectra collection

Electrospray ionization mass spectra were obtained using a Waters Micromass (Milford, Massachusetts) Quattro Ultima Pt triple quadrupole mass spectrometer, equipped with ESI source, operating in negative ion mode.

The reaction was carried out in-situ inside an electrospray syringe (a borosilicate) while spraying its contents directly into the ESI source. Sample solutions were introduced at a flow rate of 5 µL/min into the source. Electrospray and ion focusing conditions were varied to maximize the signal of the proton-bound dimer of the 4-azidophenoxide ion. Time resolved spectra for all the samples were recorded for a duration of 1 hr where a spectrum was collected every 5 minutes. For the first 20 minutes (i.e. the initial four spectra), the sample was kept in complete dark after which the sample was exposed to irradiation using a broad-band light source from a compact fluorescent bulb. Transit time of solution from the syringe needle to the ESI source is calculated to be

approximately 5 minutes at a flow rate of 5 µL/min, which means that sampling of the reaction conditions will occur at approximately 5 minutes from a change in state (light on or off).

4.3 Results

The purpose of carrying out the photolysis experiments of 4-azidophenoxide in the presence of SET reagents is to better understand the formation of indophenols and to test for a SET mechanism. If the SET reagents seem to affect the rate of the reaction or product formation, they would act as good indicators towards a SET mechanism. This section lists the results of all the photolysis experiments carried out in the presence of different SET reagents/catalysts.

4.3.1 Photolysis of clean 4-azidophenol solution

4-azidophenol undergoes Gibbs reaction upon photolysis in a basic solution and the production of indophenol can be monitored by mass spectrometry. The time-resolved mass spectrum of the photolysis of 4-azidophenoxide is shown in figure 4.6.

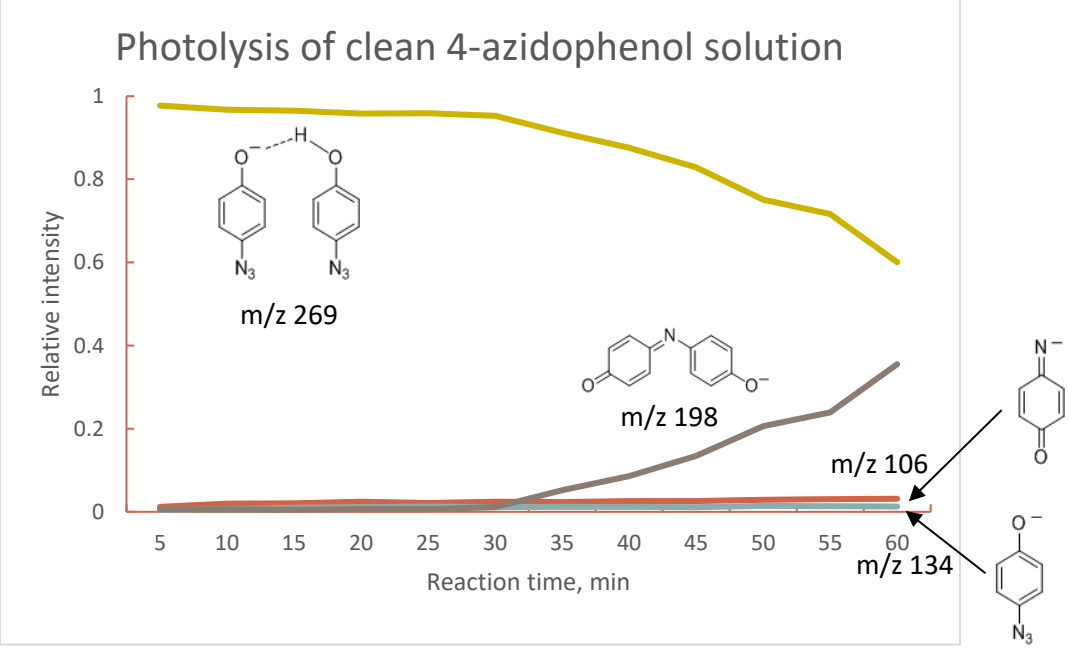

Figure 4.6. Time-resolved mass spectrum of photolysis of 4-azidophenoxide

In the dark, the predominant ions in the mass spectrum are deprotonated azidophenol (m/z 134), m/z 106 which is the quinonimide formed by loss of N_2 from the azidophenol and m/z 269 which is the proton-bound dimer of the azidophenoxide with azidophenol.

This reaction is fast and produces bright blue colored indophenol. The increase in the intensity of the blue color of the solution is a representative of the formation of indophenol. Initially, m/z 269 is the primary component. The reaction is let run in the dark for 20 mins during which there is no change in the intensity of any of the species. After 20 mins, the reaction is exposed to an irradiation by light bulb which results in the formation of a new peak m/z 198, corresponding to the indophenol product. As the intensity of the m/z 198 increases, the intensity of m/z 269 goes down. The peaks of m/z 134 and m/z 106 do not change significantly.

The different types of SET reagents used in these experiments can be primarily classified into two types.

i) Photosensitizers – SET promoters

ii) Single electron inhibitors – SET inhibitors

The effects of sensitizers in the formation of m/z 198 in the presence of different SET reagents are descibed below. Each time-resolved spectrum consists of a relative comparison of the indophenol formation in a clean versus a SET reagent doped solution.

4.3.2 Photolysis in presence of photosensitizers

All these organic photosensitizers consist of a highly conjugated system of double bonds which promote electron delocalization. Due to such a high extent of conjugation, these molecules have a very small energy gap between the highest occupied molecular orbital (HOMO) and lowest energy unoccupied orbital (LUMO). The smaller band gap enables the molecules to get excited easily and enter into their triplet electronic state more efficiently, thus making them ideal SET sensitizers.[230–232] For our photolysis experiments we used some of the most notable photosensitizers such as benzophenone, acetophenone, 4-fluoroacetophenone, Methylene Blue and 2′,3′,4′,5′,6′-pentafluoroacetophenone.

Benzophenone

Benzophenone is a versatile molecule exhibiting remarkable photochemistry.[233] It can jump from its singlet electronic state to the triplet with a nearly 100% yield.[234,235] The effect of the addition of benzophenone on the formation of the indophenol can be seen in figure 4.7.

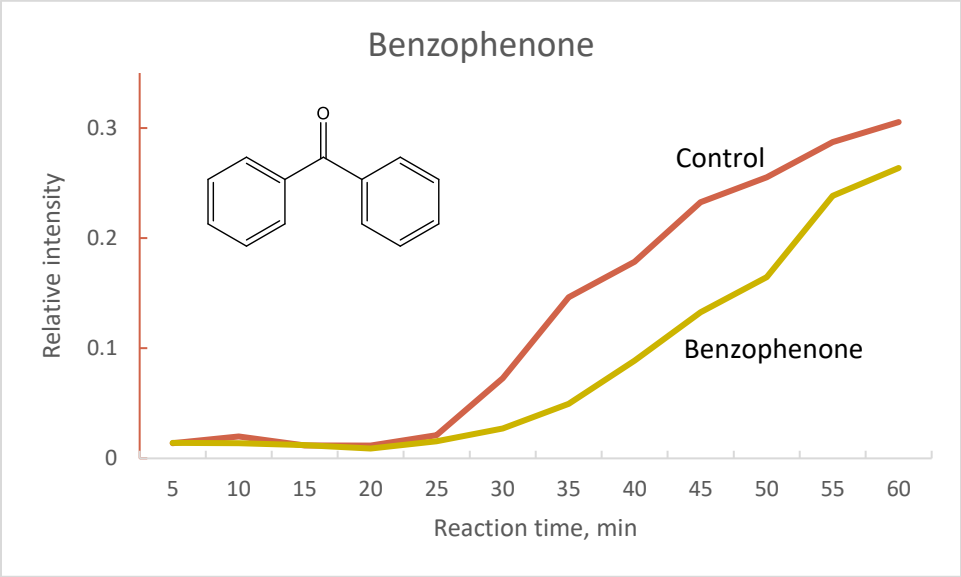

Figure 4.7. Time-resolved mass spectrum of photolysis of 4-azidophenoxide with benzophenone

Doping the reaction mixture with benzophenone produced completely opposite effects than what were expected. The initial 20 mins in dark showed no formation of m/z 198. However after exposure to light, benzophenone in fact slowed down the formation of m/z 198 relative to that of the clean azidophenol solution. This trend was also noticable while tracking the change in color of the reaction. The control solution turned from dark brown to dark green to dark blue in color over the course of 60 minutes indicating an abundance of indophenol at the end of the reaction. However, benzophenone doped solution could only induce a light blue color to the solution in the end indicating a relatively low abundance of the indophenol.

Curious with the result, we repeated the reactions in the presence of other popular photosensitizers.

4'-Fluorocetophenone

The unexpected results shown by the addition of benzophenone prompted us to investigate another ketone-based photosensitizer, 4'fluoroacetophenone. The resulting spectrum is shown in figure 4.8.

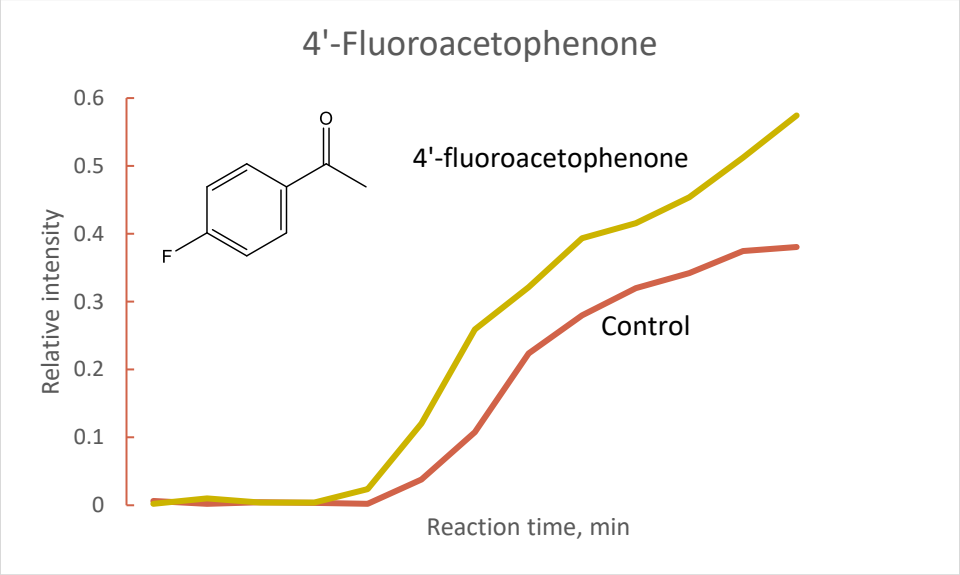

Figure 4.8. Time-resolved mass spectrum of photolysis of 4-azidophenoxide with 4'-fluoroacetophenone

The reaction is run for initial 20 minutes under dark which shows no formation of m/z 198 even in the presence of 4'-fluorocetophenone. On exposure to light, the gradual formation of m/z 198 can be observed, however with a slightly accelerated rate of formation with respect to the control experiment.

This trend is not very noticable with respect to the change in color of the reaction. Both the control and the doped 4-azidophenoxide solutions turn a similar shade of dark blue resulting from the abundant indophenol after 1 hr.

2',3',4',5',6'-Pentafluoroacetophenone

Curious from the results obtained from the 4-fluoroacetophenone experiment, we wanted to study the effect of fluorine on the acetophenone and investigate how that affects the formation of m/z 198. The time-resolved spectrum of the photolysis experiment is shown in figure 4.9.

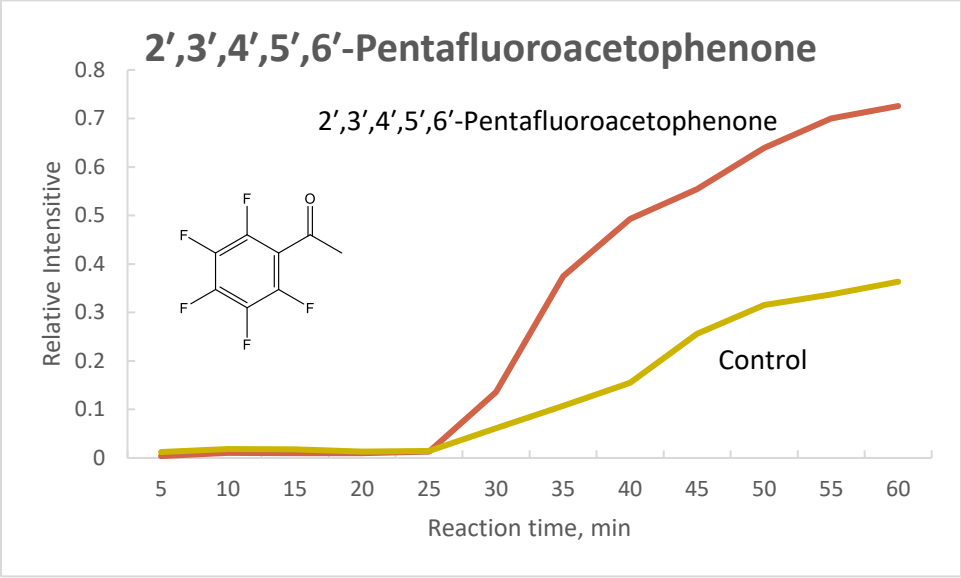

Figure 4.9. Time-resolved mass spectrum of photolysis of 4-azidophenoxide with 2′,3′,4′,5′,6′-pentafluoroacetophenone

In the presence of the pentafluoroacetophenone, the trend in the formation of m/z 198 is completely reversed from that of the previous experiments. As seen from the above spectrum, the rate of the reaction is significantly increased in relation to the control after exposure to light. At the end of 40 minutes of irradiation, the doped solution turns a very dark shade of blue backing our inferences from the mass spectrum. Thus, the presence of fluorines on the phenyl ring of acetophenone can be thought to be influencing the mechanism and the rate of the reaction.

To explore what role do structures of different photosensitizers play in the photolysis, we repeated the experiments using non-ketone based photosensitizers.

Methylene Blue

Methylene blue is a photosensitizer that belongs to phenothiazinium class of compounds. It has been widely used as a histological dye for several years[236–238] and could serve as an ideal candidate for a doped 4-azidophenol photolysis reaction.

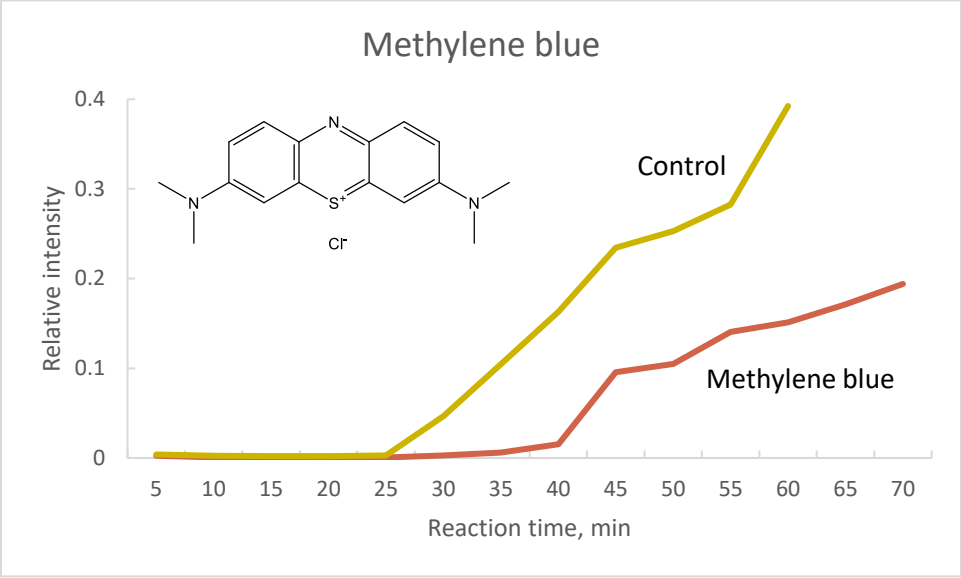

Figure 4.10. Time-resolved mass spectrum of photolysis of 4-azidophenoxide with Methylene blue

As can be seen from the mass spectrum (figure 4.10), methylene blue actually inhibits the formation of the indophenol which also explains the light blue color of the reaction mixture after irradiation by light for 40 minutes.

Next, in order to test the hypothesis that the reaction is self-catalyzed, we repeated the photolysis reactions using commercially available 2,6-dichloroindophenol as a photosensitizer.

2,6-dichloroindophenol

The time-resolved mass spectrum of the photolysis reaction in the presence of an external indophenol photosensitizer is shown in figure 4.11.

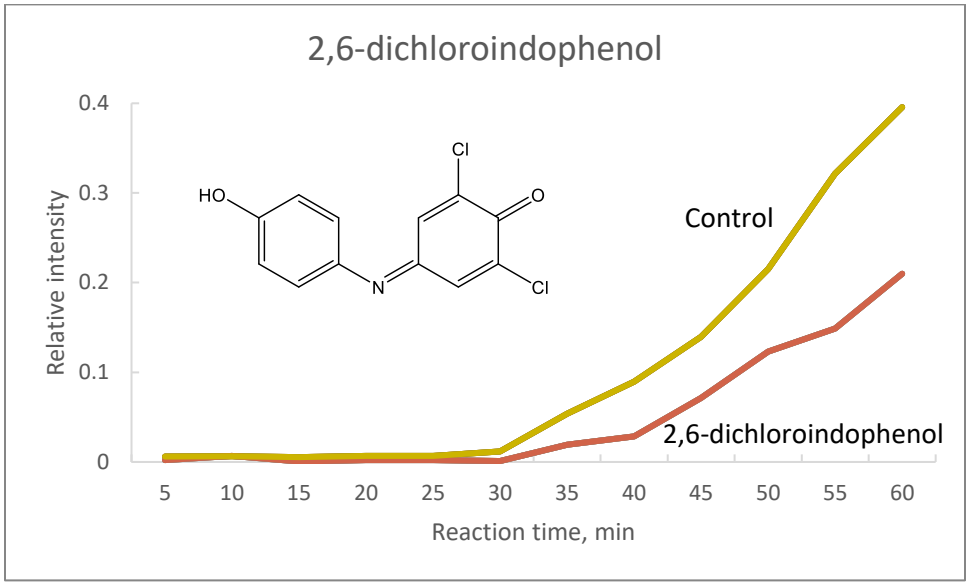

Figure 4.11. Time-resolved mass spectrum of photolysis of 4-azidophenoxide with 2,6-dichloroindophenol

The reduction in the rate of formation of m/z 198 shows that 2,6-dichloroindophenol actually has a similar effect on the photolysis as that of methylene blue resulting in a very light blue color solution at the end of 1 hr. It thus seems that indophenol itself may not be involved in photo-catalyzing its own formation.

4.3.3 Photolysis in presence of SET inhibitors

Similar to the use of SET promoters, SET inhibitors can also be expected to affect the rate of the photolysis reaction if the mechanism involves SETs. These electron scavenging molecules can also be considered as oxidizing agents where they would accept electrons transferred to them from other molecules by the virtue of which they would get reduced themselves. Assuming that the single electron mechanism is true, introducing such molecules into the photolysis reaction of 4-azidophenoxide would result in competition for the electrons between the molecules and the benzoquinone imine thus in turn affecting the rate of the reaction.

We used two notably popular electron scavengers tetracyanoquinodimethane (TCNQ) and benzoquinone.

Tetracyanoquinodimethane (TCNQ)

TCNQ is a relative of para-quinone and a well-known electron scavenger used in preparation of charge transfer salts.[239–242] TCNQ can thus be expected to get reduced during the photolysis of 4-azidophenoxide to form the reported, blue-colored radical anion. The effects of doping with TCNQ can be seen in the mass spectrum in figure 4.12.

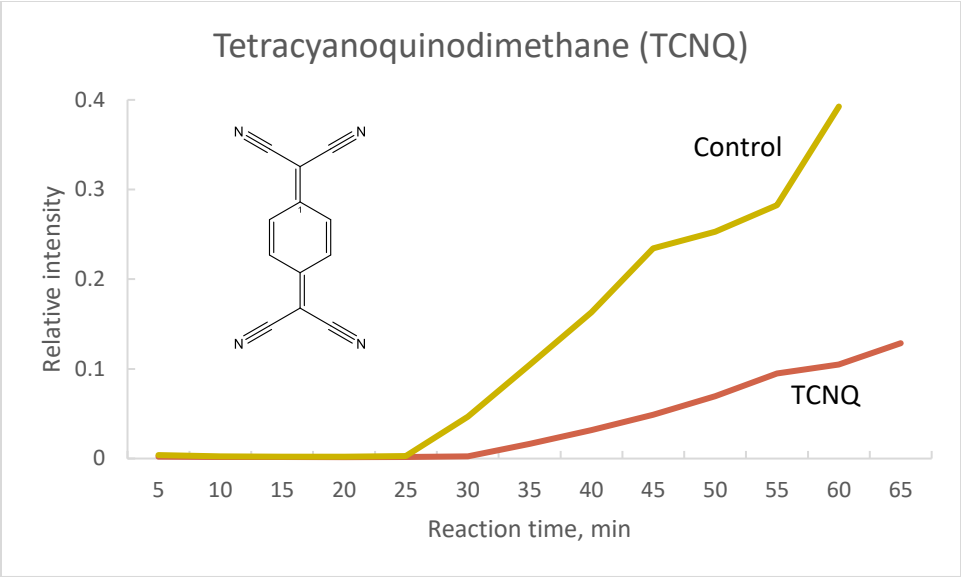

Figure 4.12. Time-resolved mass spectrum of photolysis of 4-azidophenoxide with TCNQ

For the initial 20 minutes under dark, there was no formation of the m/z 198 peak with respect in both control and the doped solutions. However, after irradiation by light bulb, the TCNQ doped solution did not show any formation of m/z 198 until the later stages of the reaction. Even then, the rate of formation of m/z 198 was much slower than that of the control. This could also be monitored by the color change of the solution which turned light green at the end of the reaction.

Para-benzoquinone

Para-benzoquinone is an another member of the quinone family that readily accepts electrons and protons from a proton source to get reduced to the more stable and aromatic hydroquinone, the driving force for the electron scavenging being the regained aromaticity.[243–249] The effect of the presence of para-benzoquinone on the photolysis reaction of 4-azidophenoxide can be seen in the mass spectrum shown in figure 4.13.

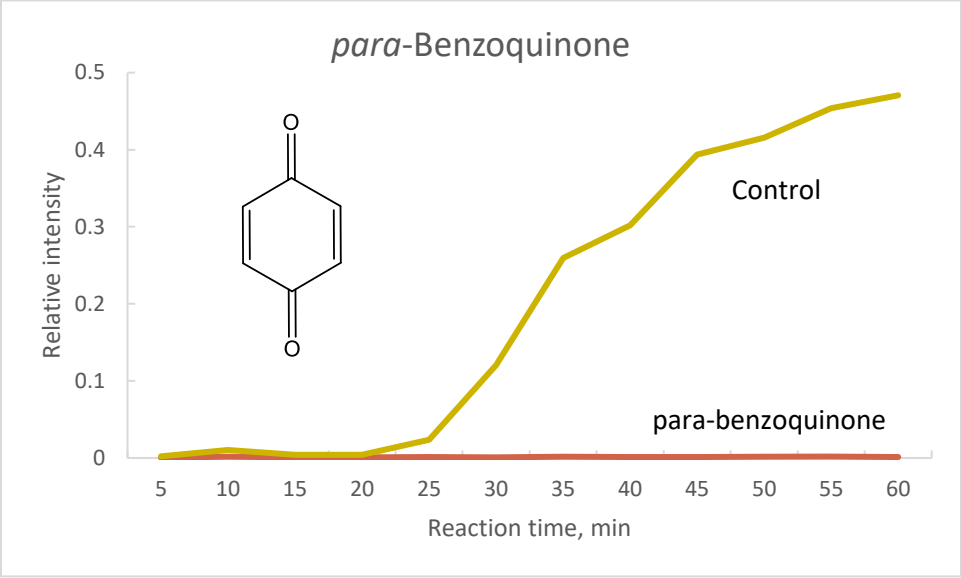

Figure 4.13. Time-resolved mass spectrum of photolysis of 4-azidophenoxide with *para*-benzoquinone

The mass spectrum shows a complete suppression of m/z 198 in the presence of para-benzoquinone even after irradiation by light for more than 40 minutes. This absence of the formation of indophenol can also be seen in the color of the solution which remains dark brown throughout the course of the reaction.

4.4 Discussion

From the photolysis of the clean 4-azidophenol solution, it can be seen that m/z 269, m/z 134 and m/z 106 exist simultaneously even under dark at time t=0. This means the photolysis/thermolysis step of azide converting into the nitrene is likely not an intermediate in the photolysis reaction. For the initial 20 minutes under dark, no photolysis reaction takes place as evident from the lack of m/z 198. This is different from the Gibbs' reaction which takes place spontaneously even in dark. Adding an external source of irradiation makes the reaction go forward as can be seen from the gradual increase in the intensity of m/z 198. Different photosensitizers can be seen to impact the reaction in different manners.

The photosensitized reactions typically occur via two types of pathways.[250,251]

Type 1 – In type 1 photochemical process, a ground-state photosensitizer gets excited into its reactive excited state by an external energy source. The excited photosensitizer undergoes electron

transfer reactions with substrates to produce products. The excited photosensitizer can also react with ground-state oxygen molecule to produce reactive singlet oxygen species. The mechanisms may involve either acquisition or loss of single electrons to form radical anion or radical cation species. The radical anions can react with oxygen to produce superoxide radical anion ($O_2^{\bullet -}$) which could undergo dismutation or one-electron reduction to give super reactive hydroxy radicals ($HO^{\bullet}$). All of these oxygen species are collectively called as reactive oxygen species (ROS).

Type 2 – In type 2 of photosensitizing reactions, the photosensitizer is excited by an external energy source and goes into the triplet state. In triplet state, it undergoes collisions with dissolved ground-state triplet oxygen and excites it into the reactive singlet state. The reactive singlet oxygen then transfers it energy to the substrate molecule by collisions to produce products. This type of pathway results in the photosensitizer being quenched by the ground-state triplet oxygen molecule.

At a given point of time, these mechanisms can run parallel with each other and occasionally even compete with each other. These pathways for photosensitization also introduce the role of dissolved molecular oxygen into the scope of our photolysis reactions.

Acetophenones are a class of photosensitizers that are known to generate free electrons on excitation.[252,253] They follow the type -1 mechanism where an acetophenone molecule donates a free electron to the molecular oxygen to produce ROS which further react with the substrate molecules to produce subsequent products. The fact that addition of fluoro derivates of acetophenone drives the reaction forward significantly, only means that the reaction is highly responsive to single electron availability. The faster rate of formation of indophenol in the presence of the fluorine substituents could be due to the fact that the more electronegative fluorines would induce more stabilization to the acetophenone radical than the hydrogens, meaning the fluoro-acetophenones would be able to "hold" free electrons much better and longer than the unsubstituted acetophenones.

In a similar manner, the drops in the rates of photolysis in the presence of TCNQ and para-benzoquinone can also be explained. Both the reagents are well known single-electron scavengers that are highly electron deficient and very prone to accept free electrons to regain their aromaticity. This behavior could result in competition with the single electron accepting benzoquinone imine, resulting in slower rate of formation of the indophenol as seen from the mass spectrum.

The failure of methylene blue to promote the SET process in the photolysis could be due to the fact that methylene blue is very sensitive to pH where the excited methylene blue could act as an electron acceptor and get quenched. This quenching of methylene blue has been reported in the literature where it is known to absorb single electrons twice followed by proton abstraction to form the colorless leuco-methylene blue[254–256] (Figure 4.14)

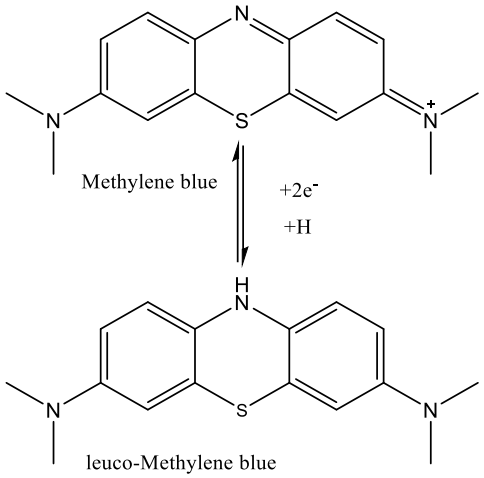

Figure 4.14. Redox conversion of Methylene blue to leuco-Methylene blue

The basis of using an external indophenol as additive was to determine if the indophenols are capable of catalyzing their own formation since they are bright blue colored with absorbance possibly in the visible light spectrum. It is possible that as indophenol is formed during photolysis, it photo-catalyzes its own formation which can be explained by the increasing reaction rate. However, the addition of indophenol only seemed to lower the rate of reaction indicating that the indophenol might only be acting as an electron scavenger. The double chlorine substitutions on the indophenol might make the indophenol more electron deficient and thus much more capable of scavenging free electrons than the indophenol product formed from the photolysis. This could explain why the indophenol product does not hinder its own formation but a 2,6-dichloroindophenol does.

All the above experiments point towards an involvement of a SET mechanism for the photolysis of 4-azidophenol to form indophenols. One of the most crucial elements for the photosensitization mechanism is the dissolved molecular oxygen. Molecular oxygen is a high energy oxidizing agent and therefore an excellent electron acceptor. That is why it plays a very

crucial role as a terminal electron acceptor in electron transport chains in biological processes.[257] In an SET mechanism, oxygen dissolved in the solvent is thus expected to play a crucial role and have an impact on the outcome of the reaction. If the photolysis of 4-azidophenol occurs from an SET mechanism, the abundance or scarcity of oxygen molecules in the solution could thus be supposed to induce drastic effects on the photolysis. In the next section, we have studied the effects of dissolved oxygen concentration on the rate of the reaction.

4.5 Effect of oxygen

In the presence of excess oxygen, the reaction should be expected to proceed at a quicker rate than that under normal conditions. Similarly, in an oxygen deficient system, the reaction rate should be expected to be slower. This would also help us to confirm or refute the possibility of SET mechanisms for the reaction.

4.5.1 Experimental

In this section, the photolysis experiments have been repeated in the presence and absence of dissolved oxygen.

4.5.1.1 General procedure for sample preparation

To prepare oxygen rich samples for analysis, oxygen gas was bubbled through 10 ml of water-methanol solvent system (1:1) in a round bottom flask for 1 hour. To a 200 µl of stock 4-azidophenol solution, 50 µl of 0.5M KOH stock solution was added and diluted to 1 ml by the oxygenated solvent. The sample was then directly sprayed by ESI-MS for mass analysis.

To prepare oxygen deficient samples, freeze pump thaw method was used. 10 ml of water-methanol solvent system (1:1) was kept in a liquid nitrogen bath for 1 hour under vacuum. After 1 hour, the vacuum was removed and the solvent was stored under positive nitrogen pressure. Samples for spraying were prepared in a similar manner as the oxygenated samples using the deoxygenated solvents for dilution.

The samples for control experiments were prepared as mentioned in the previous section.

4.5.2 Results

Oxygenated vs deoxygenated solutions

The time-resolved mass spectrum in figure 4.15, is a combination of mass spectra of two samples, one with 4-azidophenol in the presence of excess oxygen in the solution and one in a deoxygenated solution.

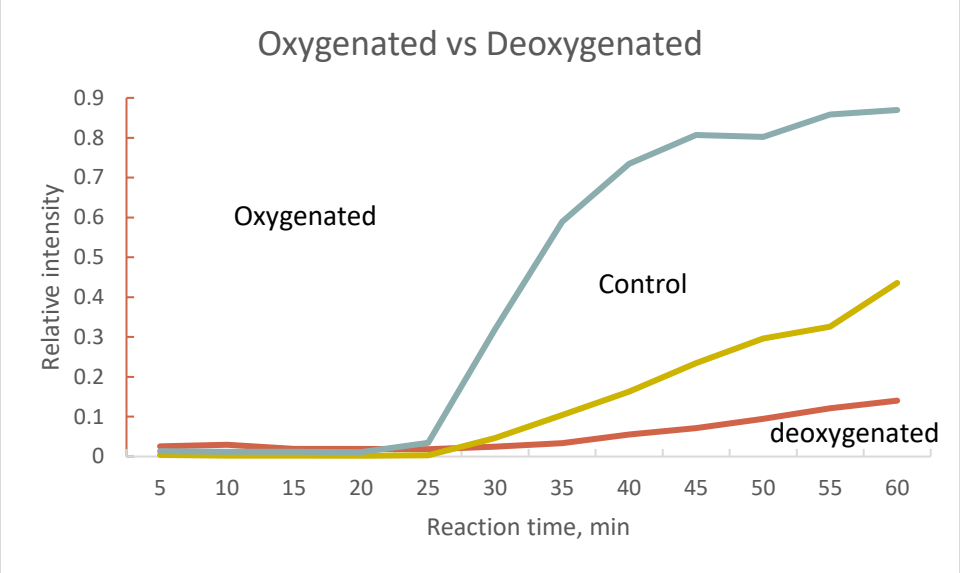

Figure 4.15. Time-resolved mass spectrum of photolysis of 4-azidophenoxide in the oxygen rich and oxygen depleted solution

As evident from the spectra, there is no formation of m/z 198 for the initial 20 minutes of the reaction under dark under any conditions. After exposure to light, m/z 198 peak in the oxygen rich sample rises dramatically as compared to that in the control experiment, whereas in the oxygen depleted sample, the formation of m/z 198 can be seen over time at a much slower rate than that of the control experiment.

Thus, it can be seen that the results obtained from these experiments align very well with the SET mechanism.

4.5.3 Discussion

The above time-resolved mass spectra show us that oxygen plays a very crucial part in the mechanism of the photolysis reaction. In a solution saturated with dissolved oxygen, electrons

from the phenoxide would be transported to the benzoquinone imine with a high efficiency resulting in increased concentration of indophenol. A reverse trend can be seen in the mass spectra of oxygen depleted samples. With a low concentration of dissolved oxygen in the solution, the electron transport is not efficient which results in the decrease in the rate of formation of indophenols.

4.6 Conclusion

From all the above experiments, it is evident that the photolysis of para-azidophenol does not proceed via a two-electron pathway, otherwise the single-electron photosensitizers, inhibitors and dissolved oxygen would have no influence on the rate of the reaction. Instead, all the results point towards SET processes, since their rates are affected by different SET reagents and molecular oxygen which are known to react only via SET mechanism.

Hence, we propose a mechanism very similar to that of the Gibbs' reaction where indophenols form photochemically from a SET from the azidophenoxide to the benzoquinone imine. Dissolved molecular oxygen serves as an electron transfer agent to facilitate the reduction of benzoquinone imine.

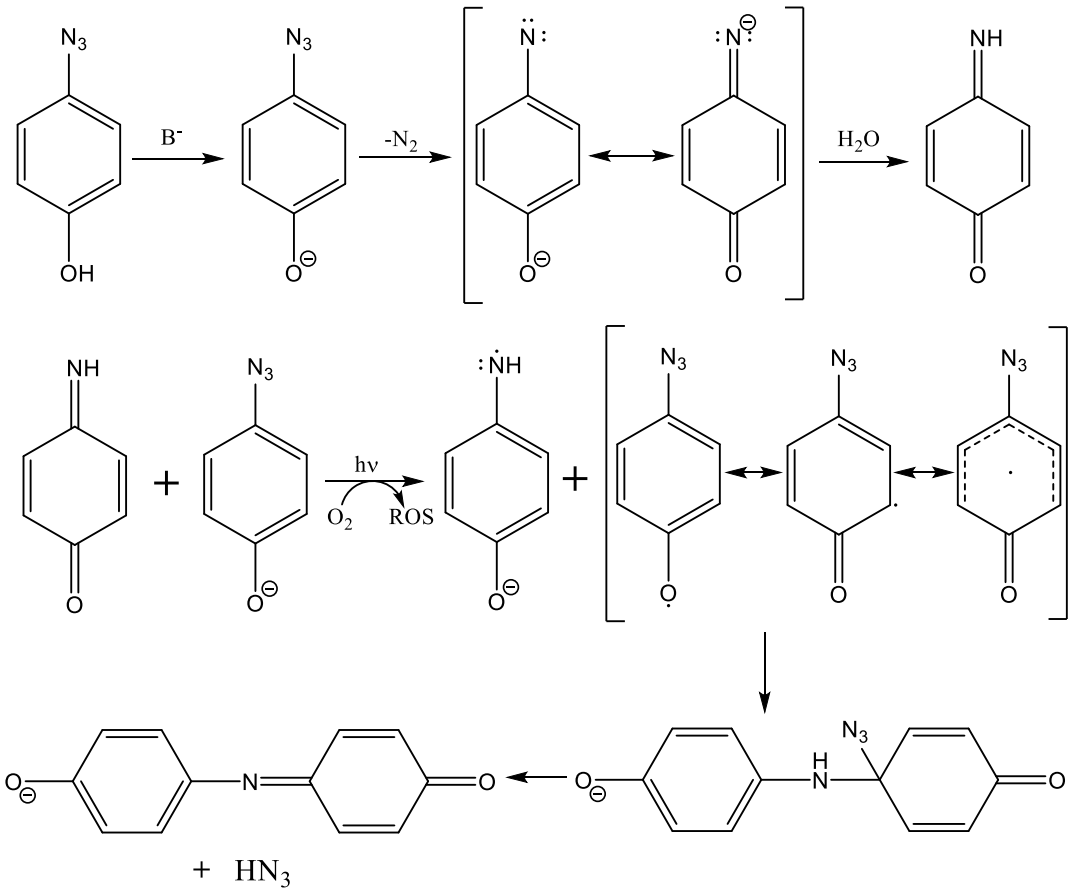

Figure 4.16. Proposed mechanism for the formation of indophenol from azidophenols by SET mechanism

This reaction is thus a photochemical version of the Gibbs' reaction which uses energy from an external incandescent light source as a driving force for SET processes.

CHAPTER 5. TUNING THE ELECTRONIC STATES OF AROMATIC NITRENES

5.1 Introduction

This chapter focuses on our efforts to control the electronic states of aromatic nitrenes. The reactivity of aromatic nitrenes depend on the difference in energy and structures of their electronic states. Manipulation of these electronic states and their energies could unlock the potential to do interesting chemistry with the aromatic nitrenes.

5.2 Electronic states of nitrenes

Nitrenes are a fascinating class of intermediates similar to carbenes but exhibit very different reactivity. For example, phenylcarbene in solution readily forms adducts with alkenes and inserts into C-H bonds,[122] whereas phenylnitrene gives mostly polymeric tar.[258] The difference in reactivity is attributed to the difference in the electronic structures and the energy barrier between ground state triplet and the lowest energy singlet.

In comparison with its carbon analogue phenylcarbene, phenylnitrene is also a ground-state triplet similar to the phenylcarbene, but whereas the lowest energy singlet in phenylcarbene is a closed-shell σ^2 state that is about 2-5 kcal/mol above the triplet, the singlet in phenyl nitrene is an open-shell, $\sigma\pi$ state, with a singlet-triplet splitting of 15 kcal/mol.[259] Even higher in energy is the closed-shell σ^2 state which is 30 kcal/mol higher than the triplet. Both the phenyl carbenes and phenyl nitrenes also have a highest energy closed-shell π^2 electronic state which has the maximum electron-electron repulsion.[117–123] The unique chemistry exhibited by the carbenes is accessed through their triplet ground state, which is achieved by a process called as intersystem crossing (ISC) from the lowest energy σ^2 singlet state to the ground-state triplet. In nitrenes however, the ISC becomes extremely slow and highly unfavorable because of the structure and energy of the low-lying open-shell singlet.

5.2.1 Impact of open-shell ground state singlet on ISC

To understand how an open-shell singlet ground state affects the ISC, it is important to consider the differences in the geometries of the phenyl carbenes and nitrenes (Figure 5.2)

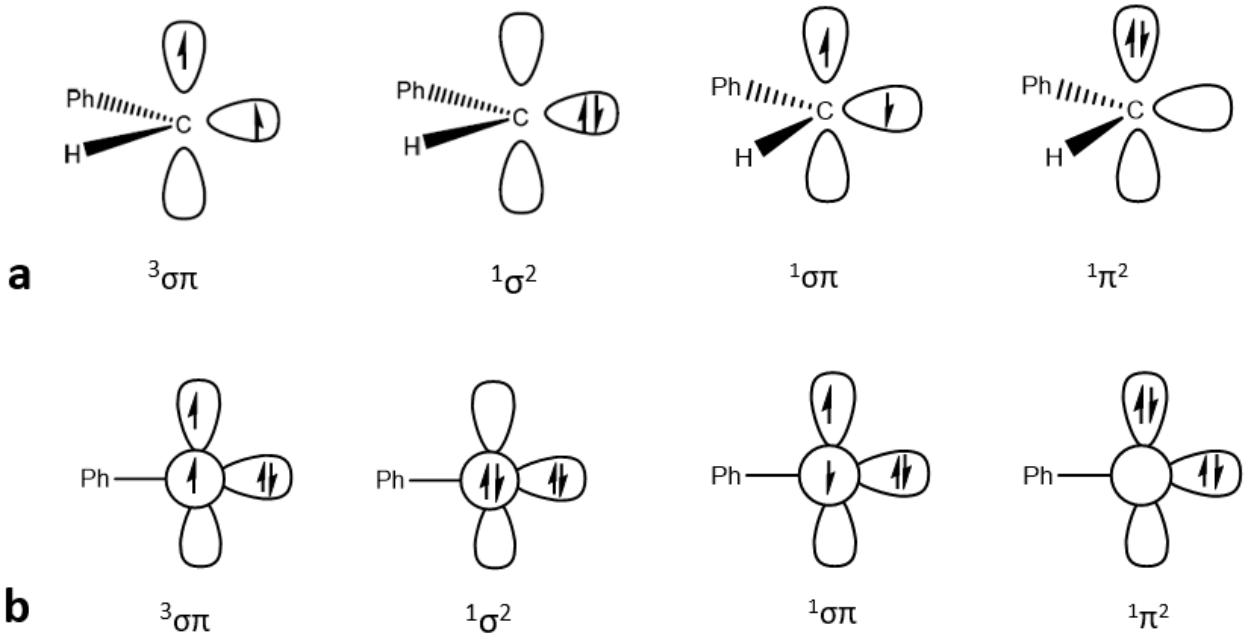

Figure 5.1. Comparison of electronic states of a) phenyl carbenes and b) phenyl nitrene

Phenyl nitrene is a monovalent, two-electron, nitrogen-centered molecule that is sp hybridized with the non-bonding electron pair lying in the sp orbital. The sp hybridization ensures that the p orbitals available to the electrons are degenerate. This degeneracy results in the differences in the ordering of the electronic states of the phenyl nitrene as compared to the phenyl carbenes, where the lowest-lying singlet state in phenyl nitrene is the open-shell in the energy diagram in contrast to the closed-shell singlet in phenyl carbene.[259]

This lowest energy open-shell singlet is responsible for drastically reducing the rates of ISC, which are found to be almost 100 to 1000 times slower (~$10^{6\text{-}7}$ s^{-1}) than that in phenylcarbene ($\geq 10^9$ s^{-1}).[260] This difference in rates can be attributed to the conservation of momentum between the molecules. In phenyl carbene, the change in the spin angular momentum of the electron is accompanied by a change in the orbital angular momentum to transition into the triplet state. However, the phenyl nitrene, in its open-shell singlet state does not have an available orbital for the same offset of the angular momentum in phenyl carbene. The lack of such offset is responsible for making the ISC more difficult and significantly slower.[121] As the phenyl nitrene is unable to transition into the triplet state, its reactivity is heavily influenced by the open-shell singlet state where the phenyl nitrene favors intramolecular rearrangements instead of a bimolecular reactivity.

These intramolecular rearrangements result from the ability of the phenyl nitrene to access its π^2 electronic state which frees an in-plane p-orbital to accept electrons from the aryl ring.[260] Such ring expansion results in the formation of a ketenimine via a benazazirine transition state. The ketenimine can further undergo polymerization processes to produce a black polymeric tar. When the reaction is carried out in the gas phase, the phenyl nitrene can undergo a ring contraction to form cyclopentadiene nitriles (Figure 5.1).

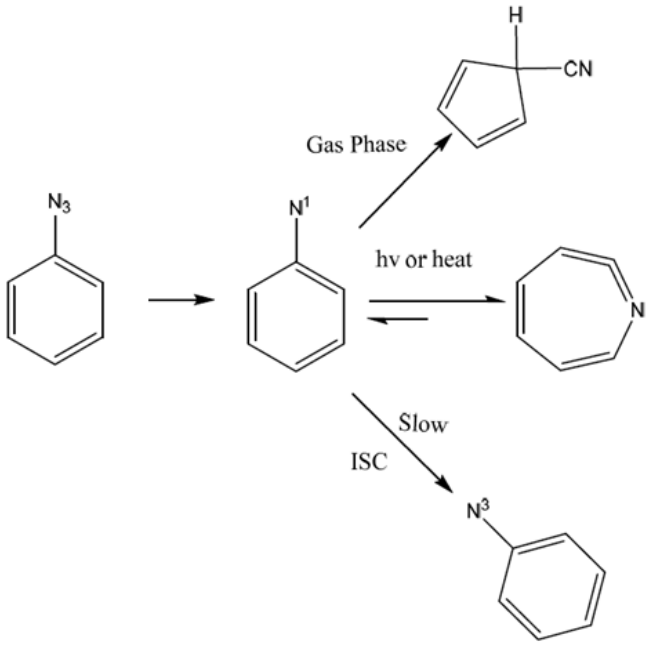

Figure 5.2. Undesirable reactivity of phenyl nitrenes

Thus, for singlet nitrenes, most of the reactivity is dominated by these rearrangement processes which are significantly faster than the ISC resulting in limited access to develop useful bimolecular chemistry for synthesis of more complex products.[121,122,215,261]

5.2.2 Promoting ISC

Our lab has mainly focused on two different ways to make the ISC more favorable -

i) Lowering the energy of the closed-shell σ^2 singlet than the open-shell $\sigma\pi$ singlet to attain a more carbene like electronic arrangement allowing access to the spin-orbit

coupling mechanism This would ensure that ISC becomes the favored process through the accessible ground-state closed shell singlet[260]

ii) Hindering the rearrangement process and lowering the energy of the ground state σπ singlet to reduce the energy barrier and make it easier for ISC to occur.

Our attempts to use anionic substitution to obtain a lowest energy singlet of σ^2 electronic state have met with success and have been discussed in the earlier chapters. Here, I describe our attempts to follow the other route to promote ISC which is to lower the energy of the σπ singlet.

During the studies on chloro-substituted phenyl nitrenes, our lab found systematic effects on the singlet-triplet splitting of chlorosubstituted phenylnitrenes despite only minor differences in energy among the different substituents.[262] Negative ion photoelectron spectroscopy revealed a difference in the geometries between the ortho and para isomers and the meta and unsubstituted isomers. The effects were particularly seen in ortho- and para-substituted phenyl nitrenes where the stabilization of the open-shell structure was observed due to the quinoidal resonance structures (Figure 5.3).

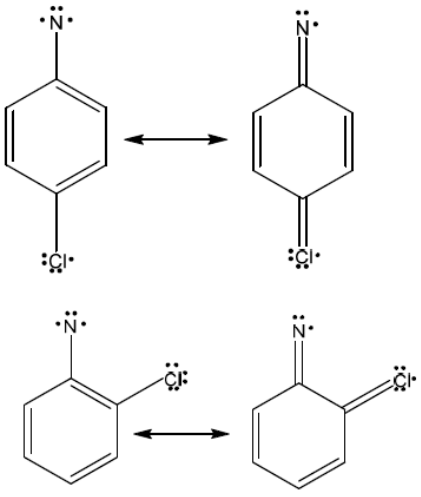

Figure 5.3. Quinoidal resonance structures of ortho and para-chloro substituted phenyl nitrenes

This stabilization however, cannot be associated with the standard two-electron resonance structures as they can only affect the closed-shell systems. Only a single-electron resonance model will allow the stabilization of open-shell electronic states.[263] Thus, the ortho and para-isomers can

be stabilized by the quinoidal resonance structures formed by π-radical delocalization and consisting of neutral diradicals with electrons localized on both the chlorine and nitrogen atoms.

This stabilization has been studied in a great detail by Borden and Davidson.[208,264] These quinoidal resonance structures allow the two electrons of the open-shell singlet to be separated in space by keeping them localized on separate atoms, thus minimizing the electron-electron repulsion. As these electrons are non-disjoint, the stabilization of the triplet state can occur through exchange interactions. However, separating the electrons spatially in the quinone resonance structures would minimize any stabilization of the triplet state that could occur through exchange interactions of spin-paired electrons.

In alignment with the study mentioned above, we attempted to develop a suitable aromatic nitrene model with the appropriate substitution that should reduce the open-shell singlet and triplet energy gaps and promote ISC into the triplet electronic state.

5.2.3 Towards developing an efficient system for σπ singlet stabilization

From the aforementioned studies, it is clear that spatial separation of the two electrons in the σπ singlet is very critical for minimizing electron-electron repulsions. One obvious way of ensuring maximum spatial separation is to increase the length of conjugation in the aromatic backbone that would keep the electrons further away from each other. Some extensions on the phenyl ring system are the fused ring systems such as 9-anthrylnitrene, 1-napthylnitrene, and 2-napthylnitrene (Figure 5.4).

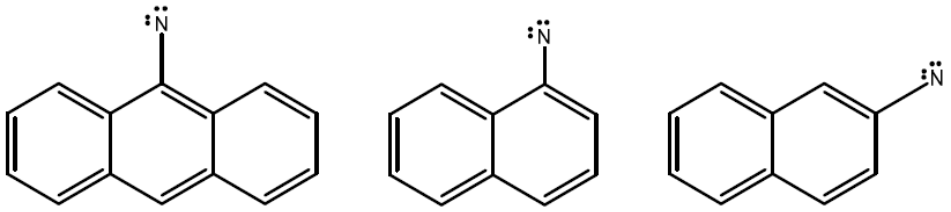

Figure 5.4. Fused ring nitrenes

Tsao and coworkers calculated the singlet-triplet energy gap to be 16.6 kcal/mol and 13.9 kcal/mol for 2-napthyl nitrene and 1-napthyl nitrene respectively.[265,266] Even though the singlet-

triplet splitting energy of these molecules does not differ from phenylnitrene, there is a significant extension in the lifetime of the singlet nitrene.

With very little difference in the energies of the phenyl and napthyl nitrenes, their reactivities were also expected to be similar even after introduction of asymmetry due to the extra phenyl ring. As predicted, the photolysis reactions of 1- and 2-napthyl nitrenes produced the respective ketenimines avoiding the azirines that are formed using the bridgehead carbons to maintain aromaticity of atleast one phenyl ring.[267–275] The ketenimines were formed reluctantly at the expense of loss of aromaticity of the molecule. Although, a crucial observation were the longer-lasting azirine transition states with lifetimes ≥150μs that enabled the transition into the triplet state to form azo dimers.[265]

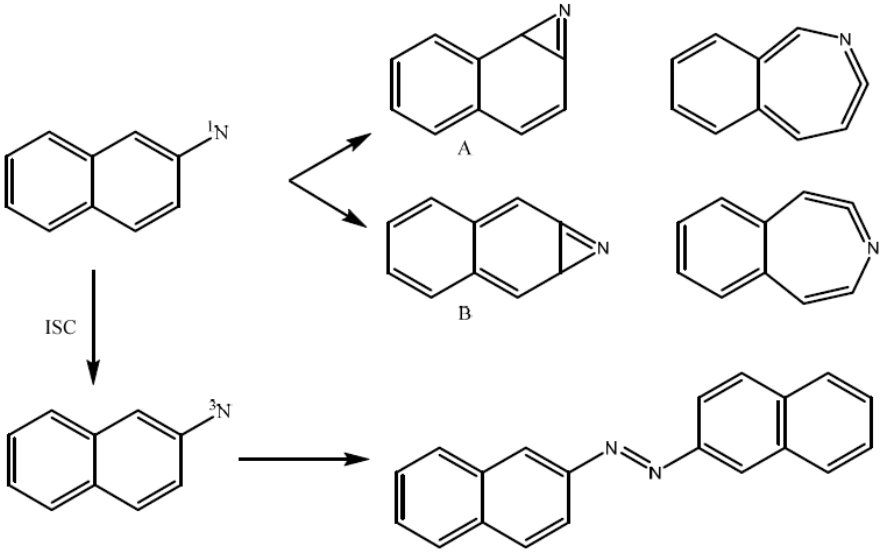

Figure 5.5. photochemistry of 2-napthyl nitrene

In case of the napthyl nitrenes, azirines were formed quite easily as the molecules were still able to retain the aromaticity of atleast one of the phenyl rings by avoiding the bridgehead carbons. However, this was not the case with 9-anthryl nitrenes. With the incorporation of one more phenyl ring, the nitrene is forced to incorporate one of the bridgehead carbons into azirine formation which would result in the loss of aromaticity of two phenyl rings. This process is expectedly much slower than in either of phenyl or napthyl nitrene. Initial calculations at CASPT2(14, 14)//CASSCF(14,14) level of theory with 6-31G* basis set showed a singlet-triplet splitting energy of 5.27 kcal/mol in

9-anthrylnitrene.[276] This value is nearly one third of the energy gap of phenylnitrene. The calculations also showed the formation of the azirine to have a transition state 23 kcal/mol higher in energy than the low lying open-shell singlet. Even if the azirine forms, the barrier is less than 1 kcal/mol to revert to the nitrene. The formation of the triplet anthryl nitrene can also be observed during laser flash photolysis experiments from the decay of singlet anthryl nitrene. In addition, the lifetime of the singlet anthryl nitrene was calculated to be 17 ns which is significantly shorter than the napthyl nitrene.[277] In can thus be concluded that, increasing the length of conjugation by expanding the aromatic system seem to drastically favor the ISC.

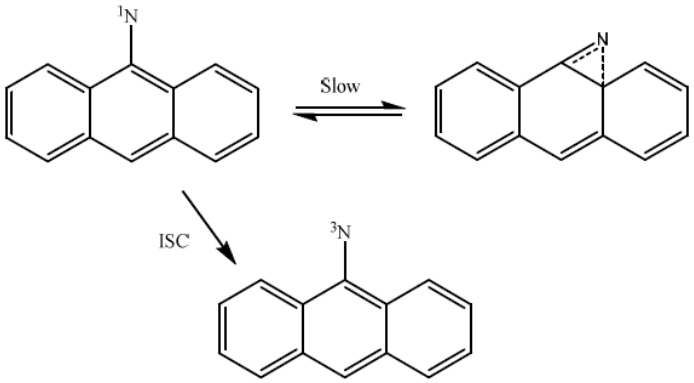

Figure 5.6. Chemistry of 9-anthryl nitrene

Another way of stabilizing the open-shell singlet nitrene is the incorporation of hetereoatoms in the aromatic systems. It has been shown that, using a furan backbone in furanyl nitrenes, significant decrease in the singlet-triplet splitting can be obtained due to the induction of "super radical stabilizers".[278,279] The furanyl nitrenes are very similar to phenyl nitrenes with respect to the ordering of electronic states on the energy scale and the spatial separation of the two electrons.[280] However, in case of 2-furanyl nitrene, the singlet-triplet splitting is calculated to be 10.9 kcal/mol which is significantly smaller than the phenyl nitrene or even the 3-furanyl nitrene. Although 2-furanyl nitrene has a relatively stabilized triplet state when compared to phenyl nitrene due to the induction of the oxonium ions in the polar resonance structures, it also has a highly stabilized singlet state. This is because the oxygen atom enables more efficient separation of the two electrons owing to the "super radical stabilizer" properties of the furan ring system at a very

small cost of the aromatic stabilization energy.[281] This effect is not observed in the 3-furanyl nitrene as the electron is not completely delocalized into the π-system (Figure 5.7).

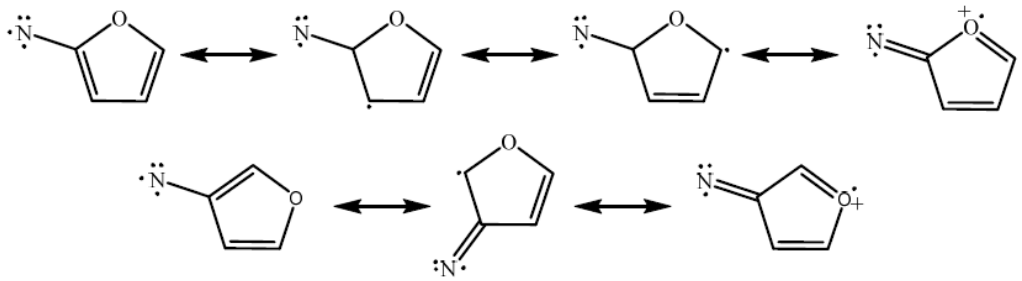

Figure 5.7. Delocalization of an electron in furanyl ring systems

With the incorporation of one radical stabilizer into the aromatic system, there is a scope of addition of another "super radical stabilizer" in the system, whose combined effects can be expected to have desirable outcomes. One such radical stabilizer is the N-oxide. The N-oxide not only enables the inclusion of an additional heteroatom stabilizer but also increases the length of conjugation for the delocalization of the electrons. Such studies have been done using oxazole- and isoxazolenitrene-n-oxides and have been shown to have drastic effects on the singlet-triplet splitting (Figure 5.8).[3]

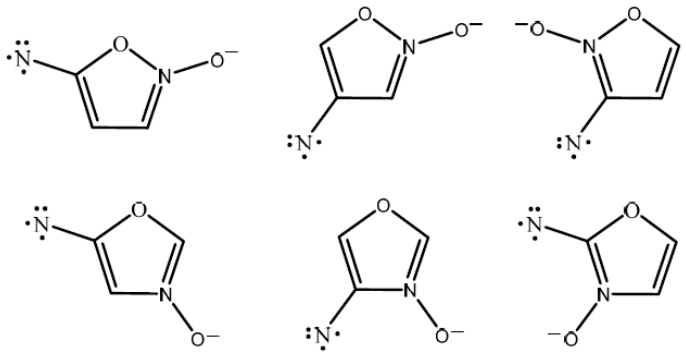

Figure 5.8. Delocalization of an electron in oxazole- and isoxazolenitrene-n-oxide systems

Although the ordering of the electronic states still remain unchanged when compared to phenyl nitrenes, remarkable differences were observed in energies of the electronic states. Most of the isomers had stabilized singlet states with respect to phenyl nitrenes. However, 2-oxazolylnitrene-n-oxide and 5-isoxazolylnitrene-noxide in particular, showed a very small singlet-

triplet splitting of about 4.7 kcal/mol and 6.3kcal/mol, respectively.[3] The reason for this can be deduced by examining their resonance structures, where the maximum delocalization of the electrons can be achieved in their most stable resonance forms that involve both the radical stabilizers (Figure 5.9).

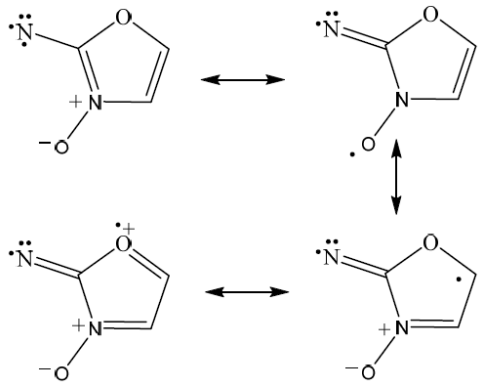

Figure 5.9. Delocalization of an electrons in 2-oxazolylnitrene-n-oxide and 5-isoxazolylnitrene-noxide

It can be presumed that the integration of more of such radical stabilizers in the aromatic system could have net stabilization effects on the nitrenes which would be additive. However, that is not always the case. For example, when a second N-oxide is added to the above system, the singlet-triplet splitting was found to be increased by 0.5 kcal/mol, which could be due to the diminished returns from delocalization resulting from the addition of a second N-oxide moiety (Figure 5.10)

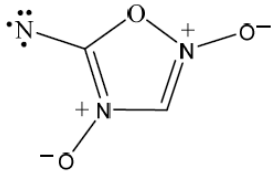

Figure 5.10. Diminished returns in the 5-Azoximylnitrene system

5.2.4 Designing a nitrene model to incorporate all the stabilization effects

All the above studies suggest that the extent of singlet-triplet splitting in phenyl nitrenes can be greatly affected by a combination of various factors that contribute to extended

delocalization of the electrons in the aromatic system. These effects can be additive as can be seen from the oxazolylnitrene-n-oxide systems. Thus, designing a system that consists of an expanded aromatic back bone such as an anthracene to promote extensive delocalization of electrons in the presence of a radical stabilizer such as an N-oxide could possibly result in sufficient reduction in the singlet-triplet splitting to cause reordering of the electronic states to favor ISC.

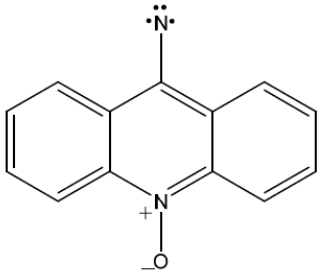

Figure 5.11. An anthracenyl-n-oxide nitrene model

The miniscule splitting energy of 5-azoximylnitrene suggests that it may be possible to have a ground state open-shell singlet. This encouraged us to develop an anthracenyl-n-oxide nitrene model system that can be presumed to affect the reordering of the electronic states.

5.3 Efforts in the synthesis of anthracenyl-n-oxide nitrene

This section will list some of the efforts made in the synthesis of the anthracenyl-n-oxide model.

9-chloroacridine was chosen as the appropriate starting material which would afford the precursor 9-azidoanthracenyl-n-oxide in two steps.

The first step in the synthesis was chosen to be the oxidation of the nitrogen of the acridine, followed by electrophilic aromatic substitution since the N-oxidation could involve use of harsher conditions which could result in azide decomposition.

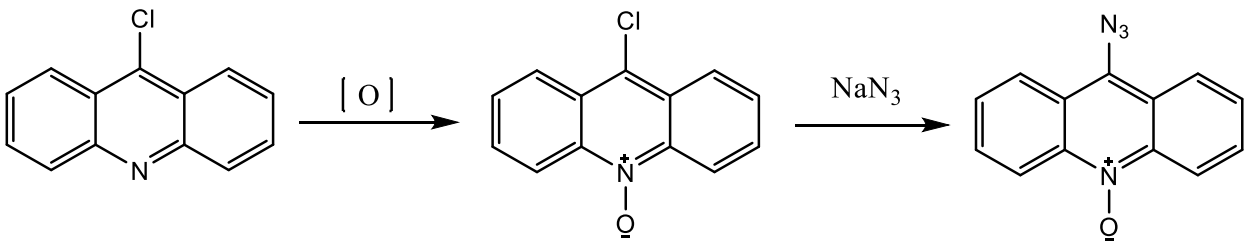

Figure 5.12. Synthetic scheme for 9-azidoanthracenyl-n-oxide

A total of three different reagents were tried to carry out the oxidation.

Meta-chloroperoxybenzoic acid (mCPBA)

One of the most popular reagents for oxidation is the mCPBA. The procedure is as follows-

mCPBA (2.5 eqv) was added to acridine (2.3 mmol) in chloroform (3.9 ml) and the mixture was refluxed for 4h. After 4h, the mixture was cooled to room temperature and 15.3 ml of saturated aqueous sodium bicarbonate solution was added to it. The aqueous layer was extracted with DCM (10 x 3ml) and the organic layers were combined, dried over magnesium sulfate, filtered and concentrated in vacuo.

A quick mass spectrum analysis of the crude product revealed no formation of the 9-chloroanthracenyl-n-oxide intermediate. The procedure was repeated several times with varying amounts of mCPBA, reagent concentration and longer reflux times. However, no formation of the N-oxide intermediate was observed in the mass spectrometer.

Hypofluorous acid (HOF)

Hypofluorous acid is the only known oxyacid of fluorine and the only known oxoacid in which the main atom gains electrons from oxygen to create a negative oxidation state. It is an intermediate formed during oxidation of water by fluorine gas. We found out that Prof. Davin Piercey in the mechanical engineering department at Purdue University often uses the intermediate to oxidize his nitrogen-based heterocycles that serve as explosives. We used his help to come up with a procedure for synthesizing the chloroantracenyl-n-oxide -

A solvent system comprising of 10 ml water and 90 ml acetonitrile was pre-cooled in ice. A solution of 10 mg of KI in 100 ml water and 10 mg of sodium thiosulfate in 500-600ml water

were prepared. Fluorine gas was then bubbled through the acetonitrile solution in an ice bath with constant stirring. The apparatus was connected to an empty trap which had the sodium thiosulfate solution in water in order to quench the HF gas liberated from the reaction. The reaction produces HOF almost immediately. 10 ml of the HOF in acetonitrile/water was then pipetted out in an Erlenmeyer flask and mixed with 10 ml of KI solution and 0.5 ml of concentrated sulfuric acid. This was done in order to measure the concentration of the HOF reagent which was calculated to be 0.37M. The reagent was then used to oxidize 9-chloroacridine in THF for 6-7 hr with constant stirring.

The reaction worked better than with the mCPBA where 5% crude yield of the product was obtained. Mass spectrometry analysis revealed that most of the starting material, 9-chloroacridine still remained unconsumed. The procedure was repeated with varying conditions of concentrations, temperatures and time but the maximum yield obtained was only 10%.

Hydrogen peroxide (H_2O_2)

Next, we tried the oxidation using hydrogen peroxide which is another popular reagent for oxidations. The procedure was as follows-

1 equivalent of 9-chloroacridine was dissolved in DCM to make a 1M concentration of the solution. To the solution, 0.03 equivalents of methyl trioxorehenium ($MeReO_3$) was added as a catalyst followed by 30 weight%, 20 equivalents of hydrogen peroxide. The mixture was stirred at room temperature for 12 hrs. Later, excess hydrogen peroxide was quenched with manganese dioxide and the reaction was diluted with DCM and water. Any excess manganese dioxide was filtered out of the solution. The organic and the aqueous layers were separated, and the organic layer was dried over sodium sulfite, filtered and concentrated.

Using hydrogen peroxide provided yields of upto 70% for the 9-chloroacridine-N-oxide which was detected and characterized on the mass spectrometer. The mass spectrum showed the molecular ion peak at m/z 230 with the chlorine isotopic peak at m/z 232. Interestingly, the mass spectrum had a base peak of m/z 196 which could be originating from the replacement of the chlorine with a hydrogen (M-35+1) on the acridine. The crude product was taken to the next step without further purification.

Synthesis of 9-azidoacridine-n-oxide

The selection of a procedure to synthesize the azide precursor faced limitations with regards to the conditions being used for the reactions as harsher conditions would cause decomposition of the azide group. Thus, a unique procedure using microwave conditions was selected and is listed below-

A model reaction of 9-chloroacridine to produce 9-azidoacridine was done using the procedure as a preliminary experiment to determine its efficiency. Two solutions of 25 mg of 9-chloroacridine in 7.5 ml acetone and 25 mg of sodium azide in 2 ml water were prepared and mixed in a Teflon vessel. The vessel was closed and irradiated in a conventional microwave at 100W for 30 seconds. The vessel was then cooled to room temperature and concentrated in vacuo. The 9-azidoacridine was filtered with suction and washed with 5 ml of water to give 76% of the crude product. The product was characterized using mass spectrometry where a product peak at m/z 220.6 was seen which on CID produced m/z 193 corresponding to the loss of a nitrogen molecule

Having achieved desirable results with the model reaction of 9-chloroacridine, we proceeded to synthesize the 9-azidoacridine-N-oxide from 9-chloroacridine-N-oxide using the same procedure. After completion of the reaction as monitored by TLC, the crude product was introduced into the mass spectrometer for characterization. However, similar to the mass spectrometric analysis of 9-chloroacridine-N-oxide, a loss of 34 mass units was observed which indicated replacement of the chlorine on the acridine with a hydrogen.

5.4 Discussion

The synthesis of 9-azidoacridine from 9-chloroacridine in the model reaction was completed without any problems indicating that the microwave mediated approach was indeed an effective way of conducting electrophilic aromatic substitutions. However, oxidation at the N-atom of the acridine induced drastic effects on the aromatic rings that are not fully understood. N-oxide substituents are known to be highly π-electron donating. It is possible that the strong π-donation results in increased stability of the carbocation intermediate formed after the release of the chloride leaving group. This effect could be exacerbated due to the additional conjugation present in the acridine. The effects could be seen directly impacting the 9-postion on the acridine

making the nucleophilic leaving group highly labile and prone to aromatic substitution by a hydrogen. In the absence of a suitable nucleophilic leaving group, the azide could not add on to the 9-position of the acridine to produce the desired product.

5.5 Conclusion and future directions

More studies need to be done in order to determine the effects of an N-oxide on different positions on aromatic rings. Literature survey reveals that presence of N-oxide does not impact a chlorine substituent in a quinoline-N-oxide system, clearly indicating that addition of an extra phenyl ring has a huge effect on the system.

Meanwhile, different routes to synthesize the 9-azidoacrdine-N-oxide which don't involve electrophilic aromatic substitution pathways need to be developed. An alternative approach could be azidation followed by the N-oxidation if a suitable process applying mild conditions and shorter reaction times can be developed for the N-oxidation. Considering that there is no evidence of an azide being a good nucleophilic leaving group, it is possible that presence of N-oxide does not impact azide to undergo replacements with hydrogen.

REFERENCES

(1) S. Singh, G. Synthetic Aziridines in Medicinal Chemistry: A Mini-Review. *Mini-Reviews Med. Chem.* **2016**, *16* (11), 892–904.

(2) Wijeratne, N. R.; Munsch, T. E.; Haupert, L. J.; Wenthold, P. G. Thermochemical Studies of Substituted Phenylnitrenes: Enthalpies of Formation of Chlorophenylnitrenes. *J. Chem. Thermodyn.* **2014**, *73*. https://doi.org/10.1016/j.jct.2013.12.035.

(3) Hossain, E.; Wenthold, P. G. Singlet Stabilization of Oxazole- and Isoxazolenitrene-n-Oxides by Radical Delocalization. *Comput. Theor. Chem.* **2013**, *1020*, 180–186. https://doi.org/10.1016/j.comptc.2013.07.028.

(4) Wenthold, P. G.; Squires, R. R. Gas-Phase Acidities of o-, m- and p-Dehydrobenzoic Acid Radicals. Determination of the Substituent Constants for a Phenyl Radical Site. *Int. J. Mass Spectrom. Ion Process.* **1998**, *175* (1–2), 215–224. https://doi.org/10.1016/S0168-1176(98)00120-7.

(5) Rau, N. J.; Welles, E. A.; Wenthold, P. G. Anionic Substituent Control of the Electronic Structure of Aromatic Nitrenes. *J. Am. Chem. Soc.* **2013**, *135* (2). https://doi.org/10.1021/ja306364z.

(6) Ju, M.; Schomaker, J. M. Nitrene Transfer Catalysts for Enantioselective C–N Bond Formation. *Nat. Rev. Chem.* **2021**, *5* (8), 580–594. https://doi.org/10.1038/s41570-021-00291-4.

(7) G. Soderberg, B. Synthesis of Heterocycles via Intramolecular Annulation of Nitrene Intermediates. *Curr. Org. Chem.* **2000**, *4* (7), 727–764. https://doi.org/10.2174/1385272003376067.

(8) Hemetsberger, H.; Knittel, D.; Weidmann, H. Enazide, 3. Mitt.: Thermolyse von ?-Azidozimtestern; Synthese von Indolderivaten. *Monatshefte für Chemie* **1970**, *101* (1), 161–165. https://doi.org/10.1007/BF00907536.

(9) Swenton, J. S.; Ikeler, T. J.; Williams, B. H. Photochemistry of Singlet and Triplet Azide Excited States. *J. Am. Chem. Soc.* **1970**, *92* (10), 3103–3109. https://doi.org/10.1021/ja00713a031.

(10) Kwart, H.; Khan, A. A. Copper-Catalyzed Decomposition of Benzenesulfonyl Azide in Cyclohexene Solution. *J. Am. Chem. Soc.* **1967**, *89* (8), 1951–1953. https://doi.org/10.1021/ja00984a035.

(11) Kwart, H.; Kahn, A. A. Copper-Catalyzed Decomposition of Benzenesulfonyl Azide in Hydroxylic Media. *Journal of the American Chemical Society*. 1967. https://doi.org/10.1021/ja00984a034.

(12) Breslow, R.; Feiring, A.; Herman, F. Intermolecular Insertion Reactions of Phosphoryl Nitrenes. *Journal of the American Chemical Society*. 1974. https://doi.org/10.1021/ja00825a042.

(13) Migita, T.; Chiba, M.; Takahashi, K.; Saitoh, N.; Nakaido, S.; Kosugi, M. Reinvestigation of the Pd-Catalyzed Reaction of Azidoformate with Allylic Ethers. *Bull. Chem. Soc. Jpn.* **1982**, *55* (12). https://doi.org/10.1246/bcsj.55.3943.

(14) Migita, T.; Hongoh, K.; Naka, H.; Nakaido, S.; Kosugi, M. Nitrene-Transfer Reaction between Azide and Unsaturated Ether in the Presence of Pd(II) Catalyst. *Bull. Chem. Soc. Jpn.* **1988**, *61* (3). https://doi.org/10.1246/bcsj.61.931.

(15) Migita, T.; Chiba, M.; Kosugi, M.; Nakaido, S. The Reaction Of Azidoformates With Allyl Ethers In The Presence Of Transition Metal Complexes. *Chem. Lett.* **1978**, *7* (12). https://doi.org/10.1246/cl.1978.1403.

(16) Groves, J. T.; Nemo, T. E.; Myers, R. S. Hydroxylation and Epoxidation Catalyzed by Iron-Porphine Complexes. Oxygen Transfer from Iodosylbenzene. *J. Am. Chem. Soc.* **1979**, *101* (4). https://doi.org/10.1021/ja00498a040.

(17) Chang, C. K.; Ming-Shang, K. Reaction of Iron(III) Porphyrins and Iodosoxylene. The Active Oxene Complex of Cytochrome P-450. *J. Am. Chem. Soc.* **1979**, *101* (12). https://doi.org/10.1021/ja00506a063.

(18) Mansuy, D.; Bartoli, J.-F.; Momenteau, M. Alkane Hydroxylation Catalyzed by Metalloporhyrins : Evidence for Different Active Oxygen Species with Alkylhydroperoxides and Iodosobenzene as Oxidants. *Tetrahedron Lett.* **1982**, *23* (27), 2781–2784. https://doi.org/10.1016/S0040-4039(00)87457-2.

(19) Groves, J. T.; Takahashi, T. Cheminform Abstract: Activation And Transfer Of Nitrogen From A Nitridomanganese(V) Porphyrin Complex. Aza Analog Of Epoxidation. *Chem. Informationsd.* **1983**, *14* (28). https://doi.org/10.1002/chin.198328298.

(20) Au, S.-M.; Fung, W.-H.; Cheng, M.-C.; Che, C.-M.; Peng, S.-M. Synthesis, Characterisation and Reactivity of Novel Bis(Tosyl)Imidoruthenium(vi) Porphyrin Complexes; X-Ray Crystal Structure of a Tosylamidoruthenium(Iv) Porphyrin. *Chem. Commun.* **1997**, No. 17, 1655–1656. https://doi.org/10.1039/a702093g.

(21) Cenini, S.; Tollari, S.; Penoni, A.; Cereda, C. Catalytic Amination of Unsaturated Hydrocarbons: Reactions of p- Nitrophenylazide with Alkenes Catalysed by Metallo-Porphyrins. *J. Mol. Catal. A Chem.* **1999**, *137* (1–3). https://doi.org/10.1016/S1381-1169(98)00116-2.

(22) Caselli, A.; Gallo, E.; Fantauzzi, S.; Morlacchi, S.; Ragaini, F.; Cenini, S. Allylic Amination and Aziridination of Olefins by Aryl Azides Catalyzed by CoII(Tpp): A Synthetic and Mechanistic Study. *Eur. J. Inorg. Chem.* **2008**, No. 19. https://doi.org/10.1002/ejic.200800156.

(23) Li, Z.; Quan, R. W.; Jacobsen, E. N. Mechanism of the (Diimine)Copper-Catalyzed Asymmetric Aziridination of Alkenes. Nitrene Transfer via Ligand-Accelerated Catalysis. *J. Am. Chem. Soc.* **1995**, *117* (21), 5889–5890. https://doi.org/10.1021/ja00126a044.

(24) Mueller, P.; Baud, C.; Naegeli, I. Rhodium(II)-Catalyzed Nitrene Transfer with Phenyliodonium Ylides. *J. Phys. Org. Chem.* **1998**, *11* (8–9). https://doi.org/10.1002/(sici)1099-1395(199808/09)11:8/9<597::aid-poc45>3.0.co;2-m.

(25) Li, Z.; Conser, K. R.; Jacobsen, E. N. Asymmetric Alkene Aziridination with Readily Available Chiral Diimine-Based Catalysts. *J. Am. Chem. Soc.* **1993**, *115* (12), 5326–5327. https://doi.org/10.1021/ja00065a067.

(26) Dauban, P.; Sanière, L.; Tarrade, A.; Dodd, R. H. Copper-Catalyzed Nitrogen Transfer Mediated by Iodosylbenzene PhI=O [2]. *Journal of the American Chemical Society*. 2001. https://doi.org/10.1021/ja010968a.

(27) Omura, K.; Uchida, T.; Irie, R.; Katsuki, T. Design of a Robust Ru(Salen) Complex: Aziridination with Improved Turnover Number Using N-Arylsulfonyl Azides as PrecursorsElectronic Supplementary Information (ESI) Available: Typical Experimental Procedures, Determination of Enantiomeric Excess and Elem. *Chem. Commun.* **2004**, No. 18, 2060. https://doi.org/10.1039/b407693a.

(28) Kawabata, H.; Omura, K.; Katsuki, T. Asymmetric Aziridination: A New Entry to Optically Active Non-N-Protected Aziridines. *Tetrahedron Lett.* **2006**, *47* (10), 1571–1574. https://doi.org/10.1016/j.tetlet.2005.12.124.

(29) Kawabata, H.; Omura, K.; Uchida, T.; Katsuki, T. Construction of Robust Ruthenium(Salen)(CO) Complexes and Asymmetric Aziridination with Nitrene Precursors in the Form of Azide Compounds That Bear Easily RemovableN-Sulfonyl Groups. *Chem. – An Asian J.* **2007**, *2* (2), 248–256. https://doi.org/10.1002/asia.200600363.

(30) Brands, K. M. J.; Jobson, R. B.; Conrad, K. M.; Williams, J. M.; Pipik, B.; Cameron, M.; Davies, A. J.; Houghton, P. G.; Ashwood, M. S.; Cottrell, I. F.; Reamer, R. A.; Kennedy, D. J.; Dolling, U.-H.; Reider, P. J. Efficient One-Pot Synthesis of the 2-Aminocarbonylpyrrolidin-4-Ylthio-Containing Side Chain of the New Broad-Spectrum Carbapenem Antibiotic Ertapenem. *J. Org. Chem.* **2002**, *67* (14), 4771–4776. https://doi.org/10.1021/jo011170c.

(31) Jones, J. E.; Ruppel, J. V.; Gao, G.-Y.; Moore, T. M.; Zhang, X. P. Cobalt-Catalyzed Asymmetric Olefin Aziridination with Diphenylphosphoryl Azide. *J. Org. Chem.* **2008**, *73* (18), 7260–7265. https://doi.org/10.1021/jo801151x.

(32) Jones, S.; Selitsianos, D. Stereochemical Consequences of the Use of Chiral N-Phosphoryl Oxazolidinones in the Attempted Kinetic Resolution of Bromomagnesium Alkoxides. *Tetrahedron: Asymmetry* **2005**, *16* (18), 3128–3138. https://doi.org/10.1016/j.tetasy.2005.08.025.

(33) Chen, Y.; Fields, K. B.; Zhang, X. P. Bromoporphyrins as Versatile Synthons for Modular Construction of Chiral Porphyrins: Cobalt-Catalyzed Highly Enantioselective and Diastereoselective Cyclopropanation. *J. Am. Chem. Soc.* **2004**, *126* (45), 14718–14719. https://doi.org/10.1021/ja044889l.

(34) Ruppel, J. V.; Jones, J. E.; Huff, C. A.; Kamble, R. M.; Chen, Y.; Zhang, X. P. A Highly Effective Cobalt Catalyst for Olefin Aziridination with Azides: Hydrogen Bonding Guided Catalyst Design. *Org. Lett.* **2008**, *10* (10), 1995–1998. https://doi.org/10.1021/ol800588p.

(35) Subbarayan, V.; Ruppel, J. V.; Zhu, S.; Perman, J. A.; Zhang, X. P. Highly Asymmetric Cobalt-Catalyzed Aziridination of Alkenes with Trichloroethoxysulfonyl Azide (TcesN3). *Chem. Commun.* **2009**, No. 28, 4266. https://doi.org/10.1039/b905727g.

(36) Abramovitch, R. A.; Bailey, T. D.; Takaya, T.; Uma, V. The Reaction of Methanesulfonyl Nitrene with Benzene. Attempts to Generate Sulfonyl Nitrenes from Sources Other than the Azides. *J. Org. Chem.* **1974**, *39* (3). https://doi.org/10.1021/jo00917a013.

(37) Yamada, Y.; Yamamoto, T.; Okawara, M. Synthesis And Reaction Of New Type I–N Ylide, N-Tosyliminoiodinane. *Chem. Lett.* **1975**, *4* (4). https://doi.org/10.1246/cl.1975.361.

(38) Nishikori, H.; Katsuki, T. Catalytic and Highly Enantioselective Aziridination of Styrene Derivatives. *Tetrahedron Lett.* **1996**, *37* (51), 9245–9248. https://doi.org/10.1016/S0040-4039(96)02195-8.

(39) Evans, D. A.; Paul, M. M.; Bilodeau, M. T. Development of the Copper-Catalyzed Olefin Aziridination Reaction. *J. Am. Chem. Soc.* **1994**, *116* (7). https://doi.org/10.1021/ja00086a007.

(40) Evans, D. A.; Faul, M. M.; Bilodeau, M. T. Copper-Catalyzed Aziridination of Olefins by (N-(p-Toluenesulfonyl)Imino)Phenyliodinane. *J. Org. Chem.* **1991**, *56* (24), 6744–6746. https://doi.org/10.1021/jo00024a008.

(41) Mansuy, D.; Mahy, J.-P.; Dureault, A.; Bedi, G.; Battioni, P. Iron- and Manganese-Porphyrin Catalysed Aziridination of Alkenes by Tosyl- and Acyl-Iminoiodobenzene. *J. Chem. Soc. Chem. Commun.* **1984**, No. 17, 1161. https://doi.org/10.1039/c39840001161.

(42) Breslow, R.; Gellman, S. H. Cheminform Abstract: Intramolecular Nitrene Carbon-Hydrogen Insertions Mediated By Transition-Metal Complexes As Nitrogen Analogs Of Cytochrome P-450 Reactions. *Chem. Informationsd.* **1984**, *15* (6). https://doi.org/10.1002/chin.198406084.

(43) Breslow, R.; Gellman, S. H. Tosylamidation of Cyclohexane by a Cytochrome P-450 Model. *J. Chem. Soc. Chem. Commun.* **1982**, No. 24. https://doi.org/10.1039/C39820001400.

(44) Mahy, J.-P.; Bedi, G.; Battioni, P.; Mansuy, D. Aziridination of Alkenes Catalysed by Porphyrinirons: Selection of Catalysts for Optimal Efficiency and Stereospecificity. *J. Chem. Soc. Perkin Trans. 2* **1988**, No. 8, 1517. https://doi.org/10.1039/p29880001517.

(45) Mahy, J. P.; Battioni, P.; Mansuy, D. Formation of an Iron(III)-Porphyrin Complex with a Nitrene Moiety Inserted into an Iron-Nitrogen Bond during Alkene Aziridination by (Tosylimidoiodo)Benzene Catalyzed by Iron(III) Porphyrins. *J. Am. Chem. Soc.* **1986**, *108* (5), 1079–1080. https://doi.org/10.1021/ja00265a037.

(46) Evans, D. A.; Faul, M. M.; Bilodeau, M. T.; Anderson, B. A.; Barnes, D. M. Bis(Oxazoline)-Copper Complexes as Chiral Catalysts for the Enantioselective Aziridination of Olefins. *J. Am. Chem. Soc.* **1993**, *115* (12), 5328–5329. https://doi.org/10.1021/ja00065a068.

(47) Halfen, J. A.; Hallman, J. K.; Schultz, J. A.; Emerson, J. P. Remarkably Efficient Olefin Aziridination Mediated by a New Copper(II) Complex. *Organometallics* **1999**, *18* (26), 5435–5437. https://doi.org/10.1021/om9908579.

(48) Vedernikov, A. N.; Caulton, K. G. Angular Ligand Constraint Yields an Improved Olefin Aziridination Catalyst. *Org. Lett.* **2003**, *5* (15). https://doi.org/10.1021/ol034681p.

(49) Amisial, L. T. D.; Dai, X.; Kinney, R. A.; Krishnaswamy, A.; Warren, T. H. Cu(I) β-Diketiminates for Alkene Aziridination: Reversible Cu-Arene Binding and Catalytic Nitrene Transfer from PhI=NTs. *Inorg. Chem.* **2004**, *43* (21). https://doi.org/10.1021/ic048968+.

(50) Badiei, Y. M.; Dinescu, A.; Dai, X.; Palomino, R. M.; Heinemann, F. W.; Cundari, T. R.; Warren, T. H. Copper-Nitrene Complexes in Catalytic C-H Amination. *Angew. Chemie - Int. Ed.* **2008**, *47* (51). https://doi.org/10.1002/anie.200804304.

(51) Müller, P.; Baud, C.; Jacquier, Y. A Method for Rhodium(II)-Catalyzed Aziridination of Olefins. *Tetrahedron* **1996**, *52* (5), 1543–1548. https://doi.org/10.1016/0040-4020(95)00999-X.

(52) Müller, P.; Baud, C.; Jacquier, Y.; Moran, M.; Nägeli, I. Rhodium(II)-Catalyzed Aziridinations and Ch Insertions with [N-(p-Nitrobenzenesulfonyl)Imino]Phenyliodinane. *J. Phys. Org. Chem.* **1996**, *9* (6). https://doi.org/10.1002/(SICI)1099-1395(199606)9:6<341::AID-POC791>3.0.CO;2-5.

(53) Müller, P.; Baud, C.; Jacquier, Y. The Rhodium(II)-Catalyzed Aziridination of Olefins with {[(4-Nitrophenyl)Sulfonyl]Imino}phenyl-Lambda^3-Iodane. *Can. J. Chem.* **1998**, *76* (6), 738–750. https://doi.org/10.1139/cjc-76-6-738.

(54) Yu, X. Q.; Huang, J. S.; Zhou, X. G.; Che, C. M. Amidation of Saturated C-H Bonds Catalyzed by Electron-Deficient Ruthenium and Manganese Porphyrins. A Highly Catalytic Nitrogen Atom Transfer Process. *Org. Lett.* **2000**, *2* (15). https://doi.org/10.1021/ol000107r.

(55) Espino, C. G.; Du Bois, J. A Rh-Catalyzed C-H Insertion Reaction for the Oxidative Conversion of Carbamates to Oxazolidinones. *Angew. Chemie - Int. Ed.* **2001**, *40* (3). https://doi.org/10.1002/1521-3773(20010202)40:3<598::AID-ANIE598>3.0.CO;2-9.

(56) Espino, C. G.; Wehn, P. M.; Chow, J.; Du Bois, J. Synthesis of 1,3-Difunctionalized Amine Derivatives through Selective C-H Bond Oxidation. *Journal of the American Chemical Society*. 2001. https://doi.org/10.1021/ja011033x.

(57) Ghosh, A. K.; Mathivanan, P.; Cappiello, J. C2-Symmetric Chiral Bis(Oxazoline)-Metal Complexes in Catalytic Asymmetric Synthesis. *Tetrahedron Asymmetry* **1998**, *9* (1). https://doi.org/10.1016/S0957-4166(97)00593-4.

(58) Lowenthal, R. E.; Masamune, S. Asymmetric Copper-Catalyzed Cyclopropanation of Trisubstituted and Unsymmetrical Cis-1,2-Disubstituted Olefins: Modified Bis-Oxazoline Ligands. *Tetrahedron Lett.* **1991**, *32* (50), 7373–7376. https://doi.org/10.1016/0040-4039(91)80110-R.

(59) Harm, A. M.; Knight, J. G.; Stemp, G. Asymmetric Copper-Catalysed Alkene Cyclopropanation and Aziridination Using Tartrate-Derived Bis-Oxazoline Ligands. *Tetrahedron Lett.* **1996**, *37* (34), 6189–6192. https://doi.org/10.1016/0040-4039(96)01320-2.

(60) Södergren, M. J.; Alonso, D. A.; Bedekar, A. V.; Andersson, P. G. Preparation and Evaluation of Nitrene Precursors (PhI=NSO2Ar) for the Copper-Catalyzed Aziridination of Olefins. *Tetrahedron Lett.* **1997**, *38* (39), 6897–6900. https://doi.org/10.1016/S0040-4039(97)01589-X.

(61) Gullick, J.; Taylor, S.; Kerton, O.; McMorn, P.; King, F.; Hancock, F. E.; Bethell, D.; Bulman Page, P. C.; Hutchings, G. J. Heterogeneous Catalytic Aziridination of Styrene Using Transition-Metal-Exchanged Zeolite Y. *Catal. Letters* **2001**, *75* (3–4). https://doi.org/10.1023/A:1016739904897.

(62) Langham, C.; Bethell, D.; Lee, D. F.; McMorn, P.; Bulman Page, P. C.; Willock, D. J.; Sly, C.; Hancock, F. E.; King, F.; Hutchings, G. J. Heterogeneous Aziridination of Alkenes Using Cu2+ Exchanged Zeolites. *Appl. Catal. A Gen.* **1999**, *182* (1). https://doi.org/10.1016/S0926-860X(98)00423-2.

(63) Langham, C.; Taylor, S.; Bethell, D.; McMorn, P.; Bulman Page, P. C.; Willock, D. J.; Sly, C.; Hancock, F. E.; King, F.; Hutchings, G. J. Catalytic Asymmetric Heterogeneous Aziridination of Alkenes Using Zeolite CuHY with [N-(p-Tolylsulfonyl)Imino]Phenyliodinane as Nitrene Donor. *J. Chem. Soc. Perkin Trans. 2* **1999**, No. 5. https://doi.org/10.1039/a806409a.

(64) Langham, C.; Piaggio, P.; Bethell, D.; Lee, D. F.; McMorn, P.; Bulman Page, P. C.; Willock, D. J.; Sly, C.; Hancock, F. E.; King, F.; Hutchings, G. J. Catalytic Heterogeneous Aziridination of Alkenes Using Microporous Materials. *Chem. Commun.* **1998**, No. 15. https://doi.org/10.1039/a801997e.

(65) Taylor, S.; Gullick, J.; McMorn, P.; Bethell, D.; Bulman Page, P. C.; Hancock, F. E.; King, F.; Hutchings, G. J. Catalytic Asymmetric Heterogeneous Aziridination of Styrene Using CuHY: Effect of Nitrene Donor on Enantioselectivity. *J. Chem. Soc. Perkin Trans. 2* **2001**, *9* (9), 1714–1723. https://doi.org/10.1039/b104522a.

(66) Bennani, Y. L.; Hanessian, S. Trans -1,2-Diaminocyclohexane Derivatives as Chiral Reagents, Scaffolds, and Ligands for Catalysis: Applications in Asymmetric Synthesis and Molecular Recognition. *Chem. Rev.* **1997**, *97* (8), 3161–3196. https://doi.org/10.1021/cr9407577.

(67) Cho, D. J.; Jeon, S. J.; Kim, H. S.; Cho, C. S.; Shim, S. C.; Kim, T. J. Chiral C2-Symmetric Bisferrocenyldiamines as Ligands for Transition Metal Catalyzed Asymmetric Cyclopropanation and Aziridination. *Tetrahedron Asymmetry* **1999**, *10* (19). https://doi.org/10.1016/S0957-4166(99)00423-1.

(68) Cho, D. J.; Jeon, S. J.; Kim, H. S.; Kim, T. J. Catalytic Cyclopropanation and Aziridination of Alkenes by a Cu(I) Complex of Ferrocenyldiimine. *Synlett* **1998**, No. 6. https://doi.org/10.1055/s-1998-1743.

(69) Song, J. H.; Cho, D. J.; Jeon, S. J.; Kim, Y. H.; Kim, T. J.; Jeong, J. H. Synthesis of Chiral C2-Symmetric Bisferrocenyldiamines. X-Ray Crystal Structure of Ru(2)Cl2&2CHCl3 (2 = N1,N2-Bis{(R)-1-[(S)-2-(Diphenylphosphino)]Ferrocenylethyl}N1,N2-Dimethyl-1,2-Ethanediamine). *Inorg. Chem.* **1999**, *38* (5). https://doi.org/10.1021/ic980433r.

(70) Shi, M.; Wang, C.-J.; Chan, A. S. C. Axially Dissymmetric Binaphthyldiimine Chiral Salen-Type Ligands for Copper-Catalyzed Asymmetric Aziridination. *Tetrahedron: Asymmetry* **2001**, *12* (22), 3105–3111. https://doi.org/10.1016/S0957-4166(01)00534-1.

(71) Adam, W.; Roschmann, K. J.; Saha-Möller, C. R. Catalytic Asymmetric Aziridination of Enol Derivatives in the Presence of Chiral Copper Complexes to Give Optically Active α-Amino Ketones. *European J. Org. Chem.* **2000**, No. 3. https://doi.org/10.1002/(SICI)1099-0690(200002)2000:3<557::AID-EJOC557>3.0.CO;2-B.

(72) Gillespie, K. M.; Sanders, C. J.; O'Shaughnessy, P.; Westmoreland, I.; Thickitt, C. P.; Scott, P. Enantioselective Aziridination Using Copper Complexes of Biaryl Schiff Bases. *J. Org. Chem.* **2002**, *67* (10), 3450–3458. https://doi.org/10.1021/jo025515i.

(73) Brandt, P.; Södergren, M. J.; Andersson, P. G.; Norrby, P.-O. Mechanistic Studies of Copper-Catalyzed Alkene Aziridination. *J. Am. Chem. Soc.* **2000**, *122* (33), 8013–8020. https://doi.org/10.1021/ja993246g.

(74) Catalytic Asymmetric Synthesis. *Synth. React. Inorg. Met. Chem.* **1994**, *24* (7), 1239–1240. https://doi.org/10.1080/00945719408001399.

(75) Zhang, W.; Lee, N. H.; Jacobsen, E. N. Nonstereospecific Mechanisms in Asymmetric Addition to Alkenes Result in Enantiodifferentiation after the First Irreversible Step. *J. Am. Chem. Soc.* **1994**, *116* (1), 425–426. https://doi.org/10.1021/ja00080a070.

(76) Davies, H. M. L.; Panaro, S. A. Effect of Rhodium Carbenoid Structure on Cyclopropanation Chemoselectivity. *Tetrahedron* **2000**, *56* (28), 4871–4880. https://doi.org/10.1016/S0040-4020(00)00202-7.

(77) Halfen, J. A.; Fox, D. C.; Mehn, M. P.; Que, L. Enhanced Reactivity of Copper Catalysts for Olefin Aziridination by Manipulation of Ligand Denticity. *Inorg. Chem.* **2001**, *40* (20), 5060–5061. https://doi.org/10.1021/ic015551k.

(78) Handy, S. T.; Czopp, M. Simple, Tunable Aziridination Catalysts Based on Poly(Pyrazolyl)Borate−Copper Complexes. *Org. Lett.* **2001**, *3* (10), 1423–1425. https://doi.org/10.1021/ol015539w.

(79) Dias, H. V. R.; Lu, H.-L.; Kim, H.-J.; Polach, S. A.; Goh, T. K. H. H.; Browning, R. G.; Lovely, C. J. Copper(I) Ethylene Adducts and Aziridination Catalysts Based on Fluorinated Tris(Pyrazolyl)Borates [HB(3-(CF 3),5-(R)Pz) 3] - (Where R = CF 3 , C 6 H 5 , H; Pz = Pyrazolyl). *Organometallics* **2002**, *21* (7), 1466–1473. https://doi.org/10.1021/om010886v.

(80) Dauban, P.; Dodd, R. H. Synthesis of Cyclic Sulfonamides via Intramolecular Copper-Catalyzed Reaction of Unsaturated Iminoiodinanes. *Org. Lett.* **2000**, *2* (15), 2327–2329. https://doi.org/10.1021/ol000130c.

(81) Dauban, P.; Sanière, L.; Tarrade, A.; Dodd, R. H. Copper-Catalyzed Nitrogen Transfer Mediated by Iodosylbenzene PhIO. *J. Am. Chem. Soc.* **2001**, *123* (31), 7707–7708. https://doi.org/10.1021/ja010968a.

(82) Duran, F.; Leman, L.; Ghini, A.; Burton, G.; Dauban, P.; Dodd, R. H. Intramolecular PhIO Mediated Copper-Catalyzed Aziridination of Unsaturated Sulfamates: A New Direct Access to Polysubstituted Amines from Simple Homoallylic Alcohols. *Org. Lett.* **2002**, *4* (15), 2481–2483. https://doi.org/10.1021/ol0200899.

(83) Doyle, M. P.; Davies, S. B.; May, E. J. High Selectivity from Configurational Match/Mismatch in Carbon−Hydrogen Insertion Reactions of Steroidal Diazoacetates Catalyzed by Chiral Dirhodium(II) Carboxamidates. *J. Org. Chem.* **2001**, *66* (24), 8112–8119. https://doi.org/10.1021/jo015932f.

(84) Doyle, M. P.; Davies, S. B.; Hu, W. Dirhodium(II) Tetrakis[Methyl 2-Oxaazetidine-4-Carboxylate]: A Chiral Dirhodium(II) Carboxamidate of Exceptional Reactivity and Selectivity. *Org. Lett.* **2000**, *2* (8), 1145–1147. https://doi.org/10.1021/ol005730q.

(85) Doyle, M. P.; Hu, W.; Phillips, I. M.; Wee, A. G. H. A New Approach to Macrocyclization via Alkene Formation in Catalytic Diazo Decomposition. Synthesis of Patulolides A and B. *Org. Lett.* **2000**, *2* (12), 1777–1779. https://doi.org/10.1021/ol005983j.

(86) Doyle, M. P.; Chapman, B. J.; Hu, W.; Peterson, C. S.; McKervey, M. A.; Garcia, C. F. Catalytic Intramolecular Addition of Metal Carbenes to Remote Furans. *Org. Lett.* **1999**, *1* (9), 1327–1329. https://doi.org/10.1021/ol990168t.

(87) Doyle, M. P.; Forbes, D. C. Recent Advances in Asymmetric Catalytic Metal Carbene Transformations. *Chem. Rev.* **1998**, *98* (2), 911–936. https://doi.org/10.1021/cr940066a.

(88) Qu, Z.; Shi, W.; Wang, J. A Kinetic Study on the Pairwise Competition Reaction of α-Diazo Esters with Rhodium(II) Catalysts: Implication for the Mechanism of Rh(II)-Carbene Transfer. *J. Org. Chem.* **2001**, *66* (24), 8139–8144. https://doi.org/10.1021/jo0107352.

(89) Müller, P.; Bernardinelli, G.; Nury, P. Synthesis of Bicyclo[3.2.2]Nonadienones via Enantioselective Cyclopropanation of Racemic Cyclohexen-3-Yl Diazoacetate. *Tetrahedron: Asymmetry* **2002**, *13* (5), 551–558. https://doi.org/10.1016/S0957-4166(02)00105-2.

(90) Pirrung, M. C.; Zhang, J. Asymmetric Dipolar Cycloaddition Reactions of Diazocompounds Mediated by a Binaphtholphosphate Rhodium Catalyst. *Tetrahedron Lett.* **1992**, *33* (40), 5987–5990. https://doi.org/https://doi.org/10.1016/S0040-4039(00)61107-3.

(91) Guthikonda, K.; Du Bois, J. A Unique and Highly Efficient Method for Catalytic Olefin Aziridination. *J. Am. Chem. Soc.* **2002**, *124* (46), 13672–13673. https://doi.org/10.1021/ja028253a.

(92) Levites-Agababa, E.; Menhaji, E.; Perlson, L. N.; Rojas, C. M. Amidoglycosylation via Metal-Catalyzed Internal Nitrogen Atom Delivery. *Org. Lett.* **2002**, *4* (5), 863–865. https://doi.org/10.1021/ol025634k.

(93) Padwa, A.; Stengel, T. Stereochemical Aspects of the Iodine(III)-Mediated Aziridination Reaction of Some Cyclic Allylic Carbamates. *Org. Lett.* **2002**, *4* (13), 2137–2139. https://doi.org/10.1021/ol0259490.

(94) Müller, P.; Boléa, C. Carbenoid Pathways in Copper-Catalyzed Intramolecular Cyclopropanations of Phenyliodonium Ylides. *Helv. Chim. Acta* **2001**, *84* (5), 1093–1111. https://doi.org/10.1002/1522-2675(20010516)84:5<1093::AID-HLCA1093>3.0.CO;2-T.

(95) Müller, P.; Boléa, C. Asymmetric Induction in Cu-Catalyzed Intramolecular Cyclopropanations of Phenyliodonium Ylides. *Synlett* **2000**, *2000* (06), 0826–0828. https://doi.org/10.1055/s-2000-6697.

(96) Müller, P.; Fernandez, D. Carbenoid Reactions in Rhodium(II)-Catalyzed Decomposition of Iodonium Ylides. *Helv. Chim. Acta* **1995**, *78* (4), 947–958. https://doi.org/10.1002/hlca.19950780417.

(97) Moriarty, R. M.; Prakash, O.; Vaid, R. K.; Zhao, L. A Novel Intramolecular Cyclopropanation Using Iodonium Ylides. *J. Am. Chem. Soc.* **1989**, *111* (16), 6443–6444. https://doi.org/10.1021/ja00198a078.

(98) O'Connor, K. J.; Wey, S.-J.; Burrows, C. J. Alkene Aziridination and Epoxidation Catalyzed by Chiral Metal Salen Complexes. *Tetrahedron Lett.* **1992**, *33* (8), 1001–1004. https://doi.org/10.1016/S0040-4039(00)91844-6.

(99) Groves, J. T.; Takahashi, T.; Butler, W. M. Synthesis and Molecular Structure of a Nitrido(Porphyrinato)Chromium(V) Complex. *Inorg. Chem.* **1983**, *22* (6), 884–887. https://doi.org/10.1021/ic00148a009.

(100) Du Bois, J.; Hong, J.; Carreira, E. M.; Day, M. W. Nitrogen Transfer from a Nitridomanganese(V) Complex: Amination of Silyl Enol Ethers. *J. Am. Chem. Soc.* **1996**, *118* (4), 915–916. https://doi.org/10.1021/ja953659r.

(101) Du Bois, J.; Tomooka, C. S.; Hong, J.; Carreira, E. M. Novel, Stereoselective Synthesis of 2-Amino Saccharides. *J. Am. Chem. Soc.* **1997**, *119* (13), 3179–3180. https://doi.org/10.1021/ja964381l.

(102) Du Bois, J.; Tomooka, C. S.; Hong, J.; Carreira, E. M. Nitridomanganese(V) Complexes: Design, Preparation, and Use as Nitrogen Atom-Transfer Reagents. *Acc. Chem. Res.* **1997**, *30* (9), 364–372. https://doi.org/10.1021/ar960222v.

(103) Bois, J. Du; Tomooka, C. S.; Hong, J.; Carreira, E. M.; Day, M. W. Synthesis and Structure of Novel MnIII and Mnv Complexes: Development of a New, Mild Method for Forming Mn□N Bonds. *Angew. Chemie Int. Ed. English* **1997**, *36* (15), 1645–1647. https://doi.org/10.1002/anie.199716451.

(104) Minakata, S.; Ando, T.; Nishimura, M.; Ryu, I.; Komatsu, M. Novel Asymmetric and Stereospecific Aziridination of Alkenes with a Chiral Nitridomanganese Complex. *Angew. Chemie Int. Ed.* **1998**, *37* (24), 3392–3394. https://doi.org/10.1002/(SICI)1521-3773(19981231)37:24<3392::AID-ANIE3392>3.0.CO;2-G.

(105) Nishimura, M.; Minakata, S.; Takahashi, T.; Oderaotoshi, Y.; Komatsu, M. Asymmetric N1 Unit Transfer to Olefins with a Chiral Nitridomanganese Complex: Novel Stereoselective Pathways to Aziridines or Oxazolines. *J. Org. Chem.* **2002**, *67* (7), 2101–2110. https://doi.org/10.1021/jo016146d.

(106) Nishimura, M.; Minakata, S.; Thongchant, S.; Ryu, I.; Komatsu, M. Selective [2+1] Aziridination of Conjugated Dienes with a Nitridomanganese Complex: A New Route to Alkenylaziridines. *Tetrahedron Lett.* **2000**, *41* (36), 7089–7092. https://doi.org/10.1016/S0040-4039(00)01219-3.

(107) Ho, C.-M.; Lau, T.-C.; Kwong, H.-L.; Wong, W.-T. Activation of Manganese Nitrido Complexes by Brønsted and Lewis Acids. Crystal Structure and Asymmetric Alkene Aziridination of a Chiral Salen Manganese Nitrido Complex. *J. Chem. Soc. Dalt. Trans.* **1999**, No. 15, 2411–2414. https://doi.org/10.1039/a903605i.

(108) Katsuki, T. Some Recent Advances in Metallosalen Chemistry. *Synlett* **2003**, No. 3, 0281–0297. https://doi.org/10.1055/s-2003-37101.

(109) Noda, K.; Hosoya, N.; Irie, R.; Ito, Y.; Katsuki, T. Asymmetric Aziridination by Using Optically Active (Salen)Manganese(III) Complexes. *Synlett* **1993**, *1993* (07), 469–471. https://doi.org/10.1055/s-1993-22494.

(110) Lai, T.-S.; Che, C.-M.; Kwong, H.-L.; Peng, S.-M. Catalytic and Asymmetric Aziridination of Alkenes Catalysed by a Chiral Manganese Porphyrin Complex. *Chem. Commun.* **1997**, No. 24, 2373–2374. https://doi.org/10.1039/a706395d.

(111) Liang, J.-L.; Huang, J.-S.; Yu, X.-Q.; Zhu, N.; Che, C.-M. Metalloporphyrin-Mediated Asymmetric Nitrogen-Atom Transfer to Hydrocarbons: Aziridination of Alkenes and Amidation of Saturated C−H Bonds Catalyzed by Chiral Ruthenium and Manganese Porphyrins. *Chem. - A Eur. J.* **2002**, *8* (7), 1563–1572. https://doi.org/10.1002/1521-3765(20020402)8:7<1563::AID-CHEM1563>3.0.CO;2-V.

(112) Simonato, J.-P.; Pécaut, J.; Marchon, J.-C.; Robert Scheidt, W. Antagonistic Metal-Directed Inductions in Catalytic Asymmetric Aziridination by Manganese and Iron Tetramethylchiroporphyrins. *Chem. Commun.* **1999**, No. 11, 989–990. https://doi.org/10.1039/a901559k.

(113) Au, S.-M.; Huang, J.-S.; Yu, W.-Y.; Fung, W.-H.; Che, C.-M. Aziridination of Alkenes and Amidation of Alkanes by Bis(Tosylimido)Ruthenium(VI) Porphyrins. A Mechanistic Study. *J. Am. Chem. Soc.* **1999**, *121* (39), 9120–9132. https://doi.org/10.1021/ja9913481.

(114) Liang, J.-L.; Yu, X.-Q.; Che, C.-M. Amidation of Silyl Enol Ethers and Cholesteryl Acetates with Chiral Ruthenium(Ii) Schiff-Base Catalysts: Catalytic and Enantioselective StudiesElectronic Supplementary Information (ESI) Available: Experimental Details. See Http://Www.Rsc.Org/Suppdata/Cc/B. *Chem. Commun.* **2002**, *2* (2), 124–125. https://doi.org/10.1039/b109272c.

(115) Zhang, J.-L.; Che, C.-M. Soluble Polymer-Supported Ruthenium Porphyrin Catalysts for Epoxidation, Cyclopropanation, and Aziridination of Alkenes. *Org. Lett.* **2002**, *4* (11), 1911–1914. https://doi.org/10.1021/ol0259138.

(116) Jeon, H.-J.; Nguyen, S. T. Nitrene-Transfer to Olefins Catalyzed by Methyltrioxorhenium: A Universal Catalyst for the [1+2] Cycloaddition of C-, N-, and O-Atom Fragments to Olefins. *Chem. Commun.* **2001**, No. 3, 235–236. https://doi.org/10.1039/b007906p.

(117) Cullin, D. W.; Soundararajan, N.; Platz, M. S.; Miller, T. A. Laser-Induced Fluorescence Spectrum of the Cyanocyclopentadienyl Radical: A Band System Long Attributed to Triplet Phenylnitrene. *J. Phys. Chem.* **1990**, *94* (26), 8890–8896. https://doi.org/10.1021/j100389a009.

(118) Cullin, D. W.; Yu, L.; Williamson, J. M.; Platz, M. S.; Miller, T. A. Reinvestigation of the Electronic Spectrum of the Phenylnitrene Radical. *J. Phys. Chem.* **1990**, *94* (9), 3387–3391. https://doi.org/10.1021/j100372a010.

(119) Poe, R.; Grayzar, J.; Young, M. J. T.; Leyva, E.; Schnapp, K. A.; Platz, M. S. Remarkable Catalysis of Intersystem Crossing of Singlet (Pentafluorophenyl)Nitrene. *J. Am. Chem. Soc.* **1991**, *113* (8), 3209–3211. https://doi.org/10.1021/ja00008a080.

(120) Poe, R.; Schnapp, K.; Young, M. J. T.; Grayzar, J.; Platz, M. S. Chemistry and Kinetics of Singlet Pentafluorophenylnitrene. *J. Am. Chem. Soc.* **1992**, *114* (13), 5054–5067. https://doi.org/10.1021/ja00039a016.

(121) Young, M. J. T.; Platz, M. S. Mechanistic Analysis of the Reactions of (Pentafluorophenyl)Nitrene in Alkanes. *J. Org. Chem.* **1991**, *56* (22), 6403–6406. https://doi.org/10.1021/jo00022a036.

(122) Schnapp, K. A.; Poe, R.; Leyva, E.; Soundararajan, N.; Platz, M. S. Exploratory Photochemistry of Fluorinated Aryl Azides. Implications for the Design of Photoaffinity Labeling Reagents. *Bioconjug. Chem.* **1993**, *4* (2), 172–177. https://doi.org/10.1021/bc00020a010.

(123) Schnapp, K. A.; Platz, M. S. A Laser Flash Photolysis Study of Di-, Tri- and Tetrafluorinated Phenylnitrenes; Implications for Photoaffinity Labeling. *Bioconjug. Chem.* **1993**, *4* (2), 178–183. https://doi.org/10.1021/bc00020a011.

(124) Keana, J. F. W.; Cai, S. X. New Reagents for Photoaffinity Labeling: Synthesis and Photolysis of Functionalized Perfluorophenyl Azides. *J. Org. Chem.* **1990**, *55* (11), 3640–3647. https://doi.org/10.1021/jo00298a048.

(125) Cai, S. X.; Glenn, D. J.; Keana, J. F. W. Toward the Development of Radiolabeled Fluorophenyl Azide-Based Photolabeling Reagents: Synthesis and Photolysis of Iodinated 4-Azidoperfluorobenzoates and 4-Azido-3,5,6-Trifluorobenzoates. *J. Org. Chem.* **1992**, *57* (4), 1299–1304. https://doi.org/10.1021/jo00030a046.

(126) Platz, M. S. Comparison of Phenylcarbene and Phenylnitrene. *Acc. Chem. Res.* **1995**, *28* (12). https://doi.org/10.1021/ar00060a004.

(127) Johnson, S. L.; Hilinski, M. K. Organocatalytic Olefin Aziridination via Iminium-Catalyzed Nitrene Transfer: Scope, Limitations, and Mechanistic Insight. *J. Org. Chem.* **2019**, *84* (13), 8589–8595. https://doi.org/10.1021/acs.joc.9b01023.

(128) Schock, M.; Bräse, S. Reactive & Efficient: Organic Azides as Cross-Linkers in Material Sciences. *Molecules* **2020**, *25* (4), 1009. https://doi.org/10.3390/molecules25041009.

(129) Bräse, S.; Gil, C.; Knepper, K.; Zimmermann, V. Organic Azides: An Exploding Diversity of a Unique Class of Compounds. *Angew. Chemie Int. Ed.* **2005**, *44* (33), 5188–5240. https://doi.org/10.1002/anie.200400657.

(130) Katritzky, A.; Scriven, E. Organic Azides: Syntheses and Applications. *J. Am. Chem. Soc.* **2010**, *132* (34), 12156–12156. https://doi.org/10.1021/ja106712z.

(131) Chiba, S. Application of Organic Azides for the Synthesis of Nitrogen-Containing Molecules. *Synlett* **2012**, *2012* (01), 21–44. https://doi.org/10.1055/s-0031-1290108.

(132) Nair, V.; Suja, T. D. Intramolecular 1,3-Dipolar Cycloaddition Reactions in Targeted Syntheses. *Tetrahedron* **2007**, *63* (50), 12247–12275. https://doi.org/10.1016/j.tet.2007.09.065.

(133) Lang, S.; Murphy, J. A. Azide Rearrangements in Electron-Deficient Systems. *Chem. Soc. Rev.* **2006**, *35* (2), 146–156. https://doi.org/10.1039/B505080D.

(134) Xu, M.; Kuang, C.; Wang, Z.; Yang, Q.; Jiang, Y. A Novel Approach to 1-Monosubstituted 1,2,3-Triazoles by a Click Cycloaddition/Decarboxylation Process. *Synthesis (Stuttg).* **2011**, *2011* (02), 223–228. https://doi.org/10.1055/s-0030-1258357.

(135) Hansen, S. G.; Jensen, H. H. ChemInform Abstract: Microwave Irradiation as an Effective Means of Synthesizing Unsubstituted N-Linked 1,2,3-Triazoles from Vinyl Acetate and Azides. *ChemInform* **2010**, *41* (18). https://doi.org/10.1002/chin.201018128.

(136) Khalili, D.; Kavoosi, L.; Khalafi-Nezhad, A. Copper Aluminate Spinel in Click Chemistry: An Efficient Heterogeneous Nanocatalyst for the Highly Regioselective Synthesis of Triazoles in Water. *Synlett* **2019**, *30* (19), 2136–2142. https://doi.org/10.1055/s-0039-1690719.

(137) Varvaresou, A.; Tsantili-Kakoulidou, A.; Siatra-Papastaikoudi, T.; Tiligada, E. Synthesis and Biological Evaluation of Indole Containing Derivatives of Thiosemicarbazide and Their Cyclic 1,2,4-Triazole and 1,3,4-Thiadiazole Analogs. *Arzneimittelforschung* **2011**, *50* (01), 48–54. https://doi.org/10.1055/s-0031-1300163.

(138) Jiang, Y.; Kuang, C.; Yang, Q. The Use of Calcium Carbide in the Synthesis of 1-Monosubstituted Aryl 1,2,3-Triazole via Click Chemistry. *Synlett* **2009**, *2009* (19), 3163–3166. https://doi.org/10.1055/s-0029-1218346.

(139) Boren, B. C.; Narayan, S.; Rasmussen, L. K.; Zhang, L.; Zhao, H.; Lin, Z.; Jia, G.; Fokin, V. V. Ruthenium-Catalyzed Azide−Alkyne Cycloaddition: Scope and Mechanism. *J. Am. Chem. Soc.* **2008**, *130* (28), 8923–8930. https://doi.org/10.1021/ja0749993.

(140) Rostovtsev, V. V.; Green, L. G.; Fokin, V. V.; Sharpless, K. B. A Stepwise Huisgen Cycloaddition Process: Copper(I)-Catalyzed Regioselective "Ligation" of Azides and Terminal Alkynes. *Angew. Chemie Int. Ed.* **2002**, *41* (14), 2596–2599. https://doi.org/10.1002/1521-3773(20020715)41:14<2596::AID-ANIE2596>3.0.CO;2-4.

(141) Himo, F.; Lovell, T.; Hilgraf, R.; Rostovtsev, V. V.; Noodleman, L.; Sharpless, K. B.; Fokin, V. V. Copper(I)-Catalyzed Synthesis of Azoles. DFT Study Predicts Unprecedented Reactivity and Intermediates. *J. Am. Chem. Soc.* **2005**, *127* (1), 210–216. https://doi.org/10.1021/ja0471525.

(142) Palmer, M. H.; Camp, P. J.; Hoffmann, S. V.; Jones, N. C.; Head, A. R.; Lichtenberger, D. L. The Electronic States of 1,2,4-Triazoles: A Study of 1H- and 1-Methyl-1,2,4-Triazole by Vacuum Ultraviolet Photoabsorption and Ultraviolet Photoelectron Spectroscopy and a Comparison with Ab Initio Configuration Interaction Computations. *J. Chem. Phys.* **2012**, *136* (9), 094310. https://doi.org/10.1063/1.3692164.

(143) Bonandi, E.; Christodoulou, M. S.; Fumagalli, G.; Perdicchia, D.; Rastelli, G.; Passarella, D. The 1,2,3-Triazole Ring as a Bioisostere in Medicinal Chemistry. *Drug Discov. Today* **2017**, *22* (10), 1572–1581. https://doi.org/10.1016/j.drudis.2017.05.014.

(144) Mohammed, I.; Kummetha, I. R.; Singh, G.; Sharova, N.; Lichinchi, G.; Dang, J.; Stevenson, M.; Rana, T. M. 1,2,3-Triazoles as Amide Bioisosteres: Discovery of a New Class of Potent HIV-1 Vif Antagonists. *J. Med. Chem.* **2016**, *59* (16), 7677–7682. https://doi.org/10.1021/acs.jmedchem.6b00247.

(145) Song, W.-H.; Liu, M.-M.; Zhong, D.-W.; Zhu, Y.; Bosscher, M.; Zhou, L.; Ye, D.-Y.; Yuan, Z.-H. Tetrazole and Triazole as Bioisosteres of Carboxylic Acid: Discovery of Diketo Tetrazoles and Diketo Triazoles as Anti-HCV Agents. *Bioorg. Med. Chem. Lett.* **2013**, *23* (16), 4528–4531. https://doi.org/10.1016/j.bmcl.2013.06.045.

(146) Peyton, L. R.; Gallagher, S.; Hashemzadeh, M. Triazole Antifungals: A Review. *Drugs of Today*. 2015. https://doi.org/10.1358/dot.2015.51.12.2421058.

(147) Roberts, J.; Schock, K.; Marino, S.; Andriole, V. T. Efficacies of Two New Antifungal Agents, the Triazole Ravuconazole and the Echinocandin LY-303366, in an Experimental Model of Invasive Aspergillosis. *Antimicrob. Agents Chemother.* **2000**, *44* (12), 3381–3388. https://doi.org/10.1128/AAC.44.12.3381-3388.2000.

(148) Espinel-Ingroff, A. In Vitro Activity of the New Triazole Voriconazole (UK-109,496) against Opportunistic Filamentous and Dimorphic Fungi and Common and Emerging Yeast Pathogens. *J. Clin. Microbiol.* **1998**, *36* (1), 198–202. https://doi.org/10.1128/JCM.36.1.198-202.1998.

(149) Johnson, L. B.; Kauffman, C. A. Voriconazole: A New Triazole Antifungal Agent. *Clin. Infect. Dis.* **2003**, *36* (5), 630–637. https://doi.org/10.1086/367933.

(150) Chai, B.; Qian, X.; Cao, S.; Liu, H.; Song, G. Synthesis and Insecticidal Activity of 1,2,4-Triazole Derivatives. *Arkivoc* **2003**, *2003* (2), 141–145. https://doi.org/10.3998/ark.5550190.0004.216.

(151) Maddila, S.; Pagadala, R.; Jonnalagadda, S. B. Synthesis and Insecticidal Activity of Tetrazole-Linked Triazole Derivatives. *J. Heterocycl. Chem.* **2015**, *52* (2), 487–491. https://doi.org/10.1002/jhet.2078.

(152) Zheng, T.; Rouhanifard, S. H.; Jalloh, A. S.; Wu, P. Click Triazoles for Bioconjugation; 2012; pp 163–183. https://doi.org/10.1007/7081_2011_72.

(153) Dondoni, A. Heterocycles in Organic Synthesis: Thiazoles and Triazoles as Exemplar Cases of Synthetic Auxiliaries. *Org. Biomol. Chem.* **2010**, *8* (15), 3366. https://doi.org/10.1039/c002586k.

(154) Haas, K. L.; Franz, K. J. Application of Metal Coordination Chemistry To Explore and Manipulate Cell Biology. *Chem. Rev.* **2009**, *109* (10), 4921–4960. https://doi.org/10.1021/cr900134a.

(155) Soto, J.; Otero, J. C.; Avila, F. J.; Peláez, D. Conical Intersections and Intersystem Crossings Explain Product Formation in Photochemical Reactions of Aryl Azides. *Phys. Chem. Chem. Phys.* **2019**, *21* (5), 2389–2396. https://doi.org/10.1039/C8CP06974C.

(156) Marcinek, A.; Leyva, E.; Whitt, D.; Platz, M. S. Evidence for Stepwise Nitrogen Extrusion and Ring Expansion upon Photolysis of Phenyl Azide. *J. Am. Chem. Soc.* **1993**, *115* (19), 8609–8612. https://doi.org/10.1021/ja00072a013.

(157) Xue, J.; Du, Y.; Chuang, Y. P.; Phillips, D. L.; Wang, J.; Luk, C.; Hadad, C. M.; Platz, M. S. Time-Resolved Resonance Raman Observation of the Dimerization of Didehydroazepines in Solution. *J. Phys. Chem. A* **2008**, *112* (7), 1502–1510. https://doi.org/10.1021/jp077215g.

(158) Kwok, W. M.; Chan, P. Y.; Phillips, D. L. Direct Observation of the 4-Methoxyphenylnitrene Intersystem Crossing from S 1 to T 1 Using Picosecond Kerr-Gated Time-Resolved Resonance Raman Spectroscopy. *J. Phys. Chem. A* **2005**, *109* (10), 2394–2400. https://doi.org/10.1021/jp044670t.

(159) Nunes, C. M.; Reva, I.; Kozuch, S.; McMahon, R. J.; Fausto, R. Photochemistry of 2-Formylphenylnitrene: A Doorway to Heavy-Atom Tunneling of a Benzazirine to a Cyclic Ketenimine. *J. Am. Chem. Soc.* **2017**, *139* (48), 17649–17659. https://doi.org/10.1021/jacs.7b10495.

(160) Mieres-Perez, J.; Costa, P.; Mendez-Vega, E.; Crespo-Otero, R.; Sander, W. Switching the Spin State of Pentafluorophenylnitrene: Isolation of a Singlet Arylnitrene Complex. *J. Am. Chem. Soc.* **2018**, *140* (49), 17271–17277. https://doi.org/10.1021/jacs.8b10792.

(161) Gritsan, N. P.; Platz, M. S. Kinetics, Spectroscopy, and Computational Chemistry of Arylnitrenes. *Chemical Reviews*. 2006. https://doi.org/10.1021/cr040055+.

(162) Aranda, D.; Avila, F. J.; López-Tocón, I.; Arenas, J. F.; Otero, J. C.; Soto, J. An MS-CASPT2 Study of the Photodecomposition of 4-Methoxyphenyl Azide: Role of Internal Conversion and Intersystem Crossing. *Phys. Chem. Chem. Phys.* **2018**, *20* (11), 7764–7771. https://doi.org/10.1039/C8CP00147B.

(163) Abramovitch, R. A.; Jeyaraman, R. Azides and Nitrenes: Reactivity and Utility. In *Azides and Nitrenes: Reactivity and Utility*; 1984.

(164) Tanimoto, H.; Kakiuchi, K. Recent Applications and Developments of Organic Azides in Total Synthesis of Natural Products. *Natural Product Communications*. Natural Product Incorporation 2013, pp 1021–1034. https://doi.org/10.1177/1934578x1300800730.

(165) Lord, S. J.; Lee, H. D.; Samuel, R.; Weber, R.; Liu, N.; Conley, N. R.; Thompson, M. A.; Twieg, R. J.; Moerner, W. E. Azido Push−Pull Fluorogens Photoactivate to Produce Bright Fluorescent Labels. *J. Phys. Chem. B* **2010**, *114* (45), 14157–14167. https://doi.org/10.1021/jp907080r.

(166) Streitwieser, A.; Pulver, S. The Azide Group as a Neighboring Group. Acetolysis of Trans-2-Azidocyclohexyl p-Toluenesulf Onate. *J. Am. Chem. Soc.* **1964**, *86* (8), 1587–1588. https://doi.org/10.1021/ja01062a028.

(167) Drost, P. Nitro-Derivatives of Orthodinitrosobenzene. *Justus Liebigs Ann. der Chemie.* **1899**, *307*, 49–69.

(168) Forster, M. O.; Fierz, H. E. CLXXXIX.—Aromatic Azoimides. Part III. The Naphthylazoimides and Their Nitro-Derivatives. *J. Chem. Soc., Trans.* **1907**, *91*, 1942–1953. https://doi.org/10.1039/CT9079101942.

(169) Smith, P. A. S.; Hall, J. H.; Kan, R. O. The Electronic Character of the Azido Group Attached to Benzene Rings. *J. Am. Chem. Soc.* **1962**, *84* (3),. https://doi.org/10.1021/ja00862a033.

(170) Stankovsky, S.; Kovac, S. Infrared Spectra of Heterocumulenes. IV. The Influence of Substituents on the Vas(NNN) Bands of Some Substituted Phenyl Azides. *Chem. zvesti* **1974**, *2*, 243–246.

(171) Hammett, L. P. The Effect of Structure upon the Reactions of Organic Compounds. Benzene Derivatives. *J. Am. Chem. Soc.* **1937**, *59* (1), 96–103. https://doi.org/10.1021/ja01280a022.

(172) Hehre, W. J.; Taft, R. W.; Topsom, R. D. Ab Initio Calculations of Charge Distributions in Monosubstituted Benzenes and in Meta- and Para-Substituted Fluorobenzenes. Comparison with 1 H, 13 C, and 19 F Nmr Substituent Shifts. In *Progress in Physical Organic Chemistry*; 2007; pp 159–187. https://doi.org/10.1002/9780470171912.ch6.

(173) Armentrout, P. B. Entropy Measurements and the Kinetic Method: A Statistically Meaningful Approach. *J. Am. Soc. Mass Spectrom.* **2000**, *11* (5), 371–379. https://doi.org/10.1016/S1044-0305(00)00102-1.

(174) Zilla, M. K.; Nayak, D.; Vishwakarma, R. A.; Sharma, P. R.; Goswami, A.; Ali, A. A Convergent Synthesis of Alkyne–Azide Cycloaddition Derivatives of 4-α,β-2-Propyne Podophyllotoxin Depicting Potent Cytotoxic Activity. *Eur. J. Med. Chem.* **2014**, *77*, 47–55. https://doi.org/10.1016/j.ejmech.2014.02.030.

(175) Demeter, O.; Fodor, E. A.; Kállay, M.; Mező, G.; Németh, K.; Szabó, P. T.; Kele, P. A Double-Clicking Bis-Azide Fluorogenic Dye for Bioorthogonal Self-Labeling Peptide Tags. *Chem. – A Eur. J.* **2016**, *22* (18), 6382–6388. https://doi.org/10.1002/CHEM.201504939.

(176) Fujio, M.; McIver, R. T.; Taft, R. W. Effects of the Acidities of Phenols from Specific Substituent-Solvent Interactions. Inherent Substituent Parameters from Gas-Phase Acidities. *J. Am. Chem. Soc.* **1981**, *103* (14), 4017–4029. https://doi.org/10.1021/ja00404a008.

(177) Hernandez-Gil, N.; Wentworth, W. E.; Chen, E. C. M. Electron Affinities of Fluorinated Phenoxy Radicals. *J. Phys. Chem.* **1984**, *88* (25), 6181–6185. https://doi.org/10.1021/j150669a025.

(178) Drahos, L.; Vékey, K. How Closely Related Are the Effective and the Real Temperature. *J. Mass Spectrom.* **1999**, *34* (2), 79–84. https://doi.org/10.1002/(SICI)1096-9888(199902)34:2<79::AID-JMS793>3.0.CO;2-V.

(179) Ervin, K. M. Microcanonical Analysis of the Kinetic Method. *Int. J. Mass Spectrom.* **2000**, *195–196*, 271–284. https://doi.org/10.1016/S1387-3806(99)00176-1.

(180) Ervin, K. M.; Armentrout, P. B. Systematic and Random Errors in Ion Affinities and Activation Entropies from the Extended Kinetic Method. *J. Mass Spectrom.* **2004**, *39* (9), 1004–1015. https://doi.org/10.1002/jms.682.

(181) Ervin, K. M. Microcanonical Analysis of the Kinetic Method. The Meaning of the "Apparent Entropy." *J. Am. Soc. Mass Spectrom.* **2002**, *13* (5), 435–452. https://doi.org/10.1016/S1044-0305(02)00357-4.

(182) Hahn, I.-S.; Wesdemiotis, C. Protonation Thermochemistry of β-Alanine. *Int. J. Mass Spectrom.* **2003**, *222* (1–3), 465–479. https://doi.org/10.1016/S1387-3806(02)01018-7.

(183) Cheng, X.; Wu, Z.; Fenselau, C. Collision Energy Dependence of Proton-Bound Dimer Dissociation: Entropy Effects, Proton Affinities, and Intramolecular Hydrogen-Bonding in Protonated Peptides. *J. Am. Chem. Soc.* **1993**, *115* (11), 4844–4848. https://doi.org/10.1021/ja00064a052.

(184) Cooks, R. G.; Kruger, T. L. Intrinsic Basicity Determination Using Metastable Ions. *J. Am. Chem. Soc.* **1977**, *99* (4), 1279–1281. https://doi.org/10.1021/ja00446a059.

(185) Nold, M. J.; Cerda, B. A.; Wesdemiotis, C. Proton Affinities of the N- and C-Terminal Segments Arising upon the Dissociation of the Amide Bond in Protonated Peptides. *J. Am. Soc. Mass Spectrom.* **1999**, *10* (1), 1–8. https://doi.org/10.1016/S1044-0305(98)00120-2.

(186) Wenthold, P. G. Determination of the Proton Affinities of Bromo- and Iodoacetonitrile Using the Kinetic Method with Full Entropy Analysis. *J. Am. Soc. Mass Spectrom.* **2000**, *11* (7), 601–605. https://doi.org/10.1016/S1044-0305(00)00120-3.

(187) Angel, L. A.; Ervin, K. M. Competitive Threshold Collision-Induced Dissociation: Gas-Phase Acidity and O−H Bond Dissociation Enthalpy of Phenol. *J. Phys. Chem. A* **2004**, *108* (40), 8346–8352. https://doi.org/10.1021/jp0474529.

(188) Hansch, C.; Leo, A.; Taft, R. W. A Survey of Hammett Substituent Constants and Resonance and Field Parameters. *Chem. Rev.* **1991**, *91* (2), 165–195. https://doi.org/10.1021/cr00002a004.

(189) Poole, J. S. A Computational Study of the Chemistry of Substituted 3-Nitrenopyridine 1-Oxides. *J. Mol. Struct. Theochem* **2009**, *894* (1–3), 93–102. https://doi.org/10.1016/j.theochem.2008.10.002.

(190) Bull, J. A.; Mousseau, J. J.; Pelletier, G.; Charette, A. B. Synthesis of Pyridine and Dihydropyridine Derivatives by Regio- and Stereoselective Addition to N -Activated Pyridines. *Chem. Rev.* **2012**, *112* (5), 2642–2713. https://doi.org/10.1021/cr200251d.

(191) Andersson, H.; Gustafsson, M.; Olsson, R.; Almqvist, F. Selective Synthesis of 2-Substituted Pyridine N-Oxides via Directed Ortho-Metallation Using Grignard Reagents. *Tetrahedron Lett.* **2008**, *49* (48), 6901–6903. https://doi.org/10.1016/j.tetlet.2008.09.104.

(192) Mongin, O.; Rocca, P.; Thomas-Dit-Dumont, L.; Trecourt, F.; Marsais, F.; Godard, A.; Queguiner, G. ChemInform Abstract: Metalation of Pyridine N-Oxides and Application to Synthesis. *ChemInform* **2010**, *27* (5), no-no. https://doi.org/10.1002/chin.199605164.

(193) Abramovitch, R. A.; Smith, E. M.; Knaus, E. E.; Saha, M. Direct Alkylation of Pyridine 1-Oxides. *J. Org. Chem.* **1972**, *37* (11), 1690–1696. https://doi.org/10.1021/jo00976a003.

(194) YAMANAKA, H.; ARAKI, T.; SAKAMOTO, T. Site-Selectivity in the Reaction of 3-Substituted Pyridine 1-Oxides with Phosphoryl Chloride. *Chem. Pharm. Bull.* **1988**, *36* (6), 2244–2247. https://doi.org/10.1248/cpb.36.2244.

(195) Clark, R. B.; He, M.; Fyfe, C.; Lofland, D.; O'Brien, W. J.; Plamondon, L.; Sutcliffe, J. A.; Xiao, X.-Y. 8-Azatetracyclines: Synthesis and Evaluation of a Novel Class of Tetracycline Antibacterial Agents. *J. Med. Chem.* **2011**, *54* (5), 1511–1528. https://doi.org/10.1021/jm1015389.

(196) Yin, J.; Xiang, B.; Huffman, M. A.; Raab, C. E.; Davies, I. W. A General and Efficient 2-Amination of Pyridines and Quinolines. *J. Org. Chem.* **2007**, *72* (12), 4554–4557. https://doi.org/10.1021/jo070189y.

(197) Borden, W. T.; Gritsan, N. P.; Hadad, C. M.; Karney, W. L.; Kemnitz, C. R.; Platz, M. S. The Interplay of Theory and Experiment in the Study of Phenylnitrene. *Acc. Chem. Res.* **2000**, *33* (11). https://doi.org/10.1021/ar990030a.

(198) Kim, S. J.; Hamilton, T.; Schaefer, H. Phenylnitrene: Energetics, Vibrational Frequencies, and Molecular Structures. *J. Am. Chem. Soc.* **1992**, *114* (13).

(199) Hrovat, D. A.; Waali, E. E.; Borden, W. T. Ab Initio Calculations of the Singlet-Triplet Energy Difference in Phenylnitrene. *J. Am. Chem. Soc.* **1992**, *114* (22). https://doi.org/10.1021/ja00048a052.

(200) Smith, B. A.; Cramer, C. J. How Do Different Fluorine Substitution Patterns Affect the Electronic State Energies of Phenylnitrene? *J. Am. Chem. Soc.* **1996**, *118* (23). https://doi.org/10.1021/ja960687g.

(201) Castell, O.; García, V. M.; Bo, C.; Caballol, R. Relative Stability of the 3A2, 1A2, and 1A1 States of Phenylnitrene: A Difference-Dedicated Configuration Interaction Calculation. *J. Comput. Chem.* **1996**, *17* (1).

(202) Kemnitz, C. R.; Karney, W. L.; Borden, W. T. Why Are Nitrenes More Stable than Carbenes? An Ab Initio Study. *J. Am. Chem. Soc.* **1998**, *120* (14). https://doi.org/10.1021/ja973935x.

(203) Burdzinski, G. T.; Middleton, C. T.; Gustafson, T. L.; Platz, M. S. Solution Phase Isomerization of Vibrationally Excited Singlet Nitrenes to Vibrationally Excited 1,2-Didehydroazepine. *J. Am. Chem. Soc.* **2006**, *128* (46). https://doi.org/10.1021/ja065783o.

(204) Grote, D.; Sander, W. Photochemistry of Fluorinated 4-Iodophenylnitrenes: Matrix Isolation and Spectroscopic Characterization of Phenylnitrene-4-Yls. *J. Org. Chem.* **2009**, *74* (19). https://doi.org/10.1021/jo901145h.

(205) Tsao, M. L.; Platz, M. S. Photochemistry of Ortho, Ortho' Dialkyl Phenyl Azides. *J. Am. Chem. Soc.* **2003**, *125* (39). https://doi.org/10.1021/ja035833e.

(206) Gritsan, N. P.; Zhu, Z.; Hadad, C. M.; Platz, M. S. Laser Flash Photolysis and Computational Study of Singlet Phenylnitrene. *J. Am. Chem. Soc.* **1999**, *121* (6). https://doi.org/10.1021/ja982661q.

(207) Johnson, W. T. G.; Sullivan, M. B.; Cramer, C. J. Meta and Para Substitution Effects on the Electronic State Energies and Ring-Expansion Reactivities of Phenylnitrenes. In *International Journal of Quantum Chemistry*; 2001; Vol. 85.

(208) Karney, W. L.; Borden, W. T. Ab Initio Study of the Ring Expansion of Phenylnitrene and Comparison with the Ring Expansion of Phenylcarbene. *J. Am. Chem. Soc.* **1997**, *119* (6), 1378–1387. https://doi.org/10.1021/ja9635241.

(209) Sankaranarayanan, J.; Rajam, S.; Hadad, C. M.; Gudmundsdottir, A. D. The Ability of Triplet Nitrenes to Abstract Hydrogen Atoms. *J. Phys. Org. Chem.* **2010**, *23* (4). https://doi.org/10.1002/poc.1654.

(210) Winkler, M. Singlet - Triplet Energy Splitting and Excited States of Phenylnitrene. *J. Phys. Chem. A* **2008**, *112* (37). https://doi.org/10.1021/jp802547c.

(211) Travers, M. J.; Cowles, D. C.; Clifford, E. P.; Ellison, G. B. Photoelectron Spectroscopy of the Phenylnitrene Anion. *J. Am. Chem. Soc.* **1992**, *114* (22). https://doi.org/10.1021/ja00048a053.

(212) Geise, C. M.; Hadad, C. M. Computational Study of the Electronic Structure of Substituted Phenylcarbene in the Gas Phase. *J. Org. Chem.* **2000**, *65* (24).

(213) Salem, L.; Rowland, C. The Electronic Properties of Diradicals. *Angew. Chemie Int. Ed. English* **1972**, *11* (2). https://doi.org/10.1002/anie.197200921.

(214) Geiger, U.; Haas, Y.; Grinstein, D. The Photochemistry of an Aryl Pentazole in Liquid Solutions: The Anionic 4-Oxidophenylpentazole (OPP). *J. Photochem. Photobiol. A Chem.* **2014**, *277*. https://doi.org/10.1016/j.jphotochem.2013.12.008.

(215) Gibbs, H. D. Phenol Tests. IV. A Study of the Velocity of Indophenol Formation 2, 6-Dibromobenzenoneindophenol. *J. Phys. Chem.* **1927**, *31* (7), 1053–1081. https://doi.org/10.1021/j150277a005.

(216) Sowjanya, K.; Thejaswini, J. C.; Gurupadayya, B. M.; Indupriya, M. Spectrophotometric Determination of Pregabalin Using Gibb's and MBTH Reagent in Pharmaceutical Dosage Form. *Der Pharma Chem.* **2011**, *3* (1).

(217) Gousuddin, M.; Appala Raju, S.; Sultanuddin; Manjunath, S. Development and Validation of Spectrophotometric Methods for Estimation of Formoterol Bulk Drug and Its Pharmaceutical Dosage Forms. *Int. J. Pharm. Pharm. Sci.* **2011**, *3* (3).

(218) Karimi, M.; Hassanshahian, M. Isolation and Characterization of Phenol Degrading Yeasts from Wastewater in the Coking Plant of Zarand, Kerman. *Brazilian J. Microbiol.* **2016**, *47* (1). https://doi.org/10.1016/j.bjm.2015.11.032.

(219) Rao Somisetty, V. S.; Bichala, P. K.; Prasada Rao, C. M. M.; Kirankumar, V. Development and Validation of Newer Analytical Methods for the Estimation of Deferasirox in Bulk and in Tablet Dosage Form by Calorimetric Method. *Int. J. Pharm. Pharm. Sci.* **2013**, *5* (SUPPL 3).

(220) Tuljarani, G.; Gowri Sankar, D.; Kadgapathi, P.; Suthakaran, R.; Satyanarayana, B. Quantitative determination of bisoprolol fumarate in bulk and pharmaceutical dosage forms by spectrophotometry. *Int. J. Chem. Sci* **2010**, *8* (4).

(221) Patel, K. M.; Patel, C. N.; Panigrahi, B.; Parikh, A. S.; Patel, H. N. Development and Validation of Spectrophotometric Methods for the Estimation of Mesalamine in Tablet Dosage Forms. *J. Young Pharm.* **2010**, *2* (3). https://doi.org/10.4103/0975-1483.66789.

(222) Ankita, M.; Gurupadayya, B. M.; Chandra, A. Colorimetric Estimation of Acenocoumarol in Bulk and Pharmaceutical Formulations. *Asian J. Chem.* **2008**, *20* (7).

(223) Mohler, E. F.; Jacob, L. N. Determination of Phenolic-Type Compounds in Water and Industrial Waste Waters. Comparison of Analytical Methods. *Anal. Chem.* **1957**, *29* (9). https://doi.org/10.1021/ac60129a036.

(224) Ettinger, M. B.; Ruchhoft, C. C. Determination of Phenol and Structurally Related Compounds by the Gibbs Method. *Anal. Chem.* **1948**, *20* (12). https://doi.org/10.1021/ac60024a018.

(225) Pallagi, I.; Toro, A.; Farkas, O. Mechanism of the Gibbs Reaction. 3. Indophenol Formation via Radical Electrophilic Aromatic Substitution (SREAr) on Phenols. *J. Org. Chem.* **1994**, *59* (22), 6543–6557. https://doi.org/10.1021/jo00101a013.

(226) Pallagi, I.; Toró, A.; Horváth, G. Mechanism of the Gibbs Reaction. Part 4. 1 Indophenol Formation via N -Chlorobenzoquinone Imine Radical Anions. The Aza-S RN 2 Chain Reaction Mechanism. Chain Initiation with 1,4-Benzoquinones and Cyanide Ion. *J. Org. Chem.* **1999**, *64* (18), 6530–6540. https://doi.org/10.1021/jo982113v.

(227) Pallagi, I.; Toro, A.; Farkas, O. ChemInform Abstract: Mechanism of the Gibbs Reaction. Part 3. Indophenol Formation via Radical Electrophilic Aromatic Substitution (SREAr) on Phenols. *ChemInform* **2010**, *26* (20), no-no. https://doi.org/10.1002/chin.199520027.

(228) Pallagi, I.; Dvortsák, P. Gibbs Reaction. Part 1. Reduction of Benzoquinone N-Chloroimines to Benzoquinone Imines. *J. Chem. Soc., Perkin Trans. 2* **1986**, No. 1, 105–110. https://doi.org/10.1039/P29860000105.

(229) Pallagi, I.; Toró, A.; Müller, J. The Mechanism of the Gibbs Reaction. Part 2: The Ortho ⇉ Ortho 2,4-Cyclohexadiene-1-One Rearrangement of the Reaction Product of 2,6-Di-Tert-Butyl-4-Chlorophenol and 2,6-Dichlorobenzoquinone N-Chloroimine. *Tetrahedron* **1994**, *50* (29), 8809–8814. https://doi.org/10.1016/S0040-4020(01)85354-0.

(230) Letard, J.; Guionneau, P.; Goux-Capes, L. Spin Crossover in Transition Metal Compounds III. *Spin Crossover Transit. Met. Coumpounds III* **2004**, *235*. https://doi.org/10.1007/b96439.

(231) Gómez Alvarez, E.; Wortham, H.; Strekowski, R.; Zetzsch, C.; Gligorovski, S. Atmospheric Photosensitized Heterogeneous and Multiphase Reactions: From Outdoors to Indoors. *Environ. Sci. Technol.* **2012**, *46* (4). https://doi.org/10.1021/es2019675.

(232) Romero, N. A.; Nicewicz, D. A. Organic Photoredox Catalysis. *Chemical Reviews*. 2016. https://doi.org/10.1021/acs.chemrev.6b00057.

(233) Sergentu, D. C.; Maurice, R.; Havenith, R. W. A.; Broer, R.; Roca-Sanjuán, D. Computational Determination of the Dominant Triplet Population Mechanism in Photoexcited Benzophenone. *Phys. Chem. Chem. Phys.* **2014**, *16* (46). https://doi.org/10.1039/c4cp03277b.

(234) Zhao, J.; Wu, W.; Sun, J.; Guo, S. Triplet Photosensitizers: From Molecular Design to Applications. *Chem. Soc. Rev.* **2013**, *42* (12). https://doi.org/10.1039/c3cs35531d.

(235) Cuquerella, M. C.; Lhiaubet-Vallet, V.; Cadet, J.; Miranda, M. A. Benzophenone Photosensitized DNA Damage. *Acc. Chem. Res.* **2012**, *45* (9). https://doi.org/10.1021/ar300054e.

(236) Steffen, J.; Rice, J.; Lecuona, K.; Carrara, H. Identification of Ocular Surface Squamous Neoplasia by in Vivo Staining with Methylene Blue. *Br. J. Ophthalmol.* **2014**, *98* (1). https://doi.org/10.1136/bjophthalmol-2013-303956.

(237) Tandon, A.; Singh, N. N.; Brave, V. R.; Sreedhar, G. Image Analysis Assisted Study of Mitotic Figures in Oral Epithelial Dysplasia and Squamous Cell Carcinoma Using Differential Stains. *J. Oral Biol. Craniofacial Res.* **2016**, *6*. https://doi.org/10.1016/j.jobcr.2016.09.003.

(238) Veuthey, T. V.; Herrera, G.; Dodero, V. I. Dyes and Stains: From Molecular Structure to Histological Application. *Frontiers in Bioscience - Landmark*. 2014. https://doi.org/10.2741/4197.

(239) Kaim, W.; Moscherosch, M. The Coordination Chemistry of TCNE, TCNQ and Related Polynitrileπ Acceptors. *Coord. Chem. Rev.* **1994**, *129* (1–2). https://doi.org/10.1016/0010-8545(94)85020-8.

(240) Bespalov, B. P.; Titov, V. V. 7,7,8,8-Tetracyanoquinodimethane in Addition, Substitution, and Complex Formation Reactions. *Russ. Chem. Rev.* **1975**, *44* (12). https://doi.org/10.1070/rc1975v044n12abeh002559.

(241) Acker, D. S.; Hertler, W. R. Substituted Quinodimethans. I. Preparation and Chemistry of 7, 7, 8, 8-Tetracyano Quino Dimethan. *J. Am. Chem. Soc.* **1962**, *84* (17). https://doi.org/10.1021/ja00876a028.

(242) Acker, D. S.; Harder, R. J.; Hertler, W. R.; Mahler, W.; Melby, L. R.; Benson, R. E.; Mochel, W. E. 7,7,8,8-Tetracyanoquinodimethane and Its Electrically Conducting Anion-Radical Derivatives. *Journal of the American Chemical Society*. 1960. https://doi.org/10.1021/ja01509a052.

(243) Miller, J. R.; Calcaterra, L. T.; Closs, G. L. Cheminform Abstract: Intramolecular Long-Distance Electron Transfer In Radical Anions. The Effects Of Free Energy And Solvent On The Reaction Rates. *Chem. Informationsd.* **1984**, *15* (34). https://doi.org/10.1002/chin.198434111.

(244) Indelli, M. T.; Ballardini, R.; Scandola, F. Experimental Investigation of Highly Exergonic Outer-Sphere Electron-Transfer Reactions. *J. Phys. Chem.* **1984**, *88* (12). https://doi.org/10.1021/j150656a023.

(245) Closs, G. L.; Calcaterra, L. T.; Green, N. J.; Penfield, K. W.; Miller, J. R. Distance, Stereoelectronic Effects, and the Marcus Inverted Region in Intramolecular Electron Transfer in Organic Radical Anions. *J. Phys. Chem.* **1986**, *90* (16). https://doi.org/10.1021/j100407a039.

(246) Calcaterra, L. T.; Closs, G. L.; Miller, J. R. Fast Intramolecular Electron Transfer in Radical Ions over Long Distances across Rigid Saturated Hydrocarbon Spacers. *J. Am. Chem. Soc.* **1983**, *105* (3). https://doi.org/10.1021/ja00341a084.

(247) Rehm, D.; Weller, A. Kinetics of Fluorescence Quenching by Electron and H-Atom Transfer. *Isr. J. Chem.* **1970**, *8* (2). https://doi.org/10.1002/ijch.197000029.

(248) A., W. Kinetics and Mechanics of Electron Transfer During Fluorescence Quenching in Acetonitrile. *Ber. Bunsenges. Phys. Chem.* 1969.

(249) Marcus, R. A.; Sutin, N. Electron Transfers in Chemistry and Biology. *BBA Reviews On Bioenergetics*. 1985. https://doi.org/10.1016/0304-4173(85)90014-X.

(250) Baptista, M. S.; Wainwright, M. Photodynamic Antimicrobial Chemotherapy (PACT) for the Treatment of Malaria, Leishmaniasis and Trypanosomiasis. *Brazilian Journal of Medical and Biological Research*. 2011. https://doi.org/10.1590/S0100-879X2010007500141.

(251) Abrahamse, H.; Hamblin, M. R. New Photosensitizers for Photodynamic Therapy. *Biochemical Journal*. 2016. https://doi.org/10.1042/BJ20150942.

(252) Lamola, A. A.; Yamane, T. Sensitized Photodimerization of Thymine in DNA. *Proc. Natl. Acad. Sci. U. S. A.* **1967**, *58* (2). https://doi.org/10.1073/pnas.58.2.443.

(253) Consuelo Cuquerella, M.; Lhiaubet-Vallet, V.; Bosca, F.; Miranda, M. A. Photosensitised Pyrimidine Dimerisation in DNA. *Chem. Sci.* **2011**, *2* (7).

(254) Tucker, D.; Lu, Y.; Zhang, Q. From Mitochondrial Function to Neuroprotection—an Emerging Role for Methylene Blue. *Molecular Neurobiology*. 2018. https://doi.org/10.1007/s12035-017-0712-2.

(255) Papadopoulou, E.; Gale, N.; Thompson, J. F.; Fleming, T. A.; Brown, T.; Bartlett, P. N. Specifically Horizontally Tethered DNA Probes on Au Surfaces Allow Labelled and Label-Free DNA Detection Using SERS and Electrochemically Driven Melting. *Chem. Sci.* **2016**, *7* (1). https://doi.org/10.1039/c5sc03185k.

(256) Gaudette, N. F.; Lodge, J. W. Determination of Methylene Blue and Leucomethylene Blue in Male and Female Fischer 344 Rat Urine and B6C3F1 Mouse Urine. *J. Anal. Toxicol.* **2005**, *29* (1). https://doi.org/10.1093/jat/29.1.28.

(257) D'Autréaux, B.; Toledano, M. B. ROS as Signalling Molecules: Mechanisms That Generate Specificity in ROS Homeostasis. *Nature Reviews Molecular Cell Biology*. 2007. https://doi.org/10.1038/nrm2256.

(258) Hossain, E.; Deng, S. M.; Gozem, S.; Krylov, A. I.; Wang, X.-B.; Wenthold, P. G. Photoelectron Spectroscopy Study of Quinonimides. *J. Am. Chem. Soc.* **2017**, *139* (32), 11138–11148. https://doi.org/10.1021/jacs.7b05197.

(259) Doering, W. vo. E.; Odum, R. A. Ring Enlargement in the Photolysis of Phenyl Azide. *Tetrahedron* **1966**, *22* (1), 81–93. https://doi.org/10.1016/0040-4020(66)80104-7.

(260) Meijer, E. W.; Nijhuis, S.; Van Vroonhoven, F. C. B. M. Poly-1,2-Azepines by the Photopolymerization of Phenyl Azides. Precursors for Conducting Polymer Films. *J. Am. Chem. Soc.* **1988**, *110* (21), 7209–7210. https://doi.org/10.1021/ja00229a043.

(261) Banks, R. E.; Sparkes, G. R. Studies in Azide Chemistry. Part V. Synthesis of 4-Azido-2,3,5,6-Tetrafluoro-, 4-Azido-3-Chloro-2,5,6-Trifluoro-, and 4-Azido-3,5-Dichloro-2,6-Difluoro-Pyridine, and Some Thermal Reactions of the Tetrafluoro-Compound. *J. Chem. Soc. Perkin Trans. 1* **1972**, No. 0, 2964. https://doi.org/10.1039/p19720002964.

(262) Banks, R. E.; Prakash, A. New Reactions of Azidopentafluorobenzene; Intermolecular ′insertions′ into n-h Bonds. *Tetrahedron Lett.* **1973**, *14* (2), 99–102. https://doi.org/https://doi.org/10.1016/S0040-4039(01)95587-X.

(263) Banks, R. E.; Prakash, A. Studies in Azide Chemistry. Part VI. Some Reactions of Perfluoroazidobenzene and Perfluoro-4-Azidotoluene. *J. Chem. Soc. Perkin Trans. 1* **1974**, 1365. https://doi.org/10.1039/p19740001365.

(264) Borden, W. T.; Davidson, E. R. Effects of Electron Repulsion in Conjugated Hydrocarbon Diradicals. *J. Am. Chem. Soc.* **1977**, *99* (14), 4587–4594. https://doi.org/10.1021/ja00456a010.

(265) Schrock, A. K.; Schuster, G. B. Photochemistry of Naphthyl and Pyrenyl Azides: Chemical Properties of the Transient Intermediates Probed by Laser Spectroscopy. *J. Am. Chem. Soc.* **1984**, *106* (18), 5234–5240. https://doi.org/10.1021/ja00330a033.

(266) Dunkin, I. R.; Thomson, P. C. P. Infrared Evidence for Tricyclic Azirines and Didehydrobenzazepines in the Matrix Photolysis of Azidonaphthalenes. *J. Chem. Soc. Chem. Commun.* **1980**, No. 11, 499. https://doi.org/10.1039/c39800000499.

(267) Gritsan, N. P.; Pritchina, E. A. The Mechanism of Photolysis of Aromatic Azides. *Russ. Chem. Rev.* **1992**, *61* (5), 500–516. https://doi.org/10.1070/RC1992v061n05ABEH000959.

(268) Smith, P. A. S.; Boyer, J. H. The Synthesis of Heterocyclic Compounds from Aryl Azides. II. Carbolines and Thienoindole 1. *J. Am. Chem. Soc.* **1951**, *73* (6), 2626–2629. https://doi.org/10.1021/ja01150a061.

(269) Hilton, S. E.; Scriven, E. F. V.; Suschitzky, H. Thermal and Photolytic Decomposition of α- and β-Naphthyl Azides. *J. Chem. Soc., Chem. Commun.* **1974**, No. 21, 853–854. https://doi.org/10.1039/C39740000853.

(270) Carde, R. N.; Jones, G.; McKinley, W. H.; Price, C. Intramolecular Nitrene Insertions into Aromatic and Heteroaromatic Systems. Part 4. Insertions Using Triphenylmethanes, Unactivated or Bearing Electron-Donating Groups. *J. Chem. Soc. Perkin Trans. 1* **1978**, No. 10, 1211. https://doi.org/10.1039/p19780001211.

(271) Carroll, S. E.; Nay, B.; Scriven, E. F. V; Suschitzky, H. Photolysis of Naphthyl and Quinolyl Azides: A Practicable Synthesis of Naphthyl and Quinolyl o-Diamines. *Synthesis (Stuttg).* **1975**, *1975* (11), 710–711.

(272) Iddon, B.; Suschitzky, H.; Taylor, D. S. Condensed Thiophen Ring Systems. Part XIV. Photolysis of Azidobenzo[b]Thiophens in Secondary Amines. *J. Chem. Soc. Perkin Trans. 1* **1974**, No. 0, 579. https://doi.org/10.1039/p19740000579.

(273) Rigaudy, J.; Igier, C.; Barcelo, J. Bicyclic Aziridines as Intermediates in the Photolysis of Polycyclic Aromatic Azides. *Tetrahedron Lett.* **1979**, *20* (21), 1837–1840. https://doi.org/10.1016/S0040-4039(01)86854-4.

(274) Gallagher, P. T.; Iddon, B.; Suschitzky, H. Synthesis and Photolysis of Azido-Benzo[b]Thiophens, -Benzothiazoles, -Benzimidazoles, and -Indazoles: Novel 6,7-Diamino-Benzothiazoles, -Benzimidazoles, and -Indazoles and 6-Diethylamino-8H-Thiazolo [5,4-c]Azepines. *J. Chem. Soc. Perkin Trans. 1* **1980**, No. 0, 2362. https://doi.org/10.1039/p19800002362.

(275) Reiser, A.; Willets, F. W.; Terry, G. C.; Williams, V.; Marley, R. Photolysis of Aromatic Azides. Part 4.—Lifetimes of Aromatic Nitrenes and Absolute Rates of Some of Their Reactions. *Trans. Faraday Soc.* **1968**, *64* (0), 3265–3275. https://doi.org/10.1039/TF9686403265.

(276) Tsao, M.-L.; Platz, M. S. A Laser Flash Photolysis and Computational Chemistry Study of 9-Anthrylnitrene. *J. Phys. Chem. A* **2003**, *107* (42), 8879–8884. https://doi.org/10.1021/jp035281m.

(277) Maltsev, A.; Bally, T.; Tsao, M.-L.; Platz, M. S.; Kuhn, A.; Vosswinkel, M.; Wentrup, C. The Rearrangements of Naphthylnitrenes: UV/Vis and IR Spectra of Azirines, Cyclic Ketenimines, and Cyclic Nitrile Ylides. *J. Am. Chem. Soc.* **2004**, *126* (1), 237–249. https://doi.org/10.1021/ja038458z.

(278) Creary, X. Super Radical Stabilizers. *Acc. Chem. Res.* **2006**, *39* (10), 761–771. https://doi.org/10.1021/ar0680724.

(279) Creary, X.; Mehrsheikh-Mohammadi, M. E.; McDonald, S. Methylenecyclopropane Rearrangement as a Probe for Free Radical Substituent Effects. .Sigma..Bul. Values for Commonly Encountered Conjugating and Organometallic Groups. *J. Org. Chem.* **1987**, *52* (15), 3254–3263. https://doi.org/10.1021/jo00391a015.

(280) Wenthold, P. G. Spin-State Dependent Radical Stabilization in Nitrenes: The Unusually Small Singlet–Triplet Splitting in 2-Furanylnitrene. *J. Org. Chem.* **2012**, *77* (1), 208–214. https://doi.org/10.1021/jo2016967.

(281) Sengupta, D.; Nguyen, M. T. Why α-Azido Five-Membered Heterocycles Decompose so Fast? An Ab Initio Molecular Orbital Study. *Tetrahedron* **1997**, *53* (28). https://doi.org/10.1016/S0040-4020(97)00637-6.

PUBLICATIONS

Investigation of the Substituent Effects of the Azide Functional Group Using the Gas-Phase Acidities of 3- and 4-Azidophenols

By

Harshal Jawale, Sabyasachy Mistry, Cory Conder and Paul G. Wenthold*

a contribution from

The Department of Chemistry and Biochemistry
Purdue University
560 Oval Drive, West Lafayette, IN 47907

Table of Contents Graphic

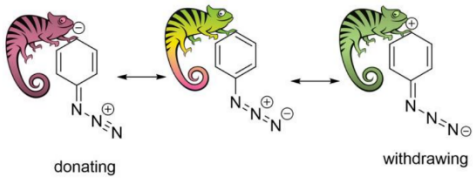

Abstract

The electronic effect of the azide functional group on an aromatic system has been investigated by using Hammett-Taft parameters obtained from the effect of azide-substitution on the gas-phase acidity of phenol. Gas-phase acidities of 3- and 4-azidophenol have been measured by using mass spectrometry and the kinetic method and found to be 340.8 ± 2.2 and 340.3 ± 2.0 kcal/mol respectively. The relative electronic effects of the azide substituent on an aromatic system have been measured by using Hammett-Taft parameters. The σ_F and σ_R values are determined to be 0.38 and 0.02 respectively, consistent with predictions based on electronic structure calculations. The values of σ_F and σ_R demonstrate that azide acts an inductively withdrawing group but has negligible resonance contribution on the phenol. In contrast, acidity values calculated for azide-substituted benzoic acids gives values of $\sigma_F = 0.69$ and $\sigma_R = -0.39$, indicating that the azide is a strong π donor, comparable to that of a hydroxyl group. The difference is explained as being the result of "chimeric" electronic behavior of the azide, similar to that observed previously for the n-oxide moiety, which can be more or less resonance donating depending on the electronic effects of other groups in the system.

Introduction

Phenyl azides have garnered significant interest since their discovery in 1864 due to their applicability in various fields.[1–6] Currently, the azide is one of the most commonly used functional groups in click chemistry,[7–14] which involves combining a biomolecule and a substrate of choice to generate a large library of compounds that find employment in various disciplines. A typical click reaction is the combination of an azide with an alkyne to yield a very useful, 5-membered triazole ring: an azide-alkyne cycloaddition (eq 1).[14]

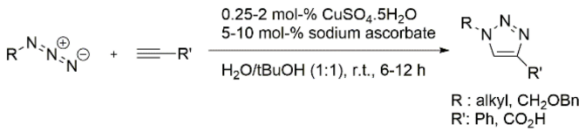

(1)

Synthesis of drug analogs is an important aspect of medicinal chemistry and drug discovery, and triazoles constitute a vital part of multiple bioactive molecules,[15] being one of the most widely used bio-isosteres.[16–18] Triazoles have good stability and various structural characteristics, such as rigidity and polarity, along with the ability to act as both a hydrogen bond donor and acceptor that helps them to mimic the traits of various functional groups. As such, they have potential applicability in medicinal chemistry,[10,19–22] agriculture,[23,24] bioconjugation,[25] chemical synthesis,[26] and supramolecular chemistry.[27]

Azides are also popular precursors of nitrenes in nitrene chemistry. Azides readily decompose in the presence of light, heat, and catalysts under reagent free conditions to yield nitrenes which have attracted tremendous interests recently.[28–36] The presence of an exceedingly good leaving group, dinitrogen, imparts a high chemical reactivity to the azide functionality, enabling it to act as electrophile, nucleophile, and radical acceptor, making it highly useful in

synthetic chemistry.[37] However, even though the azide is a versatile and energy-rich functional group widely studied for its applications, not much is known about its electronic nature. Considering that the azide is a cumulated system of π-electrons, it would be expected to interact with π system, such as in aromatic molecules, though conjugation. On examining the possible resonance structures, the azide can be rationalized to be either a π-electron donor or an acceptor as shown in Scheme 1.

SCHEME 1

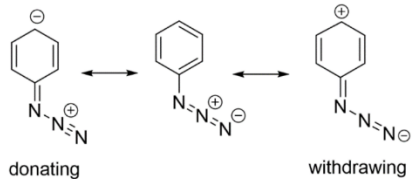

For example, an azide could exhibit π-electron donating capabilities, as shown in the left side of Scheme 1. The advantage in this case is that all the atoms maintain filled octets, at the cost of transferring negative charge from nitrogen to carbon. In contrast, as a withdrawing group, negative charge stays on the nitrogen and positive charge is transferred to the carbon. Literature reports have supported characteristics of azide that sometimes contradict each other. Azides are found to not participate as π-electron donors in charge transfer, resulting in blue-shifted absorptions.[38] On the contrary, Streitwieser and Pulver have shown that azides can act as powerful electron donors in situations of strong electron demands in non-aromatic systems.[39] It has been found that an azide permits direct nitration of benzene and naphthalene rings with the nitro groups directed to the ortho and para positions of the phenyl azide[40] or α- and β- positions in napthyl azide.[41] Bromination of phenyl azide is known to produce para-bromophenyl azide whereas that of 2-napthyl azide produces 1-bromo-2-napthyl azides.[42] These instances of

electrophilic aromatic substitutions demonstrate a π-donating character of azides. Another study by Stankovský and Kováč found that the integrated absorption intensity in the ν_{as}(NNN) band increases in the presence of electron-donating substituents or electron-withdrawing substituent, hinting at a possibly dual electronic nature of the azide group.[43] With all the uncertainty surrounding the true electronic nature of an azide group, it warrants a systematic investigation to elucidate the electronic effects of an azide group.

The electronic properties of the azide group can be interpreted by evaluating their Hammett parameters. The original Hammett equation related substituent constant, σ with the reaction constant, ρ by the following equation:

$$\rho\sigma_x = log\ (k_x/k_H)$$

where k_H is the ionization constant of unsubstituted compound and k_x is the corresponding constant for meta- and para-substituted compound. The parameter σ is dependent on the position of the substituent whereas, ρ was position independent.[44] Although this idea of quantifying substituent effects in terms of the substituent constants was a milestone, it combined all the different types of substituent effects into just one variable resulting in lack of a detailed study of the substituents. Taft and co-workers[45] have provided an alternate approach where the substituent effects are separated into different components, the inductive/field effects, σ_F, mesomeric/resonance effect, σ_R, polarizability, σ_α, and electronegativity, σ_χ. Each component contributes relates to the difference in reaction free energies, $\partial\Delta G°$, for the substituted and unsubstituted compounds. For most substituents and reactions, the most important parameters are the inductive/field and resonance effects, σ_F and σ_R, respectively. In the Hammett-Taft model, the effect on the energetics for a defined chemical process such as gas-phase acidity (ΔG_{acid}) follows the relationship in eq 2, where A° is a small constant.

$$\delta\Delta G_{acid} = \rho_F \sigma_F + \rho_R \sigma_R + A^o \quad (2)$$

Because different reactions respond differently to the inductive and mesomeric effects, the reaction constants ρ are considered to be position dependent, whereas the substituent constants, σ, are position independent. The Hammett-Taft parameters obtained by using this approach provide a fundamental understanding of the substituent behavior[45] and can be very effective in gaining insights into the electronic nature of a wide variety of substituents.

In this work, we report an experimental investigation of the Hammett-Taft parameters of the azide substituent within 3- and 4-azidophenol (**3AP** and **4AP**, respectively) by using the relationship shown in eq 2.

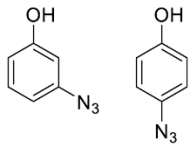

3AP **4AP**

The gas-phase acidities of **3AP** and **4AP** have not been reported in the literature, and thus have now been determined using the kinetic method with mass spectrometry.[46] The electronic effects of the azide substituent have also been investigated in the azidobenzoic acid system by using computational methods, and predict the azide to have a dual electronic nature in terms of π-electron delocalization, which is influenced by the nature of other substituents in the aromatic system.

Experimental section

All the reagents, solvents and reference phenols were obtained from commercial sources and used as supplied. The azidophenols were synthesized by using procedures similar to those reported previously.[47,48]

Procedure for synthesis of 3-azidophenol

To a solution of 3-hydroxyaniline (9.16 mmol) in DCM (15 mL) at 0°C was added 8 ml of concentrated HCl with constant stirring. A solution of sodium nitrite (11.0 mmol) in 10 mL water was then added dropwise over a period of 10 min with stirring. After 1h, a solution of sodium azide (11.91 mmol) in water (5 mL) was added to the reaction mixture with constant stirring. The reaction mixture was warmed to room temperature and stirred for further 4 h. The solution was then poured into water, extracted with DCM (3 × 20 mL), dried over magnesium sulfate, filtered and concentrated in vacuo to give 3-azidophenol as viscous yellow oil, which was used for the studies without any further purification.

Procedure for synthesis of 4-azidophenol

To a round bottom flask, 9.16 mmol of 4-hydroxyaniline was dissolved in 25 ml of deionized water and 8 ml of concentrated HCl with stirring. The solution was then cooled to 0ºC in an ice bath. Once cooled, 9.16 mmol of sodium nitrite was added to the solution in small portions and the mixture was allowed to stir for 10 minutes. 10.89 mmol of sodium azide was then added to the solution in small portions with constant stirring. Once the addition was

complete, the solution was allowed to warm to room temperature and stirred for an additional hour. The solution was then extracted with ethyl acetate (3 x 25 ml). The combined organic layers were washed with sodium bicarbonate and brine, dried over magnesium sulfate and the solvent was evaporated under reduced pressure to yield 4-azidophenol as dark brown oil which was used without further purification.

TLC analyses shows the azidophenols as the predominant products, with only trace amounts of aminophenol starting material detected as impurities. For prolonged use, the azidophenols were stored under cold and dark conditions.

General procedure for sample preparations

The substituted reference phenols selected for the experiments along with their gas-phase acidities are listed in Table 1.

Table 1. Reference phenols and their gas-phase acidities

Reference	Gas-phase acidities[b]
3-fluorophenol	343.7 ± 2.8[b]
ethyl-3-hydroxybenzoate	343.9 ± 2.1
4-fluorophenol	346.7 ± 2.1
3-trifluoromethyl phenol	339.2 ± 2.1
3-hydroxybenzaldehyde	340.5 ± 2.1
methyl-3-hydroxybenzoate	343.8 ± 2.1

[a] Values in kcal/mol. All the gas-phase acidity values from ref 49 unless otherwise noted.
[b] Ref 50

One molar stock solutions of each of the reference phenols and the azido phenols were prepared by dissolving the necessary amounts in methanol. The stock solutions of the azido

phenols were kept in the dark and stored in a freezer. Samples were prepared by mixing 7 µl of a reference stock solution with 7 µl of the azido phenol stock solution and 7 µl of 0.5 M potassium hydroxide (in water). The solutions were diluted to 1ml in water-methanol solvent system (1:1) for ESI-MS analysis. All of the samples were stored and analyzed in the dark.

Spectra collection

Electrospray ionization mass spectra were obtained on a Waters Micromass (Milford, Massachusetts) Quattro Ultima Pt triple quadrupole mass spectrometer, equipped with ESI source, operating in negative ion mode. Sample solutions were introduced into the source directly at a flow rate of 10 µL/min. Electrospray and ion focusing conditions were varied to maximize the signal of the proton bound dimer of the phenoxide ions. No significant products were observed in the ESI mass spectra besides the appropriate phenoxide ions and the proton-bound dimers.

Collision-induced dissociation (CID) studies

The phenoxide cluster ions were isolated on the basis of their mass-to-charge ratio and subjected to collision with argon target at energies of 4, 6, 8, 10, 13, 17 and 20 volts (center-of-lab frame). Primary product ions observed were *m/z* 134 (azido phenoxide) and the phenoxide of the corresponding reference phenol. CID of ions containing *p*-azidophenoxide also resulted in formation *m/z* 106, presumably the quinonimide ion (*p*-$NC_6H_4O^-$) formed by secondary fragmentation. Intensities of the product ions were recorded for each collision energy. The experiments were repeated at least four times on separate days.

Kinetic method for determination of gas-phase acidities

As mentioned in the introduction, gas-phase acidities of azido phenols required to determine their Hammett-Taft parameters have not been reported. In this work, we have measured them by using the kinetic method.[46]

Deprotonated phenols form proton-bound dimers with neutral phenols in the gas phase. When such dimers are subjected to collision with neutral molecules, they undergo fragmentation and the yields of the products depend on the relative gas-phase acidities of the respective phenols. Knowing this, it is possible to determine the gas-phase acidities of the azido phenols by using the set of substituted reference phenols with known gas-phase acidities. In the kinetic method, we consider the dissociation of a proton bound dimer $[AP^- H^+ P_i^-]$, where AP^- is the azido phenoxide and P_i^- is the reference whose corresponding phenol has known gas-phase acidity. Fragmentation of this complex leads to either APH + P_i^-species or AP^- + P_iH species.

In the mass spectroscopic measurement for the kinetic method, the difference in the acidities of the reference phenols (P_iH) and the azido phenol (APH) is related to the branching ratios $R_{E,i}$ of the AP^- and P_i^- species, by eq 3, where T_{eff} is the effective temperature of the dissociation,[51,52] $\delta\Delta S$ is the difference in activation entropies for the formation of P_i^- and AP^- from the proton-bound dimer,[53–56] and the E and i subscripts indicate the terms that are dependent on the collision energy of the dissociation and the reference phenol respectively. The branching ratio $R_{E,i}$ is the ratio of *m/z* 134 + *m/z* 106 (corresponding to AP^-) to the *m/z* of the reference phenoxide (P_i^-).

$$lnR_{E,i} = \frac{\Delta H_{acid}(P_iH) - \Delta H_{acid}(APH) - T_{eff,E}\,\delta\Delta S}{-RT_{eff,E}} \quad (3)$$

The kinetic method, in its simplest form,[57] relies on the entropy term in the equation to be negligible, thus enabling acidity calculations through a plot of $\ln R_i$ Calculated at a single collision energy vs ΔH_{acid}, for a series of reference acid P_iH. However, the extended kinetic method,[56,58] includes the entropy component to the branching ratio. Thus, from eq 3, a plot of $\ln R_{E,i}$ vs $\Delta H_{acid}(P_iH)$ at a given energy has a slope $m_E = -1/RT_{eff,E}$ and an intercept $y_E = [\Delta H_{acid}(APH) + T\delta\Delta S]/RT_{eff,E}$. In accordance with the extended kinetic method, when the dissociation is carried out at a series of collision energies, a second regression plot of y_E vs $-m_E$ can be constructed, where the slope would be the acidity, $\Delta H_{acid}(APH)$ and the intercept would be $\delta\Delta S/R$.

It has been noted[46] that the slopes and intercepts obtained from the best fit of the data in the first linear regression are interdependent. This means that, the second regression plot will result in an excessive correlation between the derived slopes and intercepts. This correlation can be removed[46] by simply plotting $\ln R_{E,i}$ versus $\Delta H_{acid}(P_iH) - \Delta H_{acid}(P_iH_{,avg})$, as the first regression plot where $\Delta H_{acid}(P_iH_{,avg})$ is the average of the gas-phase acidities of the reference phenols. In this approach, the second regression plot has an intercept of $\delta\Delta S/R$ and a slope of $\Delta H_{acid}(APH) - \Delta H_{acid}(P_iH_{,avg})$, from which the acidity of azidophenol can be obtained.

Results

The collision-induced dissociation of phenoxide proton-bound dimers was carried out at seven different energies, from 4-20 V in the lab frame. The first regression plots of $\ln R_{E,i}$ versus $\Delta H_{acid}(P_iH) - \Delta H_{acid}(P_iH_{,avg})$ for **3AP** and **4AP** at all the collision energies are provided in Figure 1, where $\Delta H_{acid}(P_iH_{,avg}) = 343.0$ kcal/mol

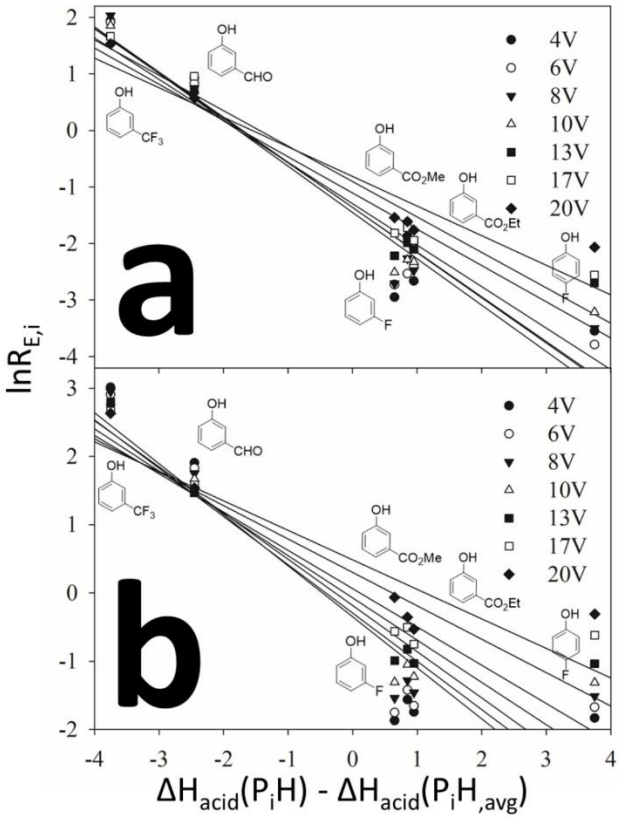

Figure 1. First regression plots of $\ln R_{eff,E}$ vs $\Delta H_{acid}(P_iH) - \Delta H_{acid}(P_iH_{,avg})$ at a series of energies for a) 3-azidophenol and b) 4-azidophenol

The subsequent second regression plots have slopes equal to 2.2 and 2.7 kcal/mol and intercepts equal to 0.3 and 1.6 eu for **3AP** and **4AP**, respectively (Figure 2).

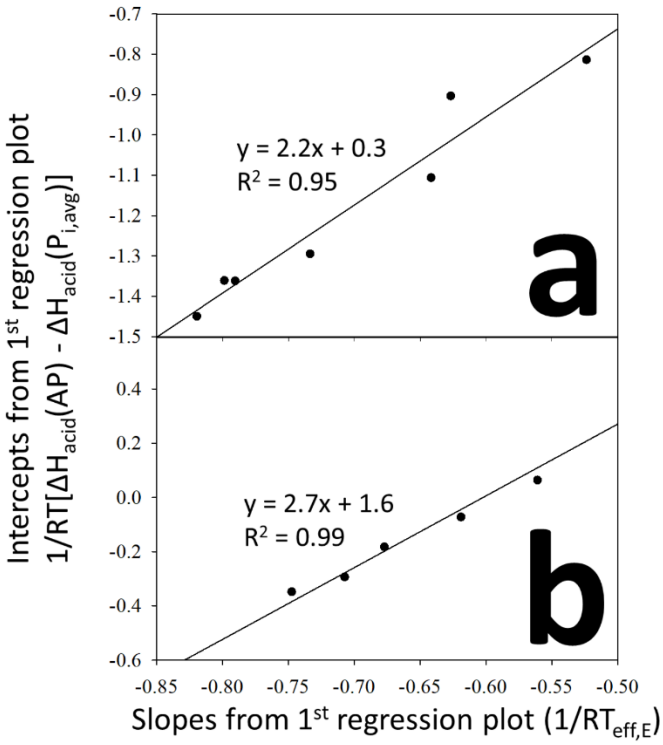

Figure 2. Second regression plot for a) 3-azidophenol and b) 4-azidophenol

In the analysis, the gas-phase acidities of the azidophenols are calculated from the slopes of the 2nd regression plot by the equation $\Delta H_{acid}(APH) = \Delta H_{acid}(P_iH_{,avg}) -$ slope. From this work, the gas-phase acidities of **3AP** and **4AP** are found to be 340.8 kcal/mol and 340.3 kcal/mol, respectively. From the intercept values, $\delta\Delta S$ is calculated to be 0.6 and 3.2 eu for the meta and para isomer, respectively. The small values of $\delta\Delta S/R$ indicate minimal differences in the activation entropies for the two dissociation pathways.

The slopes obtained from fitting the data shown in Figure 2, have uncertainties (δ_{slope}) of ±0.6 and ±0.3 kcal/mol for **3AP** and **4AP**, respectively, referring to statistical 95% confidence

levels.[46] This, however, does not include the possible errors due to uncertainties in the reference gas-phase acidities, and those intrinsic to the kinetic method itself. The uncertainty in the measured gas-phase acidities is determined by combining the uncertainties in the slope with the uncertainty in $\Delta H_{acid}(P_iH_{,avg})$. If the uncertainties of the reference acidity values are the same, then the uncertainty in $\Delta H_{acid}(P_iH_{,avg})$ would nominally be $\frac{\partial \Delta H_{acid}}{\sqrt{n}}$, where n is the number of references. However, the gas-phase acidities for the references are likely not independent and random, many having come from the same source using the same methodology, utilizing relative measurements that are anchored to the same reference. Therefore, the systematic uncertainty is not improved with more references. As described previously,[59] we approximate that half of the uncertainty in the reference values is independent and random whereas half are due to systematic errors, as shown in eq 4. Using the reported $\delta\Delta H_{acid} = 2.1$ for the references, that gives independent and random and systematic uncertainties of ±1.5 kcal/mol.

$$\delta^2\Delta H_{acid} = \delta^2\Delta H_{acid,i\&r} + \delta^2\Delta H_{acid,systematic} \qquad (4)$$

Finally, in calculating the uncertainty we conservatively include a ±1 kcal/mol contribution due to potential error in the kinetic method model. Combining the systematic error, random statistical uncertainty, uncertainty in the kinetic method model and the δ_{slope}, the overall uncertainties in the ΔH_{acid}(APH) for **3AP** and **4AP** are calculated to be ± 2.0 and ± 1.9 kcal/mol, respectively.

The measured acidities and the corresponding ΔG values for both the azidophenols are listed in Table 2, where $\Delta G = \Delta H - T\Delta S$. The entropy term, ΔS_{acid}(APH), required for the calculation is obtained by using frequencies calculated at the B3LYP/6-31+G* level of theory.

Table 2. Gas-phase acidities of azidophenols determined in this work.

Phenol	ΔH_{acid}[a]	ΔS_{acid}[b]	ΔG_{acid}[c]
3-azidophenol, **3AP**	340.8 ± 2.0	25.5	333.1 ± 2.0
4-azidophenol, **4AP**	340.3 ± 1.9	25.4	332.7 ± 1.9
phenol	349.0[d]		340.8[d]

[a] Values in kcal/mol
[b] Values in eu, obtained by using unscaled calculated frequencies of neutral azidophenol and conjugate base anion azidophenoxide obtained at B3LYP/6-31+G* level of theory.
[c] Values in kcal/mol at 300 K, obtained by using the equation $\Delta G_{acid} = \Delta H_{acid} - T\Delta S_{acid}$
[d] Reference 60

Hammett parameters for the azide group

The determination of the Hammett parameters σ_F and σ_R, for the azide group from the gas-phase acidities are described in this section. As discussed earlier, Taft[45] related the Hammett parameters of the azide to the difference in the gas-phase acidities of 3- and 4- azidophenols with the unsubstituted phenol as shown in eq 5a and 5b.

$$7.7 = 12.2\sigma_R + 19\,\sigma_F + 0.2 \qquad (5a)$$

$$8.1 = 49\sigma_R + 18.6\,\sigma_F + 0.1 \qquad (5b)$$

Solving this pair of equations gives values of σ_F and σ_R to be 0.38 and 0.02, respectively.

Discussion

To help understand the electronic behavior of the azide, the calculated Hammett-Taft parameters of the azide can be compared with those of some of the common substituents in Table 3.

Table 3. Substituent parameters for some common substituents[a]

Substituent	σ_F	σ_R
Pyridine – infused nitrogen[b]	-0.18	0.76
COCN	0.66	0.28
CHO	0.31	0.19
NO_2	0.65	0.18
CN	0.60	0.10
CF_3	0.44	0.07
N_3	**0.38**	**0.02**
CH_3	0.00	-0.08
Cl	0.45	-0.17
F	0.44	-0.25
HO	0.30	-0.38
C_2H_5OH	0.25	-0.45
σ radical[c]	0.57	-0.47
NH_2	0.14	-0.52

[a] All values are from ref 45 and 61 unless noted [b] Reference 62 [c] Reference 63

The large, positive σ_F value for N_3 is interpreted to mean that the azide group on an aromatic ring is an inductively electron withdrawing group, comparable to that of CF_3 (0.44), Cl (0.45) and F (0.44) (Table 3).[61] For σ_R, a positive value indicates π-electron withdrawing properties of a functional group, whereas a negative value is characteristic of it having π-electron donating abilities. As shown in the Table 3, the azido group in a phenol has a value nearly 0 for σ_R, which indicates it has little resonance contribution, and, if there is any, it is withdrawing. This value of σ_R is somewhat surprising in that the azide, a system consisting of multiple π-

electrons in conjugation with the aromatic ring and cumulative double bonds, has effectively no contribution to the resonance in the aromatic ring whereas even functional groups like CF_3 and CH_3 have σ_R values of 0.07 and -0.08 respectively.

Comparison with theory

To explore whether the σ_R value could be a result of an error in our acidity measurements, we have corroborated the results by using electronic structure calculations. The energies of the proton transfer reactions (eq 6) have been computed at the B3LYP/6-31+G* and M06-2X/6-311++G** levels of theory.

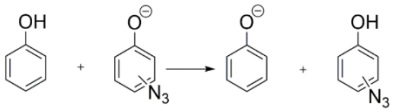

(6)

The calculated relative acidities for the azidophenols are shown in Table 4. The B3LYP results are in good agreement with the experimental values. For the M06-2X calculations, the relative values are reversed, but only slightly so, and there is very little difference between the meta and para isomers. Moreover, there is less agreement between the experimental $\delta\Delta G_{acid}$ values and the results from the M06-2X calculations.

Table 4. Experimental and calculated $\partial\Delta G_{acid}$ and $\partial\Delta H_{acid}$ of the azidophenol isomers[a]

	3-azidophenol, **3AP**			4-azidophenol, **4AP**		
	Exp[b]	B3LYP	M06-2X	Exp[b]	B3LYP	M06-2X
$\partial\Delta G_{acid}$[c]	7.7	7.8	7.2	8.1	8.3	6.9
$\partial\Delta H_{acid}$	8.2	8.3	7.7	8.7	8.9	7.5

[a] Values in kcal/mol.
[b] Values obtained by using the experimental acidities of the azidophenols measured in this work and the literature values of ΔG_{acid} and ΔH_{acid} of unsubstituted phenol (ref 60)
[c] Calculated from ΔH_{acid} by using the experimental value of ΔS_{acid}(phenol) = 27.3 eu (ref 60) and the ΔS_{acid} values for the azidophenols from Table 2.

Although the agreement between the $\delta\Delta G_{acid}$ values and the M06-2X computed values is only fair, the deviation makes very little difference in the resulting Hammett-Taft parameters. As shown in Table 5, there is essentially no difference between the predicted and experimental values of σ_F and σ_R. In particular, the predicted values for σ_R are indicative of a negligible π-withdrawing ability of the azide group, similar to what was deduced from the experimental acidities.

Table 5. Experimental and calculated values of σ_F and σ_R for the azide substituent[a]

	Exp	B3LYP	M06-2X
σ_F	0.38	0.39	0.37
σ_R	0.02	0.02	0.00

[a] Obtained by using the $\delta\Delta G_{acid}$ values from Table 4 along with eq 5a and 5b

Although the lack of π-donating ability seems surprising, it likely can be attributed to the presence of the oxide (O^-) in the phenoxide ring. Considering that the azide is capable of π-

donation, there is a competition between its electron donating abilities with that of the other substituents in the system, including the hydroxyl group in the phenol and the oxide in the anion. As shown at the bottom of Scheme 2, electron donation to the ring via resonance would be

Scheme 2

Azide is donating

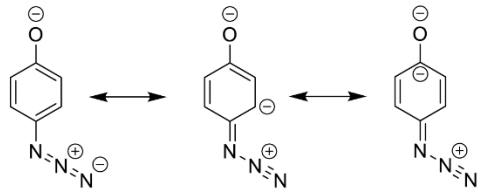

opposed by electron density donated by the oxide anion. In other words, the azide is not able to act effectively as a donor because it has to compete with the strong donor ability of the oxide group. In fact, in that situation, the azide has the ability to act as an electron withdrawing group (Scheme 3) that can accommodate the increased charge density in the ring.

Scheme 3

Azide is withdrawing

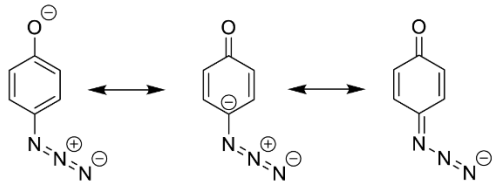

Differences in the calculated geometries of phenoxide ions are consistent with the resonance interpretation shown in Schemes 2 and 3. The optimized C-O bond lengths in phenoxide and 4-azidophenoxide are found to be 1.275 Å and 1.270 Å, respectively. The shorter C-O bond length in 4-azidophenoxide can be attributed to the increased contribution of the

carbonyl-containing resonance structure in the overall resonance hybrid, which can happen when the azide is a π-accepting group. If the azide were acting as a π donating group, the C-O bond length would be expected to increase due to the increased electron density in the aromatic ring.

Similarly, the calculated bond length of the terminal N-N bond in 4-azidophenoxide (1.157 Å) is slightly longer than that in 3-azidophenoxide (1.150 Å), suggesting more double-bond character between the atoms than in a non-resonant azide group. Therefore, the effects on the geometry are consistent with what would be expected for a π withdrawing group.

Although the electronic effects of the azide in the presence of the strong π donor can be understood in light of this resonance model, the analysis does not provide insight into the electronic effects of the azide that occur in the absence of the competing substituent. Therefore, we have carried out further investigation of the azide in a different electronic environment.

Effects of azide in benzoic acids

To determine the effect of an azide by itself, it can be studied without a competing group. For example, the π-electrons on a carboxylate oxygen are delocalized within the carboxylate group, thus effectively isolating the system from taking part in any type of resonance contribution with the benzene ring ($\sigma_R = 0$).[45] Therefore, a carboxylate does not create a competing resonance effect, and presents a very different electronic environment to study the azide, and carboxylic acids can be used to determine Hammett-Taft parameters for that situation. Unfortunately, proton-bound dimer clusters of the benzoates are not formed easily in our mass spectrometer. However, as shown with the phenols, the electronic effects can be accurately predicted by using electronic structure calculations.

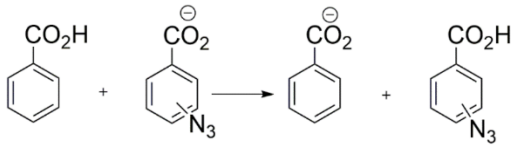

(7)

Given the success of B3LYP/6-31+G* calculations to reproduce the results for the phenol, we have used this approach to calculate the energy for the the proton exchange reaction in eq 7, obtaining $\partial\Delta G_{acid}$ values of 5.6 and 4.5 kcal/mol for 3-azido- and 4-azidobenzoic acid, respectively. The corresponding σ_F and σ_R values for azide in benzoic acid are determined using the relative acidities and the ρ values for deprotonation to be 0.69 and -0.39 respectively.[45] While still having strong electron-withdrawing inductive effects, the large negative value of σ_R indicates a very strong π-donating effect, similar to that of the hydroxy group (σ_R = -0.38). This result is in stark contrast to the negligible π-effect of the azide as in the azidophenols.

This difference in behavior can be explained by the simple resonance model discussed above. In contrast to the azidophenol system, there is no competition between the π-donating (or withdrawing) abilities of the carboxylate and the azide. However, resonance theory favors the structures with complete octets and minimal charge separation (Scheme 2) which are only possible when the oxide acts as a π-donor and the azide as a π-acceptor. The azide as a π donor (Scheme 3) creates unfavorable interaction of negative charges in the ring.

With the carboxylate (Scheme 4), a π-accepting azide does not have as much stabilizing

Scheme 4

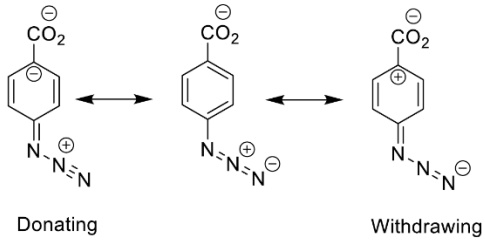

effect by resonance when compared to the azidophenoxide system. Conversely, a π-donating azide does not have any unfavorable resonance effects on the molecule unlike in the case of the azidophenoxide system. Hence, in situations where the electron demands of the system do not require it to be a π-acceptor, azide acts nominally as a π-donor, reflected in its σ_R value of -0.39.

This interpretation is also supported by comparing the bond lengths for the azidocarboxylate and phenoxides. The calculated terminal N-N bond length for 4-azidobenzoate is 1.148 Å, very similar to that for 3-azidophenoxide, and, again, shorter than that in 4-azidophenoxide. This is consistent with greater contribution from the electron withdrawing resonance structures in 4-azidophenoxide as in Scheme 3.

Additional computed properties reflect the resonance differences between 4-azidophenoxide and 4-azidobenzoate. For example, the calculated absorption frequency of the NNN stretch for 4-azidobenzoate (2229 cm^{-1}) is higher than that for 4-azidophenoxide (2201 cm^{-1}) for 4-azidophenoxide is also consistent with increased bond order between the terminal nitrogen atoms. Finally, although Mulliken charges may not provide the most accurate reflection of charge distribution, the calculated values at the terminal nitrogen atoms are -1.083 and -1.211

for 4-azidobenzoate and 4-azidophenoxide, respectively, consistent with the interpretation that azide in azidophenoxide is more π accepting.

Comparison with an N-oxide moiety

The different results depending on the competing substituents are indicative of a rare (but not novel) dual electronic nature. The ability to change the electronic effect in response to the environment has been described by Poole as a "*chimeric*" behavior.[64] This dual electronic nature demonstrated by the azide is very similar to that displayed by the N-oxide moiety, which can similarly be explained by its resonance structures (Scheme 5). Pyridine N-oxides are known to be more reactive than pyridines, displaying penchants for both nucleophiles[65–68] and electrophiles[69–71] depending on the electronic environments.[64] In this respect, we might also consider the azide group to be chimeric, or, perhaps, chameleonic may be more appropriate, in that it can change its properties in response to the environment.

SCHEME 5

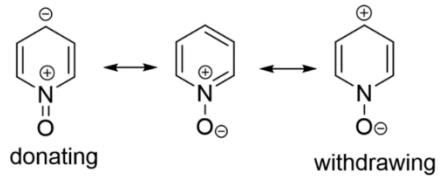

Poole's assessment is also in agreement with our theoretical predictions of the electronic effect of the N-oxide. By using the same computational procedures as in the preceding section, with gas-phase acidities calculated at the B3LYP/6-31+G* level of theory, the effective

substituent parameter, σ_R, for the N-oxide moiety, is found to be -0.43 (donating) when using carboxylic acids and 0.07 (withdrawing) with phenols, reflecting chimeric behavior.[64]

The dual nature of the electronic effects of azide have been described previously in the literature. For example, the electron withdrawing and donating abilities of the azide affect the integrated absorption intensities of the NNN bands in infrared spectroscopic studies of substituted phenyl azides.[43,50] Our observations are consistent with the conclusions described in these reports.

Conclusion

Analysis of the dissociation of proton bound dimers of azidophenols over a series of collision energies provide the gas-phase acidities of 340.8 ± 2.2 and 340.3 ± 2.0 kcal/mol for 3- and 4-azidophenol, respectively, resulting in resonance (σ_R) and inductive (σ_F) values of 0.02 and 0.38, respectively. The absence of a significant resonance effect for substitution at the para-position of the azidophenoxide is surprising considering that the azide functional group is a system with delocalizable π-electrons in conjugation with an aromatic system. To test the influence of the strongly donating oxide group in the phenoxide on the substituent parameters, they have been re-examined computationally using the carboxylic acids, and, in that system, the azide is found to be a strong π-donating group, similar to a fluorine, hydroxyl or alkoxy group. However, unlike the other strong π-donors, the azide can modulate the amount of π donation depending on the electronic needs of the system. In this way, the azide group is chameleonic in its resonance effect, always adapting to provide the maximum benefit.

Associated Content

Supporting Information

Calculated structures, energies and frequencies calculated for molecules obtained in this work.

Author Information

Corresponding Author

Paul Wenthold – Department of Chemistry, Purdue University, 560 Oval Drive, West Lafayette Indiana; Email: pgw@purdue.edu **ORCID:** 0000-0002-8257-3907

Authors

Harshal Jawale - Department of Chemistry, Purdue University, 560 Oval Drive, West Lafayette Indiana; Email: hjawale@purdue.edu

Sabyasachy Mistry - Department of Chemistry, Purdue University, 560 Oval Drive, West Lafayette Indiana; Email: Sabyasachy.Mistry@fda.hhs.gov

Cory Conder - Department of Chemistry, Purdue University, 560 Oval Drive, West Lafayette Indiana; Email: cjconder@salisbury.edu

Notes

The authors declare no competing financial interest

Acknowledgements

This work was financially supported by the National Science Foundation (CHE15-65755).

References

(1) Schock, M.; Bräse, S. Reactive & Efficient: Organic Azides as Cross-Linkers in Material Sciences. *Molecules* **2020**, *25* (4), 1009.

(2) Bräse, S.; Gil, C.; Knepper, K.; Zimmermann, V. Organic Azides: An Exploding Diversity of a Unique Class of Compounds. *Angew. Chemie Int. Ed.* **2005**, *44* (33), 5188–5240.

(3) Katritzky, A.; Scriven, E. Organic Azides: Syntheses and Applications. *J. Am. Chem. Soc.* **2010**, *132* (34), 12156–12156.

(4) Chiba, S. Application of Organic Azides for the Synthesis of Nitrogen-Containing Molecules. *Synlett* **2012**, *2012* (01), 21–44.

(5) Nair, V.; Suja, T. Intramolecular 1,3-Dipolar Cycloaddition Reactions in Targeted Syntheses. *Tetrahedron* **2007**, *63* (50), 12247–12275.

(6) Lang, S.; Murphy, J.. Azide Rearrangements in Electron-Deficient Systems. *Chem. Soc. Rev.* **2006**, *35* (2), 146–156.

(7) Xu, M.; Kuang, C.; Wang, Z.; Yang, Q.; Jiang, Y. A Novel Approach to 1-Monosubstituted 1,2,3-Triazoles by a Click Cycloaddition/Decarboxylation Process. *Synthesis (Stuttg).* **2011**, *2011* (02), 223–228.

(8) Hansen, S.; Jensen, H. Microwave Irradiation as an Effective Means of Synthesizing Unsubstituted N-Linked 1,2,3-Triazoles from Vinyl Acetate and Azides. *Synlett.* **2009**, *20* 3275-3278.

(9) Khalili, D.; Kavoosi, L.; Khalafi-Nezhad, A. Copper Aluminate Spinel in Click Chemistry: An Efficient Heterogeneous Nanocatalyst for the Highly Regioselective

Synthesis of Triazoles in Water. *Synlett* **2019**, *30* (19), 2136–2142.

(10) Varvaresou, A.; Tsantili-Kakoulidou, A.; Siatra-Papastaikoudi, T.; Tiligada, E. Synthesis and Biological Evaluation of Indole Containing Derivatives of Thiosemicarbazide and Their Cyclic 1,2,4-Triazole and 1,3,4-Thiadiazole Analogs. *Arzneimittelforschung* **2011**, *50* (01), 48–54.

(11) Jiang, Y.; Kuang, C.; Yang, Q. The Use of Calcium Carbide in the Synthesis of 1-Monosubstituted Aryl 1,2,3-Triazole via Click Chemistry. *Synlett* **2009**, *2009* (19), 3163–3166.

(12) Boren, B. C.; Narayan, S.; Rasmussen, L. K.; Zhang, L.; Zhao, H.; Lin, Z.; Jia, G.; Fokin, V. V. Ruthenium-Catalyzed Azide−Alkyne Cycloaddition: Scope and Mechanism. *J. Am. Chem. Soc.* **2008**, *130* (28), 8923–8930.

(13) Rostovtsev, V. V.; Green, L. G.; Fokin, V. V.; Sharpless, K. B. A Stepwise Huisgen Cycloaddition Process: Copper(I)-Catalyzed Regioselective "Ligation" of Azides and Terminal Alkynes. *Angew. Chemie Int. Ed.* **2002**, *41* (14), 2596–2599.

(14) Himo, F.; Lovell, T.; Hilgraf, R.; Rostovtsev, V. V.; Noodleman, L.; Sharpless, K. B.; Fokin, V. V. Copper(I)-Catalyzed Synthesis of Azoles. DFT Study Predicts Unprecedented Reactivity and Intermediates. *J. Am. Chem. Soc.* **2005**, *127* (1), 210–216.

(15) Palmer, M. H.; Camp, P. J.; Hoffmann, S. V.; Jones, N. C.; Head, A. R.; Lichtenberger, D. L. The Electronic States of 1,2,4-Triazoles: A Study of 1H- and 1-Methyl-1,2,4-Triazole by Vacuum Ultraviolet Photoabsorption and Ultraviolet Photoelectron Spectroscopy and a Comparison with Ab Initio Configuration Interaction Computations. *J. Chem. Phys.* **2012**, *136* (9), 094310.

(16) Bonandi, E.; Christodoulou, M. S.; Fumagalli, G.; Perdicchia, D.; Rastelli, G.; Passarella, D. The 1,2,3-Triazole Ring as a Bioisostere in Medicinal Chemistry. *Drug Discov. Today* **2017**, *22* (10), 1572–1581.

(17) Mohammed, I.; Kummetha, I. R.; Singh, G.; Sharova, N.; Lichinchi, G.; Dang, J.; Stevenson, M.; Rana, T. M. 1,2,3-Triazoles as Amide Bioisosteres: Discovery of a New Class of Potent HIV-1 Vif Antagonists. *J. Med. Chem.* **2016**, *59* (16), 7677–7682.

(18) Song, W.-H.; Liu, M.-M.; Zhong, D.-W.; Zhu, Y.; Bosscher, M.; Zhou, L.; Ye, D.-Y.; Yuan, Z.-H. Tetrazole and Triazole as Bioisosteres of Carboxylic Acid: Discovery of Diketo Tetrazoles and Diketo Triazoles as Anti-HCV Agents. *Bioorg. Med. Chem. Lett.* **2013**, *23* (16), 4528–4531.

(19) Peyton, L. R.; Gallagher, S.; Hashemzadeh, M. Triazole Antifungals: A Review. *Drugs of Today*. **2015**, *51*(12), 705-718.

(20) Roberts, J.; Schock, K.; Marino, S.; Andriole, V. T. Efficacies of Two New Antifungal Agents, the Triazole Ravuconazole and the Echinocandin LY-303366, in an Experimental Model of Invasive Aspergillosis. *Antimicrob. Agents Chemother.* **2000**, *44* (12), 3381–3388.

(21) Espinel-Ingroff, A. In Vitro Activity of the New Triazole Voriconazole (UK-109,496) against Opportunistic Filamentous and Dimorphic Fungi and Common and Emerging Yeast Pathogens. *J. Clin. Microbiol.* **1998**, *36* (1), 198–202.

(22) Johnson, L. B.; Kauffman, C. A. Voriconazole: A New Triazole Antifungal Agent. *Clin. Infect. Dis.* **2003**, *36* (5), 630–637.

(23) Chai, B.; Qian, X.; Cao, S.; Liu, H.; Song, G. Synthesis and Insecticidal Activity of 1,2,4-Triazole Derivatives. *Arkivoc* **2003**, *2003* (2), 141–145.

(24) Maddila, S.; Pagadala, R.; Jonnalagadda, S. B. Synthesis and Insecticidal Activity of Tetrazole-Linked Triazole Derivatives. *J. Heterocycl. Chem.* **2015**, *52* (2), 487–491.

(25) Zheng, T.; Rouhanifard, S. H.; Jalloh, A. S.; Wu, P. Click Triazoles for Bioconjugation; 2012; pp 163–183.

(26) Dondoni, A. Heterocycles in Organic Synthesis: Thiazoles and Triazoles as Exemplar Cases of Synthetic Auxiliaries. *Org. Biomol. Chem.* **2010**, *8* (15), 3366.

(27) Haas, K. L.; Franz, K. J. Application of Metal Coordination Chemistry To Explore and Manipulate Cell Biology. *Chem. Rev.* **2009**, *109* (10), 4921–4960.

(28) Soto, J.; Otero, J. C.; Avila, F. J.; Peláez, D. Conical Intersections and Intersystem Crossings Explain Product Formation in Photochemical Reactions of Aryl Azides. *Phys. Chem. Chem. Phys.* **2019**, *21* (5), 2389–2396.

(29) Marcinek, A.; Leyva, E.; Whitt, D.; Platz, M. S. Evidence for Stepwise Nitrogen Extrusion and Ring Expansion upon Photolysis of Phenyl Azide. *J. Am. Chem. Soc.* **1993**, *115* (19), 8609–8612.

(30) Xue, J.; Du, Y.; Chuang, Y. P.; Phillips, D. L.; Wang, J.; Luk, C.; Hadad, C. M.; Platz, M. S. Time-Resolved Resonance Raman Observation of the Dimerization of Didehydroazepines in Solution. *J. Phys. Chem. A.* **2008**, *112* (7), 1502–1510.

(31) Kwok, W. M.; Chan, P. Y.; Phillips, D. L. Direct Observation of the 4-Methoxyphenylnitrene Intersystem Crossing from S 1 to T 1 Using Picosecond Kerr-

Gated Time-Resolved Resonance Raman Spectroscopy. *J. Phys. Chem. A* **2005**, *109* (10), 2394–2400.

(32) Nunes, C. M.; Reva, I.; Kozuch, S.; McMahon, R. J.; Fausto, R. Photochemistry of 2-Formylphenylnitrene: A Doorway to Heavy-Atom Tunneling of a Benzazirine to a Cyclic Ketenimine. *J. Am. Chem. Soc.* **2017**, *139* (48), 17649–17659.

(33) Mieres-Perez, J.; Costa, P.; Mendez-Vega, E.; Crespo-Otero, R.; Sander, W. Switching the Spin State of Pentafluorophenylnitrene: Isolation of a Singlet Arylnitrene Complex. *J. Am. Chem. Soc.* **2018**, *140* (49), 17271–17277.

(34) Gritsan, N. P.; Platz, M. S. Kinetics, Spectroscopy, and Computational Chemistry of Arylnitrenes. *Chemical Reviews*. 2006.

(35) Aranda, D.; Avila, F. J.; López-Tocón, I.; Arenas, J. F.; Otero, J. C.; Soto, J. An MS-CASPT2 Study of the Photodecomposition of 4-Methoxyphenyl Azide: Role of Internal Conversion and Intersystem Crossing. *Phys. Chem. Chem. Phys.* **2018**, *20* (11), 7764–7771.

(36) Abramovitch, R. A.; Jeyaraman, R. Azides and Nitrenes: Reactivity and Utility. In *Azides and Nitrenes: Reactivity and Utility*; **1984**.

(37) Tanimoto, H.; Kakiuchi, K. Recent Applications and Developments of Organic Azides in Total Synthesis of Natural Products. *Natural Product Communications*. Natural Product Incorporation 2013, pp 1021–1034.

(38) Lord, S. J.; Lee, H. D.; Samuel, R.; Weber, R.; Liu, N.; Conley, N. R.; Thompson, M. A.; Twieg, R. J.; Moerner, W. E. Azido Push−Pull Fluorogens Photoactivate to Produce

Bright Fluorescent Labels. *J. Phys. Chem. B* **2010**, *114* (45), 14157–14167.

(39) Streitwieser, A.; Pulver, S. The Azide Group as a Neighboring Group. Acetolysis of Trans-2-Azidocyclohexyl p-Toluenesulf Onate. *J. Am. Chem. Soc.* **1964**, *86* (8), 1587–1588.

(40) Drost, P. Nitro-Derivatives of Orthodinitrosobenzene. *Justus Liebigs Ann. der Chemie.* **1899**, *307*, 49–69.

(41) Forster, M. O.; Fierz, H. E. CLXXXIX.—Aromatic Azoimides. Part III. The Naphthylazoimides and Their Nitro-Derivatives. *J. Chem. Soc., Trans.* **1907**, *91*, 1942–1953.

(42) Smith, P. A. S.; Hall, J. H.; Kan, R. O. The Electronic Character of the Azido Group Attached to Benzene Rings. *J. Am. Chem. Soc.* **1962**, *84* (3), 485-489.

(43) Stankovsky, S.; Kovac, S. Infrared Spectra of Heterocumulenes. IV. The Influence of Substituents on the Vas(NNN) Bands of Some Substituted Phenyl Azides. *Chem. zvesti* **1974**, *2*, 243–246.

(44) Hammett, L. P. The Effect of Structure upon the Reactions of Organic Compounds. Benzene Derivatives. *J. Am. Chem. Soc.* **1937**, *59* (1), 96–103.

(45) Hehre, W. J.; Taft, R. W.; Topsom, R. D. Ab Initio Calculations of Charge Distributions in Monosubstituted Benzenes and in Meta- and Para-Substituted Fluorobenzenes. Comparison with 1 H, 13 C, and 19 F Nmr Substituent Shifts. In *Progress in Physical Organic Chemistry*; 2007; pp 159–187.

(46) Armentrout, P. B. Entropy Measurements and the Kinetic Method: A Statistically

Meaningful Approach. *J. Am. Soc. Mass Spectrom.* **2000**, *11* (5), 371–379.

(47) Zilla, M. K.; Nayak, D.; Vishwakarma, R. A.; Sharma, P. R.; Goswami, A.; Ali, A. A Convergent Synthesis of Alkyne–Azide Cycloaddition Derivatives of 4-α,β-2-Propyne Podophyllotoxin Depicting Potent Cytotoxic Activity. *Eur. J. Med. Chem.* **2014**, *77*, 47–55.

(48) Demeter, O.; Fodor, E. A.; Kállay, M.; Mező, G.; Németh, K.; Szabó, P. T.; Kele, P. A Double-Clicking Bis-Azide Fluorogenic Dye for Bioorthogonal Self-Labeling Peptide Tags. *Chem. – A Eur. J.* **2016**, *22* (18), 6382–6388.

(49) Fujio, M.; McIver, R. T.; Taft, R. W. Effects of the Acidities of Phenols from Specific Substituent-Solvent Interactions. Inherent Substituent Parameters from Gas-Phase Acidities. *J. Am. Chem. Soc.* **1981**, *103* (14), 4017–4029.

(50) Hernandez-Gil, N.; Wentworth, W. E.; Chen, E. C. M. Electron Affinities of Fluorinated Phenoxy Radicals. *J. Phys. Chem.* **1984**, *88* (25), 6181–6185.

(51) Drahos, L.; Vékey, K. How Closely Related Are the Effective and the Real Temperature. *J. Mass Spectrom.* **1999**, *34* (2), 79–84.

(52) Ervin, K. M. Microcanonical Analysis of the Kinetic Method. *Int. J. Mass Spectrom.* **2000**, *195–196*, 271–284.

(53) Ervin, K. M.; Armentrout, P. B. Systematic and Random Errors in Ion Affinities and Activation Entropies from the Extended Kinetic Method. *J. Mass Spectrom.* **2004**, *39* (9), 1004–1015.

(54) Ervin, K. M. Microcanonical Analysis of the Kinetic Method. The Meaning of the

"Apparent Entropy." *J. Am. Soc. Mass Spectrom.* **2002**, *13* (5), 435–452.

(55) Hahn, I.-S.; Wesdemiotis, C. Protonation Thermochemistry of β-Alanine. *Int. J. Mass Spectrom.* **2003**, *222* (1–3), 465–479.

(56) Cheng, X.; Wu, Z.; Fenselau, C. Collision Energy Dependence of Proton-Bound Dimer Dissociation: Entropy Effects, Proton Affinities, and Intramolecular Hydrogen-Bonding in Protonated Peptides. *J. Am. Chem. Soc.* **1993**, *115* (11), 4844–4848.

(57) Cooks, R. G.; Kruger, T. L. Intrinsic Basicity Determination Using Metastable Ions. *J. Am. Chem. Soc.* **1977**, *99* (4), 1279–1281.

(58) Nold, M. J.; Cerda, B. A.; Wesdemiotis, C. Proton Affinities of the N- and C-Terminal Segments Arising upon the Dissociation of the Amide Bond in Protonated Peptides. *J. Am. Soc. Mass Spectrom.* **1999**, *10* (1), 1–8.

(59) Wenthold, P. G. Determination of the Proton Affinities of Bromo- and Iodoacetonitrile Using the Kinetic Method with Full Entropy Analysis. *J. Am. Soc. Mass Spectrom.* **2000**, *11* (7), 601–605.

(60) Angel, L. A.; Ervin, K. M. Competitive Threshold Collision-Induced Dissociation: Gas-Phase Acidity and O−H Bond Dissociation Enthalpy of Phenol. *J. Phys. Chem. A* **2004**, *108* (40), 8346–8352

(61) Hansch, C.; Leo, A.; Taft, R. W. A Survey of Hammett Substituent Constants and Resonance and Field Parameters. *Chem. Rev.* **1991**, *91* (2), 165–195.

(62) Schafman, B. S.; Wenthold, P. G. Regioselectivity of Pyridine Deprotonation in the Gas Phase. *J. Org. Chem.* **2007**, *72*, 1645-1651

(63) Wenthold, P. G.; Squires, R. R. Gas-Phase Acidities of o-, m- and p-Dehydrobenzoic Acid Radicals. Determination of the Substituent Constants for a Phenyl Radical Site. *Int. J. Mass Spectrom. Ion Process.* **1998**, *175* (1–2), 215–224.

(64) Poole, J. S. A Computational Study of the Chemistry of Substituted 3-Nitrenopyridine 1-Oxides. *J. Mol. Struct. THEOCHEM* **2009**, *894* (1–3), 93–102.

(65) Bull, J. A.; Mousseau, J. J.; Pelletier, G.; Charette, A. B. Synthesis of Pyridine and Dihydropyridine Derivatives by Regio- and Stereoselective Addition to N -Activated Pyridines. *Chem. Rev.* **2012**, *112* (5), 2642–2713.

(66) Andersson, H.; Gustafsson, M.; Olsson, R.; Almqvist, F. Selective Synthesis of 2-Substituted Pyridine N-Oxides via Directed Ortho-Metallation Using Grignard Reagents. *Tetrahedron Lett.* **2008**, *49* (48), 6901–6903.

(67) Mongin, O.; Rocca, P.; Thomas-dit-Dumont, L.; Trecourt, F.; Marsais, F.; Godard, A.; Queguiner, G. Metalation of Pyridine N-Oxides and Application to Synthesis. *J. Chem. Soc. Perkin Trans. I. Organic and Bio-Organic Chemistry.* **1995**, *19*, 2503-2508.

(68) Abramovitch, R. A.; Smith, E. M.; Knaus, E. E.; Saha, M. Direct Alkylation of Pyridine 1-Oxides. *J. Org. Chem.* **1972**, *37* (11), 1690–1696.

(69) Yamanaka, H.; Araki, T.; Sakamoto, T. Site-Selectivity in the Reaction of 3-Substituted Pyridine 1-Oxides with Phosphoryl Chloride. *Chem. Pharm. Bull.* **1988**, *36* (6), 2244–2247.

(70) Clark, R. B.; He, M.; Fyfe, C.; Lofland, D.; O'Brien, W. J.; Plamondon, L.; Sutcliffe, J. A.; Xiao, X.-Y. 8-Azatetracyclines: Synthesis and Evaluation of a Novel Class of

Tetracycline Antibacterial Agents. *J. Med. Chem.* **2011**, *54* (5), 1511–1528.

(71) Yin, J.; Xiang, B.; Huffman, M. A.; Raab, C. E.; Davies, I. W. A General and Efficient 2-Amination of Pyridines and Quinolines. *J. Org. Chem.* **2007**, *72* (12), 4554–4557.

Received: 6 May 2021 | Accepted: 3 November 2021

DOI: 10.1002/mas.21751

REVIEW ARTICLE

WILEY

Mass spectrometry studies of nitrene anions

Cory J. Conder | **Harshal Jawale** | **Paul G. Wenthold**

Department of Chemistry, Purdue University, West Lafayette, Indiana, USA

Correspondence
Paul G. Wenthold, Department of Chemistry, Purdue University, 560 Oval Dr, West Lafayette, IN 47906, USA.
Email: pgw@purdue.edu

Abstract

Nitrene anions are a class of reactive intermediates that provide a means for studying the corresponding neutral molecules via electron photodetachment spectroscopy and photoelectron spectroscopy. The added electron makes it possible for protected nitrene anions to be manipulated by external electric and magnetic fields of a mass spectrometer. Nitrene anions also display their own unique reactivities as reagents, which have been investigated using ion/molecule reactions. Mass spectrometry of negative ions has thereby provided information on the electronic states, reactivities, and thermochemical properties of nitrene intermediates. This review also includes a discussion of condensed-phase nitrene anions.

KEYWORDS

ion/molecule reactions, nitrene anions, spectroscopy

1 | INTRODUCTION

1.1 | Nitrenes

Nitrenes are a fascinating class of reactive intermediates that contain a neutral hypovalent nitrogen atom (R–N) and are isoelectronic with carbenes. Because of their unique chemical reactivity, nitrenes have been utilized in applications such as organic synthesis (Dequirez et al., 2012; Iddon et al., 1979; Wang et al., 2021), photoaffinity labeling (Fleming, 1995; Kotzyba-Hibert et al., 1995), and cross-linking experiments (Schock & Bräse, 2020). They have also been observed in the interstellar medium (Meyer & Roth, 1991). Nitrenes are commonly formed by thermolysis or photolysis of azides, which undergo expulsion of N_2, analogous to how carbenes are formed from diazo compounds. Despite their similarities, nitrenes and carbenes have very different reactivity. For example, carbenes easily react with C-H bonds to form adducts (Bach et al., 1993; Closs & Closs, 1969; Hirai et al., 1994; Sander et al., 1996; Tomioka et al., 1997) whereas nitrenes tend to undergo intramolecular rearrangements resulting in the formation of polymeric tar (Meijer et al., 1988; Platz, 1995).

In the early 1980s, spectroscopy studies resulted in conflicting information about the chemical properties and spin states of nitrenes due to the extreme difficulty of isolating them as intermediates. Photolysis of nitrene precursors generates nitrenes in an excited state (Wang et al., 2013), and the excess energy causes nitrenes to quickly isomerize into multiple intermediates that all absorb in a similar range. For example, the photolysis of phenylazide (PhN_3) produces phenylnitrene (PhN), ketenimine, and cyanocyclopentadienyl radical that all absorb between 300 and 400 nm, which complicated the isolation and characterization of PhN (Cullin et al., 1990; Gritsan & Platz, 2001; Platz, 1995; Wentrup, 1974; Wentrup & Crow, 1970). Similarly, it was assumed that alkylnitrenes could not be detected because of a barrierless 1,2-shift of hydrogen or alkyl groups (Travers et al., 1999).

With improvements in trapping experiments and other methods such as flash photolysis, spectroscopic assignments of many nitrenes have now been well established. Many observations of nitrenes or their primary

Abbreviations: EA, electron affinity; EI, electron ionization; EPD, electron photodetachment spectroscopy; ICR, ion cyclotron resonance; ISC, intersystem crossing; NIPES, negative ion photoelectron spectroscopy; NO, nitric oxide; PD, photodetachment; PES, photoelectron spectroscopy; PhN, phenylnitrene; SOC, spin-orbit coupling; TME, tetramethyleneethane; TMM, trimethylenemethane; TOF, time of flight.

photolysis products have been made in low-temperature matrices (Chapyshev & Wentrup, 2001; Inui et al., 2005; Maltsev et al., 2004; Nunes et al., 2016; Wentrup, 2013). These experiments were often carried out using nanosecond laser flash photolysis or nanosecond time-resolved infrared spectroscopy (Gritsan & Platz, 2006; Wang et al., 2013). However, the lifetime of some reactive intermediates such as ^{1}PhN is about 1 ns in organic solvents at room temperature (Wang et al., 2013). Other singlet nitrenes, such as *o*-biphenylnitrene and 1-napthylnitrene have even shorter lifetimes (16 and 12ps, respectively) (Burdzinski et al., 2005, 2006); thus, ultra-fast absorption spectroscopy is often required for their detection.

1.2 | Nitrene anions

An alternate approach to isolating reactive intermediates is to introduce a negative charge and manipulate the resulting anions using mass spectrometry. Anions have the advantage of being easier to generate and detect in the gas phase than their neutral counterparts. They are also less prone to undergo rearrangement reactions and fragmentations, as an added electron can function as a "protecting group" (Broadus & Kass, 2000, 2001; Reed et al., 2000). This negative ion approach can be used to produce high yields of ions of reactive species, including biradical negative ions or distonic radical anions, regioselectively (Wenthold et al., 1994). These protected intermediates can then be used in mass spectrometric studies to investigate free-radical chemistry, the acid-base properties of radicals, and in electron photodetachment spectroscopy (EPD) (Drzaic et al., 1984; Wetzel & Brauman, 1987) and negative ion photoelectron spectroscopy (NIPES) (Dessent & Johnson, 1999; Ervin & Lineberger, 1992) to probe the singlet-triplet energy gaps of the corresponding neutral biradicals and to measure their electron affinities (Wenthold et al., 1997, 1998).

Pioneering work in this area by Squires, Wenthold, and coworkers produced a series of radical anions, diradical anions, and even triradical anions such as benzynes (Wenthold et al., 1998), *m*-xylylene (Wenthold et al., 1997), trimethylenemethane (Wenthold et al., 1994; Wenthold et al., 1996), tetramethyleneethane (Lee et al., 1993), diazocarbene (Clifford et al., 1998b), dehydrophenols (Reed et al., 2003), naphthynes (Broadus & Kass, 2001; Reed et al., 2000), bicyclo[1.1.0]but-1(3)-ene (Chou & Kass, 1991), and cubene (Staneke et al., 1994). Mass spectrometry of negative anions has also been used to study a number of other transient species such as cubyl radical, phenyl radical, and vinyl radical (Davico et al., 1995; Ervin et al., 1990; Hare et al., 1997; Clifford et al., 1998a; Tian & Kass, 2013).

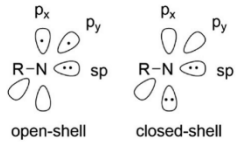

FIGURE 1 Two possible ways that the nonbonding electrons in neutral nitrenes can be distributed, as an open-shell structure, and a closed-shell structure

Nitrenes are likewise diradical intermediates with short lifetimes due to incomplete orbital occupancy (Figure 1). In contrast, nitrene anions have an extra valence electron, which effectively slows down rearrangement reactions and increases their lifetimes (McDonald & Chowdhury, 1980a). Nitrene anions are thus kinetically more stable than neutral nitrenes and can be used to determine a wide range of thermochemical data (Reed et al., 2000; Wijeratne et al., 2014).

In addition to providing valuable insights into the nature of neutral nitrenes, nitrene anions have their own unique properties as reactants, which can also be investigated using mass spectrometry. Anionic derivatives have been shown to be capable of tuning the reactivity of nitrenes, and their products have been explored using ion/molecule reactions (McDonald & Chowdhury, 1980a, 1980b, 1981, 1982, 1983; McDonald et al., 1981; Pellerite & Brauman, 1981; Rau & Wenthold, 2015; Wijeratne & Wenthold, 2007a). In this study, we review advancements in the field of nitrene anion chemistry, from their formal synthesis and reactivity to their characterization via spectroscopy and mass spectrometry, and characterization of the thermochemical properties of nitrenes.

2 | ELECTRONIC STRUCTURE OF NITRENES

Because any work on nitrene anions is intrinsically linked to nitrenes, it is useful to begin with a discussion on the underlying electronic structure of nitrenes. In any case, the electronic configuration of nitrenes and nitrene anions are closely related because they differ by only one electron. Nitrenes have nominally an sp hybridized nitrogen with a bonding sp orbital, a nonbonding sp orbital, and two (nonhybridized) p orbitals. A lone pair of electrons fills the nonbonding sp orbital, and two more electrons are distributed between the p_x and p_y orbitals. Most nitrenes have a triplet ground state with singlet excited states that can have electronic configurations p_x^2, p_y^2 or p_xp_y. The lowest-energy excited state for nitrenes is usually an open-shell singlet, in contrast to what occurs in isoelectronic carbenes,

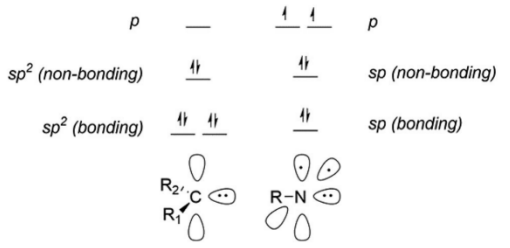

FIGURE 2 Molecular orbital diagrams for carbenes (left) and nitrenes (right)

where the lowest-energy excited state generally is a closed-shell singlet (Hrovat et al., 1992; Platz, 1995). This can be explained by looking at the molecular orbital diagrams for carbenes and nitrenes. Because carbenes are sp^2 hybridized, the closed-shell singlet is made by pairing two nonbonding electrons in a lower-energy nonbonding sp^2 orbital whereas electron repulsion in nitrenes raises the energy of the closed-shell state relative to the open-shell state (Figure 2).

The difference in the electronic structure of carbenes and nitrenes leads to a large difference in reactivity. Because of excess thermal energy that is retained upon formation, both carbenes and nitrenes are initially formed in an excited (singlet) state. However, ground-state triplet carbenes can quickly undergo intersystem crossing (ISC) from the closed-shell singlet to the ground state, which can then undergo bimolecular chemistry (Borden et al., 2000; Johnson et al., 2001; Platz, 1995). This is because the change in angular momentum from flipping the spin of an electron is accommodated by a change in orbitals ($\sigma \rightarrow \sigma\pi$) to allow for efficient spin-orbit coupling (SOC). In contrast, ISC for nitrenes is much slower because momentum is not as easily conserved going from an open-shell singlet to a triplet state without a change in orbitals ($\sigma\pi \rightarrow \sigma\pi$), resulting in slow SOC (Johnson et al., 2001; Salem & Rowland, 1972; Wijeratne et al., 2009). As a result, nitrenes are stuck in the open-shell singlet excited state, which undergoes intramolecular rearrangements faster than ISC. An example of this is seen in the photolysis of PhN_3 where the primary photolysis product ^{1}PhN isomerizes and multiple intermediates form (Figure 3). In addition to isomerizing, ^{1}PhN can also abstract a proton from its surroundings to form nitrenium ion (Falvey, 2003; Wang et al., 2013).

The singlet-triplet splitting is important in controlling the reactivity of nitrenes. A large singlet-triplet splitting leads to more intramolecular rearrangements. A smaller gap leads to faster relaxation into the triplet ground state and the possibility of bimolecular reactions. Substituents can be added to stabilize the open-shell singlet to prolong its lifetime (Johnson et al., 2001), or to stabilize the closed-shell

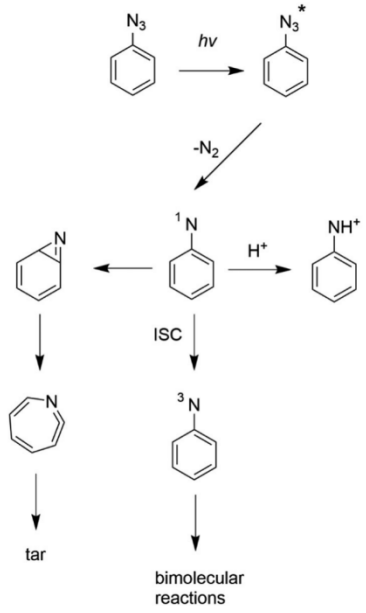

FIGURE 3 Key intermediates in the photolysis of phenylazide (Wang et al., 2013)

singlet, which undergoes ISC to the triplet ground state faster. The ground-state triplet is less likely to undergo rearrangement reactions because electrons of the same spin cannot be paired. Much theoretical and experimental work on nitrenes has been centered around tuning the singlet-triplet gap (Albini et al., 1999; Gritsan & Platz, 2001; Johnson et al., 2001; Rau et al., 2013), and nitrene anions have played a significant role in accomplishing this.

3 | CLASSES OF NITRENE ANIONS

3.1 | Introduction

Nitrene anions play many roles in addition to functioning as protected nitrene intermediates. They participate in a wide range of chemical reactions depending on their class or how they are synthesized. There are formally two approaches that could be used to introduce a negative charge into a nitrene. The first would involve the addition of an electron to a nitrene, creating a radical anion. Alternatively, anionic nitrenes can be created from neutral nitrenes by removing a cationic group, such as a proton. Because neutral nitrenes are unstable and therefore not viable as ion precursors, these approaches

are not used to synthesize the ions, but the ions that would be formed have distinguishing characteristics that provide a basis for organization and discussion.

A general description of the different classes of nitrene anions is provided in the sections below. Details of the characterization and reactivity of the ions will be given in later sections.

3.2 | Nitrene radical anions

Nitrene radical anions formally correspond to ions formed by the addition of an electron to an even-electron nitrene. Practically, they can be formed by using electron ionization (EI) of an appropriate precursor, such as an azide. Adding an electron to an azide results in dissociative attachment with loss of N_2, leaving behind a nitrene radical anion, as seen in the formation of phenylnitrene radical anion (PhN^-) from PhN_3 (Equation 1) (McDonald & Chowdhury, 1980a).

$$PhN_3 \xrightarrow{e^-} PhN^- + N_2 \quad (1)$$

Nitrene radical anions still have an sp hybridized nitrogen, so they have a lone pair of electrons in a nonbonding sp orbital and three more valence electrons distributed between two nonbonding σ and π orbitals. This reduces the number of electronic states from 4, as in the nitrene, to 2. For example, PhN^- has two possible electronic states; namely, the $^2A_1$ ground state with a $\pi^2\sigma$ configuration and a $^2B_2$ excited state with a $\sigma^2\pi$ configuration (Figure 4). Although calculations predict the $\pi^2\sigma$ configuration to be favored for PhN^- (Koirala et al., 2015; Wijeratne et al., 2009), it does not have to be so for all nitrene anions.

As mentioned earlier, nitrene radical anions contain an extra valence electron which prevents intramolecular rearrangement reactions from occurring as quickly as they do for neutral nitrenes. This aids in their most significant role as protected nitrene intermediates in photodetachment (PD) and photoelectron spectroscopy (PES) studies for probing the spectroscopic properties of nitrenes. Their reactivity has also been examined.

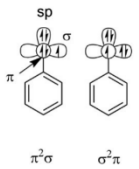

FIGURE 4 The two possible electronic configurations of phenylnitrene radical anion

3.3 | Deprotonated nitrenes

Deprotonation of nitrenes can occur if the nitrene has an acidic hydrogen. Depending on the location of the acidic hydrogen, nitrene anions formed by removing a proton can have the charge centered on the nitrogen or on a separate atom. In theory, a molecule with a proton bound to the nitrogen, such as imidogen (NH), can be deprotonated to give an even-electron anion with a formal charge of −1, as shown in Equation (2). However, this can only be done in theory as deprotonation of NH leads to a radical anion that is unbound with respect to electron detachment (Mazeau et al., 1978).

$$HN \xrightarrow{-H^+} N^- \quad (2)$$

In practice, the charge must be at a separate site from the nitrogen center such that the nitrogen atom retains its formal charge of 0. These types of ions can be formed by deprotonation of a molecule containing an azide group. Similar to electron attachment, deprotonation provides the necessary energy for spontaneous loss of N_2 to form the resulting nitrene anion, as shown in Equation (3).

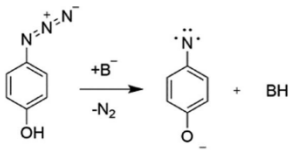

(3)

The resulting anion is not necessarily a pure nitrene and may have a mix of nitrene and imide character. For example, the *ortho*- and *para*-quinonimide anions have contributing nitrene and quinonimide resonance structures (Figure 5). In contrast, the *meta* isomer is purely a nitrene with no imide character.

Deprotonated nitrenes are still nominally nitrenes, or at least have nitrene character in that they have resonance contributions from structures with 6 electrons on nitrogen. Therefore, they will have the same electronic configurations as nitrenes, including σ^2, π^2, and σπ singlets and a σπ triplet. However, the energy ordering of the states is not necessarily the same, especially in terms of the energies of the closed-shell states, even to the extent of having a singlet ground state (Hossain et al., 2017; Rau et al., 2013).

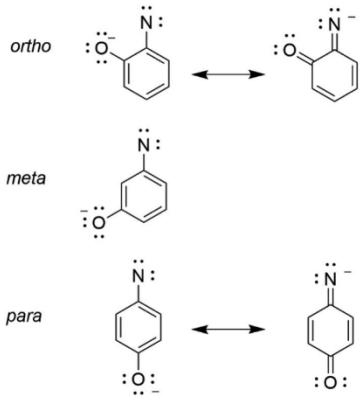

FIGURE 5 Resonance structures of quinonimide anions show that deprotonated nitrenes may have both nitrene and quinone characteristics

3.4 | Imide anions

Deprotonation of a nitrene on the carbon connected to the nitrogen nominally would result in the formation of an imide anion, $R_2C{=}N^-$, and not a nitrene. However, nitrene character can be introduced into the ion by the addition of electron withdrawing groups. For example, Rau and Wenthold (2015) have shown that benzaldimide (deprotonated benzaldimine), formed by reaction of trimethylsilybenzaldimine with fluoride, Equation (4), has an open-shell $\sigma\pi$ electronic structure if there is a sufficiently electron-withdrawing group on the aromatic ring. However, most imide anions have negligible nitrene character.

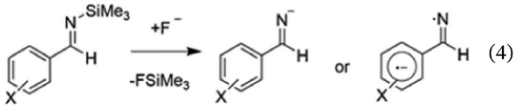

(4)

4 | SPECTROSCOPY OF NITRENE ANIONS—CHARACTERIZATION OF THE ELECTRONIC STATES OF NITRENES AND NITRENE ANIONS

4.1 | Introduction

An important application of nitrene anions is as a means for investigating the properties of nitrenes in the gas phase. Free of solvent effects that potentially stabilize electronic states, experiments with gaseous ions can simplify the characterization of nitrenes. This section discusses the advancements in the direct spectroscopic observation of nitrene anions. Some examples include imidogen (HN^-) (Al-Za'al et al., 1986, 1987; Engelking & Lineberger, 1976; Lykke et al., 1988; Miller et al., 1987; Neumark et al., 1985; Srivastava & Sathyamurthy, 2013), methylnitrene (CH_3N^-) (Travers et al., 1999), phenylnitrene (PhN^-) (Drzaic & Brauman, 1984a,b; McDonald & Davidson, 1993; Travers et al., 1992; Wijeratne et al., 2009), and substituted phenylnitrene anions (Wijeratne et al., 2009).

4.2 | NH^-

The simplest nitrene anion is NH^-. The first experimental study of NH^- was carried out by Celotta et al. (1974). In a NIPES study of NH_2^- anion, formed by glow-discharge ionization of NH_3, a small amount of NH^- was also observed, which allowed them to measure the corresponding electron affinity of NH (EA = 0.38 ± 0.03 eV). Engelking and Lineberger (1976) increased the amount of NH^- by using HN_3 for the source gas in place of NH_3 and increased the NIPES signal with a more powerful laser. Although the resolution was still limited, two peaks could be observed in the photoelectron spectrum, corresponding to transitions from the $X^2\Pi$ state of NH^- to the $X^3\Sigma^-$ and $a^1\Delta$ states of NH. The energy splitting was measured to be 1.579 ± 0.017 eV, in close agreement with theory as well as the results of photolysis experiments with neutral NH_3 (Rohrer & Stuhl, 1988; Srivastava & Sathyamurthy, 2013). They also refined the electron affinity of NH (EA = 0.381 ± 0.014 eV).

In the mid-1980s, Neumark et al. (1985) reported the infrared spectrum of NH^-, obtained by carrying out autodetachment spectroscopy using a coaxial laser-ion beam spectrometer and monitoring the neutrals and ejected electrons. As in the previous work, the NH^- was a produced by ionization of HN_3 in a hot-discharge source. The autodetachment resonances showed transitions in the R branch from NH^- ($v = 0$) to NH^- ($v = 1$) with a resolution better than 20 MHz. Transitions were also observed in the Q branch with a smaller resolution to calculate equilibrium vibrational constants, which allowed them to measure an electron affinity of 0.370 ± 0.004 eV. Later, using autodetachment spectroscopy of NH^- and detecting the kinematic velocity of the neutral molecule, Al-Za'al et al. (1987) were able to increase the resolution of the rotation-vibration spectrum and reported an electron affinity with a precision a thousand times higher than previous work (EA(NH) = 0.374362(5) eV).

4.3 | CH_3N^-

Little is known about the electronic states of alkylnitrenes. The simplest alkylnitrene, methylnitrene, is an intermediate in many combustion processes (Sadygov & Yarkony, 1997) and is thought to have a triplet ground state (X^3A_2) C_{3v} symmetry and a singlet first excited state ($\tilde{a}^1E$) (Travers et al., 1999). However, singlet CH_3N is unstable and quickly undergoes a hydrogen atom shift to become methyleneimine, CH_2NH (Equation 5).

(5)

Formation of the imine was first proposed in the early 1930s during pyrolysis studies (Leermakers, 1933) of methylazide (CH_3N_3) and later confirmed by photoionization spectroscopy (Bock & Dammel, 1987). Nevertheless, methylnitrene remained elusive despite many early attempts to isolate it. An accurate measurement of the electron affinity for CH_3N was not reported until decades later when Travers et al. (1999) reported negative ion PES of CH_3N^-, formed by ionization of methylazide in a discharge source. The electron affinity of CH_3N was found to be 0.022 ± 0.009 eV, with a singlet-triplet splitting of 130.5 ± 1.1 kJ/mol.

4.4 | PhN^-

PhN is perhaps the most famous nitrene, and PhN^- has been investigated in many spectroscopy studies. This radical anion was first investigated in the early 1980s (McDonald & Chowdhury, 1980a; McDonald et al., 1981). In the study of two primary reaction channels between aryl azides and nitrenes, they proposed that the reduction product PhN^- would avoid the competing rearrangement products of PhN. They were able to synthesize PhN^- via dissociative electron attachment with PhN_3 in a flowing afterglow apparatus. Shortly thereafter, Drzaic and Brauman (1984a, 1984b) recognized PhN^- as an approach for obtaining spectroscopic information on PhN. They reported the first direct measurement of the electron affinity of 141 ± 2 kJ/mol (1.46 ± 0.02 eV) obtained by using energy-resolved PD spectroscopy in an ion-cyclotron resonance spectrometer. They also were able to estimate a singlet-triplet splitting of 18 kJ/mol for PhN based on the increased PD yield at the corresponding energy in the spectrum.

In 1992, Travers et al. (1992) reported the 488 nm photoelectron spectrum of PhN^-, prepared from PhN_3 using a hot cathode ion source. The spectrum contained intense bands corresponding to the formation of the ground-state triplet (EA(PhN) = 1.45 ± 0.02 eV) and peaks attributed to the excited singlet state. Because the ions were rotationally and vibrationally hot, the initial peaks for the singlet band were assigned as hot bands. This assignment was confirmed by remeasuring the spectrum by taking the 351 nm photoelectron spectrum with thermal ions formed in a flowing afterglow ion source. Although the 351 nm spectrum is not shown, they explain that it confirms that the initial bands of the singlet state in the 488 nm spectrum are hot bands (see reference 5 in Travers et al., 1992) and that the singlet origin indicates a singlet-triplet splitting of approximately 75 kJ/mol.

Shortly thereafter, McDonald and Davidson (1993) reported another value for the electron affinity of PhN^- by using PD spectroscopy in a flowing afterglow. Based on the onset of the PD signal, they determined the electron affinity of PhN to be 1.429 ± 0.011 eV, in reasonable agreement with the previously reported values. On the basis of observed transitions in the PD curve, they assigned a singlet-triplet splitting of 76.64 ± 2.88 kJ/mol for PhN, in excellent agreement with the value obtained by using NIPES. Curiously, they observed lower energy transitions for the singlet, which were assigned to hot bands, as had been the case for the NIPES study (Travers et al., 1992), despite the fact that the ions formed in the flowing afterglow source should be vibrationally cooler than those in the glow-discharge.

As part of a NIPES study of chlorinated aromatic nitrenes (vide infra), Wijeratne et al. (2009) measured the 355 nm photoelectron spectrum of PhN^- for comparison with the previous work of Travers et al. (1992). Surprisingly, they found that the weak features previously described as hot bands for the singlet band were still present in the spectrum, despite using a pulsed expansion source to cool the ions. Moreover, the intense bands that had been attributed to the origin of the singlet excited state were not apparent in the 355 nm spectrum. In a reanalysis of the unpublished spectrum cited by Travers et al. (1992), it was discovered that the intense singlet-state feature was likely due to phenoxide impurity, whereas the weaker features assigned to hot bands corresponded to the standard progression of the singlet band. The reanalysis of the spectrum resulted in a revised value of the singlet triplet splitting, with $\Delta E_{ST} = 61.9 \pm 2.1$ kJ/mol, in good agreement with modern theoretical predictions (Winkler, 2008). Interestingly, the first singlet transition observed in the PD spectrum reported by McDonald and Davidson (1993), originally assigned as a hot band, is also found at an energy of 61.9 kJ/mol, suggesting that it is likely the origin for the onset of singlet formation.

4.5 | ClPhN⁻

Wijeratne et al. (2009) have carried out a PES study of chloro-substituted phenylnitrene anions to examine the effect of chlorination on electronic structure. The ions used in the study were formed from the corresponding chlorinated phenyl azides using a pulsed-expansion ionization source (Alexander et al., 1986; Metz et al., 1990; Weber et al., 2001).

The 355 nm photoelectron spectra obtained are shown in Figure 6. The lower-energy features were assigned to the triplet states, and the higher-energy features were assigned to the singlets. The origins of the triplet states are assigned as "A" and vibrational peaks are labeled "B-D." Likewise, the origins of the singlet states are labeled "a" and vibrational peaks "b-c." The spectra made it possible to measure the electron affinities for *ortho*-, *meta*-, and *para*-substituted (chlorophenyl)nitrene as 1.79 ± 0.05, 1.82 ± 0.05, and 1.72 ± 0.05 eV, respectively.

From the photoelectron spectra, it could be determined that the chlorine did not effect the order of the electronic states of the aromatic nitrene, with the open-shell singlet state still the lowest-energy singlet state. However, subtle differences observed in the shapes of the spectral features for the *ortho*- and *para*-singlet states were interpreted as indicating that the chlorine substituent has a detectable effect on the energies and structures of the open-shell singlet states. The effect was attributed to one-electron resonance delocalizaton involving the chlorine atom (Scheme 1), which allows for favorable delocalization of the π electron that reduces the electron-pair repulsion between the unpaired electrons (Karney & Borden, 1997). The result is a lowering of the singlet state energy (by about 4 kJ/mol) and a shortening of the C–N bond in the *ortho*- and *para*-isomers compared to that in the *meta*-isomer, where no resonance stabilization occurs.

4.6 | Quinonimides

The PES of quinonimides has been carried out by Hossain et al. (2017). Benzoquinones play an important role as electron acceptors in various biological processes (Ferreira et al., 2004; Srinivasan & Golbeck, 2009) as well as in chemical applications (Barrès et al., 2012; Popp & Stahl, 2007). The *ortho* and *para* isomers have Kekulé valence structures and low-energy closed-shell singlet electronic states, whereas the *meta* isomer has a non-Kekulé structure with an open-shell triplet ground state. Incorporating substituents into the aromatic ring leads to variations of lower-energy, stable Kekulé structures with closed-shell elecronic states, or to higher-energy, non-Kekulé structures with high-spin electron coupling.

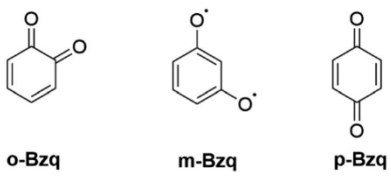

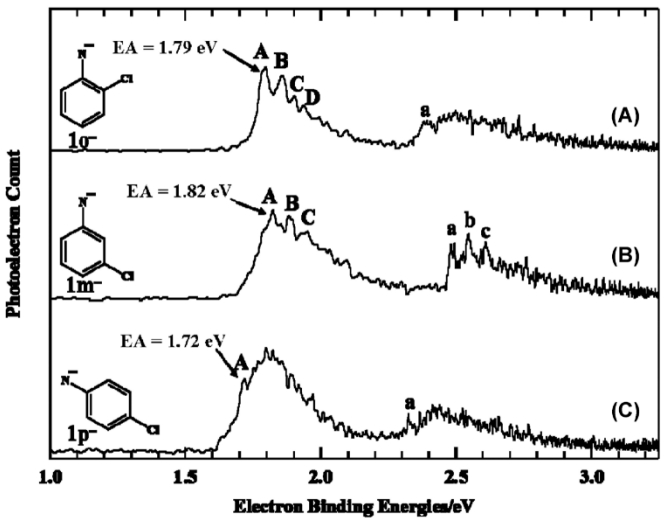

FIGURE 6 Photoelectron spectra of the (a) *ortho*-, (b) *meta*-, and (c) *para*-isomers of (chlorophenyl)nitrene anions at 355 nm. The region from 2.2 to 2.8 eV was scaled up by 2.5 to observe the origin of the singlet state more clearly. The origins of the triplet states are assigned as "A" and the other vibrational peaks are labeled as B – D. The origins of the singlet states are assigned as "a" for each isomer, and vibrational peaks are labeled b – c. Reprinted with permission from Wijeratne et al. (2009). Copyright 2009 American Chemical Society

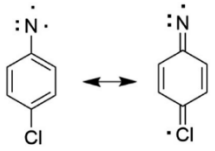

SCHEME 1

As will be discussed in the next section, the reactivity of *ortho*-, *meta*-, and *para*-quinoidal imides (Rau et al., 2013) shows that the electronic structure of the *para* isomer actually exhibits characteristics consistent with a thermally accessible triplet state. Accordingly, Hossain et al. (2017) used NIPES to study the electronic properties of the quinonimides and also determine spectroscopic properties of the corresponding quinoniminyl radicals. The NIPES experiments were carried out using a time-of-flight photoelectron spectrometer with an ESI source. ESI of *o*-, *m*- and *p*-azidophenoxide ions occurs by dissociation (M–H–N_2) to create benzoquinone product anions, **o-BzqN**$^-$, **m-BzqN**$^-$, and **p-BzqN**$^-$.

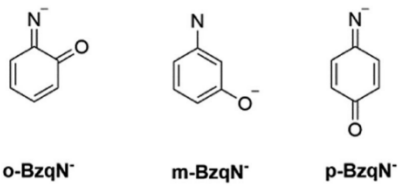

o-BzqN$^-$ **m-BzqN**$^-$ **p-BzqN**$^-$

The photoelectron spectra gave electron affinities of 1.715 and 1.67 ± 0.01 eV for **o-BzqN**$^-$ and **p-BzqN**$^-$, respectively. By modeling of the Frank-Condon profiles for the photoelectron bands, it was concluded that the *para* isomer, **p-BzqN**$^-$ is a ground state singlet whereas the *ortho* isomer is a triplet ground state nitrene. The *meta* isomer was found to rearrange to **p-BzqN**$^-$ and other unidentified isomers, and consequently could not be characterized.

5 | REACTIVITY

5.1 | Introduction

Mass spectrometry has been used in investigating the reactivity of nitrene anions in ion-molecule reactions. Nitrene anions can act as both Lewis bases and as radical intermediates. Radical chemistry stems from the configuration of valence electrons in the open-shell structure whereas two-electron chemistry can occur in either the closed-shell or open-shell structures. Because of their electron deficiency, nitrene anions are electrophilic as well. As will be discussed below, PhN$^-$ sets the basis for much of what is known about the reactivity of nitrene anions. However, as the field of nitrene anions has been increasing, a number of other rich examples have surfaced as well. This section highlights the unique reactivity that has been found for nitrene anions.

5.2 | PhN$^-$

The reactivity of PhN$^-$ has been thoroughly investigated, and a summary is shown in Figure 7. For these experiments, PhN$^-$ is generated by dissociative electron attachment of PhN_3. Because PhN$^-$ has an odd number of electrons, it is a ground-state doublet and does not have the electronic state properties like those that lead to rearrangements in neutral nitrenes (McDonald & Chowdhury, 1980a). Thus, PhN$^-$ has a longer lifetime and can easily participate in reactions with other molecules.

One of the first reactivity studies on PhN$^-$ was carried out by McDonald and Chowdhury (1980a) They observed that PhN$^-$ can react with PhN_3 by addition to N_α to produce azobenzene radical anion and nitrogen (Equation 6) and to N_γ to produce 1,4-diphenyltetrazadiene radical anion (Equation 7).

$$PhN^{\bullet-} + PhN_3 \longrightarrow Ph\text{-}N{=}N\text{-}Ph^{\bullet-} + N_2 \quad (6)$$

$$PhN^{\bullet-} + PhN_3 \longrightarrow Ph\text{-}N{=}N\text{-}N{=}N\text{-}Ph^{\bullet-} \quad (7)$$

McDonald et al. (1981) also determined the proton affinity of PhN$^-$ in a flowing afterglow using a series of proton donors with known acidity. For strong acids, PhNH was the major product. For weak acids that could not protonate PhN$^-$, bimolecular reactions were observed instead. PhN$^-$ was found to form clusters with alcohols through a sequence of reactions. PhN$^-$ also reacted with CH_3CN to form $C_8H_8N_2^-$ as the major product. On the basis of whether the proton transfer was observed, the proton affinity of the anion was deduced to be 1560 ± 8 kJ/mol, which leads to $\Delta H_f(PhN^-) = 251 \pm 2$ kJ/mol (Bartmess & McIver, 1979; McDonald et al., 1981).

PhN$^-$ also undergoes addition to certain α,β-unsaturated compounds. Gas-phase studies of 1,2 versus 1,4 additions of nucleophiles to α,β-unsaturated compounds is difficult because both reactions lead to products with the same m/z values. Additionally, solution-phase studies indicate that 1,2 additions are easily reversible, so the results from gas-phase studies

FIGURE 7 Reactions with PhN^-

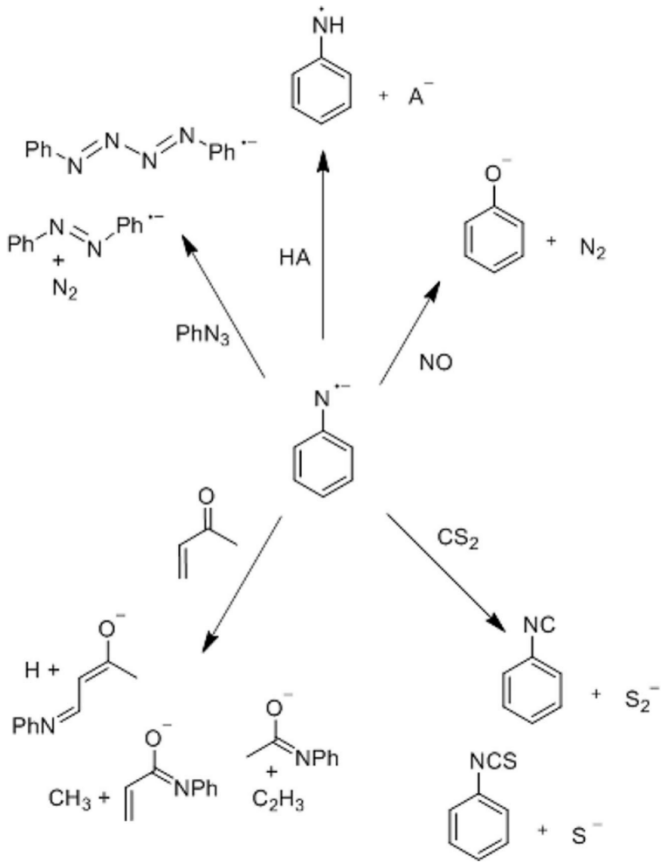

yield little information on the difference in reactivities of the two sites. However, hypovalent radical anions can be used to solve the reactivity of α,β-unsaturated compounds (McDonald & Chowdhury, 1982).

Hypovalent species such as R_2C^-, RN^-, O^-, and S^- are known to add to α,β-unsaturated compounds irreversibly because they contain both an unpaired electron and a lone pair (McDonald & Chowdhury, 1981, 1983). After the lone pair adds to the carbon, the radical can initiate irreversible β fragmentation, as shown in Scheme 2. The resulting product ions have different m/z values; thus, the preference for 1,2 versus 1,4 additions can be identified. Whereas as R_2C^-, and O^- have large H atom (HA) and H^+ (PA) affinities giving them short lifetimes, RN^- has smaller calculated HA and PA values making it a better nucleophile for gas-phase reactions (McDonald & Chowdhury, 1983).

As seen with additions to α,β-unsaturated compounds, PhN^- also adds to carbonyls. Most gas-phase nucleophiles add to carbonyls reversibly making information about the reactivity of carbonyl sites difficult to uncover. Nevertheless, addition of PhN^- followed by irreversible β fragmentation can yield valuable information on the reactivity of carbonyl sites, as shown in Scheme 3.

Nitric oxide (NO) is a reagent that reacts specifically with open-shell anions in the gas phase (Chacko & Wenthold, 2006). Ion-molecule reactions involving NO can thus aid in investigating electronic structure. Wijeratne and Wenthold (2007b) observed that PhN^- reacts with NO via nitrogen-oxygen exchange to form phenoxide, as shown in the following equation:

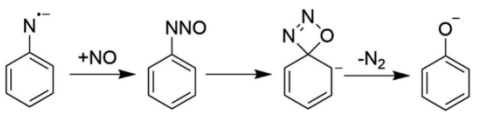

(8)

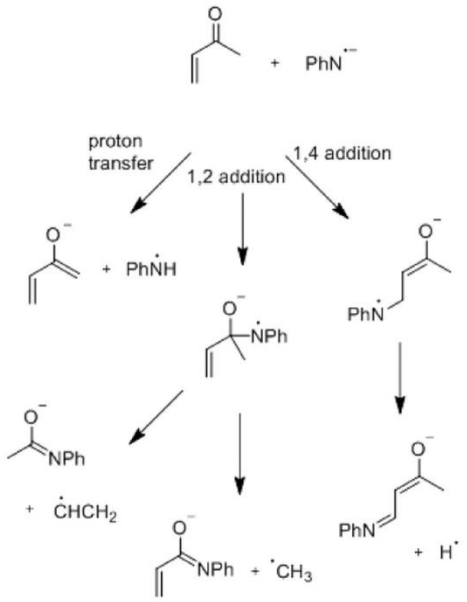

SCHEME 2

They also observed that PhN^- reacted with carbon disulfide (CS_2) by C^+ or CS^+ abstraction forming S^- and S_2^- (Equation 9).

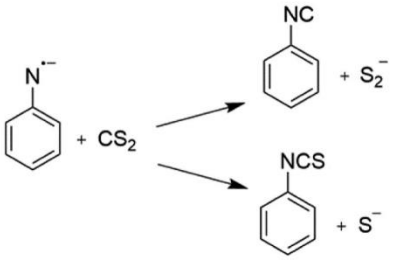

(9)

5.3 | Pyridinyl-*n*-oxide nitrenes

Radical stabilizing groups (Creary, 2006) are one route to altering the electronic structure of nitrene intermediates. Although the effect of these groups is predicted to be small, usually reducing the singlet-triplet splitting by less than 8 kJ/mol, some larger effects do occur (Hossain & Wenthold, 2013). Furthermore, other radical stabilizing groups are predicted to have an unusually small singlet-triplet splitting, as seen with 2-furanylnitrene (Wenthold, 2012). To determine the effects of a radical

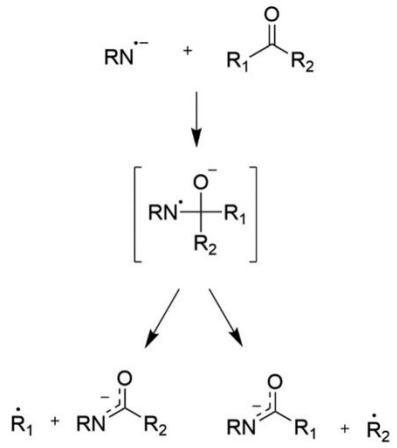

SCHEME 3

stabilizing group on PhN^-, Koirala et al. (2015) investigated the reactivity of 3- and 4-pyridinylnitrene-*n*-oxide radical anions, **3PNO**$^-$ and **4PNO**$^-$, respectively, formed by ionization of the corresponding azides in a flowing afterglow ion source.

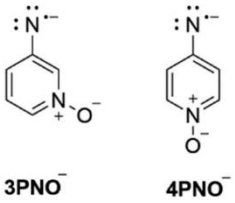

3PNO$^-$ **4PNO**$^-$

The pyridinium [ion] is an electron acceptor, but the oxide is a π donor. While the *n*-oxide does not participate in resonance at the 3-position, two types of stabilization are available at the 4-position (Figure 8).

Although the *N*-oxide is not predicted to alter the ground state of **4PNO**$^-$, differences in reactivity between **3PNO**$^-$ and **4PNO**$^-$ were observed. One significant difference is that the reaction of **4PNO**$^-$ with NO leads to more adduct ion whereas the reaction with **3PNO**$^-$ only leads to trace amounts. Both are observed to undergo N-O exchange.

Upon reaction with CS_2, **3PNO**$^-$ and **4PNO**$^-$ again displayed different reactivity. Nucleophilic attack of the oxygen in the anion at the carbon in CS_2 was only observed for **4PNO**$^-$. This led to sulfur-oxygen transfer and to formation of CS_2O^- (Equation 10), which was not observed for **3PNO**$^-$ indicating that the *N*-oxide moiety does not interact with the substituent in the *meta* position.

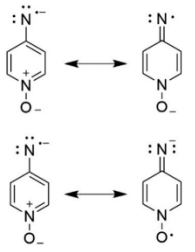

FIGURE 8 Resonance structures of **4PNO**$^-$

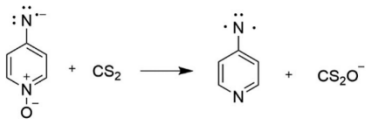

(10)

This study confirmed that sufficiently strong π-donors undergo oxygen-atom transfer, which is consistent with condensed-phase studies (Yoshimura et al., 1982) but had not previously been observed for aromatic *N*-oxides.

5.4 | Quinonimides

Rau et al. (2013) showed that anionic-π donors can affect the electronic structure of nitrenes, even to the point of leading to a closed-shell singlet ground state. They investigated reactions of anion-substituted (CH_2^-, O^-) aromatic nitrenes with O_2, NO, and CS_2. The ions were synthesized by reaction of precursor azide molecules *m*- and *p*-azidotoluene and *p*-azidophenol with hydroxide and fluoride ions, respectively, in a flow tube, resulting in closed-shell nitrene anions, as shown in Equations 11–13.

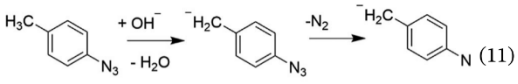

(11)

1

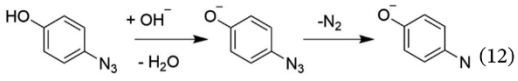

(12)

2

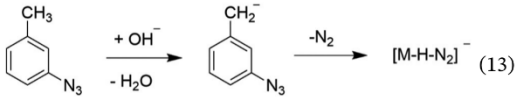

(13)

3

Differences were observed in the products of the deprotonated nitrene anions **1-3** when they react with NO. The compounds with CH_2^- (**1** and **3**) only undergo adduct formation with NO, whereas ion **2**, with the O^-, results in nitrogen-oxygen exchange in addition to adduct formation (Equation 14).

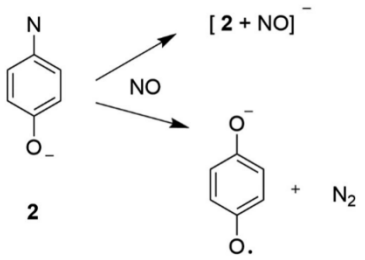

(14)

Both *para* isomers (**1** and **2)** undergo sulfur-nitrogen exchange with CS_2 to form NCS^-; however, **3** once again only undergoes adduct formation. The differences in the observed reactivity of the deprotonated nitrene anions with NO and CS_2 provide insight into the electronic structures of these ions. Because NO is known to undergo reactions with open-shell anions (Hammad & Wenthold, 2003; Wenthold et al., 1994; Wenthold & Squires, 1994), it was expected that **1** undergoes only adduct formation because it is a closed-shell anion. In contrast, **2** formed a 60/40 mixture of adduct and semiquinone anion (Equation 14), which implies it has an accessible open-shell structure. In addition, reaction of **2** with molecular oxygen results solely in nitrogen-oxygen exchange, which is indicative of a low-energy, accessible triplet state.

Calculations carried out on the singlet-triplet energy gaps of other nitrene derivatives led to the prediction that functional groups could fine tune the electronic structure of nitrenes. Figure 9 is the result of those calculations showing a series of phenyl nitrenes with a range of electron donating groups that create a spectrum of molecules with a mix of quinone (blue) and nitrene (red) resonance contributions. The stronger the electron donor, the greater the quinone contribution (blue curve), which lowers the relative energy of the closed-shell singlet state compared to that of the triplet.

5.5 | Benzoylnitrene

Wijeratne and Wenthold (2007a, 2007b, 2007c) have studied the reactivity and thermochemistry of benzoylnitrene radical anions, formed from EI of benzoylazide in a flowing afterglow. Acylnitrenes have been confirmed to be ground state singlets (Autrey & Schuster, 1987;

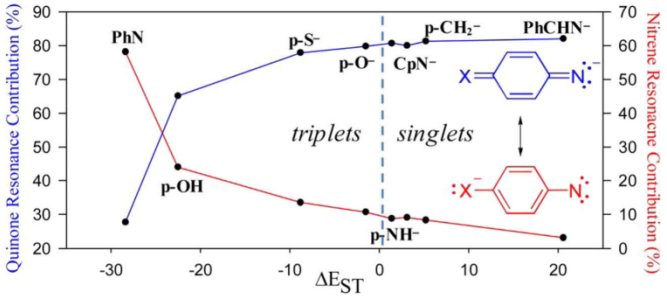

FIGURE 9 Calculated effects of anionic substituents on the singlet-triplet splitting and electronic structure of phenylnitrene. Reprinted with permission from Rau et al. (2013). Copyright 2013 American Chemical Society [Color figure can be viewed at wileyonlinelibrary.com]

Pritchina et al., 2005) because they are stabilized by the carbonyl through resonance (Gritsan & Pritchina, 2001; Pritchina et al., 2003). Similarly, benzoylnitrene radical anion is also stabilized via resonance, as shown in the following equation:

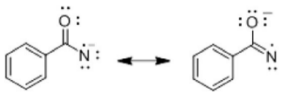

(15)

As with aromatic nitrene anions, benzoylnitrene anions react with NO by nitrogen-oxygen exchange forming benzoate anion as the major product (Equation 16) (Wijeratne & Wenthold, 2007b). The reaction is again proposed to involve an initial radical coupling of the benzoyl nitrene anion and the nitric oxide forming a benzoylnitrosate anion, followed by the formation of a 4-membered transition state that gives the benzoate after elimination of a nitrogen molecule.

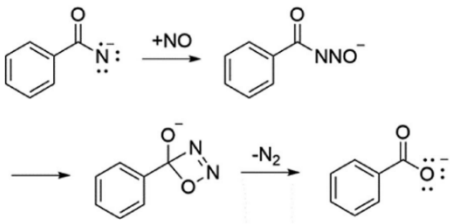

(16)

The reaction also produces a small amount of benzonitrile, which is produced by oxygen anion transfer (Equation 17).

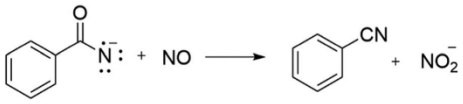

(17)

The reaction with nitrogen dioxide also undergoes a nitrogen-oxygen exchange leading to formation of benzoate anion and N_2O. This reaction is presumed to follow a similar mechanism as the reaction with NO, with initial formation of N-nitroso anion followed by a rearrangement. This reaction produced additional products, as shown in Scheme 4, but to a much smaller extent.

The reaction of benzoyl nitrene anion with the Lewis acid CS_2 yields benzonitrile as the main product along with CS_2O^- (Equation 18). Oxygen anion transfer is also observed in the reaction with SO_2, where the major products are benzonitrile and SO_3^- (Equation 19). This reaction is accompanied by the formation of SO, indicating oxygen abstraction by the benzoylnitrene anion. Reaction of benzoyl nitrene anion with other Lewis acids such as CO_2 and N_2O does not occur (Wijeratne & Wenthold, 2007b).

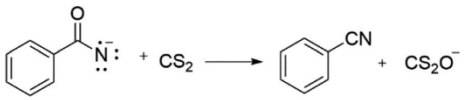

(18)

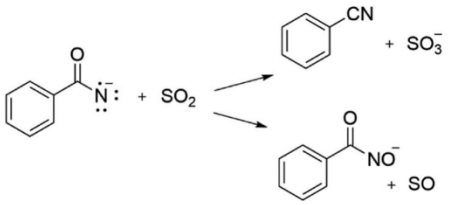

(19)

Atomic oxygen ion, O^-, is well-known to undergo reactions by H_2^+ transfer (Lee & Grabowski, 1992). Consequently, O^- has been used extensively for the synthesis of radical anions of reactive molecules, including carbenes and diradicals. A similar type of H_2^+ transfer was also observed in the reactions of benzoylnitrene anions with select reagents with high acidities. The reagents vary from various substituted phenols to other substrates such as acetic acid and

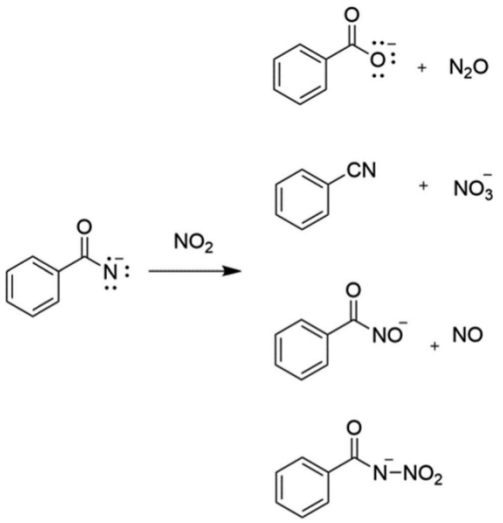

SCHEME 4

1,1,1,3,3,3-hexafluoro-2-propanol, as shown in Equations (20) and (21) (Wijeratne & Wenthold, 2007a).

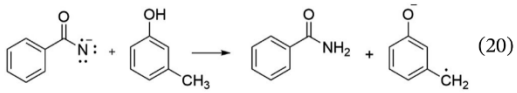
(20)

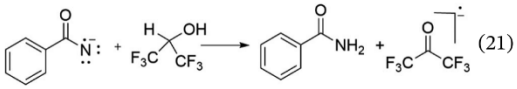
(21)

5.6 | Benzaldimides

In the same way that strong π donors can increase the quinone character of nitrenes, electron withdrawing groups can increase the nitrene character of imides. An example is *para*-substituted quinonimide anion, as shown in following equation:

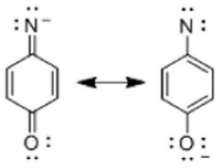
(22)

While imide anions are formally the conjugate bases of imines, they can be synthesized by reactions of *N*-trimethylsilylimines with fluoride ion (Equation 23).

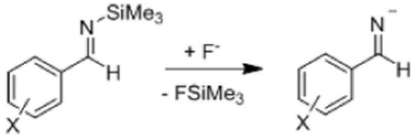
(23)

X = H, p-CH_3, p-CN, m-NO_2, p-NO_2

The nitrene character of these molecules can be confirmed through ion/molecule reactions with NO and CS_2 which have distinct reactivities towards open-shell and the closed-shell nitrenes (Rau et al., 2013). Using these reagents, Rau and Wenthold (2015) examined the reactivities of substituted benzaldimide anions (Equation 24).

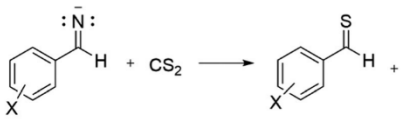
(24)

X = H, p-CH_3, p-CN, m-NO_2, p-NO_2

Typically, substituted benzaldimides react with CS_2 by nitrogen-sulfur exchange, thus confirming the presence of a nitrogen-based anion. The mechanism of the NCS^- formation is predicted to involve direct addition of CS_2 forming a thiocarboxylate which forms a 4-membered transition state followed by the substitution (Scheme 5).

Imide ions also react with CS_2 by hydride transfer forming HCS_2^- and the corresponding benzonitriles (Equation 25).

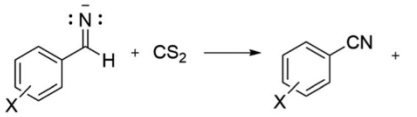
(25)

X = H, p-CH_3, p-CN, m-NO_2, p-NO_2

In reactions with NO, most imide anions form adducts indicating the presence of a closed-shell anion. In contrast, *p*-nitrobenzaldimide was found to react with NO via N–O exchange forming benzaldehyde radical anion (Equation 26). The formation of the NO adduct as well as the N–O exchange product indicates that

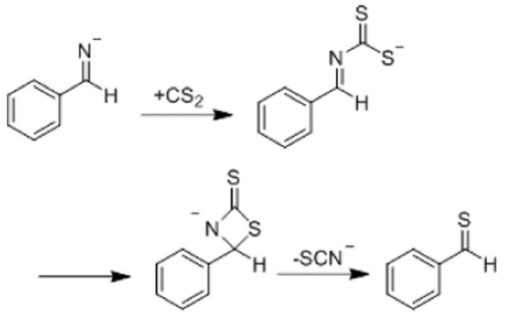

SCHEME 5

p-nitrobenzaldimide has an accessible open-shell (presumably) triplet electronic state.

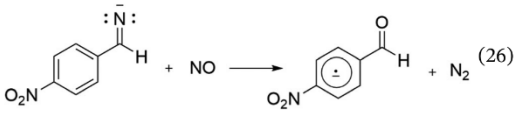

(26)

6 | THERMOCHEMISTRY

The focus of many of the studies included in this review has been on the determination of the thermochemical properties of nitrene anions and the corresponding nitrenes. Thermochemical properties, such as enthalpies of formation, gas-phase acidities, and electron affinities, aid in understanding the reactivity of nitrenes and nitrene anions, and many of the traditional mass spectrometric approaches have been used in this regard (Ervin, 2001).

As discussed in the spectroscopy section, nitrene electron affinities can be measured by using PD or PES. From features in the PD and photoelectron spectra, it can be possible to determine the energy difference between the triplet and singlet states of the nitrene, ΔE_{ST}. Anion proton affinities (or, conversely, the gas-phase acidity of the conjugate acid, $\Delta G_{acid}(RNH)$) have been measured by using proton-affinity bracketing, wherein the proton affinity is deduced from the occurrence or nonoccurrence of proton transfer in the reaction of proton donors with known gas-phase acidities. With reliable estimates of ΔS_{acid} values, the free energy values can be converted to $\Delta H_{acid}(RNH)$ (Bartmess & McIver, 1979; Berkowitz et al., 1994; Blanksby & Ellison, 2003).

From these direct measurements, additional important thermochemical quantities can be derived. In particular, by using the expression in Equation (27) (Berkowitz et al., 1994), it is possible to calculate the homolytic bond dissociation energy (BDE) in the RNH radical, D(RN–H).

$$D(R - H) = \Delta H_{acid}(RH) + E_{EA}(R) - IE(H) \quad (27)$$

Consequently, if the enthalpy of formation of RNH is known, then the BDE can be used to determine the absolute enthalpy of formation of the nitrene, $\Delta H_f(RN)$. Currently, only NH ($\Delta H_f = 376.56$ kJ/mol) (Linstrom & Mallard, 2018) and PhN ($\Delta H_f = 425 \pm 8$ kJ/mol) (Wijeratne et al., 2014) are characterized to this extent. A summary of the measured thermochemical values obtained by studies of nitrene anions is shown in Table 1.

Additional characterization of the benzoyl nitrene radical anion, **BzN**$^-$, was reported by Wijeratne and Wenthold (2007c). Collision-induced dissociation (CID) of **BzN**$^-$ occurs by loss of NCO^- to form phenyl radical (Equation 28). By using energy-resolved CID, the authors were able to determine the energy for the dissociation reaction in Equation (28) which, when combined with the well-known enthalpies of formation of phenyl radical (Ervin, 2001) and CNO^- (Linstrom & Mallard, 2018), could be used to determine the enthalpy of formation of the benzoyl nitrene radical anion.

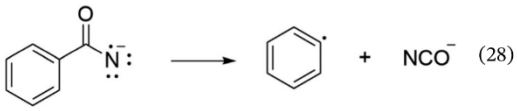

(28)

Similarly, bracketing reactions were used to determine the proton affinity of the anion, and, consequently, the gas-phase acidity of the benzamidyl radical (Equation 29). Proton transfer was observed with formic acid but not with 1,2,3-triazole, resulting in a proton affinity of 1453 ± 10 kJ/mol.

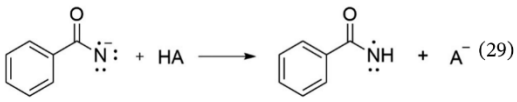

(29)

By combining these two measurements, a wealth of thermochemical data could be derived (Figure 10) including the homolytic BDE in benzoylamide (D(PhCONH-H) = 429 ± 14 kJ/mol), the electron affinity of the benzoylamidyl radical (EA(PhCONH) = 2.70 ± 0.17 eV) and the oxygen anion (O^-) affinity of benzonitrile (D(PhCN-O^-) = 294 ± 9 kJ/mol).

TABLE 1 Thermchemical properties of nitrenes and nitrene anions from mass spectrometry studies

Nitrene ion (RN^-)	$E_{EA}(RN)$ (eV)	$\Delta H_{acid}(RNH)$ (kJ/mol)	$\Delta E_{ST}(RN)$ (kJ/mol)	D(RN-H) (kJ/mol)[a]	References
NH^-	0.38 ± 0.03				Celotta et al. (1974)
	0.381 ± 0.014		152 ± 2		Engelking and Lineberger (1976)
	0.370 ± 0.004				Neumark et al. (1985)
	0.374362(5)				Al-Za'al et al. (1987)
			150.6 ± 0.1		Rohrer and Stuhl (1988)
CH_3N^-	0.022 ± 0.009		130.5 ± 1.1		Travers et al. (1999)
PhN^-	1.46 ± 0.02		18.0 ± 1.7		Drzaic and Brauman (1984a,b)
	1.45 ± 0.02		62 ± 2[b]		Travers et al. (1992)
	1.429 ± 0.011		76.6 ± 2.9		McDonald and Davidson (1993)
	1.45 ± 0.02		62 ± 2		Wijeratne et al. (2009)
		1560 ± 8		388 ± 8	McDonald et al. (1981)
o-$ClPhN^-$	1.79 ± 0.05		58 ± 8		Wijeratne et al. (2009)
		1534 ± 16		395 ± 17	Wijeratne et al. (2014)
m-$ClPhN^-$	1.82 ± 0.05		63 ± 8		Wijeratne et al. (2009)
		1535 ± 16		399 ± 17	Wijeratne et al. (2014)
p-$ClPhN^-$	1.72 ± 0.05		58 ± 8		Wijeratne et al. (2009)
		1533 ± 16		387 ± 17	Wijeratne et al. (2014)
o-$OC_6H_4N^-$	1.715 ± 0.010		149 ± 1[c]		Hossain et al. (2017)
p-$OC_6H_4N^-$	1.675 ± 0.010				Hossain et al. (2017)
$C_6H_5CON^-$		1453 ± 10			Wijeratne and Wenthold (2007c)

[a]Derived from $D(R\text{-}H) = \Delta H_{acid}(RH) + E_{EA}(R) - IE(H)$.

[b]Although this was originally reported as 75 ± 8 kJ/mol, the original data were re-interpreted by Wijeratne et al. (2009) to the value of 62 kJ/mol.

[c]This is technically the doublet-quartet splitting because the neutral nitrene is an odd-electron species; in contrast to the other nitrenes in the table, which are ground-state triplets, the low-spin (doublet) state is the ground state.

7 | CONDENSED-PHASE NITRENE ANIONS

While nitrene anions are difficult to isolate in solution, they are known to take part in condensed phase chemistry (Herbranson & Hawley, 1990; Murata et al., 1995; Van Galen et al., 1986). They fall into a category of organic molecules with low-lying high-spin electronic states that have drawn significant interest for many years because of their unique electronic properties (Perrotta & Falvey, 2013). Because of their high reactivity, they are difficult to characterize. However, a few examples have been reported in the literature, which will be discussed below.

In the electrochemical reduction of *p*-nitrophenyl azide in DMF, acetonitrile, and butyronitrile, Herbranson and Hawley (1990) proposed the formation of $p\text{-}O_2NC_6H_4N_3^-$ radical anion (Equation 30) which decomposes by loss of dinitrogen to give the corresponding phenylnitrene anion as a short-lived, unobserved intermediate (Equation 31). The formation of the dimeric dianion $4,4'\text{-}O_2NC_6H_4N{=}NC_6H_4NO_2^{2-}$ is presumed to go through the dimerization of either $p\text{-}O_2NC_6H_4N_3^-$ (Equation 32) or $p\text{-}O_2NC_6H_4N^-$ (Equation 33).

$$p\text{-}O_2NC_6H_4N_3 + e^- \rightleftharpoons p\text{-}O_2NC_6H_4N_3^{\bullet -} \quad (30)$$

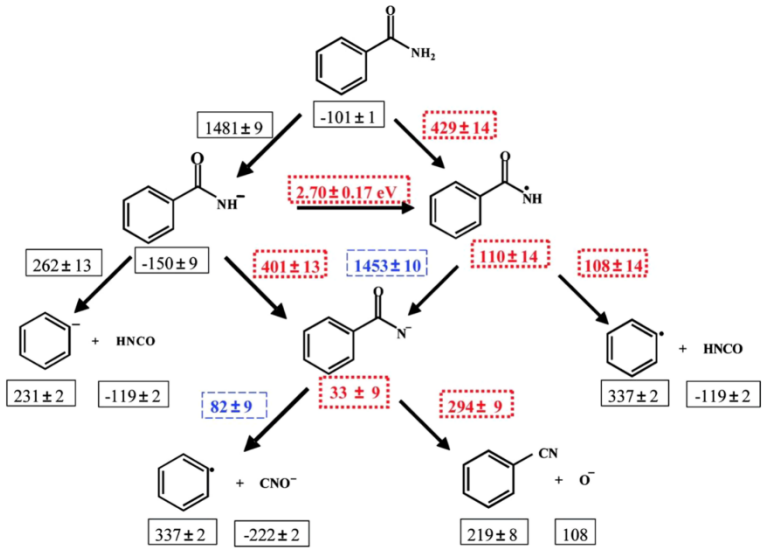

FIGURE 10 Thermochemical properties measured and derived from the studies of benzoylnitrene radical anion. All values are in kJ/mol. Values in blue dashed-line boxes were measured directly in this study, whereas values in red dotted-line boxes were derived from those measurements and literature values, shown in black. Reprinted with permission from Wijeratne and Wenthold (2007c). Copyright 2007 American Chemical Society [Color figure can be viewed at wileyonlinelibrary.com]

$$p\text{-}O_2NC_6H_4N_3^{\bullet-} \longrightarrow p\text{-}O_2NC_6H_4N^{\bullet-} + N_2 \quad (31)$$

$$2\ p\text{-}O_2NC_6H_4N_3^{\bullet-} \longrightarrow 4,4'\text{-}O_2NC_6H_4N{=}NC_6H_4NO_2^{2-} + 2N_2 \quad (32)$$

$$p\text{-}O_2NC_6H_4N^{\bullet-} \longrightarrow 4,4'\text{-}O_2NC_6H_4N{=}NC_6H_4NO_2^{2-} \quad (33)$$

The proclivity of these anion radicals to undergo a carbonyl addition/radical β-fragmentation reaction was also tested by controlled-potential electrolysis of p-$O_2NC_6H_4N_3$ in the presence of excess 2,3-butanedione $(CH_3CO)_2$. The product p-$O_2NC_6H_4N^-COCH_3$ obtained after the electrolysis was again presumed to have formed via one of the two intermediates shown in Equations 34 and 35.

$$2\ p\text{-}O_2NC_6H_4N_3^{\bullet-} + (CH_3CO)_2 \longrightarrow 4,4'\text{-}O_2NC_6H_4NCOCH_3^- + CH_3CO^{\bullet} + N_2 \quad (34)$$

$$2\ p\text{-}O_2NC_6H_4N^{\bullet-} + (CH_3CO)_2 \longrightarrow 4,4'\text{-}O_2NC_6H_4NCOCH_3^- + CH_3CO^{\bullet} \quad (35)$$

Some other experimental evidence provided by the authors for the formation of the radical anions p-$O_2NC_6H_4N_3^-$ and p-$O_2NC_6H_4N^-$ were observed during diazo transfer reactions with diethyl malonate and the formation of p-$O_2NC_6H_4N^-CON(CH_3)_2$ in DMF.

During the electrochemical reduction of fluorenone tosylhydrazone anion (Fl=NNTs$^-$), Van Galen et al. (1986) also observed evidence for the formation of tosylnitrene dianion radical (Fl=NNTs^{2-}). The dianion radical was found to be stable on the cyclic voltammetry timescale ($i_{p,a}/i_{p,c} = 1.0$) in DMF-0.1 F (n-Bu)$_4$NClO$_4$, and

could be readily protonated in the coulometric time scale or in the presence of proton donors with pKa < 29. Furthermore, the reduction of Fl=NNTs$^-$ yielded the expected product F1 = NH which further reduced reversibly to Fl=NH$^-$ radical anion on the cyclic voltammetric time scale in the absence of added proton donors.

The product studies of the decomposition reaction of Fl=NNTs^{2-} on the coulometric scale afforded the products F1NH$_2$ and TsNH$_2$, and the pathway for their formation was proposed to go through the TsN$^-$ radical anion species. Although attempts to capture TsN$^-$ were unsuccessful, the data was consistent with the formation of TsN$^-$ which was presumed to rapidly undergo hydrogen atom abstraction, proton abstraction, or other types of reactions in the condensed phase.

Formation of nitrene radical anion intermediates was also proposed by Murata et al. (1995) during pyrene-sensitized photolysis studies of *p*-butylphenylazide in the presence of diethylamine (DEA). The photolysis product *p*-butylaniline was proposed to form via one electron reduction of the azide to give the azide radical anion which then loses a dinitrogen to produce the nitrene radical anion. The nitrene radical anion would then undergo proton and hydrogen atom abstraction to yield the final aniline. The authors also proposed that the one electron reduction of the *p*-butylphenyl azide was carried out by the pyrene radical anion (Py$^-$) formed by electron transfer from DEA to the excited pyrene (Py*), as shown in Scheme 6.

Mudgal et al. (2017) studied the formation of an important biomolecule radical, aminyl radical (RNH) in 3′-azidothymidine (3′-AZT) (Figure 11), 2′-azido-2′-deoxyuridine (2′-AZdU), 4′-azido-2′-deoxycytidine (4′-AZ-2′-dC), methyl 2-azido-2-deoxy-α-D-lyxofuranoside, and methyl 2-azido-2-deoxy-β-D-ribofuranoside (Adhikary et al., 2010). The sugars were subjected to one electron reduction by radiation-produced prehydrated electrons which resulted in the formation of the corresponding, highly unstable azide anion radicals. Similar to examples discussed earlier, the azide anion radicals then underwent subsequent dinitrogen elimination to yield the corresponding nitrene anion radicals which led to rapid protonation to form RNH.

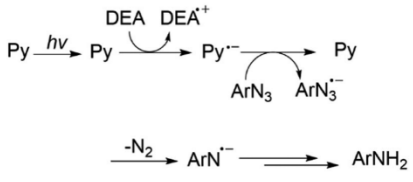

SCHEME 6

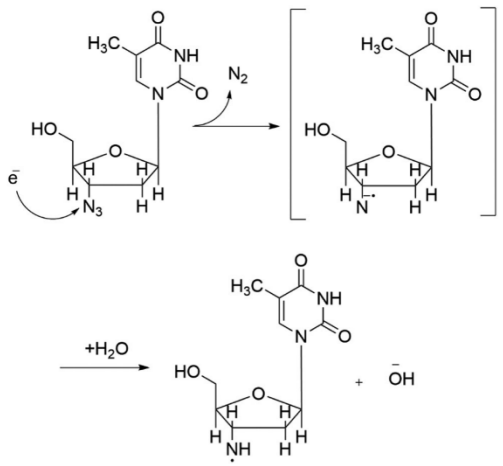

FIGURE 11 Formation of aminyl radical RNH from 3′-AZT via one-electron reduction (Mudgal et al., 2017)

Using ultraviolet and ^{1}H NMR experiments, Perrotta and Falvey (2013) characterized several ion-diradicals with low energy triplet states. Although not predicted to be the ground state, the authors found that sufficiently strong electron-withdrawing groups could lower the energy of the triplet state enough to create a population of triplet anilide (imide) anions. For example, 3,5-dinitroanilide anion, **4**, was found to have paramagnetic behavior indicating a triplet electronic state.

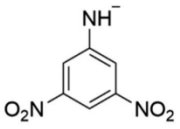

4

8 | CONCLUSIONS

Advancements in spectroscopic techniques have helped in the identification and characterization of the electronic states of many nitrenes; however, much work remains to be done to fully understand the factors that govern their energies, correlations, structures, and tunneling reactions that involve ISC and mixing of electronic states. The biggest challenge associated with these studies is the accessibility to the always decomposing nitrene intermediates. Nitrene anions serving as protected

nitrene intermediates offer easy access to spectroscopically probe their neutral counterparts because of their reluctance to undergo rearrangement reactions. Nitrene anions also exhibit their own unique reactivity, which has been discussed. Thus, investigations into nitrene anions should go hand in hand with the development of nitrene chemistry.

ACKNOWLEDGMENT

Work carried out at Purdue covered in this review has been supported by the National Science Foundation and Purdue University.

REFERENCES

Adhikary A, Khanduri D, Pottiboyina V, Rice CT, Sevilla MD. 2010. Formation of aminyl radicals on electron attachment to AZT: Abstraction from the sugar phosphate backbone versus one-electron oxidation of guanine. *J Phys Chem B 114*: 9289-9299.

Al-Za'al M, Miller HC, Farley JW. 1986. Observation of metastable states in the autodetachment continuum of the negative molecular ion NH−. *Chem Phys Lett 131*: 56-59.

Al-Za'al M, Miller HC, Farley JW. 1987. High-resolution measurement of the infrared rotation-vibration spectrum of the negative molecular ion $^{14}NH^-$. *Phys Rev A 35*: 1099-1112.

Albini A, Bettinetti G, Minoli G. 1999. Photodecomposition of some para-substituted 2-pyrazolylphenyl azides. Substituents affect the phenylnitrene S−T gap more than the barrier to ring expansion. *J Am Chem Soc 121*: 3104-3113.

Alexander ML, Johnson MA, Levinger NE, Lineberger WC. 1986. Photodissociation of mass-selected $(CO_2)_n^-$ clusters: Evaporation leading to magic numbers in fragment-ion distributions. *Phys Rev Lett 57*: 976-979.

Autrey T, Schuster GB. 1987. Are aroylnitrenes ground-state singlets? Photochemistry of.beta.-naphthoyl azide. *J Am Chem Soc 109*: 5814-5820.

Bach RD, Su MD, Aldabbagh E, Andres JL, Schlegel HB. 1993. A theoretical model for the orientation of carbene insertion into saturated hydrocarbons and the origin of the activation barrier. *J Am Chem Soc 115*: 10237-10246.

Barrès A-L, Geng J, Bonnard G, et al. 2012. High-potential reversible Li deintercalation in a substituted tetrahydroxy-p-benzoquinone dilithium salt: An experimental and theoretical study. *Chem-Eur J 18*: 8800-8812.

Bartmess JE, McIver RT. 1979. Chapter 11—The gas-phase acidity scale. In: Bowers MT editor. *Gas phase ion chemistry*. Academic Press. p 87-121.

Berkowitz J, Ellison GB, Gutman D. 1994. Three methods to measure RH bond energies. *J Phys Chem 98*: 2744-2765.

Blanksby SJ, Ellison GB. 2003. Bond dissociation energies of organic molecules. *Acc Chem Res 36*: 255-263.

Bock H, Dammel R. 1987. The pyrolysis of azides in the gas phase. *Angew Chem, Int Ed Engl 26*: 504-526.

Borden WT, Gritsan NP, Hadad CM, Karney WL, Kemnitz CR, Platz MS. 2000. The interplay of theory and experiment in the study of phenylnitrene. *Acc Chem Res 33*: 765-771.

Broadus KM, Kass SR. 2000. The electron as a protecting group. 2. Generation of benzocyclobutadiene radical anion in the gas phase and an experimental determination of the heat of formation of benzocyclobutadiene. *J Am Chem Soc 122*: 10697-10703.

Broadus KM, Kass SR. 2001. The electron as a protecting group. 3. Generation of acenaphthyne radical anion and the determination of the heat of formation of a strained cycloalkyne. *J Am Chem Soc 123*: 4189-4196.

Burdzinski G, Hackett JC, Wang J, Gustafson TL, Hadad CM, Platz MS. 2006. Early events in the photochemistry of aryl azides from femtosecond UV/Vis spectroscopy and quantum chemical calculations. *J Am Chem Soc 128*: 13402-13411.

Burdzinski GT, Gustafson TL, Hackett JC, Hadad CM, Platz MS. 2005. The direct detection of an aryl azide excited state: An ultrafast study of the photochemistry of para- and ortho-biphenyl azide. *J Am Chem Soc 127*: 13764-13765.

Celotta RJ, Bennett RA, Hall JL. 1974. Laser photodetachment determination of the electron affinities of OH, NH2, NH, SO2, and S2. *J Chem Phys 60*: 1740-1745.

Chacko SA, Wenthold PG. 2006. The negative ion chemistry of nitric oxide in the gas phase. *Mass Spectrom Rev 25*: 112-126.

Chapyshev SV, Wentrup C. 2001. Properties of triplet tetrachloro-4-pyridylnitrene isolated in inert matrices. *Chem Heterocycl Compd 37*: 1119-1129.

Chou PK, Kass SR. 1991. C_4H_4 negative ions: Formation of the bicyclo[1.1.0]but-1(3)-ene radical anion and an experimental determination of the heat of formation of bicyclo[1.1.0]but-1(3)-ene. *J Am Chem Soc 113*: 697-698.

Clifford EG, Wenthold P, Lineberger W, et al. 1998a. Properties of tetramethyleneethane (TME) as revealed by ion chemistry and ion photoelectron spectroscopy. *J Chem Soc, Perkin Trans 2*: 1015-1022.

Clifford EP, Wenthold PG, Lineberger WC, et al. 1998b. Properties of diazocarbene [CNN] and the diazomethyl radical [HCNN] via ion chemistry and spectroscopy. *J Phys Chem A 102*: 7100-7112.

Closs GL, Closs LE. 1969. Induced dynamic nuclear spin polarization in reactions of photochemically and thermally generated triplet diphenylmethylene. *J Am Chem Soc 91*: 4549-4550.

Creary X. 2006. Super radical stabilizers. *Acc Chem Res 39*: 761-771.

Cullin DW, Soundararajan N, Platz MS, Miller TA. 1990. Laser-induced fluorescence spectrum of the cyanocyclopentadienyl radical: A band system long attributed to triplet phenylnitrene. *J Phys Chem 94*: 8890-8896.

Davico GE, Bierbaum VM, DePuy CH, Ellison GB, Squires RR. 1995. The C-H bond energy of benzene. *J Am Chem Soc 117*: 2590-2599.

Dessent CEH, Johnson MA. 1999. Fundamentals of negative ion photoelectron spectroscopy, *NATO ASI Ser C 521*: 287-306.

Dequirez G, Pons V, Dauban P. 2012. Nitrene chemistry in organic synthesis: Still in its infancy? *Angew Chem, Int. Ed 51*: 7384-7395.

Drzaic PS, Brauman JI. 1984a. A determination of the triplet-singlet splitting in phenylnitrene via photodetachment spectroscopy. *J Am Chem Soc 106*: 3443-3446.

Drzaic PS, Brauman JI. 1984b. Electron photodetachment from phenylnitrene, anilide, and benzyl anions. Electron affinities of the anilino and benzyl radicals and phenyl nitrene. *J Phys Chem 88*: 5285-5290.

Drzaic PS, Marks J, Brauman JI. 1984. Electron photodetachment from gas phase molecular anions. *Gas Phase Ion Chem 3*: 167-211.

Engelking PC, Lineberger WC. 1976. Laser photoelectron spectrometry of NH−: Electron affinity and intercombination energy difference in NH. *J Chem Phys 65*: 4323-4324.

Ervin KM. 2001. Experimental techniques in gas-phase ion thermochemistry. *Chem Rev 101*: 391-444.

Ervin KM, Gronert S, Barlow SE, et al. 1990. Bond strengths of ethylene and acetylene. *J Am Chem Soc 112*: 5750-5759.

Ervin KM, Lineberger WC. 1992. Photoelectron spectroscopy of molecular anions. *Adv Gas Phase Ion Chem 1*: 121-166

Falvey DE. 2003. Nitrenium ions. *React Intermed Chem*: 593-650.

Ferreira KN, Iverson TM, Maghlaoui K, Barber J, Iwata S. 2004. Architecture of the photosynthetic oxygen-evolving center. *Science 303*: 1831-1838.

Fleming S. 1995. Chemical reagents in photoaffinity labeling. *Tetrahedron 51*: 12479-12520.

Gritsan NP, Platz MS. 2001. Kinetics and spectroscopy of substituted phenylnitrenes. In: Richard JP, Tidwell TT, editors. *Advances in physical organic chemistry*. Academic Press. p 255-304.

Gritsan NP, Platz MS. 2006. Kinetics, spectroscopy, and computational chemistry of arylnitrenes. *Chem Rev 106*: 3844-3867.

Gritsan NP, Pritchina EA. 2001. Are aroylnitrenes species with a singlet ground state? *Mendeleev Commun 11*: 94-95.

Hammad LA, Wenthold PG. 2003. An electron-catalyzed cope cyclization. The Structure of the 2,5-dicyano-1,5-hexadiene radical anion in the gas phase. *J Am Chem Soc 125*: 10796-10797.

Hare M, Emrick T, Eaton PE, Kass SR. 1997. Cubyl anion formation and an experimental determination of the acidity and C−H bond dissociation energy of cubane. *J Am Chem Soc 119*: 237-238.

Herbranson DE, Hawley MD. 1990. Electrochemical reduction of p-nitrophenyl azide: Evidence consistent with the formation of p-nitrophenylnitrene anion radical as a short-lived intermediate. *J Org Chem 55*: 4297-4303.

Hirai K, Komatsu K, Tomioka H. 1994. Reactions and kinetics of (2, 4,6-tri-tert-butylphenyl)phenylcarbene. *Chem Lett 23*: 503-506.

Hossain E, Deng SM, Gozem S, Krylov AI, Wang X-B, Wenthold PG. 2017. Photoelectron spectroscopy study of quinonimides. *J Am Chem Soc 139*: 11138-11148.

Hossain E, Wenthold PG. 2013. Singlet stabilization of oxazole- and isoxazolenitrene-n-oxides by radical delocalization. *Comput Theor Chem 1020*: 180-186.

Hrovat DA, Waali EE, Borden WT. 1992. Ab initio calculations of the singlet-triplet energy difference in phenylnitrene. *J Am Chem Soc 114*: 8698-8699.

Iddon B, Meth-Cohn O, Scriven EFV, Suschitzky H, Gallagher PT. 1979. Developments in arylnitrene chemistry: Syntheses and mechanisms [new synthetic methods (31)]. *Angew Chem, Int Ed Engl 18*: 900-917.

Inui H, Irisawa M, Oishi S. 2005. Reaction of (4-nitorophenyl) nitrene with molecular oxygen in low-temperature matrices: First IR detection and photochemistry of aryl nitroso oxide. *Chem Lett 34*: 478-479.

Johnson WTG, Sullivan MB, Cramer CJ. 2001. meta and para substitution effects on the electronic state energies and ring-expansion reactivities of phenylnitrenes. *Int J Quantum Chem 85*: 492-508.

Karney WL, Borden WT. 1997. Ab initio study of the ring expansion of phenylnitrene and comparison with the ring expansion of phenylcarbene. *J Am Chem Soc 119*: 1378-1387.

Koirala D, Poole JS, Wenthold PG. 2015. Reactivity of 3- and 4-pyridinylnitrene-n-oxide radical anions. *Int J Mass Spectrom 378*: 69-75.

Kotzyba-Hibert F, Kapfer I, Goeldner M. 1995. Recent trends in photoaffinity labeling. *Angew Chem, Int Ed Engl 34*: 1296-1312.

Lee J, Chou PK, Dowd P, Grabowski JJ. 1993. Anion-molecule approaches to non-Kekule molecules: The radical anion of tetramethyleneethane. *J Am Chem Soc 115*: 7902-7903.

Lee J, Grabowski JJ. 1992. Reactions of the atomic oxygen radical anion and the synthesis of organic reactive intermediates. *Chem Rev 92*: 1611-1647.

Leermakers JA. 1933. The thermal decomposition of methyl azide. A homogeneous unimolecular reaction. *J Am Chem Soc 55*: 3098-3105.

Linstrom PJ, Mallard WG. 2018. *NIST chemistry WebBook*. Gaithersburg, MD: National Institute of Standards and Technology.

Lykke KR, Murray KK, Neumark DM, Lineberger WC. 1988. High-resolution studies of autodetachment in negative ions. *Philos Trans R Soc, A 324*: 179-196.

Maltsev A, Bally T, Tsao M-L, et al. 2004. The rearrangements of naphthylnitrenes: UV/Vis and IR spectra of azirines, cyclic ketenimines, and cyclic nitrile ylides. *J Am Chem Soc 126*: 237-249.

Mazeau J, Gresteau F, Hall RI, Huetz A. 1978. Energy and width of N-(3P) from observation of its formation by dissociative attachment to N_2 and NO. *J Phys B: At Mol Phys 11*: L557-L560.

McDonald RN, Chowdhury AK. 1981. Gas-phase nucleophilic addition reactions of phenylnitrene anion radical with certain carbonyl-containing molecules. *J Am Chem Soc 103*: 674-676.

McDonald RN, Chowdhury AK. 1982. Hypovalent radical. Part 12. Gas-phase ion-molecule reactions of phenylnitrene anion radical with certain.alpha.,.beta.-unsaturated molecules. A study of 1,2- vs. 1,4-addition mechanisms. *J Phys Chem 86*: 3641-3645.

McDonald RN, Chowdhury AK. 1980a. Hypovalent radicals. 7. Gas-phase generation of phenylnitrene anion radical and its reaction with phenyl azide. *J Am Chem Soc 102*: 5118-5119.

McDonald RN, Chowdhury AK. 1980b. Hypovalent radicals. 8. Identification of nucleophilic 1,2- and 1,4-addition processes with.alpha.,.beta.-unsaturated molecules in the gas phase. *J Am Chem Soc 102*: 6146-6147.

McDonald RN, Chowdhury AK. 1983. Hypovalent radicals. 13. Gas-phase nucleophilic reactivities of phenylnitrene ($PhN^{-}\bullet$) and sulfur anion radicals ($S^{-}\bullet$) at sp3 and carbonyl carbon. *J Am Chem Soc 105*: 198-207.

McDonald RN, Chowdhury AK, Setser DW. 1981. Gas-phase generation of phenylnitrene anion radical–proton affinity and $\Delta H°_f$ of $PhN^{-}\bullet$ and its clustering with ROH molecules. *J Am Chem Soc 103*: 6599-6603.

McDonald RN, Davidson SJ. 1993. Electron photodetachment of the phenylnitrene anion radical: EA, $\Delta H°_f$, and the singlet-triplet splitting for phenylnitrene. *J Am Chem Soc 115*: 10857-10862.

Meijer EW, Nijhuis S, Van Vroonhoven FCBM. 1988. Poly-1,2-azepines by the photopolymerization of phenyl azides. Precursors for conducting polymer films. *J Am Chem Soc 110*: 7209-7210.

Metz RB, Weaver A, Bradforth SE, Kitsopoulos TN, Neumark DM. 1990. Probing the transition state with negative ion photodetachment: the chlorine atom + hydrogen chloride and bromine atom + hydrogen bromide reactions. *J Phys Chem 94*: 1377-1388.

Meyer DM, Roth KC. 1991. Discovery of interstellar NH. *Astrophys J 376*: L49.

Miller HC, Al-Za'al M, Farley JW. 1987. Measurement of hyperfine structure in the infrared rotation-vibration spectrum of NH^-. *Phys Rev Lett 58*: 2031-2034.

Mudgal M, Rishi S, Lumpuy DA, et al. 2017. Prehydrated one-electron attachment to azido-modified pentofuranoses: Aminyl radical formation, rapid H-atom transfer, and subsequent ring opening. *J Phys Chem B 121*: 4968-4980.

Murata S, Nakatsuji R, Tomioka H. 1995. Mechanistic studies of pyrene-sensitized decomposition of p-butylphenyl azide: Generation of nitrene radical anion through a sensitizer-mediated electron transfer from amines to the azide. *J Chem Soc, Perkin Trans 2*: 793-799.

Neumark DM, Lykke KR, Andersen T, Lineberger WC. 1985. Infrared spectrum and autodetachment dynamics of NH−. *J Chem Phys 83*: 4364-4373.

Nunes CM, Knezz SN, Reva I, Fausto R, McMahon RJ. 2016. Evidence of a nitrene tunneling reaction: Spontaneous rearrangement of 2-formyl phenylnitrene to an imino ketene in low-temperature matrixes. *J Am Chem Soc 138*: 15287-15290.

Pellerite MJ, Brauman JI. 1981. Gas-phase ion-molecule reactions of phenylnitrene anion. *J Am Chem Soc 103*: 676-677.

Perrotta RR, Falvey DE. 2013. The 3,5-dinitroanilide anion: a singlet anilide anion with evidence for a thermally accessible triplet state. *J Phys Org Chem 26*: 699-706.

Platz MS. 1995. Comparison of phenylcarbene and phenylnitrene. *Acc Chem Res 28*: 487-492.

Popp BV, Stahl SS. 2007. Palladium-catalyzed oxidation reactions: comparison of benzoquinone and molecular oxygen as stoichiometric oxidants. In: Meyer F, Limberg C, editors. *Organometallic oxidation catalysis*. Berlin, Heidelberg: Springer. p 149-189.

Pritchina EA, Gritsan NP, Bally T. 2005. Ground state multiplicity of acylnitrenes: Computational and experimental studies. *Russ Chem Bull 54*: 525-532.

Pritchina EA, Gritsan NP, Maltsev A, et al. 2003. Matrix isolation, time-resolved IR, and computational study of the photochemistry of benzoyl azide. *Phys Chem Chem Phys 5*: 1010-1018.

Rau NJ, Welles EA, Wenthold PG. 2013. Anionic substituent control of the electronic structure of aromatic nitrenes. *J Am Chem Soc 135*: 683-690.

Rau NJ, Wenthold PG. 2015. The low-lying triplet state in p-nitrobenzaldimide. *Int J Mass Spectrom 377*: 496-501.

Reed DR, Hare MC, Fattahi A, Chung G, Gordon MS, Kass SR. 2003. α,2-, α,3-, and α,4-Dehydrophenol radical anions: Formation, reactivity, and energetics leading to the heats of formation of α,2-, α,3-, and α,4-oxocyclohexadienylidene. *J Am Chem Soc 125*: 4643-4651.

Reed DR, Hare M, Kass SR. 2000. Formation of gas-phase dianions and distonic ions as a general method for the synthesis of protected reactive intermediates. Energetics of 2,3- and 2,6-dehydronaphthalene. *J Am Chem Soc 122*: 10689-10696.

Rohrer F, Stuhl F. 1988. The 193 (and 248) nm photolysis of HN3: Formation and internal energy distributions of the NH (a1Δ, b1∑+, A3Π, and c1Π) states. *J Chem Phys 88*: 4788-4799.

Sadygov RG, Yarkony DR. 1997. Electronic structure aspects of the spin-forbidden reaction CH3(X2A2″)+N(4S)→HCN(X1Σ+)+H2(X1Σg+). *J Chem Phys 107*: 4994-4999.

Salem L, Rowland C. 1972. The electronic properties of diradicals. *Angew Chem, Int Ed Engl 11*: 92-111.

Sander W, Kirschfeld A, Kappert W, Muthusamy S, Kiselewsky M. 1996. Dimesitylketone O-oxide: First NMR spectroscopic characterization of a carbonyl O-oxide. *J Am Chem Soc 118*: 6508-6509.

Schock M, Bräse S. 2020. Reactive & efficient: Organic azides as cross-linkers in material sciences. *Molecules 25*: 1009.

Srinivasan N, Golbeck JH. 2009. Protein–cofactor interactions in bioenergetic complexes: The role of the A1A and A1B phylloquinones in photosystem I. *Biochim Biophys Acta, Bioenerg 1787*: 1057-1088.

Srivastava S, Sathyamurthy N. 2013. Ab initio potential energy curves for the ground and low lying excited states of NH− and the effect of 2Σ± states on Λ-doubling of the ground state X2Π. *J Phys Chem A 117*: 8623-8631.

Staneke PO, Ingemann S, Eaton P, Nibbering NMM, Kass SR. 1994. Formation of the radical anion of cubene and determination of the heat of formation, heat of hydrogenation, and olefin strain energy of cubene. *J Am Chem Soc 116*: 6445-6446.

Tian Z, Kass SR. 2013. Carbanions in the gas phase. *Chem Rev 113*: 6986-7010.

Tomioka H, Okada H, Watanabe T, Banno K, Komatsu K, Hirai K. 1997. Polymethylated and poly(tert)butylated diphenylcarbenes. generation, reactions, kinetics, and deuterium isotope effects of sterically congested triplet carbenes. *J Am Chem Soc 119*: 1582-1593.

Travers MJ, Cowles DC, Clifford EP, Ellison GB. 1992. Photoelectron spectroscopy of the phenylnitrene anion. *J Am Chem Soc 114*: 8699-8701.

Travers MJ, Cowles DC, Clifford EP, Ellison GB, Engelking PC. 1999. Photoelectron spectroscopy of the CH3N− ion. *J Chem Phys 111*: 5349-5360.

Van Galen DA, Barnes JH, Hawley MD. 1986. The electrochemical reduction of fluorenone tosylhydrazone. Evidence consistent with the formation to the tosyl nitrene anion radical. *J Org Chem 51*: 2544-2550.

Wang J, Burdzinski G, Platz MS. 2013. Ultrafast time-resolved studies of the photochemistry of aryl azides. In: Falvey DE, Gudmundsdottir AD, editors. *Nitrenes and nitrenium ions*. Hoboken, New Jersey: John Wiley & Sons, Inc. p 1-31.

Wang YC, Lai XJ, Huang K, Yadav S, Qiu G, Zhang L, Zhou H. 2021. Unravelling nitrene chemistry from acyclic precursors: recent advances and challenges. *Org Chem Front 8*: 1677-1693.

Weber JM, Robertson WH, Johnson MA. 2001. Argon predissociation and electron autodetachment spectroscopy of

size-selected CH3NO2−·Arn clusters. *J Chem Phys 115*: 10718-10723.
Wenthold PG. 2012. Spin-state dependent radical stabilization in nitrenes: The unusually small singlet–triplet splitting in 2-furanylnitrene. *J Org Chem 77*: 208-214.
Wenthold PG, Hu J, Squires RR. 1994. Regioselective synthesis of biradical negative ions in the gas phase. Generation of trimethylenemethane, m-benzyne, and p-benzyne anions. *J Am Chem Soc 116*: 6961-6962.
Wenthold PG, Hu J, Squires RR, Lineberger WC. 1996. Photoelectron spectroscopy of the trimethylene-methane negative ion. The singlet−triplet splitting of trimethylenemethane. *J Am Chem Soc 118*: 475-476.
Wenthold PG, Kim JB, Lineberger WC. 1997. Photoelectron spectroscopy of m-xylylene anion. *J Am Chem Soc 119*: 1354-1359.
Wenthold PG, Squires RR. 1994. Gas-phase properties and reactivity of the acetate radical anion. Determination of the C-H bond strengths in acetic acid and acetate ion. *J Am Chem Soc 116*: 11890-11897.
Wenthold PG, Squires R, Lineberger WC. 1998. Ultraviolet photoelectron spectroscopy of the o-, m-, and p-benzyne negative ions. Electron affinities and singlet−triplet splittings for o-, m-, and p-benzyne. *J Am Chem Soc 120*: 5279-5290.
Wentrup C. 2013. Matrix studies on aromatic and heteroaromatic nitrenes and their rearrangements. In: Falvey DE, Gudmundsdottir AD, editors. *Nitrenes and nitrenium ions*. Hoboken, NJ: John Wiley & Sons, Inc. p 273-315.
Wentrup C. 1974. Thermochemistry of carbene and nitrene rearrangements. *Tetrahedron 30*: 1301-1311.
Wentrup C, Crow WD. 1970. Pyrolysis of 1(H)-triazoloarenes: Ring contraction to 5-ring nitriles, and CN-group migration. *Tetrahedron 26*: 3965-3981.
Wetzel DM, Brauman JI. 1987. Electron photodetachment spectroscopy of trapped negative ions. *Chem Rev 87*: 607-622.
Wijeratne NR, Fonte MD, Ronemus A, Wyss PJ, Tahmassebi D, Wenthold PG. 2009. Photoelectron spectroscopy of chloro-substituted phenylnitrene anions. *J Phys Chem A 113*: 9467-9473.
Wijeratne NR, Munsch TE, Haupert LJ, Wenthold PG. 2014. Thermochemical studies of substituted phenylnitrenes: Enthalpies of formation of chlorophenylnitrenes. *J Chem Thermodyn 73*: 213-217.
Wijeratne NR, Wenthold PG. 2007a. Benzoylnitrene radical anion: A new reagent for the generation of M-2H anions. *J Am Soc Mass Spectrom 18*: 2014-2016.
Wijeratne NR, Wenthold PG. 2007b. Structure and reactivity of benzoylnitrene radical anion in the gas phase. *J Org Chem 72*: 9518-9522.
Wijeratne NR, Wenthold PG. 2007c. Thermochemical studies of benzoylnitrene radical anion: The N−H bond dissociation energy in benzamide in the gas phase. *J Phys Chem A 111*: 10712-10716.
Winkler M. 2008. Singlet−triplet energy splitting and excited states of phenylnitrene. *J Phys Chem A 112*: 8649-8653.
Yoshimura T, Asada K, Oae S. 1982. Deoxygenation of tertiary amine oxides with carbon bisulfide. *Bull Chem Soc Jpn 55*: 3000-3003.

AUTHOR BIOGRAPHIES

Cory J. Conder is a laboratory instructor at Salisbury University (Maryland, USA). He obtained his PhD in 2021 at Purdue University (Indiana, USA) while studying under Dr. Paul Wenthold. His research interests are in isolating reactive intermediates using mass spectrometry.

Harshal Jawale is a PhD candidate at Purdue University in Dr. Paul Wenthold's research group. His research focus is at the intersection of organic chemistry and analytical chemistry, where he studies the electronic structures and reactivities of phenylnitrenes and phenylazides using mass spectrometry.

Paul G. Wenthold is an Associate Professor in the Department of Chemistry at Purdue University. He obtained a PhD from Purdue in 1994. His group investigates physical organic chemistry and reactive intermediates using mass spectrometry and ion spectroscopy.

How to cite this article: Conder CJ, Jawale H, Wenthold PG. Mass spectrometry studies of nitrene anions. *Mass Spectrometry Reviews*, (2021); e21751. https://doi.org/10.1002/mas.21751